



HAL
open science

ARN interférence : une stratégie pour cibler la protéine kinase B (Akt) dans le carcinome hépatocellulaire

Mariam Mroweh

► To cite this version:

Mariam Mroweh. ARN interférence : une stratégie pour cibler la protéine kinase B (Akt) dans le carcinome hépatocellulaire. *Virologie*. Université Grenoble Alpes [2020-..]; Université Libanaise, 2022. Français. NNT : 2022GRALV031 . tel-03771336

HAL Id: tel-03771336

<https://theses.hal.science/tel-03771336>

Submitted on 7 Sep 2022

HAL is a multi-disciplinary open access archive for the deposit and dissemination of scientific research documents, whether they are published or not. The documents may come from teaching and research institutions in France or abroad, or from public or private research centers.

L'archive ouverte pluridisciplinaire **HAL**, est destinée au dépôt et à la diffusion de documents scientifiques de niveau recherche, publiés ou non, émanant des établissements d'enseignement et de recherche français ou étrangers, des laboratoires publics ou privés.



THÈSE

Pour obtenir le grade de

DOCTEUR DE L'UNIVERSITÉ GRENOBLE ALPES

préparée dans le cadre d'une cotutelle entre l'Université Grenoble Alpes et l'Université Libanaise

Spécialité : Virologie - Microbiologie - Immunologie

Arrêté ministériel : 25 mai 2016

Présentée par

Mariam MROWEH

Thèse dirigée par **Patrice MARCHE** et **Bassam BADRAN**,
codirigée par **Nader HUSSEIN**

préparée au sein des Laboratoires : Immunologie Analytique des Pathologies Chroniques (IAPC/IAB, INSERM U1209, CNRS UMR5309, Grenoble) et Laboratoire de Biologie du Cancer et d'Immunologie Moléculaire (Beyrouth)

dans l'École Doctorale Chimie et Sciences du Vivant (EDCSV) et l'École Doctorale des Sciences et des Technologies (EDST)

ARN interférence : une stratégie pour cibler la protéine kinase B (Akt) dans le carcinome hépatocellulaire

RNA interference: a strategy for targeting protein kinase B (Akt) in hepatocellular carcinoma

Thèse soutenue publiquement le **31 mars 2022**,
devant le jury composé de :

Monsieur Patrice MARCHE

DIRECTEUR DE RECHERCHE, INSERM délégation Auvergne-Rhône-Alpes, Directeur de thèse

Madame Birke BARTOSCH

DIRECTRICE DE RECHERCHE, INSERM délégation Auvergne-Rhône-Alpes, Rapporteur

Monsieur Rabih TALHOUK

PROFESSEUR, American University of Beirut, Rapporteur

Madame Eva HAMADE

PROFESSEUR, Université Libanaise, Examinatrice

Monsieur Walid RACHIDI

PROFESSEUR DES UNIVERSITÉS, Université Grenoble Alpes, Président

Monsieur Bassam BADRAN

PROFESSEUR, Université Libanaise, Directeur de thèse

Monsieur Nader HUSSEIN

PROFESSEUR, Université Libanaise, Co-directeur de thèse

Monsieur Marc BILLAUD

DIRECTEUR DE RECHERCHE, CNRS délégation Rhône-Auvergne, Examineur



THESE de doctorat en Cotutelle
Pour obtenir le grade de Docteur délivré par
L'Université Libanaise
L'Ecole Doctorale des Sciences et Technologie

Spécialité : Immunologie

Présentée et soutenue publiquement par

MROWEH Mariam

31 Mars 2022

**ARN Interférence: Une Stratégie Pour Cibler la Protéine
Kinase B (Akt) dans le Carcinome Hépatocellulaire**

Membres du Jury

M. Walid Rachidi , Professeur, CEA Grenoble	Président
Mme. Birke Bartosch , Directrice de Recherche INSERM, CRCL	Rapportrice
M. Rabih Talhouk , Professeur, Université Américaine de Beyrouth	Rapporteur
Mme. Eva Hamade , Professeur, Université Libanaise	Examinatrice
M. Marc Billaud , Directeur de Recherche CNRS, CRCL	Examineur
M. Bassam Badran , Professeur, Université Libanaise	Directeur
M. Patrice N. Marche , Directeur de Recherche INSERM, IAB	Directeur
M. Nader Hussein , Professeur, Université Libanaise	co-Directeur

ACKNOWLEDGEMENTS

To Him, for setting me on a path that led me here.

First, I would like to thank the honorable jury for taking the time to read my manuscript, namely, Dr. Birke BARTOSCH, Pr. Rabih TALHOUK, Pr. Eva HAMADE, Dr. Marc BILLAUD and Pr. Walid RACHIDI.

I would like to thank the Lebanese University for granting me the scholarship to carry out my PhD. I would also like to thank INSERM and FLORALIS for their financial assistance in the prolonged (due to Covid-19) period of my PhD. I would also like to thank my CSI jury members, namely, Pr. Walid RACHIDI, Dr. Anouk EMADALI and Dr. Xavier GIDROL for their valuable advice throughout my PhD.

I stand where I am today because of the support of the people surrounding me, I would like to take this opportunity to write a few words of gratitude to each of those people.

I would like to thank my director in Lebanon, Pr. Bassam BADRAN and co-director Pr. Nader HUSSEIN for believing in my potential and opening the door of possibility to be able to come to France to pursue my PhD.

When I came to France, I had the chance to be mentored by Dr. Patrice MARCHE. I would like to take this opportunity and express how honored I am to have been mentored by him, it has been an enlightening journey and I am eternally grateful to have had him by my side throughout it. I would like to thank him for being a beacon of light. His constant belief in me, support, encouragement and incomparable guidance have been precious in ways I cannot put into words. He passed on his invaluable wisdom not only in science but also in the matters of life and for that I consider him as family, and he will forever have my utmost respect, and hold a great place in my heart.

I have had in France another guarding angel, Flora Clément. I am deeply thankful to her. She never stopped encouraging me and helping me overcome the obstacles I faced throughout my PhD. She persists as a source of infinite inspiration and support that I hold so dearly. Thank you very much for all the time you have given me and for being a source of motivation.

Being in the team of Patrice MARCHE, in the Institute for Advanced Biosciences (IAB), I met wonderful people who made the everyday lab life something to look forward to. To all the members of the team, thank you so much for being supportive and encouraging. Especially, Zuzana MACEK-JILKOVA and Carole FOURNIER for their valuable scientific advice and support; Marion RESSEJAC for being the “mother of the lab”, who became my best friend in France, thank you for being who you are, thank you for feeding me from your own energy, for believing in me and being my person and Lydie CARRERES for being a dear friend and a companion in the PhD difficulties as we were doing our PhDs at the same time, to these two people is an extra thank you for taking the time to listen to my every morning “Mariam Story”, it has been fun; Christine CHARRAT thank you for your help throughout my PhD in helping me do the orders and for loving me; and Khaldoun GHARZEDDINE, thank you for being a reminder of Lebanon, and for supporting me throughout everything.

The IAB acquaintances I made surpassed the team, to all the members of the institute thank you so much for your help and your friendship. To the postdoc and PhD club in IAB: Ariadni, Camilla, Francesco, Dominico, Alex, and Tanveer, thank you for the support you gave me and making me a part of an international community in IAB. In addition to Anouk EMADALI who was an inspiration and a friend and Dalenda BENMEDJAHED for being a flowing source of support and love. Loris DELRIEU to him I say 3 words: “Je s’appelle Grout”. Saly SONGVILAY, thank you for your presence in my life.

Last but not least, in the IAB I met Mohamed GRAIES, words fail me when I speak of him, I am grateful for his presence. Thank you for standing with me through better and worse, thank you for keeping me going through the late nights, thank you for all the tube labelling and ice bringing. Thank you for being constant ray of sunshine and a support system that I cherish so deeply.

I have a childhood friend who has been by my side since as long as I can remember, Katia El Assaad thank you for being a constant throughout all the stages of my life. Finally, to my family, my father Ismail MROUE, my mother Rokaya FAKIH, my sister, Julia MROUEH, and my brother Hussein MROUEH, the people to whom I owe the highest grades of thanks, a MILLION thank you.

You are the four pillars of my life. Thank you for being my safety net and my backbone. Thank you for believing in me, thank you for being unconditionally giving. I love you infinitely.

This manuscript is dedicated to
Rokaya FAKIH & Ismail MROUE

ABSTRACT

Hepatocellular carcinoma (HCC) is one of the most common causes of cancer-related deaths worldwide, and its incidence is rising. HCC develops almost exclusively on the background of chronic liver inflammation, which can be caused by chronic alcohol consumption, viral hepatitis, or an unhealthy diet. HCC exhibits a deregulation of a multitude of pathways, including the PI3K/Akt pathway. Protein kinase B (Akt) exists in 3 isoforms: Akt1, Akt2 and Akt3, transcribed from three different genes and differing in their expression levels throughout the human body. While Akt3 is expressed mainly in the brain and the testes, Akt1 is expressed constitutively in the body and Akt2 is mainly expressed in insulin-sensitive tissues. Targeting Akt through chemical inhibitors has shown potent anti-cancer effect. However, chemical inhibitors fail to show a specificity over either of the isoforms, which converge and diverge in their designated roles in controlling various cellular processes. Thus, selective inhibition is needed to confer the role of each of Akt1 and Akt2 isoforms, in the context of HCC. RNA-interference (RNAi) is a highly specific strategy to target the expression of a gene at the transcriptional level and can be exploited to suppress the expression of a given gene using exogenous small interfering RNAs (siRNAs). For that, we designed siRNAs targeting solely Akt1 or Akt2 isoform in humans and rodents, simultaneously. The specificity of the siRNAs was verified by confirming, *in vitro* on human HepG2 cell line, the selective inhibition of the designated Akt1 or Akt2 expression, in addition to the absence of predicted off-target effects upon *in silico* analysis. Furthermore, the efficiency of the designed siRNAs was demonstrated; following 6 hours of exposure to designed Akt1 and Akt2 siRNAs, the Akt1 expression and Akt2 expression remained decreased up to 5 and 7 days in HepG2 cells, respectively, and showed efficacy at low concentrations, starting 20 pM. The possible inflammatory effect of the siRNAs was also assessed, and the results show that the designed siRNAs do not activate any of the Toll-like receptors. Next, we assessed the phenotypic aspect (cytotoxicity, metabolism and proliferation) of the knockdown of Akt1 and Akt2 or the simultaneous knockdown of both by the designed siRNAs whilst comparing to Sorafenib (a verified treatment of HCC) and ARQ092 (a chemical inhibitor of Akt) on 4 different liver cancer cell lines - PLCY/PRF/5, Huh7, Hep3B and HepG2 cell lines. The results show that targeting a single isoform of Akt – either Akt1 or Akt2 – or the simultaneous knockdown of both isoforms – Akt1 and Akt2 - by the designed siRNAs have no impact on the viability, metabolism or proliferation of the cells that is contradictory to the effect seen upon treatment with inhibitors Sorafenib or ARQ092. Furthermore, the vectorization of the designed siRNAs by the Amphiphilic Dendrimer (AD) and their consequent use to target Akt1 or Akt2 in an *in ovo* HepG2 and MV4-11 cell-

line graft model showed neither a toxic effect on chick embryos, nor an anti-tumorigenic effect when compared to the control. Altogether, the results show that the knockdown of a single isoform of Akt: Akt1 or Akt2 using the designed siRNAs, is not sufficient to mount an anti-cancer effect. Furthermore, the simultaneous knockdown of both isoforms using the specific siRNAs against Akt1 and Akt2 does not mimic the effect seen by chemical Akt inhibitors. These results suggest the presence of compensatory mechanisms in the case of the targeted single isoform knockdown, and that in addition to the potent global inhibition of Akt, ARQ092 may exert an off-target inhibition leading to its prominent anti-cancer activity.

RESUME

Le carcinome hépatocellulaire (CHC) est l'une des causes les plus courantes de décès liés au cancer dans le monde, et son incidence est en augmentation. Le CHC se développe presque exclusivement sur des antécédents inflammatoires chroniques du foie, qui peuvent être causés par une consommation addictive d'alcool, une hépatite virale ou une mauvaise alimentation. Le CHC présente une dérégulation d'une multitude de voies, y compris la voie PI3K/Akt. La protéine kinase B (Akt) existe sous 3 isoformes : Akt1, Akt2 et Akt3, transcrites à partir de trois gènes différant par leurs niveaux d'expression dans le corps humain. Alors qu'Akt3 est exprimé principalement dans le cerveau et les testicules, Akt1 est exprimé de manière constitutive dans tout le corps et Akt2 est principalement exprimé dans les tissus sensibles à l'insuline. Le ciblage d'Akt par des inhibiteurs chimiques a montré un puissant effet anticancéreux. Cependant, ces composés ne présentent pas de spécificité pour les différents isoformes, qui convergent et divergent dans leurs rôles dans le contrôle de divers processus cellulaires. Ainsi, une inhibition sélective est nécessaire pour attribuer le rôle de chacune des isoformes Akt1 et Akt2, dans le contexte du CHC. L'interférence par ARN (ARNi) est une stratégie hautement spécifique pour cibler l'expression d'un gène au niveau transcriptionnel. Il est possible de l'utiliser pour supprimer l'expression d'un gène donné en utilisant des siARN interférents courts et exogènes. Ainsi, nous avons conçu des siARN ciblant uniquement l'isoforme Akt1 ou Akt2 chez l'homme et le rongeur, simultanément. La spécificité des siARN a été vérifiée en confirmant, *in vitro*, sur la lignée cellulaire HepG2 humaine, l'inhibition sélective de l'expression Akt1 ou Akt2, en plus de l'absence d'effets « off-target » prédits lors de l'analyse *in silico*. De plus, l'efficacité des siARN a été observée dès 6 heures après l'exposition aux siARN Akt1 et Akt2 et est restée jusqu'à 5 et 7 jours dans les cellules HepG2. Les siRNA ont montré une efficacité à de faibles concentrations, à partir de 20 pM, à la fois au niveau des ARNm et des protéines. L'effet inflammatoire des siARN a également été évalué et les résultats montrent que les siARN conçus n'activent aucun des récepteurs de type Toll-like (TLR). Ensuite, nous avons évalué l'aspect phénotypique (cytotoxicité, métabolisme et prolifération) de l'inactivation d'Akt1 et d'Akt2 ou de l'inactivation simultanée des deux par les siARN en comparaison avec le Sorafenib (un traitement de référence en cours du CHC) et à l'ARQ092 (un inhibiteur chimique d'Akt) sur 4 lignées cellulaires différentes de cancer du foie : PLCy/PRF/5, Huh7, Hep3B et HepG2. Les résultats montrent que le ciblage d'une seule isoforme d'Akt ou l'inactivation

simultanée des deux isoformes par les siARN conçus n'a aucun impact sur la viabilité, le métabolisme ou la prolifération des cellules, ce qui est contradictoire avec l'effet observé lors d'un traitement avec les inhibiteurs Sorafenib ou ARQ092. De plus, la vectorisation des siARN par le dendrimère amphiphile (AD) et leur utilisation pour cibler Akt1 ou Akt2 dans un modèle de greffe de lignée cellulaire (HepG2 et MV4-11) *in ovo* n'ont montré aucun effet toxique sur les embryons de poulet, ni d'effet antitumoral. Dans l'ensemble, les résultats montrent que l'inactivation d'une seule isoforme d'Akt n'est pas suffisante pour monter un effet antitumoral. De plus, l'inactivation simultanée des deux n'imité pas l'effet observé par les inhibiteurs chimiques d'Akt. Ces résultats suggèrent la présence de mécanismes compensatoires dans le cas de l'inactivation d'une seule isoforme d'Akt, et qu'en plus de la forte inhibition globale d'Akt, ARQ092 pourrait exercer une inhibition pléiotrope conduisant à son importante activité anticancéreuse.

I. TABLE OF CONTENTS

ACKNOWLEDGEMENTS.....	2
ABSTRACT	5
RESUME.....	7
I. TABLE OF CONTENTS	9
II. TABLE OF FIGURES	12
III. TABLE OF TABLES	14
IV. ABBREVIATIONS	15
V. INTRODUCTION	21
1. Hepatocellular carcinoma	21
1.1. Etiology of HCC.....	22
1.2. Treatment options of HCC.....	29
1.3. Signaling pathways altered in HCC.....	33
2. Protein Kinase B (Akt).....	38
2.1. Roles of Akt1, Akt2 and Akt3 in HCC progression	43
2.2. Role of Akt1 and Akt2 in the modulation of the immune cells	45
2.3. Targeting Akt in the management of HCC.....	50
3. RNA interference overview	55
3.1. Clinical application of RNAi.....	58
3.2. Delivery vectors for RNAi	73
VI. HYPOTHESIS AND OBJECTIVES	76
VII. MATERIALS AND METHODS.....	77
1. <i>In silico</i> design of Akt1 and Akt2 siRNAs cross-reacting humans and rodents.....	77
2. Cell culture	77
3. Transfection of the different cell lines by siRNA	78
3.1. Lipofectamine-mediated transfection.....	78
3.2. Amphiphilic Dendrimer (AD)-mediated transfection.....	79
4. Treatment with Sorafenib and ARQ092.....	79

5. Gene expression analysis	80
6. Protein immuno-detection	81
7. Toll-like receptors (TLR) activation monitoring	83
8. Cell-death analysis.....	84
9. Metabolism analysis	84
10. Cell proliferation analysis.....	85
11. <i>In ovo</i> assessment of the Dendrimer-mediated delivery of designed Akt1/Akt2 siRNAs.....	85
Preparation of chicken embryos.....	86
Amplification and grafting of tumor cells	86
Treatments.....	87
Quantitative evaluation of tumor growth and embryonic tolerability	87
12. Proteome profiling of Akt kinase activity	88
13. Kinase profiling on Pamstation®12	90
14. Statistical analysis.....	91
VIII.RESULTS	92
1. Designing and screening of siRNAs simultaneously targeting human and rodent <i>Akt1</i> and <i>Akt2</i>	92
1.1 Preliminary Akt1 siRNA design and screening	92
1.2. Preliminary Akt2 siRNA design and screening	109
2. Long lasting effect of Akt1 and Akt2-targeting siRNAs.....	127
3. Efficiency of Akt1 and Akt2-targeting siRNAs	130
4. Inflammatory effect of Akt1 and Akt2-targeting siRNAs	133
5. Phenotypic effect of the designed siRNA-mediated knockdown of Akt1 and Akt2.....	134
5.1. Effect of the designed siRNA-mediated knockdown of <i>Akt1</i> and <i>Akt2</i> on cytotoxicity	134
5.2. Effect of the designed siRNA-mediated knockdown of Akt1 and Akt2 on cell metabolism	136

5.3. Effect of the siRNA-mediated knockdown of Akt1 and Akt2 on cell proliferation.....	138
6. Vectorization of the designed Akt1 and Akt2 siRNAs using AD.....	141
7. <i>In ovo</i> assessment of the cytotoxicity and tumor growth of AD-designed siRNA-mediated knockdown of Akt1 and Akt2	143
7.1. HepG2 <i>in ovo</i> graft model.....	144
7.2. MV4-11 <i>in ovo</i> graft model	146
8. Effect of Akt1 and/or Akt2 knockdown on the kinase activity	148
8.1. Effect of D2Akt1 and/or D15Akt2 siRNAs on the activity of Akt1 and Akt2	148
8.2. Effect of D2Akt1and/or D15Akt2 siRNAs on the PI3K/Akt pathway	155
9. Kinase fingerprint of Akt1 and/or Akt2 knockdown and their chemical inhibition	173
9.1. PLCγ/PRF/5 cell line.....	177
9.2. Huh7 cell line.....	180
9.3. HepG2 cell line	183
IX. DISCUSSION	186
Background and objective.....	186
Differential Activity of AKT isoforms	187
RNAi.....	188
Phenotypic consequences of siRNA-mediated knockdown of Akt1 and Akt2	190
Molecular consequences of siRNA-mediated knockdown of Akt1 and Akt2.	192
X. CONCLUSIONS AND PERSPECTIVES.....	196
XI. REFERENCES	199
XII. ANNEXES	221
Review 1	221
Review 2	248

II. TABLE OF FIGURES

Figure 1: Global distribution of incidence of liver cancer	21
Figure 2: Global distribution mortality rate of liver cancer	22
Figure 3: Etiology of HCC.....	23
Figure 4: Aberrant activation of PI3K/Akt pathway in cancer	38
Figure 5: Isoforms of Akt	39
Figure 6: Activation of the PI3K/Akt pathway	41
Figure 7: Overview of the PI3K/Akt pathway	42
Figure 8: Role of PI3/Akt in the fate of T-cells	46
Figure 9: Role of PI3K/Akt in the fate of macrophages	48
Figure 10: Possible impact of chemical Akt inhibition on HCC and its TME	50
Figure 11: Scheme of three RNAi different pathways.....	56
Figure 12: RNAi in HCC	60
Figure 13: Jess plate	83
Figure 14: Scheme of <i>in ovo</i> study.	86
Figure 15: Pamgene principle	90
Figure 16: Screening of Designed Akt1 siRNAs <i>in cellulo</i>	103
Figure 17: Specificity of D2Akt1 and D11Akt1 siRNAs	106
Figure 18: Rodent cross-reactivity and specificity of Akt1 siRNAs	108
Figure 19: Screening of Designed Akt2 siRNAs <i>in cellulo</i>	121
Figure 20: Specificity of D15Akt2 and D27Akt2 siRNAs	124
Figure 21: Rodent cross-reactivity and specificity of Akt2 siRNAs	126
Figure 22: Long-lasting effect of D2Akt1 siRNA	128
Figure 23: Long-lasting effect of D15Akt2 siRNA	129
Figure 24: Efficiency of D2Akt1 siRNA	131
Figure 25: Efficiency of D15Akt2 siRNA	132
Figure 26: Pro-inflammatory effect of D2Akt1 and D15Akt2 siRNAs	133
Figure 27: Effect of Akt1 and/or Akt2 knockdown on cytotoxicity	135
Figure 28: Effect of Akt1 and/or Akt2 knockdown on cell metabolism	137
Figure 29: Effect of Akt1 and/or Akt2 knockdown on cell proliferation	140
Figure 30: AD-mediated vectorization of siRNAs	142
Figure 31: Effect of designed siRNAs in HepG2 <i>in ovo</i> graft model.....	145
Figure 32: Effect of designed siRNAs in MV4-11 <i>in ovo</i> graft model	147
Figure 33: Phospho-Akt1/Akt2 after knockdown in PLC γ /PRF/5 cell line	150
Figure 34: Phospho-Akt1/Akt2 after knockdown in Huh7 cell line	152
Figure 35: Phospho-Akt1/Akt2 after knockdown in HepG2 cell line	154

Figure 36: Heatmap of protein modulations in Huh7 and HepG2 cell lines.....	156
Figure 37: Effect of the knockdown of Akt1 and/or Akt2 in Huh7 cell line	160
Figure 38: Effect of the knockdown of Akt1 and/or Akt2 in HepG2 cell line.....	163
Figure 39: Categories of “within cell lines” comparative analysis	165
Figure 40: Comparative analysis in Huh7 cell line	166
Figure 41: Comparative analysis of in HepG2 cell line	168
Figure 42: Categories of “inter-cell line” comparative analysis	169
Figure 43: Inter-cell line comparative analysis of Akt1 and Akt2 knockdown ...	170
Figure 44: Inter-cell line comparative analysis of Akt1 knockdown.....	171
Figure 45: Inter-cell line comparative analysis of Akt2 knockdown.....	172
Figure 46: Heatmap of phosphosites upon the siRNA knockdown	175
Figure 47: Heatmap of phosphosites ARQ092 treatment.....	176
Figure 48: Kinase fingerprint of PLCY/PRF/5 cells upon siRNA knockdown.....	178
Figure 49: Kinase fingerprint of PLCY/PRF/5 cells upon ARQ092 treatment.....	179
Figure 50: Kinase fingerprint of Huh7 cells upon siRNA knockdown.....	181
Figure 51: Kinase fingerprint of Huh7 cells upon ARQ092 treatment.....	182
Figure 52: Kinase fingerprint of HepG2 cells upon siRNA knockdown	184
Figure 53: Kinase fingerprint of HepG2 cells upon ARQ092 treatment	185

III. TABLE OF TABLES

Table 1: Akt inhibitors in the management of HCC	51
Table 2: RT-qPCR primers	81
Table 3: Description of Egg groups	87
Table 4: List of 37 tested proteins in the phosphoarray	89
Table 5: Inter-species reactivity of Akt1 siRNA candidates.....	93
Table 6: Off-target effect of Akt1 siRNA candidates in Homo sapiens	94
Table 7: Off-target effect of Akt1 siRNA candidates in Mus musculus	95
Table 8: Off-target effect of Akt1 siRNA candidates in Rattus norvegicus	97
Table 9: Off-target effect ranking of Akt1 siRNA candidates.	102
Table 10: Weighed <i>in cellulo</i> efficacy ranking of Akt1 siRNA candidates	104
Table 11: Combination of <i>in cellulo</i> and <i>in silico</i> data for Akt1 siRNA choice	104
Table 12: Inter-species reactivity of Akt2 siRNA candidates.....	109
Table 13: Off-target effect of Akt2 siRNA candidates in Homo sapiens.....	112
Table 14: Off-target effect of Akt2 siRNA candidates in Mus musculus	113
Table 15: Off-target effect of Akt2 siRNA candidates in Rattus norvegicus	114
Table 16: Off-target effect ranking of Akt2 siRNA candidates	120
Table 17: Weighed <i>in cellulo</i> efficacy ranking of Akt2 siRNA candidates	122
Table 18: Combination of <i>in cellulo</i> and <i>in silico</i> data for Akt2 siRNA choice	122
Table 19: End-point tumor weight analysis of HepG2 <i>in ovo</i> graft model.....	146
Table 20: End-point tumor weight analysis of MV4-11 <i>in ovo</i> graft model	148
Table 21: Effect of Akt1 and/or Akt2 knockdown in Huh7 cell line	161
Table 22: Effect of the knockdown of Akt1 and/or Akt2 in HepG2 cell line	164

IV. ABBREVIATIONS

3D: three dimensional

A1AD: Alpha 1-Antitrypsin Deficiency

AD: Amphiphilic Dendrimer

ADP: Adenosine DiPhosphate

AFB1: Aflatoxin B1

AFL: Alcoholic Fatty Liver

AFP: Alpha FetoProtein

Ag: Antigen

AGO: Domain Of The Argonaute

AH: Alcoholic Hepatitis

AHP: Acute Hepatic Porphyria

AIH: Autoimmune Hepatitis

Akt: Protein kinase B

ALD: Alcohol-Related Liver Diseases

ALDH: Aldehyde Dehydrogenase

Ang II: Angiotensin II

APC: Antigen Presenting Cell

Arg1: Arginase 1

ATM: Ataxia Telangiectasia Mutated

ATP: Adenosine TriPhosphate

ATR: Ataxia Telangiectasia and Rad3 Related

AurA/Aur2: Aurora Kinase A

AurB/Aur1: Aurora Kinase B

BAD: BCL2-Antagonist of Cell Death

bFGF: basic Fibroblast Growth Factor

BLAST: Basic Local Alignment Search Tool

CAF: Cancer Associated Fibroblast

CAM: Chorioallantoic Membrane

CAMK4: Calcium/calmodulin-dependent protein kinase type IV

Casp9: Caspase 9

CCL: C-C Chemokine Ligand

CCN1/CYR61: Cysteine-Rich Angiogenic Protein 61

CCN2/CTGF: Connective Tissue Growth Factor

CCN3/NOV: Nephroblastoma Overexpressed or CCN3

CD105: Endoglin CD105

C_{dendrimer}: Concentration of Dendrimer

CDK: Cyclin-Dependent Kinase

CDKL5: Cyclin-Dependent Kinase 5

CEP70: Centrosomal Protein 70
Chk-2: Checkpoint kinase-2
CDDP: Cisplatin treatment
c-Jun/AP-1: Activator Protein-1
CK1: Casein Kinase-1
COX: Cyclooxygenase
CREB cAMP-response element binding protein
C_{siRNA}: Concentration of siRNA
CTL: CD8⁺ Cytotoxic T-Cell
CTLA4: Cytotoxic T Lymphocyte Associated Protein 4
CXCR: Chemokine Receptor
DAMP: Damaged-Associated Molecular Pattern
DC: Dendritic Cell
DEN: DiEthylNitrosamine
DM: Diabetes Mellitus
DMEM: Dulbecco's Modified Eagle medium
DNL: *De Novo* Lipogenesis
DSIR: Designer of siRNA
dsRNA: double-stranded RNA
DTT: Dithiothreitol
ECM: Extra Cellular Matrix
EGF R Epidermal Growth Factor -Receptor
EGF: Epidermal Growth Factor
EGF: Epithelial Growth Factor
EMT: Epithelial-to-Mesenchymal Transition
eNOS: endothelial Nitric Oxide Synthase
ERK: Extracellular Signal-Regulated Kinase
ERK1/2: Extracellular Signal-Regulated Kinase 1/2
FAA: Fumarylacetoacetate
FBS fetal bovine serum
FDA: Food And Drug Administration
FGF: Fibroblast Growth Factor
FGFR: Fibroblast Growth Factor Receptor
Fgr/v-Fgr: Gardner-Rasheed feline sarcoma viral
Fizz1: Found In Inflammatory Zone Protein 1
FOXC1: Forkhead Box C1
FOXO: Forkhead Box Protein O
FUBP1: Far Upstream Element Binding Protein 1
GAPDH: Glyceraldehyde-3-Phosphate Dehydrogenase
GF: Growth Factor

GPC3: Glypican 3
GPI: GlycosylPhosphatidyInositol
GRK2: G Protein-Coupled Receptor Kinase
GRO- α : growth-regulated oncogene α
GSD: Glycogen Storage Disease
GSK: Glycogen Synthase Kinase
HBV: Hepatitis-B Virus
HCC: Hepatocellular Carcinoma
HCV: Hepatitis-C Virus
HER2: Human Epidermal growth factor Receptor 2
HGF Hepatocyte Growth Factor
HH: Hereditary Hemochromatosis
HIF1 α : Hypoxia-Inducible Factor 1 α
HLA: Human Leukocyte Antigen
HPRT1: Hypoxanthine Phosphoribosyltransferase 1
HRP: Horse Raddish Peroxidase (HRP)
HS: Heparin Sulfate
HSC: Hepatic stellate cell
HSP: Heat Sock Protein
HSPG: heparin sulfate proteoglycan
HT1: Hereditary Tyrosinemia Type 1
hTERT: Human Telomerase Reverse Transcriptase
IC20: Inhibitory Concentration 20
ICC: Intrahepatic Cholangiocarcinoma
IFN: Interferon-
IGF: Insulin-Like Growth Factor,
IgG: Immunoglobulin-G
IKK α : Kappab Kinase Alpha
IL: Interleukin
ILK: Integrin-Linked Kinases
IMDM: Iscove's Modified Dulbecco's Medium
iNOS: Inducible Nitric Oxide Synthase
IR: InfraRed
IRF-1: Interferon Regulatory Factor-1
JAK: Janus Kinases
JNK 1/2/3: c-Jun N-terminal Kinase 1/2/3
Lck: Lymphocyte-specific Protein tyrosine Kinase
LDH: Lactase DeHydrogenase
LKM1: Liver/Kidney microsomal antibody 1
lncRNA: long non-coding RNA

LPS: LipoPolySaccharise
Lyn: Lck/Yes-related novel protein tyrosine kinase
MAPK: Mitogen-Activated Protein Kinase
MAPKAP2: MAPK-Associated Protein 2
MCP1 Monocyte Chemoattractant Protein 1
MDM2: Murine Double Minute 2
MEK: Mitogen-activated ERK-Activating Kinase
MEM: Modified Eagle medium
MIF: Migration Inhibitory Factor
miR/miRNA: microRNA
MRI: Magnetic Resonance Imaging
mRNA: messenger RNA
MSK1/2: Mitogen-and Stress-activated protein Kinases1/2
MTNR1B: Melatonin Receptor 1B
mTORC-1/2: mammalian Target of Rapamycin-1/2
MYCBP2: MYC-Binding Protein 2
NAFLD: Non-Alcoholic Fatty Liver Disease
NASH: Non-Alcoholic Steatohepatitis
ncRNA: Non-Coding RNA
Neg Ctrl: negative control
Nfkb: Nuclear Factor Kb
NIR: Near-InfraRed
NK: natural killer
NLR: neutrophil-lymphocyte ratio
nM: nanoMolar
NOD: Nucleotide-Binding Oligomerization Domain
nt Nucleotide
NUAK1: NUAK family SNF1-like kinase 1
ORF: Open Reading Frames
OS: Overall Survival
P38 α : Protein 38
P53: Protein 53
P70 S6K: Ribosomal Protein S6 Kinase
PAMP: Pathogen-Associated Molecular Pattern
PCTRAIRE2/ CDK16: Cyclin-Dependent Kinase 16
PD-1: Programmed cell Death protein-1
PDGFR: Platelet Derived Growth Factor Receptor
PDK-1: Phosphoinositide-Dependent Kinase-1
PDL-1: Programmed Death Ligand-1
PFS: Progression Free Survival

PGLSA-OH: Poly (Glycerol Succinic Acid)
PHLPP2: PH Domain Leucine-Rich-Repeat-Containing Protein Phosphatase2
PI3K: Phosphatidyl Inositol 3 Kinase
Pim: Proviral Integration site for Moloney murine leukemia virus
PIP2: Phosphatidyl Inositol-4,5-bisphosphate
PIP3: Phosphatidyl Inositol-3,4,5-triphosphate
PIWI: P-Element Induced Wimpy Testis
PK: Protein Kinase.
PLC: Phospho Lipase C
PLL: Poly(2,2-Bis(Hydroxymethyl)Propionic Acid (Bis-MPA),
pM: picomolar
PMAM: Poly(AmidoAMine)
PP2A: Protein Phosphatase 2A
PPAR: Peroxisome Proliferator-Activated Receptor.
PPI: Polypropylenimine
PRAS40: Proline-Rich Akt Substrate of 40 kDa
Pre: Precursor
Pri: Primary
Prrs: Pattern Recognition Receptors
PTEN: Phosphatase and Tensin Homolog
PTGS: Post-Transcriptional Gene Silencing
PYK2: Protein Tyrosine Kinase 2
qPCR: quantitative PCR
RAF: Rapidly Accelerated Fibrosarcoma
RAS: Rat sarcoma virus
RIG-I: Retinoic Acid-Inducible Gene I
RISC: RNA-Induced Silencing Complex
RNAi: RNA interference
ROCK1: Rho-associated protein kinase 1
ROS: Reactive Oxygen Species
RS18: Ribosomal subunit 18
RSK: Ribosomal S6 Kinase
RSKL2: Ribosomal Protein S6 Kinase-Like 2
RTK Receptor Tyrosine Kinase
RT-qPCR: Reverse Transcriptase – quantitative Polymerase Chain Reaction
SBNO2: Strawberry Notch homologue 2
SCID: Severe Combined Immunodeficiency
SEAP: Secreted Embryonic Alkaline Phosphatase
SENP1: SUMO Specific Protease 1
Ser: Seine

SGK1: Serine/threonine-protein kinase SGK1
SH2: Src Homology 2
shRNA: short-hairpin RNA
siRNA: small interfering RNA
SMAD: Small Mothers Against Decapentaplegic
Sol: Solution
SOX: Sex-Determining Region X Box
SPARC: Secreted Protein Acidic An Rich In Cysteine
Src: Sarcoma
SREBP1: Sterol Regulatory Element-Binding Protein-1
STAT: Signal Transducers And Activators of Transcription
TAM: Tumor Associated Macrophage
TANs: Tumor-Associated Neutrophils
TAP1: Transporter associated with antigen processing 1
Tcl1: T-Cell Leukemia 1
TCR: T cell receptor
TGF- β : Transforming Growth Factor
Th: T-helper
Thr: Threonine
TLR: Toll-Like Receptor
TME: Tumor Microenvironment
TNF- α : Tumor Necrosis Factor Alpha
Tpl2: Tumor Progression Locus 2
Tregs: T regulatory cells
TSC1/2: Tuberous Sclerosis 1/2
TTP: Time To Progression
Tyr: Tyrosine
UKA: Upstream Kinase Analysis
UTR: UnTranslated Region
VEGF: Vascular Endothelial Growth Factor
VEGFR: Vascular Endothelial Growth Factor Receptor
VEGFR-2: VEGF Receptor 2
WDR7: WD Repeat Domain 7
WNK1: Lysine Deficient Protein Kinase 1
WNK1: Lysine deficient protein kinase 1
Wnt: Wingless -related integration site
YAP: Yes- Associated Protein
 μ M: micromolar

V. INTRODUCTION

1. Hepatocellular carcinoma

Liver cancer encompasses two major types: Hepatocellular Carcinoma (HCC) and Intrahepatic Cholangiocarcinoma (ICC), along with angiosarcoma, hemangiosarcoma and hepatoblastoma [1], see *Figure 1* & *Figure 2* for worldwide information on mortality and incidence. HCC is the most common type of liver malignancy (75–85%), and it ranks fourth among the causes of cancer-related deaths worldwide [2]. However, its global incidence differs among men and women with a 2.8:1 ratio [3]. Even though it ranks ninth in the rate of cancer incidence in women, it ranks fourth in the cancer-related deaths in women, stressing on its high mortality rate [4]. HCC generally emerges from a chronic inflammation of the hepatic environment caused by various reasons and has few treatment options.

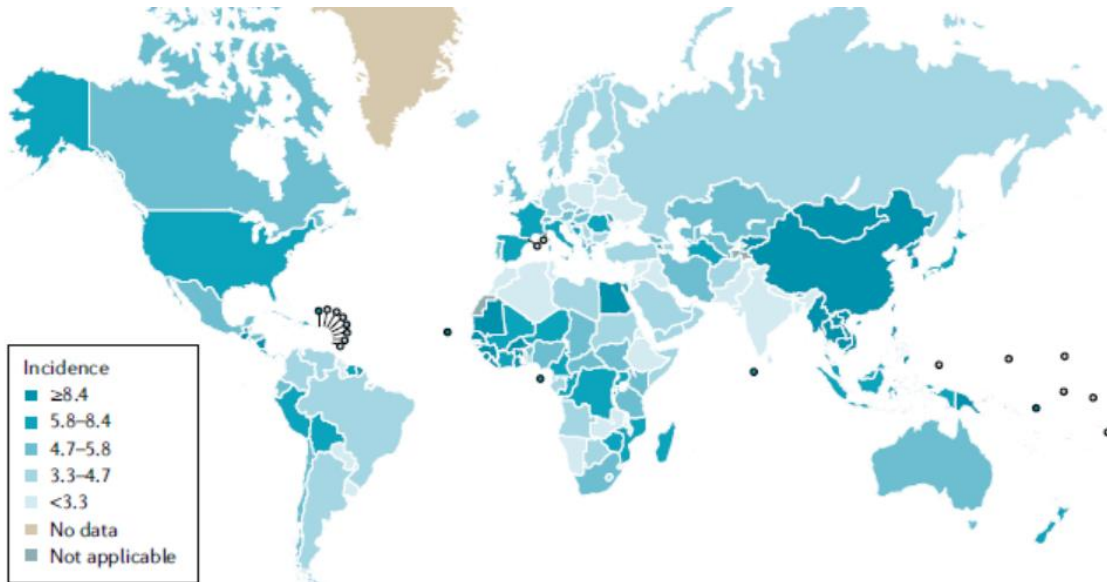


Figure 1: Global distribution of incidence of liver cancer. The incidence of liver cancer varies geographically, and is most prominent in East Asia and Sub-Saharan Africa. HCC comprises 90% of liver cancers. Numbers are per 100,000 person-year. Adapted from Yung J. et al, Nature Reviews [5].

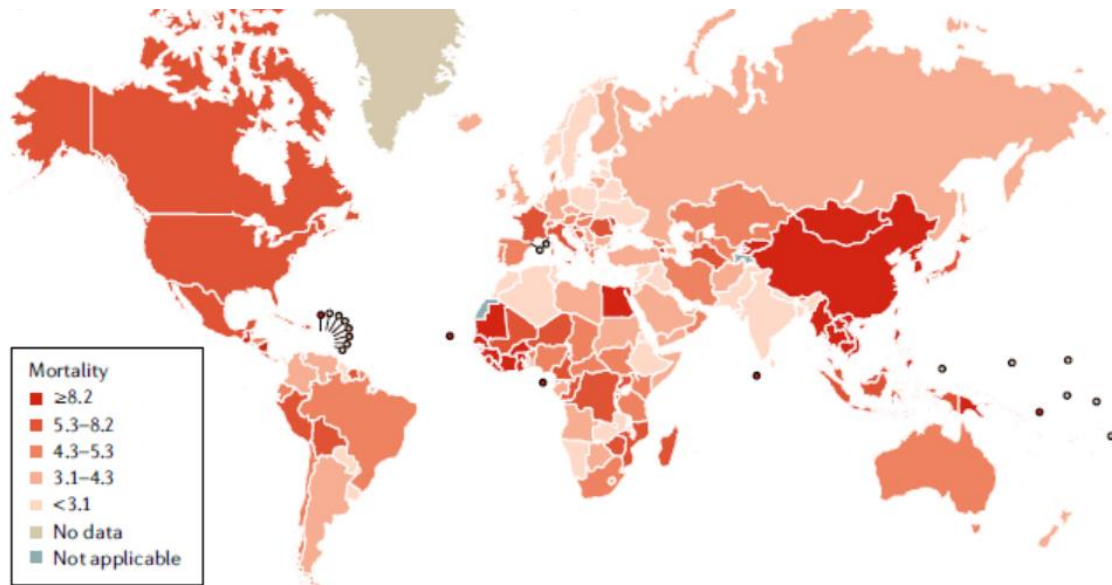


Figure 2: Global distribution mortality rate of liver cancer. The mortality rate due to liver cancer varies geographically. It is most prominent in East Asia and Sub-Saharan Africa where medical resources are scarce. Adapted from Yung J. et al, *Nature Reviews* [5].

1.1. Etiology of HCC

The complexity of HCC pathogenesis stems from the involvement of molecular failures affecting various functions of the cell (cell cycle deregulation, DNA methylation alteration, chromosomal instability, immunomodulation, Epithelial-to-Mesenchymal transition, among others...). Although the progression into HCC depends on the etiology, most of the etiologies converge into the following sequence of events: liver injury, chronic inflammation, fibrosis, cirrhosis and finally HCC [6]. Various immune responses are fired due to the liver damage to attain an inflammatory state. Damaged or necrotic cells secrete Damaged-Associated Molecular Patterns (DAMPs) whereas viruses secrete Pathogen-Associated Molecular Patterns (PAMPs). The aforementioned molecular patterns activate Pattern Recognition Receptors (PRR) like Toll-like receptor (TLR), C-type lectin Receptors, Nucleotide-binding Oligomerization Domain (NOD)-like receptors and Retinoic acid-Inducible Gene I (RIG-I)-like receptors leading to the activation immune cells [7]. Liver injury could be of viral origins, like hepatitis C and B viruses (HCV, HBV), or caused by metabolic disorders leading to Non-Alcoholic Fatty Liver Diseases (NAFLD) and Non-alcoholic Steatohepatitis (NASH). Moreover, it could be due to chronic consumption of alcohol or consumption of toxins (such as aflatoxins) and hereditary diseases such as hemochromatosis [6], see *Figure 3*.

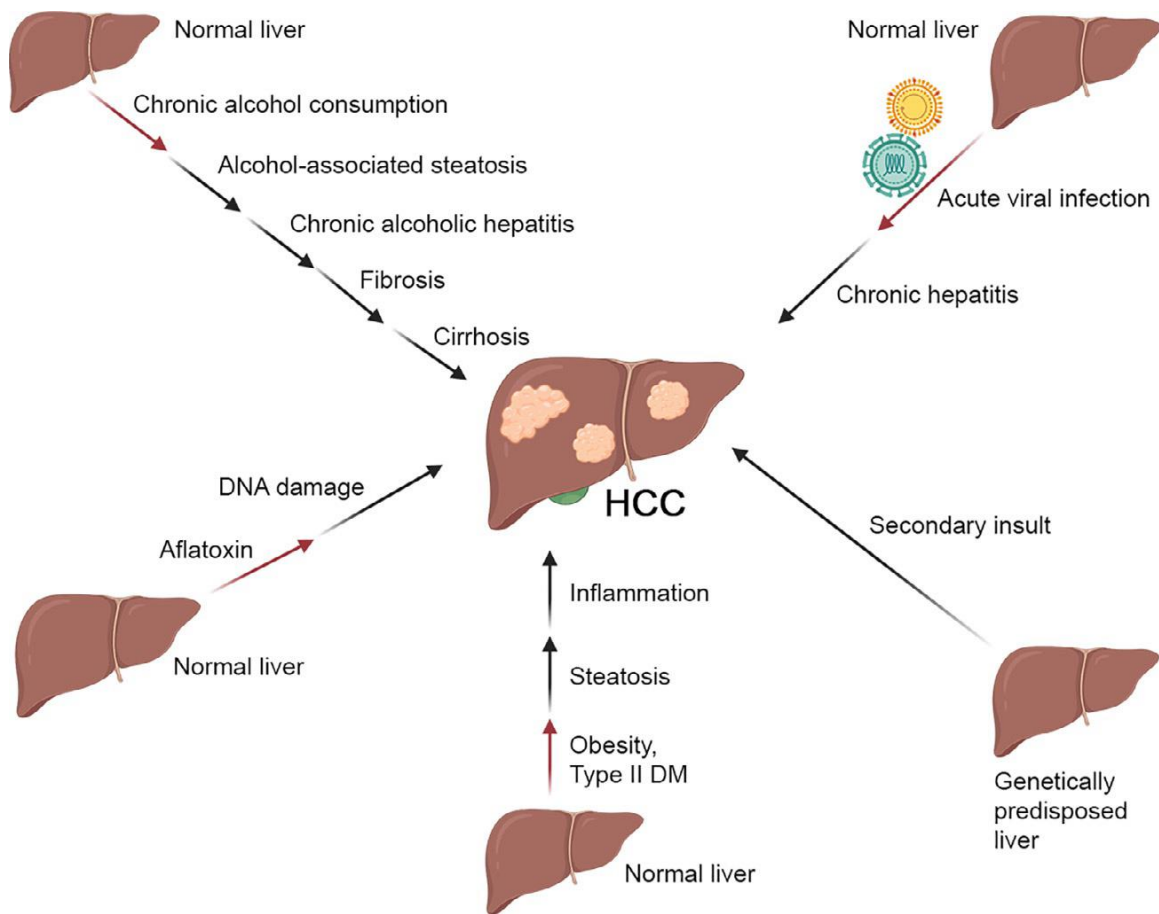


Figure 3: Etiology of HCC. Various factors drive hepatocellular carcinogenesis, among which are: chronic alcohol consumption, acute viral infection, secondary insult to a genetically predisposed liver, obesity and Type II Diabetes Meletus (DM), and aflatoxins. The liver passes through different phases, indicated above, depending on the etiologic background. Adapted from Chidambaranathan-Reghupa S. et al., *Advanced Cancer Research* [1].

1.1.1. HBV and HCC

HBV, as the name suggests, is a hepatotropic virus. It is a blood-borne pathogen possessing a 3 kb DNA genome with 4 overlapping Open Reading Frames (ORFs) [8]. Infection with HBV leads to HCC in direct and indirect ways.

On one hand, the direct ways are due to: the insertion of the viral DNA into the host DNA, causing chromosomal instability and mutations, and by the interaction of the HBV proteins with the host proteins. The oncogenesis mechanism of the integration of the HBV genome into the host's genome is dependent upon the site of integration. For instance, integration in close proximity to the human Telomerase Reverse Transcriptase (hTERT) enzyme gene leading to its reactivation and granting the cells a death evasion mechanism cell proliferation gene, cell cycle genes or metabolism genes could grant the cells malignant

properties [9]. Also, the interaction of HBV proteins like HBx with various anti-apoptotic pathways to counteract the apoptotic signals of the cells favoring survival. Among these pathways: p53 [10], Phosphatidyl inositol 3-Kinase (PI3K)/Akt/Bad pathway [11], p38/mitogen-activated protein kinase (MAPK) [12] or Wnt/ β -catenin pathway [13].

On the other hand, the indirect ways can be summarized by establishing a chronic inflammatory environment and oxidative stress thus resulting in the accumulation of genetic and epigenetic modifications along with chronic hepatitis, fibrosis, and finally cirrhosis. The chronic stage of the infection is defined as a persistence of the HBs Antigen (Ag) in the patient's blood for over 6 months [14]. Combating HBV infection is done by the efforts of both the innate and the adaptive immunity. The formerly mentioned response is dampened due to the quiescent state of the HBV during the first weeks of infection. Furthermore, the later plays a major role in the clearance, a process attributed to the T-cells activation against specific HBV antigens. However, there *seems* to be an improper maturation of memory T-cells that hinders the proper immune response. Thus, favoring a chronic inflammatory background which creates a niche for HCC [15].

1.1.2. HCV and HCC

HCV is a hepatotropic virus, which displays a genetic polymorphism. It possesses 7 genotypes with several subtypes. When compared to the other genotypes, HCV genotypes 1 and 3 have an 80% higher incidence rate of HCC [16]. Patients with genotype 1 *seem* to have a specific oncogenic mechanism, while sometimes surpassing the cirrhotic stage [17], whereas patients infected by genotype 3 have a risk of end-stage liver disease with a high HCC incidence rate even after the clearance of the virus [18]. The mechanism through which HCV induces HCC is similar to that of HBV only in the indirect approach stated earlier. Aside from the effects on the metabolism, proliferation and survival, oxidative stress and genomic instability and angiogenesis, HCV has been shown to affect the complement system; inhibiting the complement components leading to the dampening of the immune response, paving the way for cell growth ability [19]. On that note, people co-infected with HIV and HCV show a higher incidence of HCC [20].

To state a few examples of the ways chronic HCV infection favors HCC; on the metabolic level HCV has been shown to affect glucose and lipid metabolism [21].

HCV leads to insulin resistance and accumulation of glucose affecting the Akt/mammalian target of rapamycin (mTOR pathway). Moreover, the steatosis state of the liver driven by HCV has been shown to be due to an increased synthesis of lipids, a decreased lipogenesis and disrupted lipid transportation. HCV upregulates the expression of the enzyme responsible for *de novo* lipid synthesis (fatty acid synthase) while decreasing the expression of Peroxisome Proliferator-Activated Receptor (PPAR)- α/γ which in turn plays a major role in the transportation of lipids [22-24]. Concerning the cell proliferation, HCV tends to fire up the signaling cascades leading to an increase in the proliferation and survival of hepatocyte cells [25]. Due to the chronic HCV infection, the inflammatory response triggers hepatocarcinogenesis, indirectly, by acting on various pathways including DNA repair, apoptosis, and ROS production, among others [26, 27]. The degree of inflammation directly correlated with HCV infection induces changes in the liver morphology and promotes the sequential events of fibrosis, cirrhosis and finally HCC [28].

1.1.3. Alcohol and HCC

In the language of numbers, 30% of HCC cases come from the background of Alcohol-related Liver Diseases (ALD) including those co-existing with other risk factors. The degree of ALD is directly related to the amount of alcohol consumed [29]. Alcohol abuse leads to Alcohol-associated Fatty Liver (AFL), an asymptomatic state of liver disease that is usually reversible upon the decrease in the alcohol consumption. The deposition of fat in hepatocytes due to an increase in lipogenesis and/or a decreased fatty-acid oxidation [30]. A steatotic liver favors Alcoholic Hepatitis (AH) or liver inflammation, thus favoring HCC. Alcohol dehydrogenase (ADH) and Aldehyde Dehydrogenase (ALDH) enzymes are responsible for the processing of alcohol in the liver. Polymorphisms of ADH and ALDH genes lead in some cases to the accumulation of acetaldehydes which tend to interact with DNA and/or proteins forming adducts that deregulate their functions and/or lead to the induction of immune responses [31]. In fact, alcohol metabolites disrupt the barrier between the gut and the liver leading to the infiltration of bacteria (Lipopolysaccharide (LPS)) which in small amount can be cleared by the liver harmless however with a higher infiltration rate, leads to the activation of resident macrophages and migratory monocytes leading to inflammation [32]. AH is also reversible once alcohol intake is stopped. On the

other hand, chronic alcohol hepatitis leads to fibrosis and cirrhosis and finally, HCC.

1.1.4. NAFLD and HCC

NAFLD comprises 25% of liver injury cases and is associated to several risk factors such as obesity and diabetes. Moreover 20% of patients suffering from NAFLD manifest the advanced stage of the disease: NASH among which 2.6% further advance into HCC [33].

The literature diverges when it comes to the etiology of NAFLD into NASH. Firstly, the two-hit hypothesis proposes the simple accumulation of fat in the hepatocytes, and is followed by a mounted immune response leading to NASH, cirrhosis and then HCC. Secondly, the multi-hit hypothesis, is similar to the former but with the addition of genetic and environmental factors.; accumulation of fat in the liver cells in this scenario can be due to increase lipolysis of visceral adipose tissue and its import to the liver, excess *de novo* lipogenesis (DNL), or high-fat diet consumption. As a result, the cells experience an organelle-damage, leading to cell injury and death, an increased reactive oxygen species (ROS) production, supporting inflammatory signals, and a direct activation of hepatocyte TLR4, further supporting an inflammatory reaction. The previous events are all added up into the classical sequence of events – fibrosis, cirrhosis and finally HCC [34, 35].

1.1.5. Aflatoxins and HCC

Aflatoxins are mycotoxins produced by fungal species and are known to be hepatotoxins. Nuts and grains are the major carriers of aflatoxins, an incident that might occur upon their harvest or storage. They are known to cause acute or chronic poisoning [36]. Aflatoxins are known to result in liver failure and can be fatal. Mycotoxins, on the other hand, progresses into HCC. Metabolic processing of aflatoxin leads to the production of metabolites which form DNA adducts leading to DNA damage. In addition, it is capable of causing chromosomal alteration and chromosomal strand breaking in human cells [37]. Aflatoxin B1 (AFB1) is the most potent aflatoxin. AFB1-related HCC is attributed to a missense mutation in the p53 gene and thus affecting differentiation and metastasis [38].

1.1.6. Genetic predisposition and HCC

Genetic factors often play a role in the etiology of HCC. An array of genetic predispositions, when added to other factors, have been shown to support the HCC initiation and progression. To name some: Alpha 1-Antitrypsin Deficiency (A1AD), Autoimmune hepatitis (AIH), Hereditary Hemochromatosis (HH), Glycogen Storage Disease (GSD), porphyria, and tyrosinemia type 1.

alpha 1-antitrypsin deficiency (A1ATD)

Alpha 1-antitrypsin inhibits the serine protease neutrophil elastase which in turn cleaves a number of connective tissue substrates. The latter plays a role in the anti-inflammatory response (blocking Tumor Necrosis Factor (TNF)- α) against tissue injury and inflammation [39]. People with A1ATD have been shown to have a higher risk of cirrhosis and HCC [40].

Autoimmune hepatitis (AIH)

As the name suggests, the disease manifests in an immune response against the host's liver cells. A variety of mutations are attributed to this disease: a mutation in the Human Leukocyte Antigen (HLA) class II DR (HLA-DR) (involved in the expression of antigens to the CD4⁺ T-cells), a mutation in the fas cell surface death receptor and TNF- α and cytotoxic T lymphocyte associated protein 4 (CTLA4) [41]. The phenomenon of "molecular mimicry" is also a player in this disease. For instance, autoantigen cytochrome P450IID6 shows a molecular similarity to HCV antigens, thus anti-Liver/Kidney microsomal antibody 1 (LKM1) antibody cross-reacts the before mentioned antigens [42]. Thus, fostering an inflammatory environment in the liver.

Hereditary Hemochromatosis (HH)

As the name suggests, HH is a genetically inherited disease characterized by the increased uptake of iron into the cells and their deposition in various organs: heart, pancreas, joints and liver. The effects of iron deposition can be summarized by: increased cell proliferation, DNA damage by increasing ROS levels, and dismantling of subcellular organelles' membranes through peroxidative damage [43]. Cirrhosis incidence in HH patients is 10-25% while that of HCC is 8-10% with a 20-fold increase in the latter's incidence in comparison to healthy people [44, 45].

Glycogen storage diseases (GSD)

The liver is the prime site of glycogen anabolism and catabolism and thus the most affected by errors occurring in this pathway. GSD forms a group of hereditary diseases affecting the glycogen pathway. There are 12 types of GSD, each with a defect in a different enzyme. The most prominent ones are types I, II, III, and IV whilst type I is the most common of them all. It is characterized by a deficiency in the glucose-6-phosphatase enzyme [46]. Numerically speaking 57% and 8% of people suffering from GSD type I develop hepatocellular adenoma and HCC respectively. Several functional consequences on the liver cells can lead to oncogenesis: autophagy impairment, mitochondrial dysfunction, metabolic reprogramming, oncogene activation and downregulation of tumor suppressors [47].

Porphyria

Porphyria is a rare genetic disease fostering a deficiency in the enzyme involved in heme biosynthesis and consequently leading to the accumulation of porphyrin and porphyrin metabolites in the cells [48]. Of great relevance is the Acute Hepatic Porphyria (AHP) type that is associated with an increases risk of HCC. However, the manifestation of HCC cannot be accomplished by AHP, alone, it requires the addition of other risk factors. However, AHP patients have been shown to have a 35-fold higher incidence rate of HCC than healthy people [49].

Tyrosinemia type1

Hereditary Tyrosinemia type 1 (HT1) is an autosomal recessive genetic disorder. It affects an enzyme, fumarylacetoacetate hydrolase, which upon its dysfunction leads to the accumulation of 4-fumarylacetoacetate (FAA) and its toxic metabolites in the liver. HT1 can be treated by medication and a specific diet regimen [50]. However, due to the lack of screening and the asymptomatic feature of the disease, HCC manifests in people having HT1 in 25-75% of the cases. This is due to: oxidative stress, inhibition of DNA repair enzymes, endoplasmic reticulum (ER) stress, Golgi complex disruption, and apoptosis resistance [51].

1.2. Treatment options of HCC

HCC faces obstacles in diagnosis and has limited therapeutic options. Patients suffering from HCC often remain asymptomatic until the disease reaches an advanced stage. This hinders its diagnosis. Alpha Fetoprotein (AFP), the most widely used biomarker for HCC surveillance and diagnosis, is ineffective in accurately detecting early HCC [52, 53]. At an early stage of the disease, HCC can be treated by surgical resection, percutaneous ablation, or liver transplantation. However, at a later stage, the therapeutic options are limited and vary according to the stage of the disease. During the last decade, the therapeutic options have been limited to Sorafenib (a multikinase inhibitor) [54, 55]. Recently, other first-line treatments such as Lenvatinib and second-line treatments such as regorafenib and Cabozantinib have been proposed for treatment. However, these drugs demonstrate no superior efficacy compared to Sorafenib [56]. In 2020, immunotherapy re-shuffled the cards with the combination Atezolizumab (an anti-Programmed Death-Ligand 1 (PDL-1) antibody) plus Bevacizumab (an anti-Vascular Endothelial Growth Factor (VEGF) antibody), that considerably increase tumor response and survival outcomes thus becoming the new first line therapy of advanced HCC [57]. Nevertheless, only a minority of HCC patients benefit from this therapy, and alternative strategies are needed to augment host immune response [58]. The treatment options are further illustrated below.

1.2.1. First-line treatments

Sorafenib

Also termed Nexavar, Sorafenib has been the first systemic treatment option to be approved for HCC treatment after 30 years of research. It showed an increased Overall Survival (OS) of Sorafenib over the placebo by approximately 3 months (10.7 vs 7.9 months). It was approved by the Food and Drug Administration (FDA) in December 2007 [59]. Mechanistically speaking, Sorafenib is a multi-tyrosine kinase inhibitor. It inhibits a variety of intracellular kinases: c-RAF, B-RAF and mutant B-RAF, along with cell surface kinases: Fms-related tyrosine kinases, vascular endothelial growth factor receptors (VEGFR)-1,2,3, and Platelet-Derived Growth Factor Receptor (PDGFR)- β [60]. The efficacy of Sorafenib as a treatment option can be inferred from the roles played by the kinases it inhibits. They play an impeccable role in the various cell signaling pathways supporting malignancy: cell proliferation, survival and apoptosis. Despite the fact that Sorafenib has been

the sole standard therapy for the last decade, it failed to dampen the development of HCC and showed relatively high levels of systemic toxicity along with the emergence of resistant tumors [61]. Hence the emergence of novel therapies is much needed.

Lenvantinib

In July 2018, the FDA approved Lenvantinib as another first-line treatment strategy against HCC. It is also a multiple-receptor tyrosine kinase inhibitor targeting VEGFR1,2,3 in addition to Fibroblast Growth Factors (FGF) and receptors: FGFR1,2,3 and 4. A comparative study between the efficiency of Lenvantinib and Sorafenib, as first-line treatments, was done. The data showed an OS non-inferior to Sorafenib (13.6 *vs* 12.3 months) however with a better progression free survival (PFS) (7.4 *vs* 3.7 months), and in the median time to progression (TTP) (8.9 *vs* 3.7 months), in the Lenvantinib group compared to the Sorafenib [62].

Atezolizumab and Bevacizumab

In May 2020, and following the advances done in the field of immunotherapy, a combination of Atezolizumab and Bevacizumab was approved by the FDA. Atezolizumab is a fully humanized, monoclonal IgG1 isotype against PDL-1; whereas Bevacizumab is a humanized antibody which binds to VEGF. The efficacy of combination of the previously mentioned antibodies as a treatment for HCC was shown by the randomized portion of phase 1b GO30140 trial with an overall response rate of 27%. Further, its superiority over Sorafenib was shown in the phase III randomized trial (IMbrave150). The data demonstrated longer median OS of 19.2 months compared with the 13.4 months for Sorafenib, and higher PFS (6.8 *vs* 4.3 months) [57].

1.2.2. Second-line treatments

Regorafenib

Also known as Stivarga, is also a multi-kinase inhibitor. It was approved by the FDA after Sorafenib in April 2017 as a second-line treatment for patients showing progression following Sorafenib treatment. Similarly, to the first-line treatments it acts by inhibiting VEGFRs 2 and 3, PDGFR and Raf kinases and thus leading to

the inhibition of tumor cell proliferation and angiogenesis. The median OS of the group treated with Regorafenib after a course of Sorafenib treatment was 10.6 months which is higher than that of the placebo group (7.8 months). However, given the structural similarity between Sorafenib and Regorafenib, possible toxic effects are expected. Indeed, Regorafenib has showed higher toxicity when compared to sorafenib and its use was restricted to patients tolerating Sorafenib treatment whilst those intolerant to Sorafenib were not considered eligible [63, 64].

Cabozantinib

In January 2019, Cabozantinib was approved by the FDA as a treatment for advanced HCC who has been treated with at least one first-line systemic treatment. It is a multi-kinase inhibitor which inhibits VEGFR2, c-Met, TIE-2 and AXL. This approval was issued following the CELESTIAL study which revealed a better OS in the group treated with Cabozantinib *vs* the group treated with placebo (10.2 *vs* 8.0 months) in HCC patients that are refractory/intolerant to Sorafenib treatment, regardless the duration of the treatment, along with a better PFS. Unfortunately, Cabozantinib showed serious side effects, the most common being palmar-plantar erythridysesthia (17%), hypertension (16%) and increased aspartate aminotransferase level (12%) [65].

Nivolumab

In September 2017, Nivolumab a fully human immunoglobulin-G4 (IgG4) neutralizing Programmed cell Death protein (PD)-1 and thus inhibiting its binding to its corresponding receptors Programmed Death Lingand-1 (PD-L1) and PD-L2 was approved by the FDA. This was after the CheckMate-040 and the CheckMate-459 studies. The CheckMate-040 study, a phase I/II study, done on patient pre-treated with Sorafenib showed promising response rate of 15%, a median OS of 15 months and median PFS of 4 months. However, the CheckMate-459 study did not show a survival benefit of Nivolumab compared to Sorafenib therapy naïve patients. Thus, Nivolumab was recommended majorly as a second-line treatment and in some instances as a first-line treatment *i.e.* patients ineligible or intolerant to other first-line treatments [66].

In the context of the CheckMate-040 study, the combination of Nivolumab and Ipilimumab was studied. Its approval by the FDA came in March 2020 as a second-line treatment option. Ipilimumab is a human antibody targeting the cytotoxic T-lymphocyte associated receptor -4 (CTLA-4) which reverses its inhibitory effect on the immune response. The study compared the effect of a combined therapy of Nivolumab plus Ipilimumab *vs* a combined therapy followed by a monotherapeutic approach by Nivolumab. Data from the study showed a response rate of 32% *vs* 31%, and a median OS of 23 and 12 months, the response duration was shown to be 4.6 *vs* 30.5 months, respectively. Thus, the approved course of treatment was the second one attributed to a combined therapy followed by a monotherapy [67].

Pembrolizumab

In November 2018, Pembrolizumab was approved by the FDA as a second-line treatment for advanced HCC. It is an anti-PD-1 antibody. The approval was granted following the Keynote-244 trial for efficacy and safety, the median PFS and OS were 4.9 and 12.9 months respectively [68].

Ramucirumab

In May 2019, Ramucirumab was approved by the FDA as a second line treatment for advanced HCC showing an AFP level ≥ 400 ng/ml. It is a recombinant monoclonal antibody that acts as an antagonist for the VEGFR2. The approval came after studying the efficacy of Ramucirumab treatment with Sorafenib. At first, no statistical significance of the median OS *vs* the placebo was shown (9.6 *vs* 7.6 months). However, further statistical analysis of a subgroup having $\text{AFP} \geq 400$ ng/ml showed a significant increase in the median OS *vs* the placebo group (7.8 *vs* 4.2 months) [69].

It is worth mentioning that many therapeutic approaches are being assessed as first or second-line treatments for HCC: Avelumab (NCT03289533), Lenvatinib plus Pembrolizumab (NCT03006929), Nivolumab plus Cabozantinib (NCT01658878), among others [70].

1.3. Signaling pathways altered in HCC

Chronic liver inflammation often leads to fibrosis followed by cirrhosis and finally HCC. The changes in the liver's state throughout its evolution into being affected by HCC are accompanied by a change in the tumor microenvironment (TME), which sustains a niche favoring malignancy. The modulations in the status of TME affect an array of cells that include immune cells (resident and migratory), endothelial cells, hepatic stellate cells and others. This leads to the differentiation of cells into those that support tumor's development and progression: tumor-associated macrophages (TAMs), tumor-associated neutrophils (TANs), and cancer-associated fibroblasts (CAFs) [71]. The changes in the phenotypic and secretory profile of cells of TME result from the change in the transcriptome and/or an altered protein function in the cells accompanied by dysregulation of the complex signaling pathways in the cells. The alteration of the signaling pathways is common in HCC and is crucial for the progression of the tumor. RAS/RAF/MEK/ERK, MAPK, HGF/MET, VEGF, FGF, TGF- β , EGF, IGF, JAK/STAT, p53, Wnt/ β -catenin, and PI3K/Akt/mTOR [72] are among the altered signaling pathways.

1.3.1. RAS/RAF/MEK/ERK, MAPK pathway

Rat sarcoma virus (RAS) was among the first oncogenes described in humans [73]. The signaling pathway RAS/RAF/MEK/ERK (RAS/Rapidly Accelerated Fibrosarcoma/ Mitogen-activated ERK-activating Kinase/Extracellular signal-regulated kinase) controls various cellular processes among which are cell proliferation, angiogenesis and apoptosis. The activation of MAPK is initiated following external stimuli and the activation of receptor tyrosine kinases (RTK). G-proteins (RAS) are then recruited to the plasma membrane and are phosphorylated leading to their activation. Thereafter, sequentially, RAF, MEK, and finally ERK1 and ERK2 are phosphorylated and thus activated. Following their activation, ERK1 and ERK2 translocate into the nucleus and ensure the activation of c-Jun and c-Fos transcription factors. In HCC, an increased phosphorylation of MEK1/2 has been shown when compared to adjacent non-tumoral tissues. Moreover, there is a constitutive activation of the MAPK pathway due to the oncogenic mutations of RAS, an overexpression of the ligands and dysregulated epigenetic modification [74].

1.3.2. HGF/Met pathway

The mesenchymal-epithelial transition factor (c-Met) is a RTK having one known binding ligand: Hepatocyte growth factor (HGF). As its name implies, it plays a role in the epithelial-to-mesenchymal transition (EMT), a process very crucial in oncogenesis. In accordance with its role in the EMT, c-Met influences many cellular processes: cell proliferation, survival, motility, invasiveness [75]. Following its activation, c-Met mediates the phosphorylation of adaptor proteins (GRB2 and GAB1) [76] which consequently activate MAPK [77], PI3K [78], STAT and NFkB pathways. The deregulation in this pathway in HCC has been shown in 50% of HCC patients due to: mutations (4%), genetic amplification (24%) and overexpression (50%) [79].

1.3.3. Growth factor-associated signaling pathways

The following growth factors: VEGF, FGF, Transforming Growth Factor (TGF)- β , Epithelial Growth Factor (EGF), and Insulin-Like Growth Factor (IGF), among others, are known to play a prominent role in HCC [80]. This is attributed to their binding to their corresponding receptors on the cells leading to a cascade of activation of various signaling pathways, ultimately leading to the modulation of various cellular processes including cell proliferation, survival, metabolism, angiogenesis...

VEGF

VEGF has received a lot of attention when searching for a treatment for HCC thus most of the FDA approved drugs for HCC treatment target the VEGF receptor 2 (VEGFR2) signaling pathway. It plays an important role in the growth and migration of HCC cells [81]. It is worth mentioning that 5-7% of HCC patients show a high DNA amplification of VEGFA – a member of the VEGF family. The increase in the VEGF levels correlates with tumoral vascular invasion and a poor prognosis [82, 83].

FGF

FGF, on the other hand, and upon their binding to the FGFR has been shown to activate the RAS/RAF pathway along with the PI3K/Akt pathway. The main role

played by this pathway is wound healing and angiogenesis [84]. The correlation between the FGF with HCC has been established due to the evident increase in the expression of various FGFRs in HCC patients, and their consecutive effects: FGFR2 overexpression signifies poor clinical outcomes, FGFR4 plays a role in the cell proliferation and secretion of alpha-fetoprotein [85]. Furthermore, FGF19 and FGF4 exhibited high levels of DNA amplifications (8% of HCC patients) [82].

TGF- β

TGF- β exhibits a dual role in HCC, depending on the context, it acts a tumor promotor or a tumor suppressor. Its array of control spans various cellular processes including proliferation, apoptosis, differentiation, migration and invasion. Interestingly, its role is not restricted to that of tumor cells but surpass them into regulating the stroma and the inflammatory processes in the liver – regulating cytokine and matrix metalloprotease secretion. Upon its binding to the EGFR receptor, it fires the Small Mothers Against Decapentaplegic (SMAD) signaling pathway along with the PI3K-Akt pathway and MAPK [86]. In addition, it is associated with c-Myc-mediated HCC initiation and progression [87]. Moreover, a study showed that in a cohort of 488 HCC patients, 40% of them showed genomic alterations in the TGF- β signaling pathway [88].

EGF

EGF along with other ligands like amphiregulin, epiregulin, beta-regulin, heparin-binding EGF and epigen are among the growth factors that bind to the EGFR [89]. Interestingly, the signaling pathway activated by EGFR is cell dependent. Its overexpression has been shown in cirrhotic and HCC tissues, endothelial cells, and has been correlated with HCC recurrence [90]. Additionally, EGF has been shown to be implicated in the inflammatory background of HCC [91].

IGF

The association of IGF to its corresponding receptor IGFR has been shown to activate the PI3/Akt/mTOR and MAPK pathways. The consecutive activation of the previously mentioned signaling pathways leads to a modulation in the cell proliferation and the inhibition of apoptosis [92]. A cohort of 288 HCC patients

showed a > 20-fold overexpression of genes of the IGF family, thus asserting the role played by IGF in HCC (reducing apoptosis and favoring proliferation) [93].

1.3.4. JAK/STAT pathway

Janus kinases (JAKs) are proteins attached to the cytoplasmic domain of receptors on the surface of the cells – mainly cytokine receptors. Upon the binding between the ligand and the receptor, JAKs are activated, leading to phosphorylation events on the receptor. The docking sites created by the phosphorylation events allow the recruitment of Signal Transducers and Activators of Transcription (STATs). Upon the recruitment, STATs are further phosphorylated by JAKs. Then phosphorylated STATs dimerize and translocate to the nucleus leading to the transcription of target genes [94]. JAK/STAT pathway has been shown to regulate cell proliferation, stem cell maintenance, differentiation and immune system regulation. This pathway has been shown to be overactivated in HCC. This is mainly due to the loss and/or downregulation of the JAK/STAT inhibitors as a cohort of 80 HCC patients showed a promoter hypermethylation and loss of heterozygosity of JAK/STAT inhibitors [95]. Interestingly, the Interleukin-6(IL-6)/JAK/STAT branch of the pathway has been shown to be activated at a higher rate in steatohepatic HCC [96].

1.3.5. P53

A key event in cancer initiation and progression is the aberrations (genetic mutations and deletions) occurring in the tumor suppressor gene *TP53* encoding the P53 protein [97]. P53 stands in the center of regulating cell cycle, apoptosis, senescence, and maintenance of genetic integrity among other functions. In HCC, the various etiologies affect the *TP53* gene: 45% of patients with HBV-related HCC showed a mutation in the *TP53*, aflatoxin consumption is directly correlated with a characteristic mutation in *TP53* [98].

1.3.6. Wnt/ β -catenin

The Wingless -related integration site (Wnt)/ β -catenin pathway is divided into two branches: the canonical and the non-canonical branches, depending on the presence or absence of β -catenin upon its activation. The activation of the pathway

is characterized by the accumulation of β -catenin in the cytoplasm where it is ubiquitinated and degraded. In the absence of the fired cascade, β -catenin translocates into the nucleus where it interacts with DNA binding T-cell factor, Hypoxia-Inducible Factor 1 α (HIF1 α), Forkhead box protein O (FOXO) and Sex-determining region X box (SOX) leading to the transcription of genes related to cell proliferation and differentiation [99]. Normally, the pathway is inactive in adult differentiated cells, however, it is activated in HCC [100]. In 30% of HCC cases the β -catenin gene by itself is mutated and in 5-10% of HCC cases the regulators of β -catenin are mutated [101].

1.3.7. PI3K/Akt/mTOR pathway

The PI3K/Akt signaling pathway has been receiving a lot of attention in cancer research as it has been shown to be hyper-activated in different types of cancer. The PI3K/Akt hyper-activation appears often due to the activating mutations in the effector molecules often upstream of Akt rather than in Akt itself – except for the E17K mutation in the PH domain of Akt. The common activating mutations, *see Figure 4*, include the following[102]:

- i) a mutation hitting the catalytic subunit of PI3K rendering it constitutively active,
- ii) loss of PTEN whose role is to deactivate Akt), reported in up to 53% of HCC patients
- iii) activation mutations of RAS and growth factor receptors
- iv) gene amplification mutations of Akt and/or its effectors.

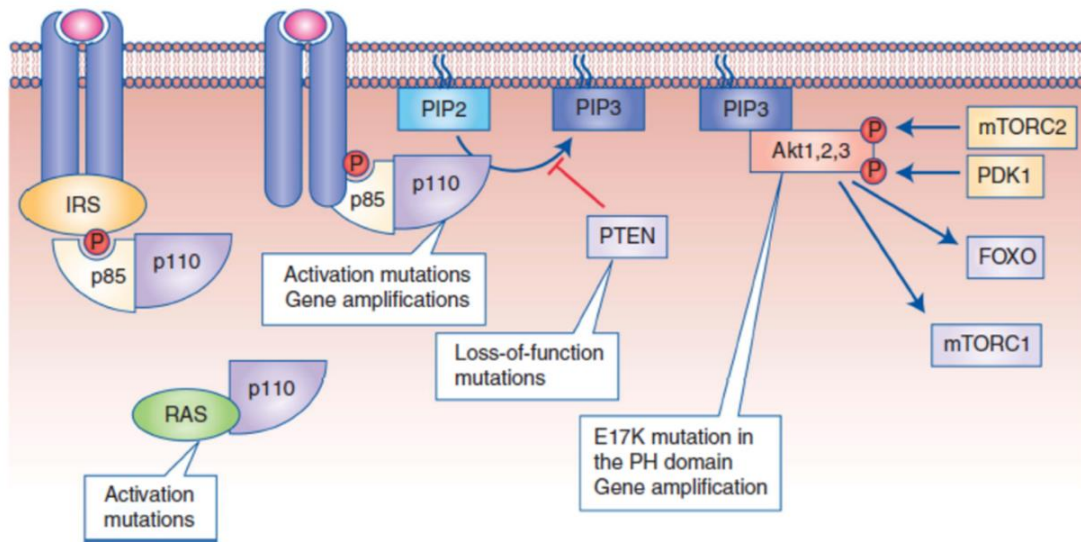


Figure 4: Aberrant activation of PI3K/Akt pathway in cancer. Driving mutations for the hyperactivation of Akt in cancer: RAS activation mutation, activation mutation of p110 subunit of PI3K, and loss of function mutation of PTEN (negative regulator of Akt). Rarely, a mutation of Akt itself: “E17K” occurs. It is a substitution of the 17th glutamine residue (E) by a Lysine (K). Adapted from Wang Q. et al, British Journal of Cancer[102].

Activation of the Akt signaling pathway is closely related to the occurrence and development of liver inflammation and fibrosis – up to 40% of early-stage HCC patients show an overactivation of PI3K/Akt/mTOR pathway [103-105] and is associated with a poor prognosis for HCC patients [106]. Importantly, a bioinformatic study analyzed 331 candidates for HCC prognostic factors among which all the three Akt isoforms were selected for further clinical validation, and the results showed a correlation between tumor aggressiveness and poor prognosis [107].

In the following section Akt will be detailed.

2. Protein Kinase B (Akt)

Akt (also known as Protein Kinase B) is a serine/threonine protein kinase family member discovered in 1991 [108]. The ~56kDa protein exists in mammals in three isoforms translated from 3 distinct genes: *Akt1* (*PKB α*), *Akt2* (*PKB β*), and *Akt3* (*PKB γ*). While the first two isoforms are constitutively expressed throughout the body – with a preference for insulin-sensitive tissues for *Akt2* – *Akt3* is said to be expressed in the brain and the testes. On the structural level, *Akt* consists of the following 3 domains: 1) the amino-terminal pleckstrin homology (PH) domain, 2)

a central domain sharing homology with other cAMP-dependent protein kinases (AGC kinases), and 3) a carboxyl-terminal domain serving as a regulatory domain, see Figure 5. These three isoforms share homologies in their catalytic domains, but they diverge in the PH and regulatory domains [109].

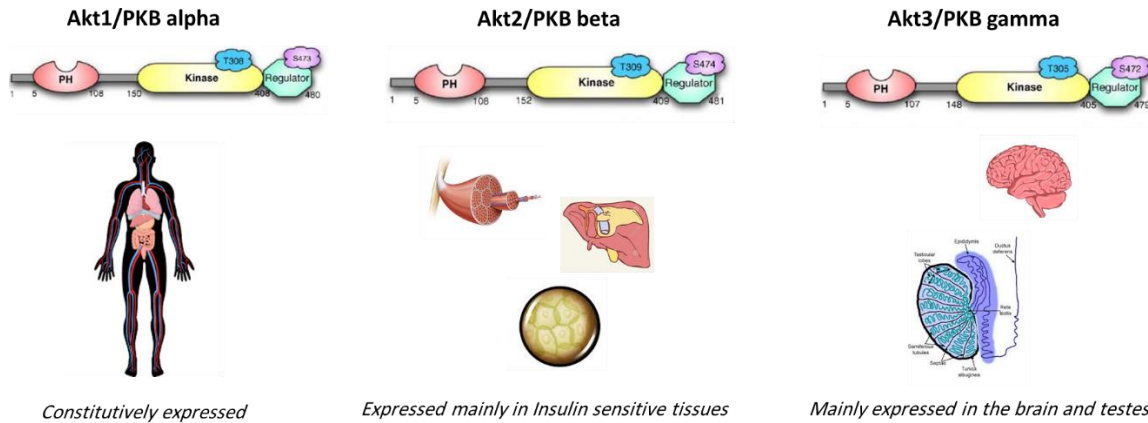


Figure 5: Isoforms of Akt. Akt has three isoforms: Akt1 (Protein kinase-B (PKB) alpha), Akt2 (Protein kinase-B (PKB) beta), and Akt3 (Protein kinase-B (PKB) gamma). They show homology in their structure (shown on the top panel of the figure), constituted of a Pleckstrin Homology (PH) domain, a kinase domain and a regulatory domain. They differ in their expression patterns: Akt1 is constitutively expressed in the human body; Akt2 is mainly expressed in insulin-sensitive tissues like muscles, pancreas and adipose tissue; Akt3 is mainly expressed in the brain and the testes.

AKT is considered as a master regulator serving as the center point in the PI3K/Akt pathway, which regulates several cellular processes encompassing cell survival, cell size/growth, survival, proliferation, glucose metabolism, transcription, protein synthesis, genome stability, and neovascularization. Thus, any disturbance in this pathway has drastic effects on the cellular homeostasis [109].

Regulation of this pathway is done at two instants: activation and inhibition. Activation of this pathway is mediated by a cascade of events exerted by the action of several proteins. One of the classical ways for the activation is through the induction of the RTKs due to their subsequent activation by external stimuli: PDGF, insulin, EGF, basic Fibroblast Growth Factor (bFGF) and IGF-1 [110]. The beforementioned induction of the RTKs leads to the activation of PIP3Ks. It is of importance to mention that the PIP3Ks are heterodimeric enzymes harboring a catalytic subunit classified into 2 classes Ia and Ib and a regulatory subunit. Class Ia of the catalytic subunit encompasses 110-kDa catalytic subunits: p110 α and p110 β , which bind to five kinds of regulatory subunits: 85 α , p55 α , p50 α , p85 β , and p55 γ . However, class Ib encompasses only the p110 γ isoform which binds only to the p101 regulatory subunit. The regulatory subunits contain either a Src

homology 2 (SH2) domains (the 5 kinds of regulatory subunits binding class Ia), or a trimeric GTP binding protein site (P101 regulatory subunit). Once PI3Ks are activated they mediate the conversion of phosphatidyl inositol 4,5-bisphosphate (PIP2) into phosphatidyl inositol-3,4,5-triphosphate (PIP3), by phosphorylating the former. The recruitment of various Akt isoforms to the plasma membrane is crucial for their activation. The PIP3 acts as a docking site. The PH domain binds to the PIP3 at the plasma membrane. In some instances, the activation of Akt surpasses the PIP3 checkpoint and can be activated by actin, heat shock protein (Hsp) 90, Hsp27, and Posh [109, 111]. Akt is prone to 2 phosphorylation events at the following threonine (Thr) and serine (Ser) residues: Thr 308 and Ser 473 for Akt1, Thr 309 and Ser 474 for Akt2, and Thr 305 and Ser 472 for Akt3. The Thr phosphorylation events are executed by phosphoinositide-dependent kinase-1 (PDK-1), whereas the Ser phosphorylation events are achieved by other kinases like the mammalian target of rapamycin complex 2 (mTORC2) and integrin-linked kinases (ILK). These two phosphorylation events are essential for Akt to attain its full function, *see Figure 6*. However, it remains functional only with the threonine phosphorylation. Recently, Tyrosine (Tyr) residues in the Akt have been shown to be prone to phosphorylation events, however these seem to be stimulus dependent. EGF mediated activation led to the phosphorylation of Tyr31 and 326 residues and IGF-1 stimulus led to the Tyr474 residue phosphorylation [112]. The inhibition of this pathway is mediated by a negative feedback loop mediated by protein phosphatase 2A (PP2A), PH domain leucine-rich-repeat-containing protein phosphatase 1/2 (PHLPP2), and phosphatase and tensin homolog (PTEN), carboxyl-terminal modulator protein, Grb10, keratin K10 and T-cell leukemia 1 (Tcl1) [113].

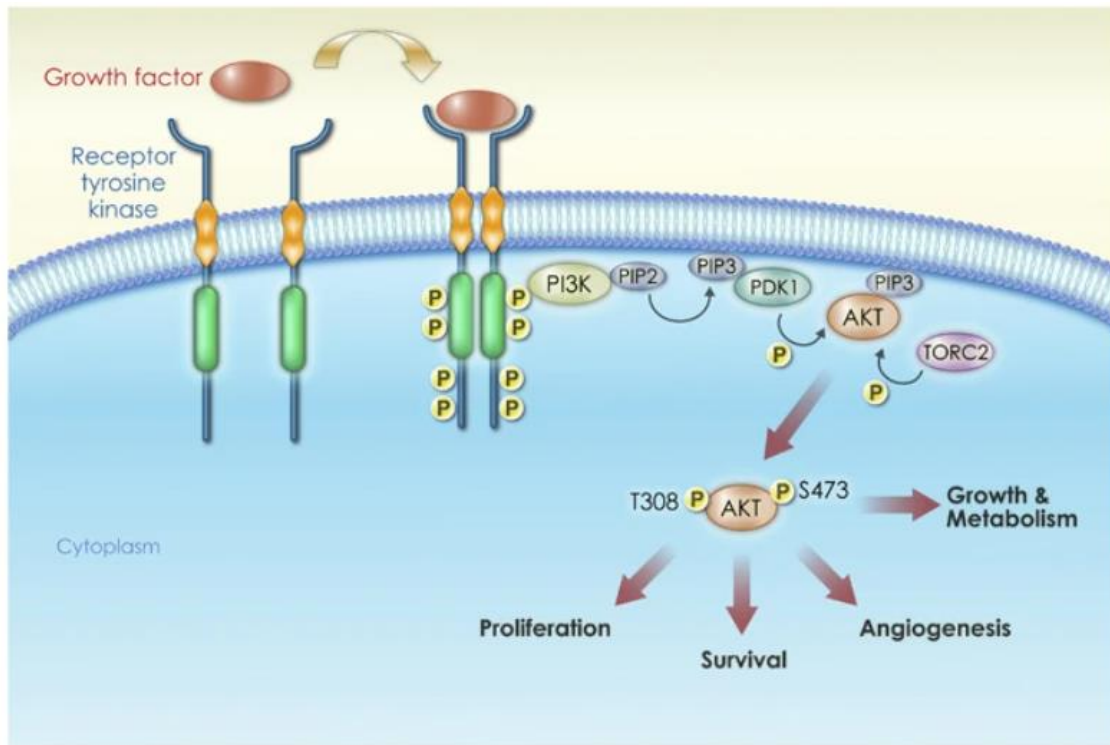


Figure 6: Activation of the PI3K/Akt pathway. Schematic representation of the common activation cascade of Akt by growth factors and receptor tyrosine kinases (RTKs). Following the binding of the growth factors to the RTK receptor, they are subject to an autophosphorylation and hence activation. Once activated, they in turn activate phosphatidylinositol 3 kinase (PI3K). Once activated it mediates the conversion of phosphatidylinositol – 4,5 bisphosphate (PIP2) into phosphatidylinositol-3,4,5-triphosphate (PIP3). The Akt is then recruited to the plasma membrane by binding to PIP3. Once there, Akt is subject to activating phosphorylations by phosphoinositide-dependent kinase-1 (PDK1), and target of rapamycin 2 (TORC2) at the Serine (S) and threonine (T) residues. Adapted from Garcia-Echeverria C. et al., *Oncogene* [114].

Various substrates are prone to phosphorylation by Akt, and are downstream effectors of this pathway to regulate the various cellular processes. Some of these that can be highlighted: proline-rich Akt substrate of 40 kDa (PRAS40), cyclin-dependent kinase (CDK) inhibitors P21 and P27, paladin and vimentin, Inhibitors of KappaB Kinase alpha (IKK α), and Tumor progression locus 2 (Tpl2). Moreover, Akt-mediated phosphorylation of tuberous sclerosis (TSC)1/2 complex and mTORC1 regulate cell growth. Survival has also been found among the cellular processes controlled by Akt through the direct inhibition of pro-apoptotic proteins like Bad or the inhibition of pro-apoptotic signals fired by the transcription factors such as FoxO1 [111]. Metabolism-related proteins like Glycogen Synthase Kinase (GSK) 3 β are also among the substrates for Akt, see Figure 7.

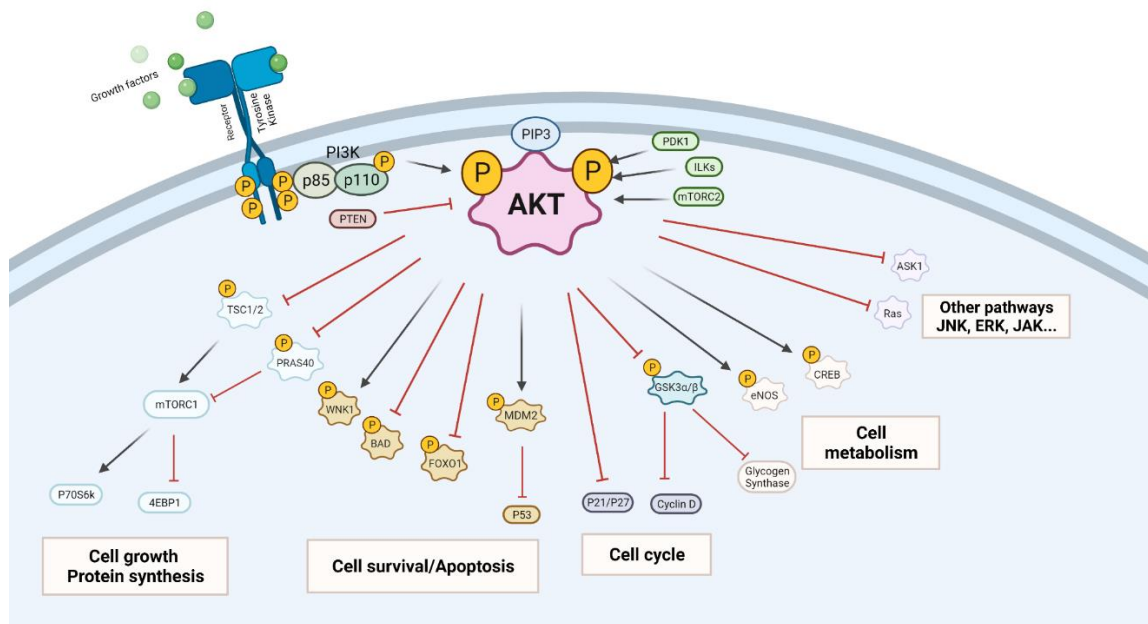


Figure 7: Overview of the PI3K/Akt pathway. Schematic representation of the Akt pathway and its downstream effector molecules. The black arrows signify an activation, the red arrows signify an inhibition. Akt pathway is implicated in the cell growth, protein synthesis, cell survival/apoptosis, cell cycle, cell metabolism, and cross-talks with other signaling pathways, either directly (by one protein intermediate) or indirectly (by one or more protein intermediates). The pathway is fired by the activation of the receptor tyrosine kinase by extracellular signals mediated by growth factors. The subsequent activation of the receptor mediates the phosphorylation and thus the activation of the Phosphatidylinositol 3 kinase (PI3K), which is made up of 2 subunits P85 and p110. The PI3K mediates the phosphorylation of phosphatidylinositol-3,4-diphosphate (PIP₂) and the production of Phosphatidylinositol-3,4,5-triphosphate (PIP₃). Once produced, it mediates the recruitment of the Akt to the cell surface where it is activated/inhibited. Protein serine/threonine kinase Phosphoinositide-Dependent Kinase-1 (PDK1), is recruited to, and activated at the cell surface and is responsible for phosphorylating and activating Akt, along with Integrin-Linked Kinase (ILK) and Mammalian Target Of Rapamycin 2 (mTORC2), among others. In contrast, Phosphatase and Tensin Homolog (PTEN) is the main negative regulator of the pathway. Phosphorylation of Tuberous Sclerosis (TSC)1/2 by Akt releases the inhibitory effect on Mammalian Target Of Rapamycin 1 (mTORC1). The latter activates p70S6K and inhibits 4E-BP1, resulting in the regulation of protein synthesis and cell growth. Phosphorylation events on the following proteins leading to their activation/inhibition mediate the regulation of the cell survival/apoptosis: Lysine Deficient Protein Kinase 1 (WNK1), BCL2-Antagonist of Cell Death (BAD), Forkhead box protein O1 (FoxO1), and P53 regulated via the activation of Murine Double Minute 2 (MDM2). The role of Akt in the regulation of cell cycle is mediated via the regulation of cell-cycle-related proteins such as P21/P27 and Cyclin D. As far as the cell metabolism is concerned, among the Akt regulated proteins are: Glycogen Synthase, endothelial Nitric Oxide Synthase (eNOS), and cAMP-Response Binding Element (CREB). It is worth mentioning that the Glycogen Synthase Kinase 3 (GSK) exerts its role in the regulation of both the cell cycle and metabolism axes. The PI3K/AKT/mTOR signaling intertwines with other signaling pathways like: c-Jun N-terminal Kinase (JNK) Extracellular Signal Regulated Kinase (ERK), and Janus Kinase (JAK), among others. This is mediated through the interaction of Akt with the Rat Sarcoma virus (RAS) and Apoptosis Signal-Regulating Kinase 1 (ASK1).

2. Protein Kinase B (Akt)

2.1. Roles of Akt1, Akt2 and Akt3 in HCC progression

The contribution of the various Akt isoforms in the progression of HCC has been explored by research carried out over the years.

2.1.1. Akt1

As far as Akt1 is concerned, a study in 2019 showed that the Akt1-mediated phosphorylation of mTORC2 is crucial for triggering hepatocarcinogenesis in humans and mice as it contributes to cellular growth through c-Myc activation [115]. Further, the altered metabolic state of the liver in HCC commonly exhibits a marked up-regulation of aldose reductase. Interestingly, aldose reductase has been shown to interact with the catalytic domain of Akt1 leading to an activation of the Akt/mTOR pathway [116]. Moreover, the TME components can lead to an activation of Akt. For instance, an *in vitro* study mimicking the augmented TME polyamine levels in HCC showed a subsequent increase in the levels of Akt1 along with those of ornithine decarboxylase, spermidine/spermine N1 acetyl transferase, hypoxia inducing factor 1 α , matrix metalloproteinase 9, VEGF, and downregulated p27. The previous fluctuations resulted in an increase in the proliferation and the migration of HepG2 cells (HCC cell line) [117]. To further stress the role of Akt1 in HCC progression, a study demonstrated that the overexpression of myristylated Akt1 – and thus constitutively active Akt1 – led to a liver tumor development in mice, and its combination with S-phase kinase-associated protein overexpression exacerbated the phenotype [118]. Interestingly a real-time imaging study of Akt1 in HCC cells demonstrated that the nuclear translocation of Akt1 is independent of the phosphorylation events at the Thr308 and Ser473 [119]. In contrast, a study showed that a decrease in β -catenin levels in the HepG2 cell line showed no change in the Akt1 expression level, while it decreased the phosphorylation and consequently decreased cell growth. This stresses the cross-communication between the different signaling pathways activated by the signals from TME, which converge onto the Akt1 activity and its effect on HCC progression [120].

2.1.2. Akt2

Akt2 has also been shown to be a contributor to HCC progression, and some researchers argue that its role in HCC prognosis surpasses that of Akt1. A study by Xu and colleagues detected overexpression of Akt2 in 38% of the HCC tissues of the studied cohort with a moderate or less expression of Akt1 in all the cases. The high expression of Akt2 correlated with the histopathological differentiation, portal invasion, and the number of tumor nodules, while Akt1 did not correlate with any of these clinicopathological features [121]. An *in vitro* study conducted to investigate the role of Akt2 in the proliferation and migration of HCC cells showed that Akt2 was regulated by STAT3. The ablation of STAT3 by small-interfering RNA (siRNA) led to a decrease in the phosphorylated form of Akt2 and led to a subsequent decrease in the proliferation and migration of HCC cells. Moreover, the *in vivo* transfection with siRNA against STAT3 decreased the pace of the tumor's growth, a process that was reversed by Akt2. This points to the significant role of Akt2 in the growth of the tumor [122]. Another *in vivo* study stressed the importance of Akt2 in the process of hepatic steatosis and carcinogenesis. In this study, the hydrodynamic transfection of a mutated form of PI3K subunit α alone into mouse livers led to hepatic steatosis, whereas the hydrodynamic transfection of mouse livers with a mutated form of PI3K subunit α combined with either NRASV12 or c-Met in the mouse liver led to the development of tumor nodules, which exhibited an increase in the activation of Akt/mTOR and RAS/MAPK signaling pathways. The ablation of Akt2 in mouse livers inhibited both the hepatic steatosis in the former case and tumorigenesis in the latter one [123]. Interestingly, a study of zebrafish (*Danio rerio*) showed that the induced expression of oncogenic Kras led to the development of HCC having great resemblance to the human tumors with an elevated Akt2 activation [124].

2.1.3. Akt3

Despite the previous knowledge about the focused expression of Akt3 in the testes and brain, some studies have shown the implication of Akt3 in HCC. A series of studies on micro-RNA (miRNA) profiles in HCC revealed the downregulation of miRNA-144, and miRNA-582-5p. The downregulation of the previously mentioned miRNAs resulted in a sustained expression of their downstream targets. Both the aforementioned miRNAs showed Akt3 among their targets, and

their subsequent downregulation supported tumor progression and growth. This indicates the contribution of Akt3 in HCC progression [125, 126].

2.2. Role of Akt1 and Akt2 in the modulation of the immune cells

In addition to direct anti-tumor activity, there is growing evidence that targeting the Akt pathway has an indirect anti-tumor activity that is mediated by the response of immune cells [127]. In fact, TME, which is generally immunosuppressive and metabolically stressed, can be modulated by Akt as this pathway is essential to the differentiation, maturation, and functioning of many immune cells. At present, the immunomodulation by Akt is best characterized at the level of T cells and macrophages.

2.2.1. Akt regulates the functions and fate of T cells

The regulation of the nutrient metabolism in the T cells is important for the control of their differentiation as it shapes their function and survival. Quiescent T cells require oxidative catabolic metabolism and use low amounts of nutrients. T-cell activation through T cell receptor (TCR) induces a metabolic switch to aerobic glycolysis and anabolic metabolism to sustain cell division and differentiation. Then, different subsets of activated T cells adopt fine-tuning of metabolism homeostasis according to their functions and fate [128]. For example, the glycolytic rates are higher in Th1, Th2, and Th17 than in the T regulatory cells (Tregs). Tregs use fatty acid oxidation for their energy demand while memory T cells use mitochondrial oxidative phosphorylation and fatty acid oxidation for their long-term persistence [129].

The PI3K-Akt pathway orchestrates the nutrient uptake and utilization within the cell. Thus, it is a key pathway to regulate the functions and fate of T cells. The TCR and CD28 co-stimulation by their respective ligands is known to engage the PI3K/Akt/mTOR cascade [130]. The differentiation into effector T cells and memory T cells is achieved, in part, by asymmetric division where daughter cells contain different amounts of active mTORC1. Thus, the high levels of active mTORC1 in effector T cells increase glycolytic activity, and the low levels in memory T cells increase lipid metabolism. This event is achieved by RagC mediated translocation of mTOR to the lysosomes through a CD98 and leucine-dependent mechanism [131]. The mTOR inhibition in T cells induces tolerance

through the T cells' energy, and blocks the differentiation to effector T cells leading to the generation of FoxP3⁺, Tregs, and CD8⁺ memory T cells [132]. This is associated with the lower activation of the transactivation factors STAT4, 6, and 3 in response to IL12, 4, and 6 stimulations. Interestingly, the Akt-dependent induction of mTORC1 activity in the T cells does not require mTORC2 for their differentiation into T-helper (Th)1 and Th17. Which is not the case with hepatocytes and the T cell differentiation into Th2 which require functional mTORC2 [133]. TCR can induce the mTOR activation through upstream PI3K/Akt activation, which is the signaling that is enhanced by costimulatory receptors (e.g., CD28) [130], see Figure 8.

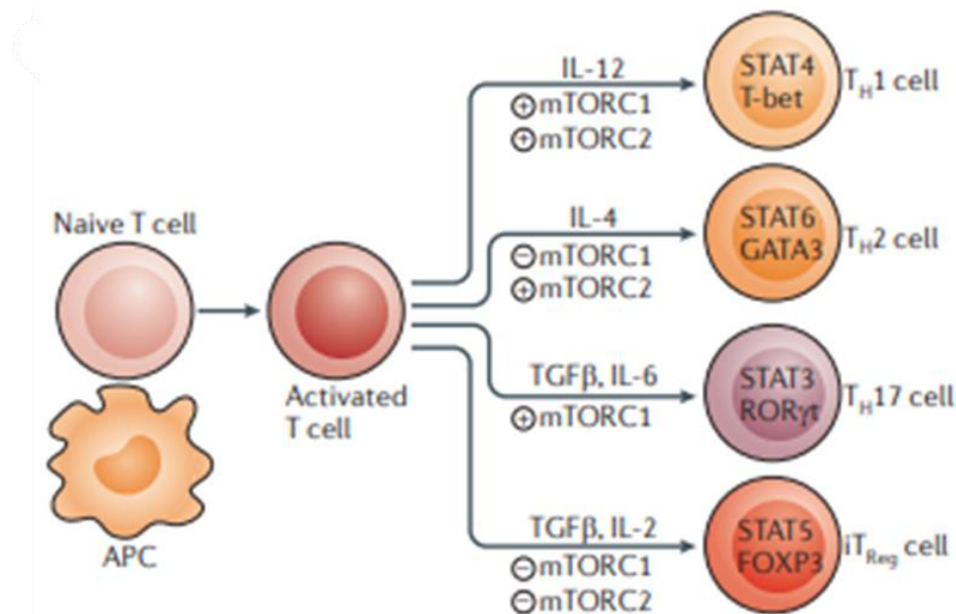


Figure 8: Role of PI3/Akt in the fate of T-cells. The fate of T-cells upon their activation by antigen presenting cells (APCs) and the applied stimuli is mediated by the state of the mammalian target of rapamycin (mTORC)1/2 regulated by the PI3/Akt pathway. IL: interleukin; Th: helper T-cell; Treg: regulatory T-cell. Adapted from Chi H. et al., *Nature Reviews Immunology* [134]

CTLA-4 and PD-1 can antagonize the mTOR activity via Akt and PI3K inhibition. Indeed, the CTLA-4 mediated inhibition of Akt is dependent on PP2A. The PD-1-induced Akt inhibition involves a blockade of the CD28 cytoplasmic tail function (probably through SHP1/2), thus, preventing the synthesis of PI3P by PI3K. In addition, the PD-1-induced PI3K/Akt pathway inhibition is more potent to block T cell differentiation than the CTLA-4-induced PI3K/Akt inhibition [135]. Notably, the PI3K/Akt/mTOR pathway also regulates lymphocyte trafficking through the modulation of CD62L and CCR-7 expression [136].

Regarding the Akt isoform dichotomization in T cell activation, recent publications suggest a divergence in Akt1, 2, or 3 functions. The Akt1 isoform downregulates proliferation of the thymus-derived Tregs, thus, facilitating Ag-specific Th1/Th17 responses. On the other hand, Akt2 increases the proliferation of Tregs and suppresses the Ag-specific Th1/Th17 responses. Furthermore, the treatment with a specific Akt1 inhibitor suppresses disease progression in a mouse model of autoimmune encephalomyelitis [137]. The Akt3 signaling in T cells, and not in neurons, is necessary for maintaining the central nervous system's integrity during an inflammatory demyelinating disease (*in vivo* model of myelin-oligodendrocyte glycoprotein-induced experimental autoimmune encephalomyelitis) [138]. Clearly, further studies are needed to clarify the role of each Akt isoform in the T cell activation process and antitumor activity.

In conclusion, the Akt pathway is at the epicenter of the T cell activation/differentiation process. This needs to be taken into consideration while choosing the therapeutic targeting of this pathway.

2.2.2. Akt plays a role in macrophage polarization

Macrophages are a heterogeneous population of cells arising from the myeloid lineage and are involved in innate immunity.[139] The roles of these cells during pathogen encounters are broad, and they encompass antigen processing, presentation, orchestration of inflammatory response, clearance, and repair. A dichotomy between “classically activated macrophages” and “alternatively activated macrophages” depending on different stimuli has been described and led to the emergence of an “M1” versus “M2” terminology. As simple as this classification sounds, in reality, such clear division was challenged by the discovery of TAMs that do not fit in the classification system for which different subsets of M2 macrophages (M2a, M2b, M2c, and M2d) were brought into the spotlight in accordance with their transcription profiles and responses to the different stimuli. Importantly, the presence of TAMs is generally associated with a poor prognosis in solid tumors [140].

The different polarization states of the macrophages result in different modes of action according to the tissue environment based on the signals that they receive from the surrounding cells. M1 macrophages exhibit a pro-inflammatory function along with a microbicide activity and resistance to pathogens. M2 macrophages

predominantly mount an anti-inflammatory response, parasite control, tissue remodeling, and immune modulation. The macrophage polarization fate is dictated by the regulation of cytokine production, phagocytosis, autophagy, apoptosis, and metabolism. All of these pathways seemed to have Akt as the converging node. In fact, signaling cascades controlled by PI3K-Akt largely contributed to macrophage polarization [141], see Figure 9.

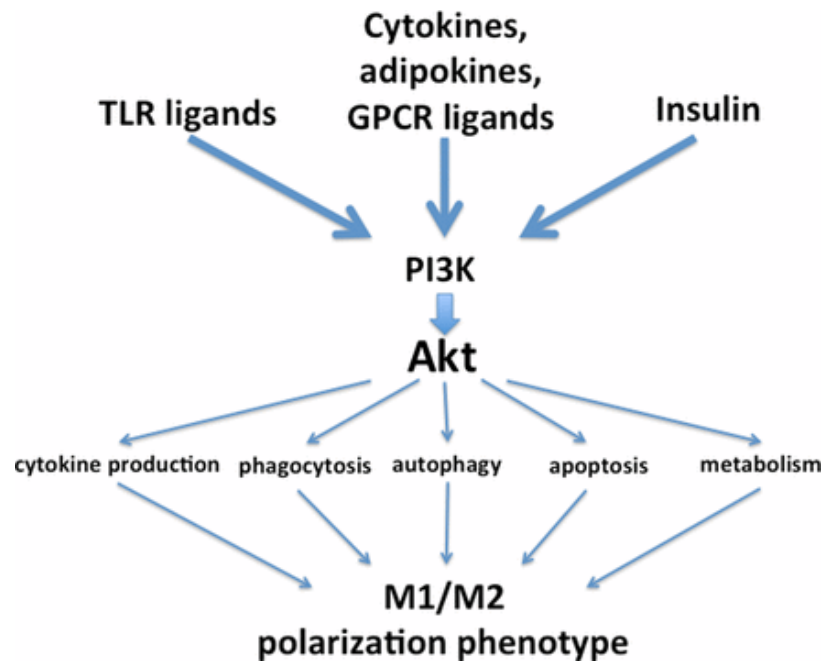


Figure 9: Role of PI3K/Akt in the fate of macrophages. Schematic representation of the converging node of the PI3k/Akt pathway in the regulation of the polarization state of macrophages into M1 and M2. Such a fate decision is mediated through the Akt pathway control of the various processes of: cytokine production, phagocytosis, autophagy, apoptosis, and metabolism. Adapted from Vergadi E. et al., *The Journal of Immunology* [141].

The PI3K/Akt pathway plays a key role in the increase of anti-inflammatory markers such as arginase-1 (Arg1) and IL-10 and inhibition of the production of pro-inflammatory cytokines [142, 143]. It has been described that activation of the PI3K-Akt pathway results in increased polarization of M2 macrophages [141], and BMP7 and SMAD 1/5/8 might play a major role in these events [144]. Expectedly, published data also suggest that the inhibition of either PI3K or mTOR results in M1 macrophage polarization [145, 146]. For example, rapamycin treatment has been found to promote M1 polarization [147]. Nevertheless, the Akt pathway can also be triggered in macrophages by TLR4 activation [148], activating downstream NFκB [149], and mTORC1 [150] which are responsible for the transcription of M1 genes.

While differences in the PI3K/Akt pathway involvement upon macrophage activation might arise from distinct tissue environments or macrophage origins between studies, the differences in the Akt isoforms (Akt 1, 2, or 3) play an important role in this matter [141]. Double and triple knockout studies support evidence that each Akt isoform possesses non-overlapping functions. Indeed, in a study using dextran sodium sulfate-induced colitis, the genetic ablation of Akt1 isoform exacerbated the disease; however, the ablation of Akt2 in these mice protected them. This difference was due to the M1 profile and M2 profile in these two cases respectively [151]. Moreover, studies have shown that knocking down of the Akt1 expression promotes the upregulation of Induced Nitric Oxide Synthase (iNOS) and IL-12 β (M1 activation) and suppresses TLR4-induced M1 macrophage activation. In contrast, as reviewed previously, the knockout of Akt2 resulted in an M2 phenotype along with elevated M2 markers (Arg1, Ym1, and Found in inflammatory zone protein-1 (Fizz1)), endotoxin tolerance, and elevated levels of IL10 [141].

Still, the importance of the subcellular localization of Akt isoforms in macrophages has been poorly documented, and a further level of complexity exists based on the acute *vs* chronic activation of Akt that remains to be tested in terms of macrophage fate.

In conclusion, activation of macrophages is highly dependent on the Akt pathway, but the full picture of Akt involvement in macrophage polarization remains to be completed, especially concerning the role of each Akt isoform in TME of HCC.

2.2.3. Akt modulates other cells in the tumor microenvironment

Neutrophils present in the tumor, termed as Tumor-associated neutrophils (TANs), are major players in the TME of HCC. They recruit both macrophages and Tregs to promote the progression of HCC [152]. Akt signaling cascade is involved in migration, degranulation, and oxygen production, and the Akt2 isoform has a predominant role in regulating neutrophil functions [153].

Besides, mast cells modulate the immune response and mediate angiogenesis. It has been demonstrated that the recruitment of mast cells increases angiogenesis by PI3K-Akt-Glycogen Synthase Kinase (GSK3) β -AM signaling, which can be reversed by Akt inhibition [154].

2.3. Targeting Akt in the management of HCC.

As the search for therapies for HCC continues, several researchers are trying to pinpoint specific effector proteins that could be targeted. Akt (also known as Protein Kinase B) is showing growing interest as a therapeutic target for HCC, *see Figure 10*. The Akt inhibitors that are capable of inhibiting the PI3K/Akt/mTOR pathway have been tested as an anti-tumor treatment in several preclinical studies and early clinical phase trials, mostly in the case of gynecologic and prostate cancers, but the data from preclinical and clinical studies are also available in HCC. (As summarized in *Table 1*).

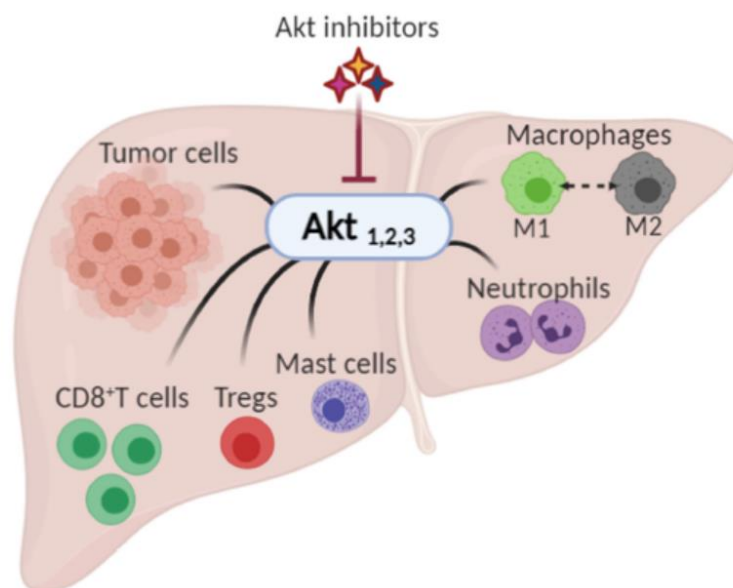


Figure 10: Possible impact of chemical Akt inhibition on HCC and its TME . Schematic representation of the targets of chemical inhibition of Akt which encompass the tumor cells as well as tumor microenvironment (TME) constituents, namely, CD8⁺ T-cells, regulatory T-cells (T-regs), mast cells, neutrophils and macrophages. Adapted from Mroweh M. et al., *International Journal of Molecular Sciences* [70].

Classical ATP-competitive Akt inhibitors such as Ipatasertib (GDC-0068) and Capivasertib (AZD5363) are currently in phase-I and phase-II clinical trials for mono- or combination-therapies. However, because the ATP-binding pocket of Akt is highly conserved among kinases, the selectivity of these inhibitors is limited, and their use is associated with side effects during treatment and lack of efficacy. The efforts to identify more specific and selective small molecules have resulted in the development of allosteric inhibitors such as MK-2206, ARQ092, and ARQ751 [155, 156].

Table 1: Akt inhibitors in the management of HCC

Inhibitor	Mechanism of action	Experiment setup	Antitumor effect	Effect on TME	Clinical trial
GDC-0068 [157-159]	ATP competitive AKT inhibitor	Combination of GDC-0068 with sorafenib in HepG2 and Huh7 sorafenib-resistant cell-lines	- synergistic antitumor effect - promotion of apoptosis - induction of autophagic cell death	Not investigated	Phase I/II including multiple solid tumors treated by GDC-0068 in monotherapy or in association with abiraterone + prednisolone: safe and tolerable in monotherapy or in combination
AZD5363 [160, 161]	ATP competitive AKT inhibitor	Single agent in Hep-G2 and Huh-7 HCC cells Combination with FH535 (β -catenin inhibitor) in THH, Hep3B and HepG2	- inhibition of tumor proliferation - induction of cell-cycle arrest - promotion of apoptosis - promotion of autophagy through p53 activation	Not investigated	Phase I, AZD5363 in monotherapy, in multiple advanced solid tumors including liver cancer (NCT01895946): safe and tolerable, no data on antitumor response Phase I including multiple solid tumors harboring AKT mutations (NCT02465060)
ARQ092 [162, 163]	allosteric pan-AKT inhibitor	Single agent and in combination with sorafenib in a DEN-induced cirrhotic rat model of HCC and in Hep3B, HepG2, Huh-7, PLC/PRF, and	- inhibition of tumor proliferation - promotion of apoptosis - synergistic antitumor effect when	- anti-angiogenic effect, - improved liver fibrosis - decrease of intrahepatic neutrophils	No clinical trial

		HR4 HCC cell lines	combined with sorafenib	and macrophages	
ARQ 751 [164]	allosteric pan-AKT inhibitor	Single agent and in combination with sorafenib in DEN-induced cirrhotic rat model of HCC	- inhibition of tumor proliferation - synergistic antitumor effect when combined with sorafenib	- Improved liver fibrosis	Phase Ib (NCT02761694) in solid tumors with PIK3CA/AKT/PTEN mutations including HCC: ongoing
MK-2206 [165, 166]	allosteric pan-AKT inhibitor	Single agent in Human Huh7, Hep3B, and HepG2 HCC cell lines	- Promotion of apoptosis - Inhibition of cell proliferation - Induction of cell cycle arrest	Not investigated	Phase II trial, MK-2206 in monotherapy in advanced HCC previously treated (NCT01239355) : discontinued due to discouraging results

First, an ATP-competitive Akt inhibitor GDC-0068 showed promising antitumor activity ranging from tumor growth delay to regression in multiple tumor xenograft models as a single agent to the potentialized antitumor activity of classic chemotherapeutic agents [157]. A high basal level of phospho-Akt, PTEN loss, and PIK3CA kinase domain mutations were predictive of a better response to GDC-0068 [157]. More specifically, in an *in vitro* model of Sorafenib-resistant HCC cells, the exposure to GDC-0068 combined with Sorafenib restored sensitivity to Sorafenib by switching autophagy, one of the known resistance mechanisms, from a cytoprotective role to a death-promoting mechanism. This association induced a synergistic antitumor effect suggesting, at the time, that GDC-0068 represents a good candidate for further clinical trials in combination with Sorafenib [158]. In clinics, to this day, GDC-0068 was tested in a phase-1 basket trial with multiple solid tumors including only one HCC patient without any further study carried out in this pathology [159]. This compound is currently mostly studied in prostate and breast cancers in combination with other anticancer agents.

AZD5363, also known as Capivasertib, is another Akt inhibitor that binds to and inhibits all Akt isoforms. In a large number of cancer cell lines, it has been shown to decrease FOXO3a phosphorylation through Akt inhibition leading to FOXO3a translocation to the nucleus where it can “switch on” the expression of genes, such as p27, FasL, and BIM by inducing cell-cycle arrest and promoting apoptosis [167]. Moreover, AZD5363, suppresses the proliferation of human HCC cell lines, HepG2 and Huh-7, by inhibiting the phosphorylation of downstream molecules in the Akt signal pathway in a dose- and time-dependent manner [160]. AZD5363 was studied in combination with the β -catenin inhibitor (FH535) *in vitro*. This combination induced a stronger effect on cell death and displayed antiproliferative effects on transformed human hepatocytes through inhibition of cell-cycle progression, enhanced autophagy marker protein expression, and autophagy-associated death. An enhanced p53 expression was also observed due to modulation of murine double minute 2 (MDM2) activation, and it led to cell proliferation inhibition and promotion of autophagy. The importance of p53 was confirmed on Hep3B cells, which do not express p53. While the combination did not induce a significant autophagy-dependent death on wild-type cells, and this was reversed after transfection with the wild-type p53 gene. These promising results suggest that inhibiting both Akt and β -catenin pathways may represent a new therapeutic way of treating HCC that would, however, require further preclinical and clinical investigations [168]. AZD5363 was tested in a phase-I trial in multiple advanced solid tumors including HCC, and it showed acceptable safety and tolerability profiles [161]. Moreover, it is still under investigation in a large phase-1 study, the MATCH screening trial, that includes multiple solid tumors harboring druggable mutations including Akt mutations (NCT02465060).

ARQ092 (also named Miransertib) is a small allosteric pan-Akt inhibitor that showed interesting results in a diethylnitrosamine- (DEN) induced rat model of HCC developing on cirrhosis, which was assessed by MRI. The ARQ092 treatment induced downregulation of the mTOR pathway with a decrease in the active phosphorylated form of Akt and its downstream actors. ARQ092 improved the tumor response, normalized the vascularization, and significantly decreased the fibrosis of the surrounding liver [162]. A combination of ARQ092 with Sorafenib synergistically decreased the tumor progression with the promotion of apoptosis and reduction of tumor proliferation and angiogenesis [163], and similar effects were observed when ARQ 751, a next-generation allosteric pan-Akt inhibitor, was used [164]. ARQ 751 is now tested in clinics, in a phase-1b basket trial, as a single

agent or in combination with other anticancer drugs in the case of solid tumors with PIK3CA/Akt/PTEN mutations including HCC (NCT02761694).

MK-2206, another allosteric Akt inhibitor, that has been studied *in vitro* and *in vivo* in many cancers has shown interesting *in vitro* activity resulting in cell-cycle arrest, inhibition of cancer cell proliferation, and promotion of apoptosis in human HCC cell lines [165]. It was, later, studied in a phase-2 trial including patients with advanced HCC that was previously treated but was prematurely arrested due to discouraging results (NCT01239355). Another phase-2 trial in the case of advanced biliary cancer was also stopped after 8 inclusions due to the absence of clinical efficacy as a single agent but with an acceptable safety profile (NCT01425879) [166]. Further trials may be needed on this front in combination with other targeted therapies.

The data concerning Akt inhibitors in HCC are still preliminary and future clinical development may have to involve combinations with other targeted therapies such as β -catenin inhibitor or immune checkpoint inhibitors to improve the care of HCC patients.

2.3.1. The impact of Akt inhibition

Although the Akt inhibitors have been intensively studied during the past decade in the context of cancer, their effect on TME has received less attention until very recently. Interestingly, recent studies suggest that apart from their direct anti-tumor activity, the Akt inhibitors have the capacity to modulate TME and switch it from pro-tumoral to anti-tumoral. The inhibition by AZD8835 in pre-clinical mouse tumor models directly increased CD8⁺ T-cell activation, while Tregs, macrophages, and myeloid-derived suppressor cells were strongly suppressed [169]. Similarly, in several different tumor-bearing mice, the Akt pathway inhibitor, MK-2206, caused the selective depletion of suppressive Tregs, which was associated with enhanced cytotoxic CD8 responses [170]. The Akt inhibitor, AZD5363, was administered as an adjuvant after radiotherapy in tumor-bearing mice which was associated with marked reductions in tumor vascular density, a decrease in the influx of CD11b⁺ myeloid cells, and a failure of tumor regrowth [171]. Similarly, in the rat model of HCC, which accurately recapitulated the scenario and TME of human HCC [172], the Akt inhibition by ARQ092 was

associated with the modulations of TME mainly in the form of a decrease in the accumulation of intrahepatic neutrophils and macrophages [163].

Recent studies have also demonstrated the effect of the Akt inhibitors on TME in cancer patients. For instance, in Human Epidermal growth factor Receptor 2 (HER2) negative breast cancer patients, two oral doses of the Akt inhibitor, MK-2206, were associated with a favorable immune profile in TME including increased CD3⁺CD8⁺ density and greater expression of interferon genes [173]. However, there are no studies that assess the impact of Akt inhibition on TME in HCC patients.

Despite being widely developed for treating HCC, all these Akt kinase activity inhibitors lack specificity. To further target Akt isoform, we aim at developing more specific therapeutic candidate, using especially RNA-interference (RNAi) strategy. Indeed, the use of the RNAi strategy has been already widely explored as a treatment strategy for HCC, especially to inhibit the crosstalk between the TME and HCC.

3. RNA interference overview

The Nobel Prize in Physiology and Medicine was awarded in 2006 to RNA interference (RNAi) discoverers: Andrew Z. Fire and Craig C. Mello [174]. RNAi involves a double-stranded ribonucleic acid that interferes with a specific messenger RNA (mRNA) and prevents its translation or leads to its degradation, therefore decreasing expression levels of the corresponding protein. This mechanism censors the output of the genome and dictates the fate of a specific transcript, inhibiting its translation into the final active form, the protein. Due to the aberrant activities of a variety of proteins in cancers, RNAi introduces itself as a promising tool in cancer therapy. Moreover, as RNAi interrupts the gene of interest (and can be specific to a mutated version of a gene), mRNA, protein flow, it can modulate the secretory profile of the cells leading to disrupted crosstalk, which is empirical for the tumor progression [175].

RNAi is a regulatory mechanism involving small regulatory RNAs (belonging to non-coding RNAs (ncRNA)) that are not translated into proteins. The RNAi mechanism is one way of inducing post-transcriptional gene silencing (PTGS) and can participate as a natural process of resistance to the presence of pathogenic exogenous double-stranded RNA (dsRNA)[176]. The presence of dsRNA in the

cell is termed to be “abnormal” and is degraded by the cellular machinery upon recognition through TLR activities. dsRNAs can be of viral origin, but could also be from endogenous genes such as transposons [177]. Therefore, by mimicking this process, *i.e.*, the introduction of RNA molecules with the ability to bind to the target mRNA and thus labelling it for degradation, it is possible to control the expression of specific genes for treatment purposes. Diverse studies have shown *in vitro* the efficiency of this mechanism in numerous pathologies, specifically in inflammatory diseases as well as cancer [178, 179]. RNAi comprises three different types of RNA molecules: microRNAs (miRNA), short hairpin RNAs (shRNA) and small interfering RNAs (siRNA), *see Figure 11*.

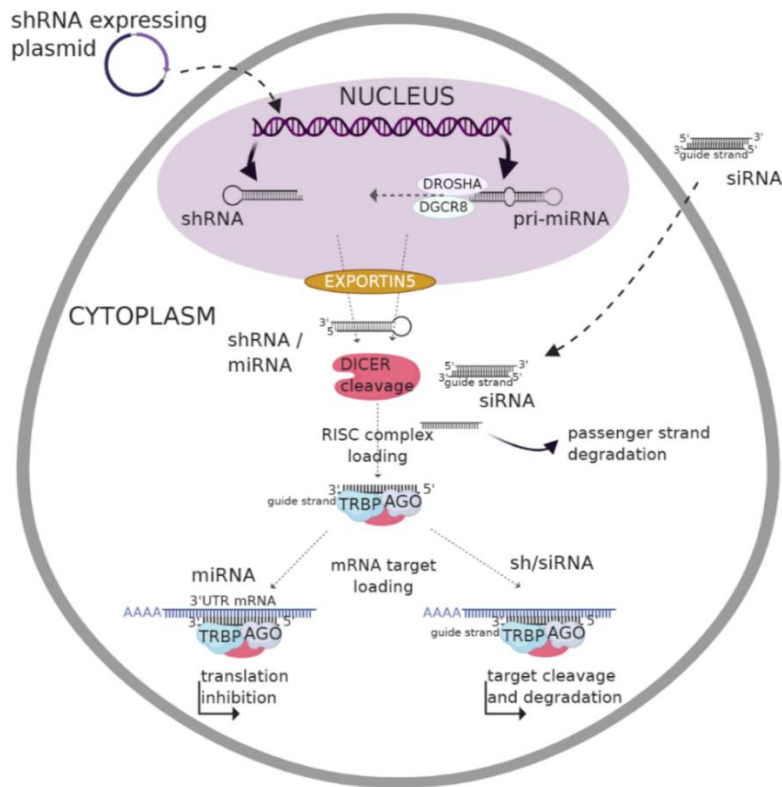


Figure 11: Scheme of three RNAi different pathways: miRNA, shRNA and siRNA. Scheme of the three different RNA interference (RNAi) pathways: micro(mi)RNA, short hairpin(sh)RNA and small interfering (si)RNA. shRNA and miRNA mediated silencing are based on a modification of the genomic content within the nucleus whereas siRNAs act directly in the cytoplasm of cells and do not require nuclear import. shRNAs and miRNAs are introduced into the cell in the form of DNA, and it is essential that they are transported into the nucleus to be transcribed into double stranded (ds)RNAs with a hairpin-like structure and are thus termed primary (pri)-shRNAs and pri-miRNAs, respectively, which are further cleaved in the nucleus by the DROSHA enzyme. The resulting transcripts are termed precursor (pre)-shRNAs and pre-miRNAs, respectively, and are exported to the cytoplasm via Exportin 5. siRNAs, on the other hand, are introduced in the form of dsRNA sequences and are not delimited by a nuclear transport step; they are cleaved by DICER enzyme to attain their final form. In the cytoplasm, the three pathways converge as they are all loaded to the RNA induced silencing (RISC) complex. After that, they diverge again in their mechanism of action to silence a target gene: a miRNA-RISC complex inhibits translation, whereas sh/siRNA-RISC complexes bind to mRNA sequences resulting in their degradation. Adapted from Mroweh M. et al, International Journal of Molecular Sciences [71].

Biogenesis and gene silencing mechanism of microRNA

MicroRNA (miRNA) is an endogenous single-stranded RNA molecule of 19–22 nucleotides (nt) derived from a double-stranded region of 60–70nt RNA hairpin precursor. The miRNA gene is usually in the form of clusters at different sites within the genome, commonly in intergenic regions and introns of protein-coding genes. Biogenesis of miRNA takes place in both the nucleus and cytoplasm. Depending on the DNA region, the miRNA gene is transcribed by either RNA polymerase II or III (generally the latter). The resulting primary miRNA (pri-miRNA) is then processed to give the precursor miRNA (pre-miRNA), which assumes a loop structure and is exported into the cytoplasm by the help of Exportin-5. Further maturation occurs in the cytosol to give a mature miRNA that binds to the target mRNA. The silencing of the target mRNA is initiated by a partial hybridization of the miRNA–RISC (microRNA–RNA-induced silencing complex) on the 3'Untranslated region (UTR) of mRNA through a base pairing [180]. The induction of miRNA, therefore, implies nucleus modification.

Biogenesis and gene silencing mechanism of shRNA

Another form of RNAi is short hairpin RNA (shRNA). These are engineered RNA sequences that can be produced within the cell from a DNA vector. The transfection of DNA that expresses shRNA into the nucleus of the target cell can be achieved by using different vectors such as lentivirus, adenovirus, plasmids, PCR amplicons or small circular DNA sequences [181] [182]. The first transcripts of shRNA known as pri-shRNA with hairpin-like structures are transcribed within the nucleus [183] and then processed to give a precursor (pre-shRNA) of 50–70nt in length, which is then exported to the cytosol through Exportin-5. After cytosolic maturation, the pre-shRNA is then cleaved to generate double-stranded fragments of 21–22nt shRNAs. Finally, the silencing mechanism is similar to that of siRNAs, as described below [184]. The strong expression of shRNA may be less beneficial as it can alter the endogenous RNAi pathway thus increasing the saturation of the miRNA pathway. Furthermore, DNA-based shRNA faces several obstacles, especially the activation of innate immune responses that can reduce cellular protein synthesis [185]. In addition to the off-targets, the lack of an efficient delivery system poses a major challenge of shRNA-based therapy [186]. Also, nonspecific binding of RNAi molecules to cellular components, such as non-targeted mRNAs, can increase the immune- and toxicity-related response.

Moreover, the use of viral vectors for delivery forces a margin of toxicity, insertional mutagenesis and immunogenicity, thus limiting their clinical application [187].

Biogenesis and gene silencing mechanism of siRNA

RNAi technology has evolved over time, with the easiest approach being delivering chemically synthesized siRNAs. Primarily siRNAs were thought to be exogenous in origin, however, several studies have identified endogenous siRNAs arising from genomic loci [188]. siRNAs have been conserved among eukaryotes and have been involved in gene expression regulation and cell proliferation [175], [189]. siRNAs are produced from a long double-stranded RNA (200–500 bp) precursor that is cleaved by Dicer via two RNase III domains. The resulting dsRNA fragments are unwound by helicase enzymes, and the antisense strand known as guide strand is associated with RISC to form siRISC. This complex is then directed to the target mRNA, and the cleavage of the latter is induced by the active site residues in the P-Element Induced Wimpy Testis (PIWI) domain of the Domain Of The Argonaute (AGO) protein [190].

3. RNA interference overview

3.1. Clinical application of RNAi

The first RNAi-based therapeutics have been introduced into clinical practice recently. Indeed, Patisiran, the first-ever therapeutic based on RNAi, was approved by the FDA in August 2018. This siRNA specifically blocks the expression of an abnormal form of the transthyretin protein in patients with hereditary transthyretin amyloidosis (ATTRh) [191]. The next-ever drug that was developed based on RNAi, Givlaari, has been approved by the FDA in November 2019 for the treatment of acute hepatic porphyria [192]. Both drugs were developed by Alnylam Pharmaceuticals, the RNAi pioneer company that managed to encase its synthetic siRNA in a lipid-based nanoparticle and deliver it into the liver. Moreover, many studies have validated the use of siRNA to treat various viral infections, including Ebola, in non-human primates in a very specific way as siRNAs can be tailored for each epidemic strain [193]. These studies highlight the therapeutic potential of siRNAs, a potential that is currently exploited to propose innovative solutions.

3.1.1. RNAi and cancer

So far, there is no RNAi-based drug approved for anticancer therapy, but several therapeutics are currently undergoing clinical trials. Originally, RNAi-based anticancer therapy was proposed to target oncogenes. In fact, proto-oncogene activation can occur through genetic alterations including gene fusion, translocation, mutation or chromosomal rearrangement [194]. Therefore, the imbalance between proto-oncogenes and tumor suppressor genes can sustain cancer development [195]. RNAi could be used to inhibit mRNA translation of oncogenic genes and improve chemotherapy efficiency by reducing the activity of multidrug resistance-related genes within cancer cells [196], [197].

The potential anticancer effects of RNAi technology showed that the gene silencing of overexpressed genes in tumor cells, involved in tumor growth, proliferation, signaling pathways, drug resistance or tumor metastasis, could provide curative benefits and reduce HCC development [198]. Moreover, RNAi could target other cells in the liver and thereby modify the crosstalk between the tumor and its surrounding microenvironment to limit the potentiation effects of either of the cells on each other [199].

3.1.2. RNAi-mediated therapeutic intervention in the context of HCC

The key to cancer progression and thriving is the presence of a milieu that sustains the cancer multiplication and helps in combating the various stresses that come its way; among them are the hypoxia and the immune response that attempts to combat the cancer. The microenvironment status is a key point in evading these stresses and creating coping mechanisms for the cancer to thrive. As it was explained above, inflammation drives HCC development. This suggests the key role of immune cells in the vicinity of the tumor before the emergence of HCC. A change in the status of the tumor microenvironment from a “combating” one to a “permissive” one is crucial. This is established by changes in the tumor microenvironment of the liver including many effectors: Extracellular Matrix (ECM) components, CAFs, endothelial cells, hepatic stellate cells and immune cells (migratory and resident). All of these mediate a crosstalk with the tumor via a profile of secretome ranging from chemokines, cytokines and growth factors to extracellular vesicles (*e.g.*, exosomes) harboring effector molecules (nucleic acids and/or proteins) that aid in the tumor progression and the

conversion of the milieu into a pro-tumorigenic one. This back-and-forth communication serves as a feedback loop to ensure a sustained adaptation according to the tumor status [200]. RNAi can be used to disrupt this loop, *see Figure 12*. For instance, in that context, the FDA has granted in 2020 an orphan drug designation to the therapeutic candidate, STP705, a siRNA targeting both the TGF β and Cyclooxygenase (COX)-2 gene for the treatment of HCC [201]. Further, studies about the use of RNAi mediated tackling of various effector molecules in an array of cells involved in HCC initiation and progression are detailed below.

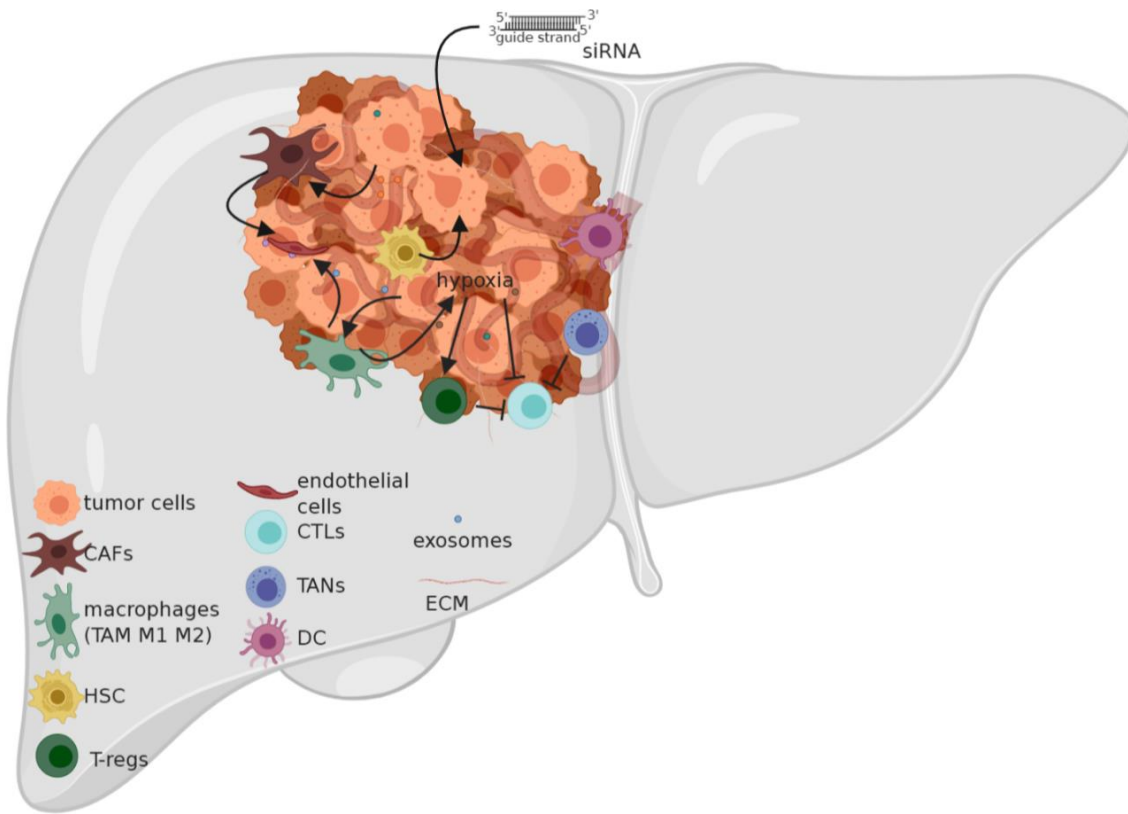


Figure 12: RNAi in HCC. Schematic representation of the tumor microenvironment and its various constituents and the use of RNAi strategy in HCC. Such a strategy can result in the targeting of a variety of cells aside from the tumor cells themselves; these are: CAFs: Cancer associated fibroblasts; TAM: tumor associated macrophages; HSC: hepatic stellate cell; Tregs: T-regulatory cells; CTLs: cytotoxic T-Lymphocytes; TANS: tumor associated neutrophils; DC: dendritic cell; ECM: extracellular matrix; siRNA: small interfering ribonucleic acid. Adapted from Mroweh M. et al, *International Journal of Molecular Sciences* [71]

Tackling communication with extracellular components

Extracellular matrix (ECM)

The ECM is a mesh of an interstitial matrix and basal membrane composed of proteoglycans and hyaluronic acid that hold the organ together. However, this mesh is not the sole matrix witnessing the evolution of the tumor in HCC; rather, it facilitates the interactions between the effectors and their corresponding effectors. It acts as a bridge in the crosstalk between the tumor and the different cells in the tumor vicinity and faces many changes due to hepatocarcinogenesis [202].

Heparin Sulfate (HS) plays an important role in HCC and mediates the binding of the growth factors to their respective RTKs. Heparin-degrading endosulfatases SULF1 and SULF2 in the ECM regulate such a process [203]. As crosstalk mediators and potentiators of HCC, RNAi approaches have been developed to target the different growth factors in the vicinity of HCC.

Besides heparin sulfate, a heparan sulphate proteoglycan Glypican 3 (GPC3) is located at the extracellular side of the cell membrane through a glycosylphosphatidylinositol (GPI) anchor. It has recently emerged as a potential biomarker and/or therapeutic target for HCC. Silencing GPC3 in CP-Hep cells and human HCC cells, by a targeted siRNA, showed a decreased proliferation and a boost in the apoptosis along with a decrease in the invasive profile. Furthermore, another study exploited the synergistic effect of the siRNA-mediated knockdown of GPC3 along with Sorafenib to combat HCC. Liposomes harboring GPC3 siRNA along with Sorafenib were delivered to HepG2 cells. The results showed a hindered proliferation, possibly due to the decrease in Cyclin D1 expression following GPC3 knockdown and Sorafenib administration, along with an increase in the apoptosis rate. *In vivo* subcutaneous xenografts of HepG2 cells in nude mice yielded results consistent with those obtained *in vitro* [204].

Heparanase, another important component of the ECM, plays a prominent role in tumorigenesis. It contributes to the cleavage of HS side chains of heparin sulfate proteoglycans (HSPGs), releasing sequestered bioactive molecules. In the context of HCC, heparanase has been shown to promote metastasis by two means: the degradation of the ECM components and a non-enzymatic alteration of the adhesive properties of HCC [205]. Reducing the heparanase expression utilizing siRNA could efficiently inhibit tumor metastasis [205].

Growth factors (GFs) such as VEGF, epidermal growth factor receptor (EGF) and hepatocyte growth factor (HGF) have been observed to be overexpressed in many cancers including HCC, as they play a crucial role in different mechanisms involving tumor proliferation, metastasis and angiogenesis[206-208]. A shRNA targeting VEGF was designed to inhibit VEGF expression of HCC cells and liver tumor tissues. The latter was administrated intratumorally or via intravenous injection into orthotopic allograft liver tumor-bearing mice. Results demonstrated a more effective suppression of tumor angiogenesis and tumor growth in different HCC models studied [209]. Moreover, a study designed a multiple targeting siRNA which could simultaneously suppress three genes: NET-1, EMS1 and VEGF. This co-silencing reduced tumor proliferation and growth and induced tumor cell death [210], [211]. Similarly, simultaneous silencing of VEGF and KSP using siRNA cocktail in Hep3B cells inhibited cell proliferation, migration and invasion and also promoted tumor apoptosis [210]. In another study, a siRNA was used to suppress migration inhibitory factor (MIF) cytokines that play an important role in HCC proliferation. Upon MIF knockdown, the tumor growth rate was reduced in both HCC cell lines and in *in vivo* xenograft model along with an increased expression of apoptosis-related proteins[212]. As growth factors have an impact on the proliferation of HCC, RNAi targeting proliferation mediators in HCC have been utilized. Cyclin E and Cyclin-Dependent Kinase 2 (Cdk2) are essential actors in cell cycle and initiation of DNA replication [213], and an overexpression of cyclin E has been found in 70% of the HCC cases. Accordingly, a siRNA targeting the coding region of cyclin E was designed, this showed a suppression of Cyclin E expression up to 90% in HCC cell lines and also inhibited HCC tumor growth in nude mice [214].

Another group of matricellular proteins involved in HCC is CCN, core regulatory proteins – named according to its first 3 members: CYR61 (cysteine-rich angiogenic protein 61 or CCN1), CTGF (connective tissue growth factor or CCN2), and NOV (nephroblastoma overexpressed or CCN3) – that modulate cell-matrix interaction to modify the cellular phenotype. CCNs play a role in differentiation, adhesion, migration, mitogenesis, chemotaxis and angiogenesis. The first four members of this family are shown to play a role in HCC: CCN1 to 4. CCNs induce the secretion of chemokines and cytokines to establish an inflammatory milieu and orchestrate the recruitment of immune cells to the tumor microenvironment. For instance, platelet-derived CCN1 increases the percentage of reactive oxygen species (ROS) in hepatocytes leading to macrophage activation and immunosuppression. CCN1

has also been shown to increase the expression of several proinflammatory signals through the activation of integrin-Nuclear Factor κ B (NF κ B) signaling in macrophages [215], [216]. Moreover, fibronectin, laminin, collagen and elastin in the ECM are involved in the chemotaxis and cell–cell interactions. Additionally, laminin-5–dependent overexpression of integrins α 3 β 1 and α 6 β 4 positively correlates with the invasive and metastatic potentials of HCC cells. Changes are introduced in the adhesive and migratory characteristics of HCC cells by the α 3 β 1 integrin by mediating the interaction between the ECM and the cells [217]. Silencing β 1 and α v integrin subunits using a nanoparticle delivery of siRNAs in mouse liver reduced tumor proliferation and increased tumor cell death without harming the healthy liver tissue [218] .

Extracellular vesicles (exosomes)

Exosomes are small membrane vesicles that are released by many different cell types, in both normal and pathological conditions. These small nanoparticles bleb out of the origin cells and have the ability to fuse with the membrane of recipient cells. Their role in crosstalk lies in the cargo they carry within them. Exosomes play important roles in the exchange of biological information as substance transport carriers and in regulation of the cellular microenvironment by delivering a variety of biological molecules, including mRNAs, miRNAs and proteins.

The shuttling of exosomes between the different effectors has been shown to reshape the TME in order to support carcinogenesis. Among the effects of exosomes are suppression of the immune response, favoring angiogenesis, remodeling of the ECM and changes in the stromal cells [219-221]. Exosomes have been shown to transfer genetic material from cancerous cells to normal ones mediating tumor progression, traverse the blood stream to distant areas to elicit a metastatic site for the tumor, and modulate the anti-tumor immunity. On the level of the nucleic acid content of exosomes, extensive research has been done on the miRNA of HCC-derived exosomes. Studies over the years provided a panel of miRs that are transported from the tumor to the adjacent cells, some of which are as follows: miR-584, miR-517c, miR-378, miR-520f, miR-142-5p, miR-451, miR-518d, miR-215, miR-376a, miR-133b and miR-367, miR-21, miR-192, miR-221, miR-122, miR-423-5p, miR-21-5, plet-7d-5p, let-7b-5p, let-7c-5p, miR-486-5p and miR-10b-5p, miR-519d and miR-1228. The different miRNAs modulate the gene expression in the recipient cells favoring metastasis, tumor progression, drug

resistance and recurrence [222]. Techniques to exploit miRNA to tackle the crosstalk between tumor cells and their vicinity have recently emerged. For instance, microRNA-320a (miR-320a) which is downregulated in several cancers, was found to inhibit c-Myc expression in HCC tissues and cell lines. Therefore, upregulation of miR-320a by transfecting the cells with miR-320a mimics inhibited tumor proliferation and invasion by decreasing the expression c-Myc in HCC cells [223].

A study in 2016 described that exosome alter drug sensitivity by releasing molecules such as mRNAs and miRNAs into neighboring cells. This study sheds the light on the activation of HGF/c-Met/Akt signaling pathway via HCC-cell derived exosomes resulting in the inhibition of Sorafenib-induced apoptosis, thus emphasizing on the role of exosomes in Sorafenib resistance in liver cancer [224]. Wang and colleagues in 2018 described that HCC cell line HepG2-derived exosomes could be actively internalized by adipocytes differentiated from mesenchymal stem cells (MSCs) and caused significant transcriptomic alterations, in particular induced inflammatory phenotype in adipocytes [225]. Additionally, 14-3-3 zeta protein in T lymphocytes induces their exhaustion by evident expression of PD-1, TIM-3, LAG3 and CTLA-4. Tumor-derived exosomes mediate the transfer of 14-3-3 zeta protein to the tumor-infiltrating lymphocytes leading to their exhaustion and/or their differentiation into T-regulatory cells (T-regs) [226].

Aside from miRNAs, exosomes have been shown to shuttle mRNAs and long non-coding RNAs (lncRNAs). Many studies have shown that HCC cell lines with a great metastatic potential secrete exosomes carrying proto-oncogenes, in the form of mRNA, such as Met S100 family members and caveolin [227]. Oncogene c-Myc abnormal expression boosts the proliferative, invasive and migration capabilities of HCC HepG2 cells, and therefore a plasmid-based polymerase III promoter system was used to deliver and express siRNA targeting to silence c-Myc in HepG2 cells. The results showed that the siRNA-based knockdown of c-Myc significantly decreased its expression in HepG2 cells up to 85%. Consequently, a significant decrease in migration, invasion and proliferation of HepG2 cells was recorded [228]. Another study demonstrated that the overexpression of c-Jun, a proto-oncogene involved in MAPK signaling, was associated with Sorafenib HCC resistance; hence using siRNA tool, c-Jun downregulation was correlated with a significantly enhanced Sorafenib-induced tumor apoptosis [229]. Another oncogene in HCC is Bmi-1, which facilitates DNA repair and promotes survival.

A recent study correlated the resistance to Cisplatin treatment (CDDP) to elevated Bmi-1 expression levels. CDDP alone or in combination with other drugs is used to combat HCC especially in non-resectable or Sorafenib-refractory HCC [230-232]. On that basis, Li and colleagues developed in 2019 a nanoparticle delivery system incorporating both nanoplatine cores and a calcium phosphate (CaP)-coated siRNA targeting Bmi-1. The efficiency of the delivery and the silencing was tested first *in vitro* on HepG2 cells, and then *in vivo* on mice xenograft model. The results showed highest tumor inhibition in the mice treated with nanoparticles loaded with CaP-Bim-1 siRNA and nanoplatine cores in comparison to the control groups[233].

Furthermore, a study showed that CD90⁺ Huh7 cells (HCC cell line) secreted exosomes harboring H19, a lncRNA, and once in the target cells, it upregulated the expression and release of VEGF, thus stimulating angiogenesis and adherence of CD90⁺ Huh7 cells with endothelial cells [234], further stressing on the importance of VEGF as a target for RNAi. A study was conducted in 2018 utilizing a galactose-derivative-modified nanoparticle harboring VEGF siRNA for an attempted knockdown. The results showed that VEGF siRNA loaded in ASGPR-targeted nanoparticles silenced VEGF both *in vitro* and *in vivo*, demonstrated potent anti-angiogenic activity in HCA-1 tumors and suppressed primary HCC growth and distal metastasis [235]. A more recent study focused on attaining a synergistic effect by co-loading Ph-sensitive liposomes with a siRNA targeting VEGF and Sorafenib. The system was tested in two-dimensional cultured HepG2 cells, three-dimensional HepG2 tumor spheroids and tumor regions of H22 tumor-bearing mice. The results showed a successful uptake of the system and decreased VEGF expression in all models along with an induction of apoptosis [236]. Moreover, and due to its role in drug resistance, a chemokine receptor (CXCR4)-targeted lipid-based nanoparticle along with a modified antagonist of CXCR4, AMD3100, was designed to specifically deliver VEGF-siRNA[237]. Results showed that efficient downregulation of VEGF expression both *in vitro* and *in vivo* and together with Sorafenib led to the synergistic tumor growth inhibition compared to Sorafenib only, suggesting that the use of siRNA in cancer therapy could increase drug efficacy[238].

Tackling Cellular components
Cancer-Associated Fibroblasts (CAFs)

CAFs are cells that trans-differentiate from different resident cells in the liver, mainly fibroblasts, but they can also derive from epithelial cells, endothelial cells, local mesenchymal cells, smooth muscle cells, pre-adipocytes and bone-marrow-derived progenitors [239-242]. Their trans-differentiation can be mediated by TNF- α and PDGF secreted by the macrophages [243]. HCC derives from a cirrhotic background, which involves a strong activation of fibroblasts, the main precursor of CAFs [243], [244]. TNF- α was shown to upregulate the expression of the transcription factor AATF via its regulatory element site of sterol regulatory element-binding protein-1 (SREBP1) in both HepG2 and Huh-7 cell lines via siRNA targeting SREBP1. Furthermore, the knockdown AATF in HCC cell line QGY-7703 inhibited proliferation, migration, anchorage-independent growth, invasion and colony formation. A decrease in the tumorigenicity was also shown in the QGY-7703 xenograft model of NSG mice harboring AATF knockdown. This study stresses the importance of TNF- α in HCC thriving [245].

On the level of TME priming, CAFs intercalate in the ECM and secrete ECM components. Among these, it is worth mentioning type 1 collagen fibers, fibronectin, tenascin and secreted protein acidic and rich in cysteine (SPARC). Immune modulation wise, CAFs secrete cytokines (Interleukin (IL)-1, IL-6...) and chemokines (monocyte chemoattractant protein-1 (MCP-1), SDF-1/CXCL12...). By the secretion of SDF-1, CAFs also recruit endothelial progenitor cells to the tumor vicinity, thus supporting tumor vascularization [243]. To further support the tumor growth, CAFs produce and secrete growth factors (EGF, FGF, HGF and TGF- β) [246], [247]. In addition, CAFs have been shown to secrete CCL-2,-5,-7 and CXCL-16 thus promoting metastasis to bone, brain and lung in severe combined immunodeficiency (SCID) mice via activation of the TGF- β pathway [248], thus stressing on the wide array of pathways activated by the crosstalk between CAFs and the tumor. These pathways are the focus of RNAi interventions.

Endothelial cells

Endothelial cells are important for the tumor as they are the nutrient and oxygen suppliers. In addition, they mediate a crosstalk with the tumor via a change in the expression profile of receptors, rendering them responsive to signals derived from

the tumor microenvironment and the tumor itself, while also secreting a variety of cytokines to communicate with the tumor [249]. The phenotype changes can be summarized by an upregulation of the expression of endoglin (CD105) along with the various angiogenic receptors: VEGFR, EGFR, PDGFR, and CXCR [246]. RNAi-based gene silencing delivered by an optimized immunoliposome showed an effective EGFR gene knockdown in mice bearing orthotopic HCC, thereby showing the potential of this promising therapy [210]. The role of CD105 is prominent as it is activated by a variety of TGF- β superfamily members. It facilitates the extravasation of leukocytes into the site of inflammation, and induces the “leaking” of chemotaxis factors into the bloodstream. Moreover, they exhibit a greater migration capacity and accelerated cell cycle, along with an array of secretions: tissue plasminogen activator, IL-6, IL-8, MCP-1 and growth-regulated oncogene alpha (GRO- α), among others [239]. Several studies underlined the importance of IL-8-mediated inflammation in metastatic HCC through the activation of the transcription factor forkhead box C1 (FOXC1) or via integrin $\alpha\beta 3$ [250]. Silencing of IL-8 with siRNA showed that it could be used to reduce tumor metastasis mediated by IL-8 [251].

Hepatic Stellate Cells (HSCs)

HSCs are normally non-proliferating cells residing in the liver, ready to be activated upon injury. These cells are primarily activated by signals from injured Kupffer cells, injured platelets or any other type of injured cells in the vicinity. In the context of HCC, HSCs are activated during the fibrogenesis process that precedes the tumorigenesis and carry on to secrete ECM components. HSCs can be activated by HBV, HCV, cathepsins B and D, PDGF, TGF- $\beta 1$, MMP-9, JNK and IGFBP-5, and they can infiltrate into the HCC stroma. Once there, they stimulate tumor vascularization through the secretion of VEGF-A and MMP-2 [203]. They are known to secrete laminin-5, increase cytokine production, and exhibit liver-specific pericyte properties [243]. Various studies have been done to stress on the importance of the reciprocal crosstalk between HSCs and the tumor. A recent study showed that the crosstalk between HSCs and HCC via PDGF- β induced the increase in the expression of REG3A in HCC cells. Furthermore, the silencing of REG3A via siRNA led to a decrease in the proliferation of LX-2 HCC cells when cocultured with HSC cell line MH134. This is shown to be a result of the modulation of the p42/44 pathway [252].

A study showed an increase in the proliferation rate of rat HSCs following culturing with conditioned tumoral hepatocyte media, accompanied by an increase in α -SMA expression, and desmins, PDGFR and Gelatinase A secretion – markers of CAFs [253]. Another study showed the reciprocal priming of HSCs to the tumor. It showed that the conditioned media of HSCs increased the growth and invasiveness of HCC. Similar results were obtained upon the co-implantation of HSCs and HCC cells in nude mice, which appears to be the result of activated NF κ B and Erk signaling pathways [254],[255]. In that context, gene silencing of Erk1 and Erk2 using siRNAs developed Fluorouracil (5-FU) sensitivity and increased 5-FU-induced apoptosis in HCC HepG2 cell line [256].

Immune cells

The landscape of the TME of HCC comprises a complex set of immune cells with their intricate cytokine and chemokine secretions. The immune responses sustained against HCC include the CD8⁺ Cytotoxic T-cells (CTLs), which produce perforin and granzymes to kill the cancer cells upon activation. The frequency of CTLs in the tumor vicinity is correlated with better survival. However, the crosstalk in the tumor vicinity between the tumor and these cells, along with effector molecules and immunosuppressive cells, namely T-regs, hinders the function of CTLs [200]. The TME plays a pivotal role in the immune evasion by establishing an immunosuppressive profile. The preferential activation of subsets of immune cells and their subsequent secreted chemokines and cytokines are the means for such process. The crosstalk mediated between the immune cells and the tumor via the different secretory components plays a major role in the tumor progression.

- **Macrophages**

As HCC is a result of a chronic inflammation, the persistent inflammatory signal drives the constant recruitment of monocytes into the inflammatory site along with an alteration in the bone marrow signal to favor the increased output of myeloid cells [257]. Thus, the pool of macrophages in the tumor site results from the invasion of circulating macrophages added to the pre-existing macrophages in the liver, termed as Kupffer cells. The pool is heterogenous in terms of macrophage subtypes: M1, M2 or Tumor Associated Macrophages (TAMs) [258]. It has been

shown that macrophages display a plasticity between the two major types of M1 and M2 macrophages. However, the line to discriminate between the two subtypes is not yet crystal clear. Principally, M1 macrophages (classically activated) are pro-inflammatory and are associated with anti-tumorigenic activity, whilst M2 macrophages (alternatively activated) are anti-inflammatory and favor tumorigenicity. The cell fate is decided by extrinsic factors ranging from growth factors, cytokines and chemokines to microenvironment stress. M1 macrophages are stimulated by interferon-gamma (IFN- γ) along with a TLR agonist such as LPS. M2 macrophages on the other hand are stimulated by IL-4, IL-10 and IL-13. The differentiation implicates phenotypical, genetic, epigenetic, metabolic and secretome changes. Of major importance in the context of cancer is the profile of secretion of each macrophage subtype. On the level of M1 macrophages, they exhibit a typical pro-inflammatory cytokine and chemokine profile: TNF alpha, IL-1, IL-6, IL-12, IL-18, IL-23, MCP-1, CXCL9, CXCL10. As for M2 macrophages they are known for the secretion of IL-10, IL-12^{low}, CC chemokine ligand (CCL)17, CCL22, CCL24 [258],[259]. M2 macrophages are active effectors in the context of HCC. A clinical study in 2014 showed a poor prognosis for patients exhibiting an increased expression of CD-163 and Scavenger A macrophages (markers for M2 macrophages). This was accompanied with increased tumor nodules and venous infiltration in HCC, along with an increased EMT potential via M2 macrophage CCL22 secretion [259]. Another study showed that M2 macrophages accumulated more in Sorafenib-resistant HCC tumors than Sorafenib-sensitive ones, and confer Sorafenib resistance by secreting HGF, which sustains tumor growth and metastasis by activation of HGF/c-Met, ERK1/2/MAPK and PI3K/AKT pathways in tumor cells [260].

Several targeting mediators of tumor cells are secreted by macrophages and have been studied in the development and progression of HCC. In the context of targeting MAPK signaling, which is overexpressed in HCC and associated with tumor growth, the downregulation of MAP4K4 using shRNA led to reduced cell proliferation, S-phase cell cycle blockade and increased tumor apoptosis [261]. Another signaling pathway targeted by RNAi is HGF/c-Met. A study showed that SUMO specific protease 1 (SEN1) silencing resulted in a downregulation of HGF-induced proliferation and migration of HCC cells through effects on the HGF/c-Met pathway [262]. Additionally, in order to inhibit the proliferation of HCC cell lines (HepG2 and Huh7), siRNA targeting a tyrosine kinase receptor known as RON showed an efficient suppression of tumor cell

migration and invasion and enhanced apoptosis by activating cleaved caspase-3 and PARP through the modulation of Akt, c-Raf and ERK signaling pathway [263]. A study in 2019 by Zhang and colleagues evaluated the expression of sirtuin 6 (SIRT6) in a variety of HCC cell lines and its effect on the Erk1/2 signaling pathway favoring proliferation and inhibiting apoptosis. The results showed an elevated expression of SIRT6 in 9 HCC cell lines in comparison to a normal liver cell line. Moreover, knockdown of SIRT6 via an siRNA approach in Huh-7 cell line resulted in a decrease in the proliferation rate along with an increase in the apoptosis rate with a downregulation of Bcl-2, and an upregulation of Bax and cleaved-caspase 3. This was accompanied by a decrease in the phosphorylation of Erk1/2 [264]. Epithelial cell transforming sequence 2 (ECT2) has been shown to be implicated in early HCC recurrence via the activation of the Rho/Erk signaling. The downregulation of ECT2 by siRNA entailed the suppression of Erk, thereby enhancing apoptosis and reducing the metastatic ability of HCC cells [265]. Further focusing on Rho, RhoC overexpression and metastatic potentials of HCC have been correlated as enhancing invasion and migration of HCC cells. Inhibition of RhoC resulted in inhibition of invasion and migration without reducing cell viability in HCCLM3 cells. In addition, silencing of the RhoC expression in an HCC metastatic mouse model showed a significant inhibition of tumor metastasis [266].

Another subset of macrophages termed “TAMs” was found in the tumor vicinity of HCC. Studies have shown that the presence of TAMs in the tumor vicinity correlates to poor prognosis in HCC. These cells exhibit an M2-like phenotype and express both M1 and M2 macrophage hallmarks. They secrete pro-inflammatory cytokines *e.g.*, IL-1 β , IL-6, IL-23 and TNF- α . A recent study demonstrated that the interaction of TNF- α and angiotensin II (Ang II) in HCC cells could enhance tumor proliferation, migration and invasion via the regulation of G protein-coupled receptor kinase (GRK2). Therefore, GRK2-siRNA was used to examine the molecular interactions of TNF- α in tumor growth, and the obtained results suggested that TNF- α could serve as a new potential therapeutic target in HCC [267]. TAMs also secrete a variety of growth factors such as TGF- β , VEGF, FGF, PDGF, angiogenic factor thymidine phosphorylase, angiogenesis-modulating enzyme cyclooxygenase-2, MMP-9 and MMP-12 [268]. On the level of immune response modulation, TAMs have been shown to suppress CD4⁺CD25⁻ T cells, activate T-regs and contribute to the expansion of Th-17 cells, which in turn favor the expression of immune-suppressing antigens PD-1, CTLA-4, GITR [152, 269].

Moreover, TGF- β in the tumor microenvironment triggers the expression of Tim-3 on the surface of TAMs and the subsequent IL-6 secretion; the TAM-derived IL-6 further activates the IL-6/STAT3 pathway in the tumor sustaining survival and proliferation [270]. When HCC cell lines (SMMC7721 cells and QGY-7703 cells) were transfected with siRNA targeting STAT3 and AKT2, a significant decrease in mRNA level of AKT2 and STAT3 was observed. Furthermore, nude mice were used to verify the correlation and a decreased ability of HCC cell proliferation, migration and invasion has been since concluded [122].

- Neutrophils

As it is the case with macrophages, TANs in the tumor microenvironment exhibit two polarizations: N1 neutrophils that are said to be anti-tumorigenic and N2 neutrophils that are said to be pro-tumorigenic [271]. Their activation is governed by type 1 IFNs and TGF- β . Their main role in tumors is to suppress CD8⁺ T-cells, thus helping the tumor evade the immune response. Nitric oxide production by TANs, induced by TNF- α in the tumor microenvironment, promotes CD8⁺ T-cell apoptosis [272]. In the context of HCC, TANs exhibit the same role as in different cancers, associating with poor prognosis and driving tumor progression. The neutrophil–lymphocyte ratio (NLR) is of great significance in patients subject to immunotherapy (PD-1/PDL-1) and correlates with the tumor progression [273], [274]. On the clinical level, NLR has been shown to be an indicator of survival after hepatectomy [275], [276]. Recent studies have shown that the accumulation of TANs via HIF-1/RANTES upregulation in NASH drives the initiation and progression into HCC [277]. While in the tumor vicinity, TANs secrete chemokines such as CCL2 and CCL17 which in turn recruit TAMs and T-regs, thus contributing to HCC progression, metastasis and resistance to Sorafenib treatment [278]. Interestingly, downregulation of CXCL5 a direct chemoattractant for neutrophils by shRNA in HCC cells reduced tumor growth, metastasis and intratumoral neutrophil infiltration [279].

- Dendritic cells

Dendritic cells (DCs) in a healthy liver play the role of bridging the innate and adaptive immunity as antigen-presenting cells (APCs) as well as of instructing lymphocytes. The most prominent role of DCs in HCC is mediating immune

tolerance. Thus, the crosstalk between DCs, the tumor and its tumor vicinity is mediated by the secretion of various cytokines leading to immune tolerance and tumor progression. At first hand, the activation of DCs is mediated by IFN- γ secretion by the tumor or effector cells in the vicinity. Upon activation, DCs tend to secrete IL-10 and IL-12. IL-12 leads to impaired activation of allogenic T-cells. IL-10 depotentiates the immune response against the tumor and excludes APC from the tumor mass [280]. It is important to mention that the DCs are emerging targets for immune therapy in the context of HCC, thus further stressing on the fact that the crosstalk between DCs, immune cells and the tumor is crucial for the tumor progression [281]. A study demonstrated that efficient shRNA-based suppression of interferon regulatory factor-1 (IRF-1) inhibited IFN- γ mediated tumor thus promoting cell death of HCC cell line, opening a new therapeutic strategy to tackle autophagic cells [282]. On another note, IFN-stimulated gene 15 (ISG15) is a ubiquitin-like molecule that has been identified as an intrinsic actor that elicits HCC tumorigenesis and metastasis; the former is overexpressed in HCC patients. Using cell lines and xenograft model, siRNA-mediated knockdown of ISG15 showed a significant inhibition of tumor growth [283].

- Natural killer cells

Natural killer (NK) cells are prominent in the liver and are the first responders against viral infections (HBV and HCV). NK cells are also in charge of maintaining a proper immune function as they regulate the tuning of the immune response between the defensive and tolerance modes [258], [284]. The effect of NK cells in HCC is majorly by their inhibited function. Growing evidence suggests that the hypoxic conditions inducing the activation of HIF1 α , along with immune modulators in the tumor microenvironment disrupt the regulating ability of NK cells, resulting in the exhaustion of the anti-tumor response and poor prognosis [285]. Interestingly, RNAi-mediated suppression of HIF1 α expression in the liver inhibited metastatic tumor growth in the hepatoma cell line (SMMC-7721) and tumor-bearing mouse liver [286, 287]. NK cells can be inhibited by HCC cells as HCC cells express MICA, a specific NK cell ligand that inhibits NK cell interaction [258]. Another mechanism of depotentiating NK cells by HCC cells is the impairment of IL-12 secretion by DCs by HCC cell-derived alpha fetoprotein A more direct effect of alpha fetoprotein has been shown on NK cells and is dictated by a time frame [288, 289]. T-regs play a role in the attenuation of the NK cell

function, either by the release of cytokines like IL-8, TGF- β 1 and IL-10, which then decrease the expression of NKR ligands on HSCs suppressing them from binding to NKG2D on NK cells, or by their competition with NK cells over the available IL-2 in the tumor microenvironment [290]. Moreover, the attenuated production of TNF- α and IFN- γ by NK cells mediated by CAF-derived IDO and PGE2 has been shown to be among the reasons of sustained fibrosis in HCC and immune cell evasion [291].

3.2. Delivery vectors for RNAi

Nanoparticles have received considerable attention due to their ability to protect RNAi molecules from enzymatic degradation and their capacity to be associated to specific peptides, increasing their selectivity to tumor cells [292],[293]. In addition, chemical modifications involving sugar and phosphate and chemical structure modifications in the oligonucleotide backbone of RNAi have been proven efficient as they considerably reduce toxicity, off-targets, as well as the degradation by nucleases [294]. The use of RNAi comprises the RNAi molecule and its vector, and the success of such an intervention is dependent on the efficiency of the delivery system along with the RNAi efficiency. Recently, non-viral vectors, especially nanoparticle carriers such as polymers: polyethylene glycol (PEG), polyethylenimine (PEI), poly-l-lysine (PLL), dendrimers and chitosan; lipids: lipid nanoparticles, liposomes, micelles, etc.; and inorganic nanoparticles: carbon nanotubes, gold, mesoporous silica nanoparticles (MSNs); have shown multiple advantages in the field of RNAi delivery [295]. Of particular interest are dendrimers.

The name “dendrimer” comes from the Greek word “dendron” meaning “tree” thus signifying their structure: a tree branching from a single central point. Dendrimers are polymeric nanoparticles that have an array of usage in biomedical research as vectors or as acting molecules *per se*. They possess a highly branched three-dimensional (3-D) structure along with their unimolecular, monodisperse, and micellar macromolecular properties. They are composed of 3 main components: the core, interior and the surface. The morphology of the dendrimer is dictated by the number/type of internal branching units. Thus, the core manages the three dimensional (3D_ architecture of the dendrimer granting either a spherical, an ellipsoid or a cylindrical scaffold [296]. The surface can be altered by polymerization with peripheral functional groups. Their polymeric structure

varies and the name attributed to the dendrimer often corresponds to the polymer on the surface along with the modifications. A dendrimer contains either one or more polymers: Poly(AMidoamine) (PMAM), PLL, poly(2,2-bis(HydroxyMethyl)Propionic Acid (bis-MPA), PolyPrIpylenimine (PPI), and Poly (Glycerol Succinic Acid) (PGLSA-OH). Their synthesis is either a convergent or a divergent process; beginning from the surface and proceeding to add monomers to the surface unit which eventually attach to the core or starting at the reactive center and construction of branching units towards the surface, respectively. Dendrimers' span of use includes many fields in the biomedical research; that of which is impacted by their generation process, core composition and peripheral modification [297].

Dendrimers have shown an antimicrobial potential, despite their overall charge. The PPI dendrimers, with a cationic charge, harboring quaternary ammonium groups on their periphery showed notable antimicrobial activity [298]. Similarly, anionic amphiphilic dendrimers showed potent antimicrobial activity [299]. Along with their antimicrobial potential, dendrimers are also studied in for their antiviral effect. VivaGel, a sulfonated polylysine dendrimer, is well-known for its use as an antiviral agent against HIV-1. Moreover, they have been used as contrast agents for Magnetic Resonance Imaging (MRI) specifically using dendrimer-based metal chelates [300].

Immunomodulation has been shown as an additional application for the dendrimers. The use of a modified dendrimer in a mouse model of arthritis showed a prominent inhibition inflammation and bone erosion. A process that involved the inhibition of monocyte-derived osteoclast differentiation and activity [301]. Vaccination also exploits the dendrimer as a delivery vector [302]. Various other applications of the dendrimer have been reported, such as burn treatments [303], prion research [304], photodynamic therapy [305], among others.

More importantly, dendrimers are also used as transfecting agents. Many variants of the dendrimer have been used as vectors for RNAi: PMAM, PPI, PLL, carbosilane dendrimers, triazine dendrimer, polyglycerol dendrimers, amphiphilic dendrimers, among others. The use of amphiphilic dendrimers (AD) in RNAi is illustrated in detail below.

Amphiphilic Dendrimer: a vector for RNAi

The amphiphilic dendrimer (AD) is said to be a hybrid between the lipid and the polymer; thus, taking advantage of both the dendrimer and the lipid aspects of a delivery vector. Thus, rendering it a safer and improved delivery vector. The AD is synthesized by Click chemistry [306], bearing a hydrophobic long alkyl chain with a low-generation hydrophilic PAMAM dendron. An added advantage is of the AD self assembles upon its association with the siRNA. Upon contact with the siRNA, it spontaneously undergoes structural rearrangement into smaller spherical micelles which in turn maximize the interaction between the AD and the siRNA and has been shown to successfully deliver siRNAs both *in vitro* and *in vivo* [307], [308]. In addition to the self-assembly property, the AD possesses the ability to be complexed to a peptide (E16RGDK) which binds to the nrp-1 receptor on the surface of various cells, thus favoring receptor-mediated endocytosis which could increase the efficiency of the delivery as well as allow a targeted delivery approach [309].

VI. HYPOTHESIS AND OBJECTIVES

Despite the advancements made in the field of HCC therapy, the current therapeutic options remain poorly efficient and some patients remain ineligible for the currently available treatments. Thus, spurs the need for better understanding of the molecular mechanisms behind HCC carcinogenesis to pinpoint new targets for therapy.

Akt inhibitors are showing prominent outcomes as a therapeutic target in HCC, However, they fail to show a specificity towards the Akt isoforms. The isoform-specific roles of Akt1 and Akt2 in HCC remain ambiguous. For that, in this study, the objective was to:

- i) Develop an RNAi strategy, specifically siRNAs, as a tool to specifically modulate the expression of Akt1 and Akt2 in HCC.
- ii) Decipher the roles played by either of the isoforms in the carcinogenesis of HCC.

Which could ultimately pave the way for a novel treatment option.

VII. MATERIALS AND METHODS

1. *In silico* design of Akt1 and Akt2 siRNAs cross-reacting humans and rodents.

Designer of siRNA (DSIR) algorithm (<http://biodev.cea.fr/DSIR/DSIR.html>) was used to generate 21-nucleotide sequences of siRNA candidates targeting *Mus musculus* Akt1 (NM_009652.3) and Akt2 (NM_001110208.2) genes. DSIR is based on a linear model which combines particular nucleotides based on a given gene sequence to ensure specificity and high rates of RISC binding and/or Ago2-mediated cleavage of the target mRNA complementary strand[310]. Within the DSIR algorithm are tools that allow the fine tuning of the candidate selection process. The set threshold for siRNA selection was set to a 90% with a mismatch tolerance of 3. A built-in option in the DSIR algorithm is that it ensures that the guide strand of the siRNA to have a perfect match with the mRNA target. In addition, during the design pro-inflammatory signals like those that activate the toll-like receptor (TLR) are automatically removed [310]. Next, in order to decipher the cross-reactivity of the siRNA candidates to human and rat Akt1 and Akt2 genes and to unravel possible off-target effect, NCBI blasting (<https://blast.ncbi.nlm.nih.gov/Blast.cgi>) bioinformatic tool was used. As the word “BLAST: basic local alignment search tool” signifies, the NCBI blasting system is an algorithm which scans primary biological sequences (amino acids, DNA, or RNA), termed “query” for homologies within an assigned database. In our case, the query was the Akt1 and Akt2 siRNA candidates generated by the DSIR, against the *Homo sapiens* and *Rattus norvegicus* genome databases. Custom synthesis of the siRNA sequences selected was done by Dharmacon company with an addition of a 5'P motif to ensure the siRNAs' processing by RISC complex.

2. Cell culture

Throughout this study 4 human cell lines were used, currently available in the team: HepG2, Hep3B, Huh7 and Phospho Lipase C (PLC) γ /PRF/5, and one mouse cell line: Hepa1.6. In addition to MV4-11 cell line provided by Inovotion (detailed in later sections)

The human cell lines are representative of different types of human liver cancer and the different status of p53. Hep3B, Huh7 and PLC γ /PRF/5 cell lines are HCC cell lines whilst HepG2 cell line is a hepatoblastoma cell line. Concerning the p53

status, Hep3B cell line is p53-depleted, Huh7 and PLC/PRF/5 cell lines present p53 mutations and HepG2 cell line expresses wild-type p53. No mutations in Akt were reported in any of the cell lines (COSMIC database) [311].

All the cell lines were cultured at 37°C and 5% CO₂. HepG2 and Hep3B cells were cultured in Modified Eagle medium (MEM) + Glutamax (Gibco cat #41090-028) supplemented with 10% fetal bovine serum (FBS) (Gibco cat #10270) and 1% Penicillin - Streptomycin (Gibco cat #P11-010). On the other hand, PLC γ /PRF/5 and Huh7 were cultured in Dulbecco's Modified Eagle medium (DMEM) + Glutamax (Gibco cat #61965-026) supplemented with 10% FBS and 1% Penicillin-Streptomycin. Additionally, PLC γ /PRF/5 medium is supplemented with 1% Sodium Pyruvate (Gibco cat #11360-039).

Hepa1.6 cell line was also used in the *in vitro* studies. It is a mouse hepatoma cell-line derived from a spontaneous BW7756 tumor in a C57L mouse. Culture conditions were also 37°C and 5% CO₂. The culture media used was DMEM with L-Glutamine (ATCC cat #30-2002) supplemented with 10% FBS and 1% Penicillin - Streptomycin.

3. Transfection of the different cell lines by siRNA

The designed siRNAs were custom-designed by Dharmacon according to the sequence, and introduced with a 5'P modification. The mock siRNA was also ordered from Qiagen (cat#1027281).

3.1. Lipofectamine-mediated transfection

PLC γ /PRF/5, Huh7, Hep3B or HepG2 cells were cultured in a 12-well plate 24 hours prior transfection (10⁵ cells/well). LipofectamineRNAiMAX (Invitrogen cat #13778075) and Opti-MEM medium (Gibco cat #11058-021) were used. According to the manufacturer's instructions, 0.8 μ l of LipofectamineRNAiMAX was mixed with the desired siRNA concentration. The time of transfection was a pulse transfection of 6 hours, after which the media was changed to the respective culture medium for each cell line.

3.2. Amphiphilic Dendrimer (AD)-mediated transfection

Cells were seeded as mentioned in the Lipofectamine-mediated transfection section 24 hours before transfection. The transfection mixture was prepared depending on the desired N/P ratio according the following equation:

$$N/P = (C_{\text{dendrimer}} \times \text{Number of terminal amine}) / (C_{\text{siRNA}} \times \text{Number of phosphate group})$$

“N” the mole of terminal amine in the dendrimer

“P” the mole of phosphate group in nucleic acid

“ $C_{\text{dendrimer}}$ ”: Concentration of Dendrimer,

“ C_{siRNA} ”: Concentration of siRNA

The N/P ratio as the equation determines the amount of the dendrimer *versus* the amount of the siRNA in the transfection mix. Once the desired N/P ratio is set, a mixture of siRNA and optiMEM and a separate AD and OptiMEM mixture were prepared, mixed together thoroughly and left at RT for 10 minutes. Then, the AD mixture was added to the siRNA mixture, mixed thoroughly and left for 30 minutes at room temperature – to allow the complexation of the siRNA and the self-assembly of the AD. The mixture was then added to the cells, cultured in OptiMEM, and left for 6 hours, after that the media was removed and changed into complete media, until the end-point of the experiment. The AD was generously supplied by Dr Ling Peng (Aix-Marseille Université, Center Interdisciplinaire de Nanoscience de Marseille, CNRS UMR 7325). AD was produced, associated with siRNA and use for transfection as already described in detail [306].

4. Treatment with Sorafenib and ARQ092

Cells were seeded in at a concentration of 10^5 cells/well in a 12-well plate and 5000 cells/well in a 96-well plate. Sorafenib Tosylate (Bay 43-9006, Sigma-Aldrich, Germany) and ARQ092, also known as Miransertib, (MedChem Express cat #HY-19719) were dissolved in pure dimethyl sulfoxide (DMSO, Sigma-Aldrich). 5 mM stock solutions of these reagents were stored at -20°C temperature and protected from light. The cells were treated with these compounds, similarly to the transfection procedure, for a 6 hour pulse before changing the media into complete cell media, depending on the cell line.

5. Gene expression analysis

RNA was extracted using Paris Kit (Life Technologies cat #AM1921) according to the manufacturer's instructions. Quantification of the RNA was done using Nanodrop ND-1000 spectrophotometer. Reverse transcription was done by SuperscriptIV Vilo mastermix with EZDNASE cDNA synthesis kit (Invitrogen cat #11766050) according to the manufacturer's instructions. cDNA was stored at -20°C before further analysis. Quantitative PCR (qPCR) was done using sequence-specific primers, *see Table 2* designed on Integrated DNA technologies (IDT) (<https://eu.idtdna.com/>) primer quest tool. The primers were chosen according to the following conditions: length of 21 nucleotides, GC content around 50%, melting temperature around 62°C and a binding site nearer to the 3' end of the gene. Afterwards, custom-designed primers were ordered from Eurogentec (<https://www.eurogentec.com/>) and verified before use. iTaq™ Universal SYBR Green Supermix (Biorad cat #1725122) and Hard-shell 384-well PCR plates (Biorad cat #HSP3805) compatible with the CFX Connect real-time PCR (Biorad) were used. The analysis was done by the Bio-Rad CFX manager software. The mean fold change of the expression of the gene was calculated after normalization to the three housekeeping genes: Glyceraldehyde-3-Phosphate Dehydrogenase (GAPDH), Ribosomal subunit 18 (RS18), and Hypoxanthine Phosphoribosyltransferase 1 (HPRT1).

Table 2: RT-qPCR primers. *HPRT1*: Hypoxanthine Phosphoribosyltransferase 1; *GAPDH*: Glyceraldehyde-3-Phosphate Dehydrogenase; *RS18*: Ribosomal subunit 18; *MTNR1B*: Melatonin Receptor 1B; *SBNO2*: Strawberry Notch homologue 2; *MYCBP2*: MYC-Binding Protein 2; *FUBP1*: Far Upstream Element Binding Protein 1; *CEP70*: Centrosomal Protein 70; *TAP1*: Transporter associated with antigen processing 1; *WDR7*: WD Repeat Domain 7.

Target	Sequence 5' → 3' (forward)	Sequence 5' → 3' (reverse)	Role
<i>AKT1</i>	CAGCACGTGTACGAGAAGAA	GCCGTGAACTCCTCATCAA	Akt family
<i>AKT2</i>	GCATCATAGGGAGACCTTCATC	CACCTCAGCCTTCCAAGTTA	
<i>HPRT1</i>	TTCTGTGGCCATCTGCTTAG	GTTTAGGAATGCAGCAACTGAC	House-keeping genes
<i>GAPDH</i>	CAAGAGCACAAGAGGAAGAGAG	CTACATGGCAACTGTGAGGAG	
<i>RS18</i>	CAGAATCCACGCCAGTACAA	GAGCTTGTTGTCCAGACCAT	
<i>MTNR1B</i>	TCTCCACCTAGCATGGACTAA	TAGTACCTCCCTCTCAGGATTG	Off-target D2Akt1 siRNA
<i>SBNO2</i>	CCAGTACTTCTCAGACACCTTC	TCCTCGTAGATCTCCTCGATAC	Off-target D11Akt1 siRNA
<i>MYCBP2</i>	GAACCACCATCACTGGAACA	CTTTCACCTCGTCGGAGATAAC	
<i>FUBP1</i>	GCACCTCAGGGCCAATAATA	TCATCAAGTCGTCTGCATCC	
<i>CEP70</i>	CTGAAGACCTCCAGAGCATTATC	CCATCACCACCAGAGATCTTAC	Off-target D15Akt2 siRNA
<i>TAP1</i>	GGACAAGAGCCACAGGTATTT	CAGCTGTGATTTCTCCATAGT	Off-target D27Akt2 siRNA
<i>WDR7</i>	GGATCTTCTCGTGGAGGTTATG	GATGGCTGGGAAACATTCTTG	

6. Protein immuno-detection

The protein immuno-detection was done using the apparatus named “Jess” developed by Biotechne (<https://www.proteinsimple.com/>). It uses a capillary-based system to execute a gel migration of protein lysates and specific-antibody mediated detection. It follows the same principle of a conventional western blot encompassing the process of migration of the reduced protein samples, blocking, primary antibody priming, secondary antibody priming (conjugated to either a peroxidase enzyme or a fluorescent conjugate in the Infrared or Near-Infrared region) and revelation. The difference with conventional western blot resides in the immuno-detection step, which is achieved within the gel without transfer of the proteins on a membrane for immuno-detection. The whole process takes place

within a plate and a 25-capillary system (Biotechne cat # SM-W004) with a size range of 12-230kDa to be placed in Jess. The plate is prefilled with stacking gel and loading gel and is filled according to the manufacturer's instructions in the designated wells. Afterwards, the plate and the capillary system in Jess, the machine is launched and 3 hours later, bands are visualized on the lanes and quantified automatically by a Jess built-in algorithm.

Protein Extraction was done by EZ buffer made fresh prior to each protein extraction from the following chemicals at the designated concentrations: 200mM Tris HCL, 100mM NaCl, 1mM EDTA, 0.5% NP40, 10% Glycerol and supplemented with protease inhibitor cocktail (Alpha Complete Roche cat #04693 24 001) and anti-phosphatase cocktails (Phosstop Roche cat #4906837001). Quantification of the protein concentration was done using BCA Protein Assay kit (Fisher Scientific cat #10741395) according to the manufacturer's instructions, in order to normalize the loading. Protein samples were reduced and denatured before loading using reagents that are supplied by the manufacturer in the form of miniature tubes of Dithiothreitol (DTT) reducing agent and an additional fluorescent 5X mastermix which come in an EZ pack along with the biotinylated ladder (Biotechne cat # SM-W004). The fluorescence harbor bands in the mix that allow the tracing of the migration in the capillary. Following the mixing of the dissolution of the DTT and the 5X fluorescent mastermix powders according to the manufacturer's instructions, the protein samples are into the desired concentration by 0.1X sample buffer (Biotechne cat # SM-W004) and 1/5 of 5X fluorescent mastermix to a final volume of 8 μ l (5 μ l for loading and the rest as dead volume).

The advantage of using Jess is that it allows multiplexing. That is, within the same capillary, 2 different proteins could be detected simultaneously, taking advantage of the different channels that Jess could use for detection. The two proteins should be detected by 2 different antibodies from 2 different species and their respective secondary antibodies should be coupled to either Horse Raddish Peroxidase (HRP) enzyme, fluorescent particles in the near-infrared (NIR) range or fluorescent particle in the infrared-range (IR). The usage of antibodies on Jess needs to be optimized taking into account the dosage to detection range and the linearity of the signal upon changing the protein concentration. The dilution to be taken was the one before the plateau with a concentration within the linear range, in this case (0.25 mg/ml). The primary antibodies that were used were monoclonal: rabbit Akt1 antibody (Cell Signaling cat #2938) at 1/10 dilution, rabbit Akt2 antibody (Cell Signaling cat #3063), rabbit phospho-Akt1 Ser473 antibody (Cell

Signaling cat #9018) and rabbit phospho-Akt2 Ser474 antibody (Cell Signaling cat #8599) both at 1/5 dilution, and mouse monoclonal β -actin antibody clone 937215 (Biotechne SAS cat #MAB8929) at a dilution 1/500. The multiplexation was always one of the rabbit antibodies with the mouse β -actin antibody as a house keeping gene. Consequently, the secondary antibody mix were selected from the panel of antibodies custom-made for Jess. These were: ready to use HRP-coupled anti-rabbit antibody (Biotechne cat #DM-001) and 20X NIR-coupled anti-mouse antibody (Biotechne cat #DM-009). Additionally, a solution of Luminol-peroxide (supplied with the HRP-coupled anti rabbit antibody) is prepared in a 1:1 ratio. Finally, the plate is filled according to the manufacturer's instructions as shown in *Figure 13*, and placed in Jess along with the capillary system.

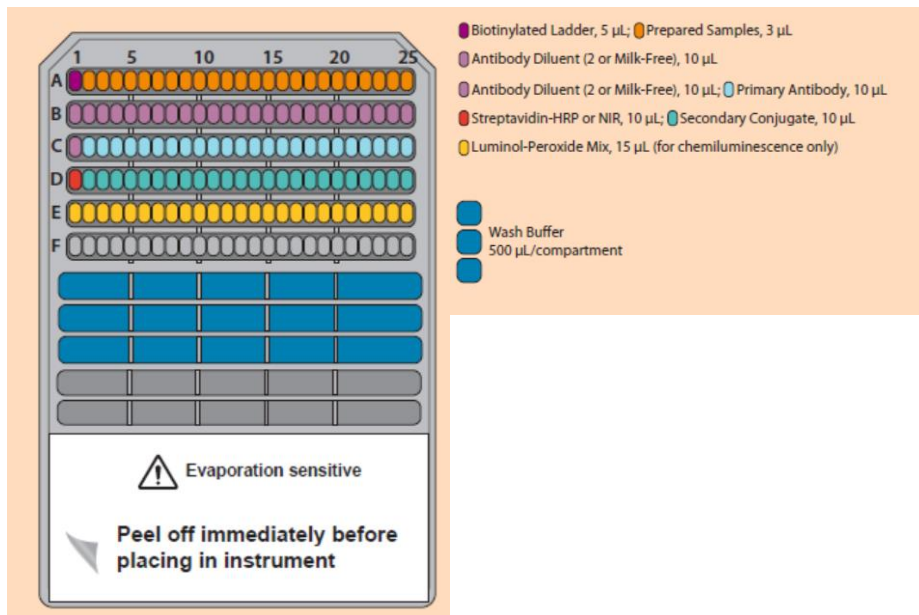


Figure 13: Jess plate. Diagram showing the plate structure of Jess and the order in which each lane is filled. (Adopted from the website: <http://www.proteinsimple.com> .

7. Toll-like receptors (TLR) activation monitoring

THP1-XBlue-MD2-CD14 cells (Invitrogen cat #thpx-mcdsp) was used to monitor the activation status of TLR receptors: TLR1/2/3/4/5/9. It is an engineered human monocyte cell line characterized by a stable expression of the TLRs and NF- κ B and AP-1-inducible Secreted Embryonic Alkaline Phosphatase (SEAP) reporter gene. It thus allows the detection of a specific TLR activation through measurement of SEAP in the supernatant. As controls Human TLR1-9 Agonist kit (Invivogen cat #tlrl-kit1hw) was used. In brief, 10^7 cells were incubated with 1 ng/ml Pam3CSK4,

10⁷ cells/ml HKLM, 10 µg/ml HMW poly(I:C), 10 µg/ml LMW poly(I:C), 10 ng/ml LPS-EK, 10 ng/ml FLA-st, 10 ng/ml FSL-1, 5 µg/ml Imiquinone, 10 µg/ml ssRNA50, or 10 µg/ml ODN2006 to respectively activate TLR1/2, TLR2, TLR3 (for both the HMW and LMW poly(I:C)), TLR4, TLR5, TLR6/2, TLR7, TLR8, and TLR9. Following 24 hours of incubation, supernatants were incubated with Quanti Blue Solution (Invitrogen cat #rep-qbs) for 1 hour. The readout was by measuring the SEAP activity by CLARIOstar® Microplate Reader at an absorbance of 655 nm.

8. Cell-death analysis

LDH assay

During cell death cytoplasmic enzymes like Lactate Dehydrogenase (LDH) are released into the culture media due to the loss of the integrity of the plasma membrane. The CytoTox-One kit (Promega #G7890) is used, according to the manufacturer's instructions, to detect the levels of LDH in the supernatant thus giving an indication about the death of the cells in the different transfection conditions. In brief, 100µl of CytoToxONE reagent is added to 100µl of the supernatant, incubated for 10 minutes at RT, then 50µl of stop solution is added. A positive control was used using a cell lysis solution supplied with the kit that induced cell death. The incubation with the CytoToxONE mediates a reaction with LDH leading to the generation of a fluorescent product measured on CLARIOstar® (excitation 560nm and emission of 590nm).

9. Metabolism analysis

ViaLight® Plus Cell Proliferation and Cytotoxicity Bioassay kit (Lonza cat #LT07-121) was used, according to the manufacturer's instructions, to study the ATP levels in the cells which reflect the cell metabolism, mirroring the cell proliferation and viability of the cells. Briefly 5000 cells were seeded in a flat-bottomed 96-well plate and transfected using LipofectamineRNAiMAX or treated with Sorafenib or ARQ092. After 24 hours, 25µl/well of lysis reagent was added followed by 50 µl of AMR PLUS reagent. The Quantification of the Adenosine Triphosphate (ATP) levels was then done by measurement of Luminescence on CLARIOstar® Microplate Reader (BMG LABTECH). As a positive control, DMSO 1000µM, inducing cell death, was used.

10. Cell proliferation analysis

Cell Titer 96® Non-Radioactive Cell Proliferation Assay (Promega cat #112) was used, according to the manufacturer's instructions, in order to assess the effect on the proliferation of the cells upon transfection or treatment with Sorafenib or ARQ092. Briefly, the cells are incubated with a premixed optimized dye solution in a 96-well plate for 4 hours at 37°C. During this time the alive cells convert the tetrazolium in the dye into formazon. The stop solution was then added and incubated overnight at 37°C in order to solubilize the formazon product. After that, the absorbance was measured at 577 nm on CIARIOstar® Microplate Reader (BMG LABTECH). As a control DMSO at 1000µM was used to kill the cells.

11. *In ovo* assessment of the Dendrimer-mediated delivery of designed Akt1/Akt2 siRNAs

The *in ovo* study was done by Inovotion (<https://www.inovotion.com/>), a company that established the egg model as a valid type of *in vivo* model situated between *in vitro* testing and the classical preclinical studies in rodents. The results obtained by such an approach gives insights into the efficiency and the cytotoxicity of a given drug. The viability of the embryo growing inside the egg and its degree of mutagenesis is said to give an insight into the cytotoxicity. Simultaneously, monitoring the size of the tumor grafted on the egg is said to give an insight into the efficacy of the used drug. In the case of this study, the delivery of the dendrimer coupled to the designed siRNAs D2Akt1 and D15Akt2 was assessed for its cytotoxicity and effect on tumor growth. In brief human cell lines (HepG2 cells and MV4-11 cells) were grafted on growing chick embryos in eggs. The grafted eggs were afterwards treated with the dendrimer at N/P ratio 5 and concentration of siRNA 50nM prepared as specified in the dendrimer-mediated transfection section and administered at 2 doses: 0.05 mg/kg and 0.025 mg/kg.

A schematic diagram of the study is presented in *Figure 14* and the details of the study are described below.

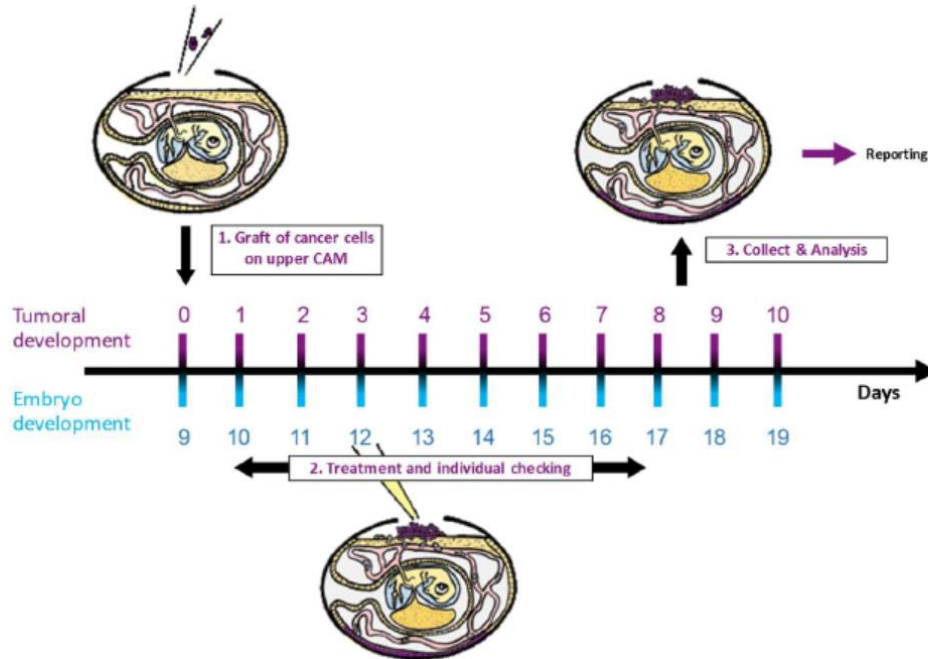


Figure 14: Scheme of in ovo study. Schematic diagram detailing the in ovo study. 1) The cancer cells are grafted into the egg through a hole in the chorioallantoic membrane (CAM), on day 9 of embryonic development (E9, in blue on the timeline), and marked as day 0 of tumoral development (in violet on the timeline). 2) The different egg groups are treated with the AD-siRNA complexes via 4 injections at 2 doses described in Table 3, while following the survival of the embryos. 3) On day E18, the tumors are collected, fixed and weighed. Figure adapted from study report presented in Annexes.

Preparation of chicken embryos

Fertilized White Leghorn eggs are incubated at 37.5°C with 50% relative humidity for 9 days. At that moment (E9), the chorioallantoic membrane (CAM) is dropped down by drilling a small hole through the eggshell into the air sac, and a 1cm² window is cut in the eggshell above the CAM. At least 15 eggs are grafted for each group.

Amplification and grafting of tumor cells

MV4-11 tumor cells are cultivated in Iscove's Modified Dulbecco's Medium (IMDM) supplemented with 10% FBS and 1% penicillin/streptomycin. On day E9, cells are detached with trypsin, washed with complete medium and suspended in graft medium. An inoculum of 3.10⁶ MV4-11 cells is added onto the CAM of each egg (E9) and then eggs are randomized into groups.

HepG2 tumor cell line is cultivated in MEM medium supplemented with 10% FBS, 1% Glutamine, 1% Pyruvate and 1% penicillin/streptomycin. On day E9, cells are detached with trypsin, washed with complete medium and suspended in graft medium. An inoculum of $0,5 \cdot 10^6$ cells is added onto the CAM of each egg (E9) and then eggs are randomized into groups

Treatments

Before the first treatment, viability of each egg is checked and surviving eggs are randomized in groups. All eggs of a group are treated with a volume of 100 μ l of the working solution of compound (freshly prepared), as detailed in *Table 3*.

Table 3: Description of Egg groups. Neg Ctrl: negative control; Sol.: Solution; E: Embryo Day.

# Group	Description	Cpd Name	[Injected Sol.]	Final [in ovo]	Dosing Regimen (Single/Multiple)
1	Neg. Ctrl.	Nanoparticle siRNA Control	- 0.03 mg/ml	- 0.05 mg/kg	E11/E13/E15/E17
2	D2 Akt1 [1]	Nanoparticle D2 Akt1	- 0.015 mg/ml	- 0.025 mg/kg	E11/E13/E15/E17
3	D2 Akt1 [2]	Nanoparticle D2 Akt1	- 0.03 mg/ml	- 0.05 mg/kg	E11/E13/E15/E17
4	D15 Akt2 [1]	Nanoparticle D15 Akt2	- 0.015 mg/ml	- 0.025 mg/kg	E11/E13/E15/E17
5	D15 Akt2 [2]	Nanoparticle D15 Akt2	- 0.03 mg/ml	- 0.05 mg/kg	E11/E13/E15/E17

Quantitative evaluation of tumor growth and embryonic tolerability

On day E18, the upper portion of the CAM (with tumor) is removed, washed by PBS buffer and then directly transferred in PFA (fixation for 24 hours). After that, tumors are carefully cut away from normal CAM tissue and weighed. Embryonic viability is checked daily. The number of dead embryos is also counted on E18, to evaluate treatment-induced embryo toxicity. The final death ratio and a Kaplan-Meyer curve are provided for all groups along with any visible abnormality observed during the study is also shortly described in the results section.

12. Proteome profiling of Akt kinase activity

Proteome Profiler Human Phospho-Kinase Array Kit (R&D cat #ARY003C) was used in order to assess the phosphorylation of a list of 37 kinase phosphorylation sites with 2 related total proteins, *see Table 4*. The assay is constituted of 2 membranes A and B which harbor capture and control antibodies, spotted in duplicate. Cell lysates were prepared according to the manufacturer's instructions using Lysis Buffer 6 (supplied with the kit) and supplemented with Halt™ Phosphatase Inhibitor Cocktail (100x) (Thermo Fischer Scientific cat #78428) and Halt™ Protease Inhibitor Cocktail, EDTA free (100x) (Thermo Fischer Scientific cat #78437) diluted 1/100. BCA protein quantification was done. Membranes were first blocked using a blocking solution supplied with the kit (Array buffer 1) and each membrane was then incubated with 200µg of protein lysate overnight. The next day, the membranes were washed 3 times (10 minutes each wash), to remove excess unbound proteins. Afterwards, the membranes were incubated with a cocktail of biotinylated detection antibodies for 2 hours at room temperature. After that, the membranes were washed again and Streptavidin-HRP and chemiluminescent detection reagents were applied, and a signal is produced at each capture spot corresponding to the amount of phosphorylated protein bound. The images of the membranes were taken using Vilber Fusion FX. The quantification of the spots was done using ImageJ giving the mean pixel intensity of each spot.

Table 4: List of 37 tested proteins in the phospho-array. S: Serine; T: Threonine; Y: Tyrosine. Abbreviations of the proteins are in the table.

Targeted Protein	Abbreviation	Phosphorylated site
CREB	cAMP-response element binding protein	S133
EGF R	Epidermal Growth Factor -Receptor	Y1086
eNOS	Endothelial Nitric Oxide Synthase	S1177
ERK1/2	Extracellular Signal-Regulated Kinase 1/2	T202/Y204, T185/Y187
Chk-2	Checkpoint kinase-2	T68
c-Jun/AP-1	Activator Protein-1	S63
Fgr/v-Fgr	Gardner-Rasheed feline sarcoma viral	Y412
GSK-3 α / β	Glycogen Synthase Kinase 3 α / β	S21/S9
GSK-3 β	Glycogen Synthase Kinase 3 β	S9
HSP27	Heat Sock Protein 27	S78/S82
P53	Protein 53	S15
P53	Protein 53	S46
P53	Protein 53	S392
JNK 1/2/3	c-Jun N-terminal Kinase 1/2/3	T183/Y185, T221/Y223
Lck	Lymphocyte-specific Protein tyrosine Kinase	Y394
Lyn	Lck/Yes-related novel protein tyrosine kinase	Y397
MSK1/2	Mitogen-and Stress-activated protein Kinases1/2	S376/S360
P70 S6 Kinase	Ribosomal Protein S6 Kinase	T389
P70 S6kinase	Ribosomal Protein S6 Kinase	T421/S424
PRAS40	Proline-RIch Akt Substrate of 40 kDa	T246
P38 α	Protein 38	T180/Y182
PDGF R β	Platelet-Derived Growth Factor – Receptor β	Y751
PLC- γ 1	PhosphoLipase-C γ 1	Y783
Src	Sarcoma	Y419
PYK2	Protein Tyrosine Kinase 2	Y402
RSK1/2	Ribosomal S6 Kinase 1/2	S221/S227
RSK1/2/3	Ribosomal S6 Kinase 1/2/3	S380/S386/S377
STAT2	Signal Transducer and Activator of Transcription 2	Y689
Stat5a/b	Signal Transducer and Activator of Transcription5a/b	Y694/Y699
WNK1	Lysine Deficient Protein Kinase 1	T60
Yes	Tyrosine-protein kinase	Y426
STAT1	Signal Transducer and Activator of Transcription 1	Y701
STAT3	Signal Transducer and Activator of Transcription 3	Y705
STAT3	Signal Transducer and Activator of Transcription 3	S727
β -Catenin	-	-
STAT6	Signal Transducer and Activator of Transcription 6	Y641
HSP60	Heat Sock Protein 60	-

13. Kinase profiling on Pamstation®12

The serine threonine kinase assay performed on PamChip® arrays on the PamStation®12 (Pamgene cat #31500) is a high-throughput flow-through microarray assay to determine the activity of serine threonine kinases. The phosphorylation activity is determined using peptides immobilized on the PamChip® (Pamgene cat #32501) arrays. The phosphorylation activity is detected with a fluorescently labelled antibody and recorded by a CCD-camera in the PamStation®12. The PamStation®12 is specifically intended for the processing of one up to three PamChip®4 microarrays. Both the instrument and the PamChip® microarrays are products of PamGene International B.V (<https://www.pamgene.com/>). A schematic diagram of the assay is shown in *Figure 15*. During the assay, the assay mix is pumped up and down through the porous 3D arrays.

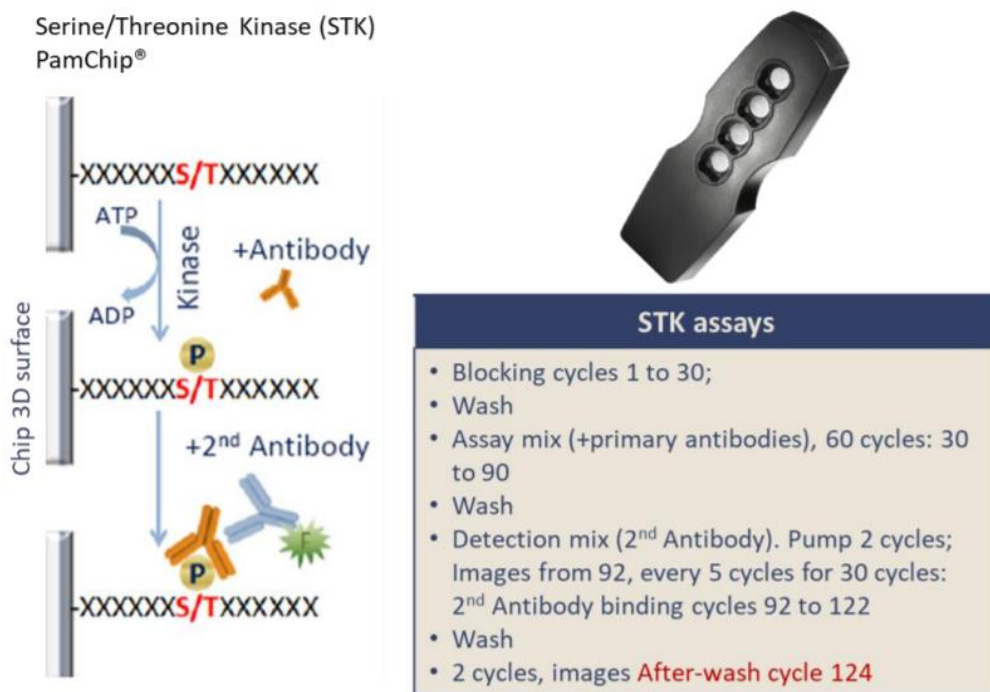


Figure 15: Pamgene principle. Representative diagram of the principle of function of the Pamchip (to the left), and a brief summary of the protocol (on the right). Abbreviations: STK: Serine/Threonine kinase; ATP: Adenosine triphosphate; ADP: Adenosine diphosphate. Figure adapted from protocol on Pamgene website (<http://www.pamgene.com/>).

The cell lysate was prepared by lysing the cells in M-PER™ Mammalian extraction buffer (Thermo Fischer Scientific cat #78503) supplemented with Halt™ Phosphatase Inhibitor Cocktail (100x) (Thermo Fischer Scientific cat #78428) and

Halt™ Protease Inhibitor Cocktail, EDTA free (100x) (Thermo Fischer Scientific cat #78437) according to the protocol advised by Pamgene. A protein dosage by BCA was done before snap freezing the samples on dry ice. The day in which the Serine/Threonine kinase assay is performed, the cell lysates are defrozed on ice, diluted with M-PER mammalian extraction buffer supplemented with the anti-protease and anti-phosphatase cocktails stated before to attain 1 µg of protein.

The reagents used from are all supplied by the STK reagent kit (Pamgene cat #32201) and follow the protocol supplied by Pamgene. In brief, first, the chips were loaded into the PamStation®12 and blocked using 1% BSA. Just before loading the samples were mixed with the reaction mix encompassing the diluted primary antibody. One hour and a half later, the detection mix is added onto the chips. At the end of the run, the images obtained by the PamStation®12 were sent to Pamgene for analysis.

14. Statistical analysis

All the statistical analysis were done with the specialized computer software Prism® (GraphPad Software). For each represented figure, the statistical test used, along with the significance (p-value) are specified in the legends.

VIII. RESULTS

1. Designing and screening of siRNAs simultaneously targeting human and rodent *Akt1* and *Akt2*

Human and rodent *Akt1* and *Akt2* isoforms share 81% nucleotide sequence similarity thus spurred the idea of designing siRNAs that simultaneously target human and rodent *Akt* isoforms [312]. The computation model Designer of siRNA (DSIR) bioinformatics tool was used to generate 21-nucleotide sequences of siRNA. For each siRNA exists 2 strands: the sense strand (SS) (or passenger) and the antisense strand (AS) (or guide).

1.1 Preliminary Akt1 siRNA design and screening

As a first step, sequence of *Mus musculus Akt1* (NM_009652.3) was used as a template for the generation of the 21-nucleotide siRNA sequences targeting *Akt1* mRNA. DSIR gave a list of 21 candidates for *Akt1* siRNA. The candidates were named according to the order they were generated in by the DSIR. For instance: the first candidate given by the DSIR for a siRNA against *Akt1* was named D1Akt1 siRNA, the second was named D2Akt1 and so on.

The screening of the candidates relied first on *in silico* analysis through NCBI blasting bioinformatics tool. The process included first blasting each siRNA sequence (SS and AS strands) against the *Rattus norvegicus* and *Homo sapiens* genome in order to decipher the cross-reactivity. NCBI blasting screens for degrees of homology between the given siRNA sequence and genes in the genome of the species. The degree of homology is attributed as a percentage of query cover and identity, *see Table 5*. Every siRNA sequence (AS and SS strands) that gave a percentage of query cover and identity of 80% or higher to *Akt1* gene in each of the species was considered as a candidate that cross-reacts the three species. Among the 21 *Akt1* siRNA candidates, 7 candidates showed a cross-reactivity between the 3 species: **D2Akt1, D6Akt1, D7Akt1, D8Akt1, D10Akt1, D11Akt1, and D15Akt1** siRNAs

Table 5: Inter-species reactivity of Akt1 siRNA candidates. The siRNA candidates in bold are the ones that show a cross reactivity to the three species. SS: sense strand; AS: anti-sense strand.

siRNA	Sequence	<i>Mus musculus</i>		<i>Rattus norvegicus</i>		<i>Homo sapiens</i>	
		Query cover	Identity	Query cover	Identity	Query cover	Identity
D1Akt1	SS sequence	100%	100%	100%	95.24%	-	-
	AS sequence	100%	100%	100%	95.24%	-	-
D2Akt1	SS sequence	100%	100%	90%	100%	90%	100%
	AS sequence	100%	100%	100%	100%	100%	100%
D3Akt1	SS sequence	100%	100%	100%	100%	-	-
	AS sequence	100%	100%	100%	100%	95%	95%
D4Akt1	SS sequence	100%	100%	-	-	-	-
	AS sequence	100%	100%	100%	95.24%	-	-
D5Akt1	SS sequence	100%	100%	90%	95%	-	-
	AS sequence	100%	100%	100%	95%	-	-
D6Akt1	SS sequence	100%	100%	100%	100%	66%	100%
	AS sequence	100%	100%	100%	100%	90%	94.74%
D7Akt1	SS sequence	100%	100%	100%	95.24%	90%	100%
	AS sequence	100%	100%	100%	100%	80%	100%
D8Akt1	SS sequence	100%	100%	100%	100%	71%	100%
	AS sequence	100%	100%	100%	100%	80%	100%
D9Akt1	SS sequence	100%	100%	-	-	-	-
	AS sequence	100%	100%	-	-	-	-
D10Akt1	SS sequence	100%	100%	100%	100%	90%	100%
	AS sequence	100%	100%	100%	100%	80%	100%
D11Akt1	SS sequence	100%	100%	100%	100%	80%	100%
	AS sequence	100%	100%	100%	100%	80%	100%
D12Akt1	SS sequence	100%	100%	100%	100%	-	-
	AS sequence	100%	100%	95%	100%	-	-
D13Akt1	SS sequence	100%	100%	80%	100%		
	AS sequence	100%	100%	71%	100%		
D14Akt1	SS sequence	100%	100%	100%	95.24%	-	-
	AS sequence	100%	100%	100%	95.24%	-	-
D15Akt1	SS sequence	100%	100%	100%	100%	80%	100%
	AS sequence	100%	100%	100%	100%	76%	100%
D16Akt1	SS sequence	100%	100%	76%	100%	-	-
	AS sequence	100%	100%	66%	100%	-	-
D17Akt1	SS sequence	100%	100%	100%	100%	-	-
	AS sequence	100%	100%	100%	100%	-	-

D18Akt1	SS sequence	100%	100%	-	-	-	-
	AS sequence	100%	100%	-	-	-	-
D19Akt1	SS sequence	100%	100%	-	-	90%	100%
	AS sequence	100%	100%	-	-	80%	100%
D20Akt1	SS sequence	100%	100%	95%	100%	-	-
	AS sequence	100%	100%	85%	100%	-	-
D21Akt1	SS sequence	100%	100%	100%	95.24%	100%	95.24%
	AS sequence	100%	100%	100%	95.24%	100%	95.24%

Afterwards, deep *in silico* analysis to select the best 4 candidates of siRNA was done. Data from the NCBI not only deciphered the cross-reactivity of Akt1 siRNA sequences to genes among the species, it also unraveled a possible targeting of other genes considered as “mismatches” and referred to as an “off-target effect”. In addition, analysis of the degree of the alignment to the seed sequence – (2nd to the 7th nucleotides of the AS strand)- was studied for each mismatched gene, since it has been shown to dictate the specificity of the siRNA [313]. Genes having a percentage of query cover and identity over 55% and/or 3 or more nucleotide alignment in the seed sequence were taken into account as an off-target gene effect, see Table 6 for the off-target effect in *Homo sapiens*, see Table 7 for that in *Mus musculus*, and see Table 8 for that in *Rattus norvegicus*.

Table 6: Off-target effect of Akt1 siRNA candidates in *Homo sapiens*. Seed sequence (from nucleotide 2 to nucleotide 7) is marked in red. Homology to the siRNA sequence is in bold.

siRNA	Gene name	Position on the siRNA sequence 5' -> 3'	Query cover	Identities
D2Akt1	<i>INTS5</i>	U UCUUGAGGAGGAAGUAGCGU	71%	15/15
	<i>MTNR1B</i>	U UCUUGAGGAGGAAGUAGCGU	71%	15/15
D6Akt1	<i>CPNE8</i>	U AGAGUUCUGCAGGACACGGU	71%	15/15
	<i>CPNE5</i>	U AGAGUUCUGCAGGACACGGU	71%	15/15
	<i>HMGCGR</i>	U AGAGUUCUGCAGGACACGGU	71%	15/15
D7Akt1	<i>RPL13A</i>	U ACACCACGUUCUUCUGGAG	71%	15/15
	<i>DNAH1</i>	U ACACCACGUUCUUCUGGAG	66%	14/14
	<i>SIX6</i>	U ACACCACGUUCUUCUGGAG	66%	14/14
D8Akt1	<i>WDR72</i>	U GUAGGGUCCUUCUUGAGCAG	95%	19/20
	<i>KDM5D</i>	U GUAGGGUCCUUCUUGAGCAG	80%	17/17
D10Akt1	<i>RP6KA4</i>	U UGCACAGCCCGAAGUCCGUU	95%	19/20
	<i>FBXL2</i>	U UGCACAGCCCGAAGUCCGUU	66%	14/14

	TBX20 TV2	UUGCACAG CCCGAAGUCCGUU	66%	14/14
D11Akt1	Akt2	UUGUCCU CCAGCACCUCAGGG	95%	20/20
	FUBP1	UUGUCCU CCAGCACCUCAGGG	85%	18/18
	SBNO2	UUGUCCU CCAGCACCUCAGGG	76%	16/16
	MYCBP2	UUGUCCU CCAGCACCUCAGGG	76%	16/16
	ZNF541	UUGUCCU CCAGCACCUCAGGG	80%	17/17
D15Akt1	KIAA1841	UG AUGGU GAUCAUCUGAGCUG	71%	15/15
	EEF2	UG AUGGU GAUCAUCUGAGCUG	71%	15/15
D21Akt1	SBK2	UUCUCCA GPUUCAGGUCCCGG	100%	20/21
	PRKCG	UUCUCCA GPUUCAGGUCCCGG	76%	16/16
	TTC22	UUCUCCA GPUUCAGGUCCCGG	76%	16/16
	GNB1L	UUCUCCA GPUUCAGGUCCCGG	76%	16/16
	PRKCZ	UUCUCCA GPUUCAGGUCCCGG	76%	16/16
	MMP2	UUCUCCA GPUUCAGGUCCCGG	76%	16/16
	OR10J1	UUCUCCA GPUUCAGGUCCCGG	76%	16/16

Table 7: Off-target effect of Akt1 siRNA candidates in *Mus musculus*. Seed sequence (from nucleotide 2 to nucleotide 7) marked in red. Homology to the siRNA sequence is in bold.

siRNA	Gene name	Position on the siRNA sequence 5' -> 3'	Query Cover	Identities
D2Akt1	<i>Cfap43</i>	UUCUUGA GGAGGAAGUAGCGU	76%	16/16
	<i>C4bp</i>	UUCUUGA GGAGGAAGUAGCGU	95%	19/20
	<i>Rrs1</i>	UUCUUGA GGAGGAAGUAGCGU	76%	16/16
	<i>Senp3</i>	UUCUUGA GGAGGAAGUAGCGU	71%	15/15
D6Akt1	<i>Zfp655</i>	U AGAGUU CUGCAGGACACGGU	71%	15/15
	<i>Ctma3</i>	U AGAGUU CUGCAGGACACGGU	71%	15/15
	<i>Olf1377</i>	U AGAGUU CUGCAGGACACGGU	71%	15/15
	<i>Ligp1</i>	U AGAGUU CUGCAGGACACGGU	71%	15/15
	<i>Gpr35</i>	U AGAGUU CUGCAGGACACGGU	71%	15/15
D7Akt1	<i>Cdcp3</i>	UACACCA CGUUCUUCUCGGAG	71%	15/15
	<i>Il20ra</i>	UACACCA CGUUCUUCUCGGAG	71%	15/15
	<i>Muc2</i>	UACACCA CGUUCUUCUCGGAG	66%	14/14
	<i>Gfod2 tv4</i>	UACACCA CGUUCUUCUCGGAG	66%	14/14
	<i>Grm2</i>	UACACCA CGUUCUUCUCGGAG	66%	14/14

	<i>SLc52a2</i>	U ACACCA CGUUCUUCUGGAG	66%	14/14
	<i>Gm34507</i>	U ACACCA CGUUCUUCUGGAG	66%	14/14
D8Akt1	<i>Mdm4</i>	U GUAGGG UCCUUCUUGAGCAG	90%	18/19
	<i>Sox14</i>	U GUAGGG UCCUUCUUGAGCAG	71%	15/15
	<i>Sox1</i>	U GUAGGG UCCUUCUUGAGCAG	71%	15/15
	<i>Dlgap4 toX19</i>	U GUAGGG UCCUUCUUGAGCAG	66%	14/14
	<i>Eif2ak3 toX2</i>	U GUAGGG UCCUUCUUGAGCAG	66%	14/14
	<i>Nkiras</i>	U GUAGGG UCCUUCUUGAGCAG	66%	14/14
D10Akt1	<i>Mical1</i>	U UGCACA GCCCGAAGUCCGUU	66%	14/14
	<i>Mical1</i>	U UGCACA GCCCGAAGUCCGUU	66%	14/14
	<i>LOC115489151</i>	U UGCACA GCCCGAAGUCCGUU	66%	14/14
	<i>Ap1s2</i>	U UGCACA GCCCGAAGUCCGUU	66%	14/14
	<i>Rab11b</i>	U UGCACA GCCCGAAGUCCGUU	61%	13/13
	<i>Rab11b</i>	U UGCACA GCCCGAAGUCCGUU	61%	13/13
	<i>Ksr1</i>	U UGCACA GCCCGAAGUCCGUU	61%	13/13
	<i>ksr1</i>	U UGCACA GCCCGAAGUCCGUU	61%	13/13
D11Akt1	<i>fubp1</i>	U UGUCCU CCAGCACCUCAGGG	85%	18/18
	<i>Majin</i>	U UGUCCU CCAGCACCUCAGGG	76%	16/16
	<i>Strn3</i>	U UGUCCU CCAGCACCUCAGGG	76%	16/16
	<i>Akt2</i>	U UGUCCU CCAGCACCUCAGGG	95%	19/20
	<i>figla</i>	U UGUCCU CCAGCACCUCAGGG	76%	16/16
	<i>Mfap2</i>	U UGUCCU CCAGCACCUCAGGG	76%	16/16
D15Akt1	<i>Cop1</i>	U GAUGGU GAUCAUCUGAGCUG	71%	15/15
	<i>Rnf216</i>	U GAUGGU GAUCAUCUGAGCUG	71%	15/15
	<i>Syn3</i>	U GAUGGU GAUCAUCUGAGCUG	71%	15/15
	<i>Eef2</i>	U GAUGGU GAUCAUCUGAGCUG	71%	15/15
D21Akt1	<i>Nuak1</i>	U UCUCCA GPUUCAGGUCCCGG	100%	20/21
	<i>Plekha7</i>	U UCUCCA GPUUCAGGUCCCGG	76%	16/16
	<i>Mmp2</i>	U UCUCCA GPUUCAGGUCCCGG	76%	16/16
	<i>Nup133</i>	U UCUCCA GPUUCAGGUCCCGG	76%	16/16
	<i>Phkg1</i>	U UCUCCA GPUUCAGGUCCCGG	95%	19/20
	<i>Rfwd3</i>	U UCUCCA GPUUCAGGUCCCGG	76%	16/16
	<i>Rps6ka4</i>	U UCUCCA GPUUCAGGUCCCGG	100%	21/21

Table 8: Off-target effect of Akt1 siRNA candidates in *Rattus norvegicus*. Seed sequence (from nucleotide 2 to nucleotide 7) is marked in red. Homology to the siRNA sequence is in bold.

siRNA	Gene name	Position on the siRNA sequence 5' -> 3'	Query Cover	Identities
D2Akt1	<i>Senp3</i>	UUCUUGA GGAGGAAGUAGCGU	76%	16/16
	<i>Slc12a6</i>	UUCUUGA GGAGGAAGUAGCGU	71%	15/15
	<i>Ptgis</i>	UUCUUGA GGAGGAAGUAGCGU	71%	15/15
	<i>Ccn4</i>	UUCUUGA GGAGGAAGUAGCGU	71%	15/15
	<i>Trip12</i>	UUCUUGA GGAGGAAGUAGCGU	66%	14/14
	<i>Baz1a</i>	UUCUUGA GGAGGAAGUAGCGU	66%	14/14
	<i>Rbmy1j</i>	UUCUUGA GGAGGAAGUAGCGU	66%	14/14
	<i>Arghap32</i>	UUCUUGA GGAGGAAGUAGCGU	66%	14/14
	<i>Syt7</i>	UUCUUGA GGAGGAAGUAGCGU	76%	16/16
	<i>Loc501116</i>	UUCUUGA GGAGGAAGUAGCGU	66%	14/14
	<i>Dot1l</i>	UUCUUGA GGAGGAAGUAGCGU	66%	14/14
	<i>Strc</i>	UUCUUGA GGAGGAAGUAGCGU	66%	14/14
	<i>Myo15a</i>	UUCUUGA GGAGGAAGUAGCGU	66%	14/14
	<i>Tmem151a</i>	UUCUUGA GGAGGAAGUAGCGU	66%	14/14
	<i>Arghef10</i>	UUCUUGA GGAGGAAGUAGCGU	80%	14/14
<i>Hikeshi</i>	UUCUUGA GGAGGAAGUAGCGU	66%	14/14	
D6Akt1	<i>Tep1</i>	UAGAGUU CUGCAGGACACGGU	66%	14/14
	<i>Cngb3</i>	UAGAGUU CUGCAGGACACGGU	71%	15/15
	<i>Ikbb</i>	UAGAGUU CUGCAGGACACGGU	66%	14/14
	<i>Cpne5</i>	UAGAGUU CUGCAGGACACGGU	66%	14/14
	<i>Pkdcc</i>	UAGAGUU CUGCAGGACACGGU	66%	14/14
	<i>Cntn6</i>	UAGAGUU CUGCAGGACACGGU	66%	14/14
	<i>Brwd1</i>	UAGAGUU CUGCAGGACACGGU	61%	13/13
	<i>Nhsl2</i>	UAGAGUU CUGCAGGACACGGU	61%	13/13
	<i>P2ry4</i>	UAGAGUU CUGCAGGACACGGU	61%	13/13
	<i>Rgd1565959</i>	UAGAGUU CUGCAGGACACGGU	61%	13/13
	<i>Slc26a10</i>	UAGAGUU CUGCAGGACACGGU	61%	13/13
	<i>Cpne8</i>	UAGAGUU CUGCAGGACACGGU	61%	13/13
	<i>Spats2</i>	UAGAGUU CUGCAGGACACGGU	61%	13/13
	<i>Sync</i>	UAGAGUU CUGCAGGACACGGU	80%	16/17
	<i>Gpr63</i>	UAGAGUU CUGCAGGACACGGU	61%	13/13
	<i>Gprin3</i>	UAGAGUU CUGCAGGACACGGU	61%	13/13
	<i>Rgd1560248</i>	UAGAGUU CUGCAGGACACGGU	61%	13/13
	<i>Gfra4</i>	UAGAGUU CUGCAGGACACGGU	61%	13/13
	<i>Sla2</i>	UAGAGUU CUGCAGGACACGGU	61%	13/13
	<i>Ctnna3</i>	UAGAGUU CUGCAGGACACGGU	61%	13/13

	<i>P4ha1</i>	UAGAGUUCUGCAGGACACGGU	61%	13/13
	<i>Zfp704</i>	UAGAGUUCUGCAGGACACGGU	61%	13/13
	<i>Plch1</i>	UAGAGUUCUGCAGGACACGGU	61%	13/13
	<i>Cd180</i>	UAGAGUUCUGCAGGACACGGU	61%	13/13
	<i>Zfp827</i>	UAGAGUUCUGCAGGACACGGU	61%	13/13
	<i>Loc684327</i>	UAGAGUUCUGCAGGACACGGU	61%	13/13
	<i>Tifab</i>	UAGAGUUCUGCAGGACACGGU	61%	13/13
	<i>Erich1</i>	UAGAGUUCUGCAGGACACGGU	61%	13/13
	<i>Gins4</i>	UAGAGUUCUGCAGGACACGGU	61%	13/13
	<i>Cdca2</i>	UAGAGUUCUGCAGGACACGGU	61%	13/13
	<i>Xpo4</i>	UAGAGUUCUGCAGGACACGGU	61%	13/13
	<i>Mettl13</i>	UAGAGUUCUGCAGGACACGGU	61%	13/13
D7Akt1	<i>Akap6</i>	UACACCA CGUUCUUCUCGGAG	66%	14/14
	<i>Gfod2</i>	UACACCA CGUUCUUCUCGGAG	66%	14/14
	<i>Kdr</i>	UACACCA CGUUCUUCUCGGAG	66%	14/14
	<i>Teddm1</i>	UACACCA CGUUCUUCUCGGAG	66%	14/14
	<i>Kcnd3</i>	UACACCA CGUUCUUCUCGGAG	61%	13/13
	<i>Rilpl1</i>	UACACCA CGUUCUUCUCGGAG	61%	13/13
	<i>Gemin5</i>	UACACCA CGUUCUUCUCGGAG	61%	13/13
	<i>Mrpl53</i>	UACACCA CGUUCUUCUCGGAG	61%	13/13
	<i>Zfp653</i>	UACACCA CGUUCUUCUCGGAG	61%	13/13
	<i>Foxc2</i>	UACACCA CGUUCUUCUCGGAG	80%	16/17
	<i>Hsp70</i>	UACACCA CGUUCUUCUCGGAG	61%	13/13
	<i>Slc46a3</i>	UACACCA CGUUCUUCUCGGAG	61%	13/13
	<i>Zfp532</i>	UACACCA CGUUCUUCUCGGAG	66%	14/14
	<i>Loc498971</i>	UACACCA CGUUCUUCUCGGAG	61%	13/13
	<i>Muc2</i>	UACACCA CGUUCUUCUCGGAG	66%	14/14
	<i>Loc684709</i>	UACACCA CGUUCUUCUCGGAG	66%	14/14
	<i>Dgkb</i>	UACACCA CGUUCUUCUCGGAG	61%	13/13
	<i>Wtp1</i>	UACACCA CGUUCUUCUCGGAG	61%	13/13
	<i>Rrh1</i>	UACACCA CGUUCUUCUCGGAG	61%	13/13
	<i>Ntn3</i>	UACACCA CGUUCUUCUCGGAG	61%	13/13
	<i>Stam</i>	UACACCA CGUUCUUCUCGGAG	61%	13/13
	<i>Loc681458</i>	UACACCA CGUUCUUCUCGGAG	61%	13/13
	<i>Stx4</i>	UACACCA CGUUCUUCUCGGAG	61%	13/13
	<i>Scd4</i>	UACACCA CGUUCUUCUCGGAG	61%	13/13
<i>Ceacam18</i>	UACACCA CGUUCUUCUCGGAG	61%	13/13	
<i>Loc103692169</i>	UACACCA CGUUCUUCUCGGAG	61%	13/13	
<i>Scd Tbx1</i>	UACACCA CGUUCUUCUCGGAG	61%	13/13	
D8Akt1	<i>Akt2</i>	UGUAGGGUCCUUCUUGAGCAG	80%	17/17
	<i>Cubn</i>	UGUAGGGUCCUUCUUGAGCAG	66%	14/14

	<i>Cdc42ep4</i>	UGUAGGGUCCUUCUUGAGCAG	66%	14/14
	<i>Luzp1</i>	UGUAGGGUCCUUCUUGAGCAG	66%	14/14
	<i>Nkiras2</i>	UGUAGGGUCCUUCUUGAGCAG	66%	14/14
	<i>Sox1</i>	UGUAGGGUCCUUCUUGAGCAG	71%	15/15
	<i>Sox3</i>	UGUAGGGUCCUUCUUGAGCAG	71%	15/15
	<i>Mdm4</i>	UGUAGGGUCCUUCUUGAGCAG	66%	14/14
	<i>Krt40</i>	UGUAGGGUCCUUCUUGAGCAG	66%	14/14
	<i>Vsig1</i>	UGUAGGGUCCUUCUUGAGCAG	61%	13/13
	<i>Tbc1d2b</i>	UGUAGGGUCCUUCUUGAGCAG	61%	13/13
	<i>Scn5a</i>	UGUAGGGUCCUUCUUGAGCAG	61%	13/13
	<i>Stac3</i>	UGUAGGGUCCUUCUUGAGCAG	61%	13/13
	<i>Pop1</i>	UGUAGGGUCCUUCUUGAGCAG	61%	13/13
	<i>Prph1</i>	UGUAGGGUCCUUCUUGAGCAG	80%	16/17
	<i>Fbxo33</i>	UGUAGGGUCCUUCUUGAGCAG	61%	13/13
	<i>Klhl29</i>	UGUAGGGUCCUUCUUGAGCAG	61%	13/13
	<i>Hpca</i>	UGUAGGGUCCUUCUUGAGCAG	61%	13/13
	<i>Myh7b</i>	UGUAGGGUCCUUCUUGAGCAG	61%	13/13
	<i>Capn7</i>	UGUAGGGUCCUUCUUGAGCAG	61%	13/13
	<i>Mtif3</i>	UGUAGGGUCCUUCUUGAGCAG	61%	13/13
	<i>Ncor2</i>	UGUAGGGUCCUUCUUGAGCAG	61%	13/13
D10Akt1	<i>Rgd1563888</i>	UUGCACAGCCCGAAGUCCGUU	66%	14/14
	<i>Cavin2</i>	UUGCACAGCCCGAAGUCCGUU	66%	14/14
	<i>Igdcc3</i>	UUGCACAGCCCGAAGUCCGUU	61%	13/13
	<i>Mical1</i>	UUGCACAGCCCGAAGUCCGUU	61%	13/13
	<i>Ksr1</i>	UUGCACAGCCCGAAGUCCGUU	61%	13/13
	<i>Prkca</i>	UUGCACAGCCCGAAGUCCGUU	80%	16/17
	<i>Olr1597</i>	UUGCACAGCCCGAAGUCCGUU	61%	13/13
	<i>Coro1b</i>	UUGCACAGCCCGAAGUCCGUU	61%	13/13
	<i>Limk2</i>	UUGCACAGCCCGAAGUCCGUU	61%	13/13
	<i>Prkcd</i>	UUGCACAGCCCGAAGUCCGUU	80%	16/17
	<i>Tns3</i>	UUGCACAGCCCGAAGUCCGUU	61%	13/13
	<i>Pkp2</i>	UUGCACAGCCCGAAGUCCGUU	61%	13/13
	<i>Slc22a23</i>	UUGCACAGCCCGAAGUCCGUU	61%	13/13
	<i>Gsap</i>	UUGCACAGCCCGAAGUCCGUU	61%	13/13
	<i>Pdgfc</i>	UUGCACAGCCCGAAGUCCGUU	61%	13/13
	<i>Loc103691267</i>	UUGCACAGCCCGAAGUCCGUU	66%	14/14
	<i>Tub</i>	UUGCACAGCCCGAAGUCCGUU	80%	16/17
	<i>Loc102552663</i>	UUGCACAGCCCGAAGUCCGUU	61%	13/13
	<i>Loc102546864</i>	UUGCACAGCCCGAAGUCCGUU	80%	16/17
	<i>Tgfb2</i>	UUGCACAGCCCGAAGUCCGUU	61%	13/13
	<i>Loc102547118</i>	UUGCACAGCCCGAAGUCCGUU	61%	13/13
	<i>Mob3c</i>	UUGCACAGCCCGAAGUCCGUU	61%	13/13

	<i>Pram1</i>	UGCACA GCCCGAAGUCCGUU	61%	13/13
	<i>Recq14</i>	UGCACA GCCCGAAGUCCGUU	66%	12/12
	<i>Tbxa2r</i>	UGCACA GCCCGAAGUCCGUU	66%	12/12
	<i>Itpk1</i>	UGCACA GCCCGAAGUCCGUU	66%	12/12
D11Akt1	<i>Arvcf</i>	UGUCCU CCAGCACCUCAGGG	80%	17/17
	<i>Akt2</i>	UGUCCU CCAGCACCUCAGGG	95%	19/20
	<i>Klhl25</i>	UGUCCU CCAGCACCUCAGGG	76%	16/16
	<i>Cabin1</i>	UGUCCU CCAGCACCUCAGGG	71%	15/15
	<i>Trem2</i>	UGUCCU CCAGCACCUCAGGG	71%	15/15
	<i>Grin2d</i>	UGUCCU CCAGCACCUCAGGG	71%	15/15
	<i>Tbc1d23</i>	UGUCCU CCAGCACCUCAGGG	66%	14/14
	<i>Urb2</i>	UGUCCU CCAGCACCUCAGGG	66%	14/14
	<i>Tmprss12</i>	UGUCCU CCAGCACCUCAGGG	71%	15/15
	<i>Tecpr2</i>	UGUCCU CCAGCACCUCAGGG	95%	18/19
	<i>Dga2</i>	UGUCCU CCAGCACCUCAGGG	71%	15/15
D15Akt1	<i>Eef2</i>	UGAUGGU GAUCAUCUGAGCUG	71%	15/15
	<i>Slc15a1</i>	UGAUGGU GAUCAUCUGAGCUG	71%	15/15
	<i>Rcor1</i>	UGAUGGU GAUCAUCUGAGCUG	66%	14/14
	<i>Adh1</i>	UGAUGGU GAUCAUCUGAGCUG	66%	14/14
	<i>Msx3</i>	UGAUGGU GAUCAUCUGAGCUG	66%	14/14
	<i>Fcgbp1</i>	UGAUGGU GAUCAUCUGAGCUG	66%	14/14
	<i>Txndc12</i>	UGAUGGU GAUCAUCUGAGCUG	66%	14/14
	<i>Rnf216</i>	UGAUGGU GAUCAUCUGAGCUG	66%	14/14
	<i>Ccer1</i>	UGAUGGU GAUCAUCUGAGCUG	66%	14/14
	<i>Itp2</i>	UGAUGGU GAUCAUCUGAGCUG	66%	14/14
	<i>Cyp4f18</i>	UGAUGGU GAUCAUCUGAGCUG	66%	14/14
	<i>Sgpp1</i>	UGAUGGU GAUCAUCUGAGCUG	61%	13/13
	<i>Igf2bp3</i>	UGAUGGU GAUCAUCUGAGCUG	61%	13/13
	<i>Klhl15</i>	UGAUGGU GAUCAUCUGAGCUG	61%	13/13
	<i>Kctn1</i>	UGAUGGU GAUCAUCUGAGCUG	61%	13/13
	<i>Gpr155</i>	UGAUGGU GAUCAUCUGAGCUG	61%	13/13
	<i>Arfrp1</i>	UGAUGGU GAUCAUCUGAGCUG	61%	13/13
	<i>Itp3</i>	UGAUGGU GAUCAUCUGAGCUG	61%	13/13
	<i>Rnf180</i>	UGAUGGU GAUCAUCUGAGCUG	61%	13/13
	<i>Tbl1xr1</i>	UGAUGGU GAUCAUCUGAGCUG	61%	13/13
	<i>Atp6ap1l</i>	UGAUGGU GAUCAUCUGAGCUG	61%	13/13
	<i>Schip1</i>	UGAUGGU GAUCAUCUGAGCUG	80%	16/17
	<i>Galnt15</i>	UGAUGGU GAUCAUCUGAGCUG	61%	13/13
	<i>Slc25a15</i>	UGAUGGU GAUCAUCUGAGCUG	61%	13/13
	<i>Rgd1561730</i>	UGAUGGU GAUCAUCUGAGCUG	61%	13/13
	<i>Gemin5</i>	UGAUGGU GAUCAUCUGAGCUG	61%	13/13
<i>Med1</i>	UGAUGGU GAUCAUCUGAGCUG	61%	13/13	

	<i>Bnc1</i>	UGAUGGU GAUCAUCUGAGCUG	61%	13/13
	<i>Loc100365212</i>	UGAUGGU GAUCAUCUGAGCUG	66%	14/14
D21Akt1	<i>Rps6ka4</i>	UUCUCCAGCUUCAGGUCCCGG	90%	19/19
	<i>Tmem110</i>	UUCUCCAGCUUCAGGUCCCGG	80%	17/17
	<i>Nuak2</i>	UUCUCCAGCUUCAGGUCCCGG	100%	20/21
	<i>Nuak1</i>	UUCUCCAGCUUCAGGUCCCGG	95%	19/20
	<i>Phkg1</i>	UUCUCCAGCUUCAGGUCCCGG	95%	19/20
	<i>Dst</i>	UUCUCCAGCUUCAGGUCCCGG	71%	15/15
	<i>Mks1</i>	UUCUCCAGCUUCAGGUCCCGG	71%	15/15
	<i>Cwf19l1</i>	UUCUCCAGCUUCAGGUCCCGG	71%	15/15
	<i>Ttc22</i>	UUCUCCAGCUUCAGGUCCCGG	71%	15/15
	<i>Aipl1</i>	UUCUCCAGCUUCAGGUCCCGG	66%	14/14
	<i>Newgene_1305243</i>	UUCUCCAGCUUCAGGUCCCGG	76%	16/16
	<i>Loc102551828</i>	UUCUCCAGCUUCAGGUCCCGG	71%	15/15
	<i>Dnah17</i>	UUCUCCAGCUUCAGGUCCCGG	71%	15/15
	<i>Ccdc88c</i>	UUCUCCAGCUUCAGGUCCCGG	71%	15/15
	<i>Cdkl5</i>	UUCUCCAGCUUCAGGUCCCGG	66%	14/14
	<i>Dgkd</i>	UUCUCCAGCUUCAGGUCCCGG	66%	14/14
	<i>Scn2b</i>	UUCUCCAGCUUCAGGUCCCGG	66%	14/14
	<i>Cdk4</i>	UUCUCCAGCUUCAGGUCCCGG	66%	14/14
	<i>Mapk11</i>	UUCUCCAGCUUCAGGUCCCGG	66%	14/14
	<i>Krt84</i>	UUCUCCAGCUUCAGGUCCCGG	85%	17/18
	<i>Nr4a3</i>	UUCUCCAGCUUCAGGUCCCGG	66%	14/14
	<i>Col5a1</i>	UUCUCCAGCUUCAGGUCCCGG	66%	14/14
<i>Cttnbp2nl</i>	UUCUCCAGCUUCAGGUCCCGG	66%	14/14	
<i>Prkaca</i>	UUCUCCAGCUUCAGGUCCCGG	66%	14/14	
<i>Alpk2</i>	UUCUCCAGCUUCAGGUCCCGG	66%	14/14	

In order to numerically represent the data, the siRNA candidates were ranked based on the total number of off-targets in each of the species. The ranking strategy was ascending as the sum of mismatched increases as shown in *Table 9*. The 4 candidates having the least off-target effect in the 3 species were then chosen for further *in cellulo* analysis. The chosen Akt1 candidates were: **D2Akt1, D8Akt1, D11Akt1 and D15Akt1.**

Table 9: Off-target effect ranking of Akt1 siRNA candidates. . In bold are the siRNA candidates showing the least off-target effect in the 3 species.

siRNA	<i>Homo sapiens</i>		<i>Mus musculus</i>		<i>Rattus norvegicus</i>		All species Sum of Ranks
	Number of off-targets	Rank	Number of off-targets	Rank	Number of off-targets	Rank	
D2Akt1	2	1	4	1	16	2	4
D6Akt1	3	2	5	2	32	8	12
D7Akt1	3	2	7	4	27	6	12
D8Akt1	2	1	5	2	22	3	6
D10Akt1	3	2	5	2	26	5	9
D11Akt1	5	3	6	3	11	1	7
D15Akt1	2	1	4	1	29	7	9
D21Akt1	7	4	7	4	25	4	12

1.1.1. *In cellulo* assessment of the efficiency of the 4 candidates of Akt1 siRNA and choice of the best 2 candidates

The *in silico* data provided candidates; however, their efficiency should be verified upon transfection *in cellulo* in order to sort out the best among them. For that, human hepatocellular carcinoma cell line, *HepG2*, exhibiting a sustained level of expression of Akt1 was chosen for testing the efficiency of the candidates. *HepG2* cells were pulse transfected for 6 hours with the **D2Akt1**, **D8Akt1**, **D11Akt1** and **D15Akt1** siRNAs at 3 concentrations (0.1nM, 1nM and 10nM), with mock siRNA as a negative control. Protein analysis of the expression of Akt1 was done by Jess 48 hours later.

The results showed a dose-dependent decrease in the expression of Akt1 with varying efficiencies depending on the candidate, *see Figure 16*. D2Akt1 siRNA showed a 73%, 31%, and 18% decrease in the expression of Akt1 protein at 10nM, 1nM and 0.1nM siRNA concentrations, respectively. On the other hand, D11Akt1 siRNA showed a decrease in the expression of Akt1 by 83% at the 10nM concentration, 43% at the 1nM concentration, and no decrease of Akt1 expression at the 0.1nM concentration. Similarly, D15Akt1 siRNA showed no decrease of Akt1 expression at the 0.1nM concentration accompanied by a decrease in the expression of Akt1 by 62% at the 10nM and 44% at the 1nM concentration. As far as D8Akt1 siRNA is concerned, no decrease of the expression of Akt1 was observed at any of the tested concentrations, *see Table 10*.

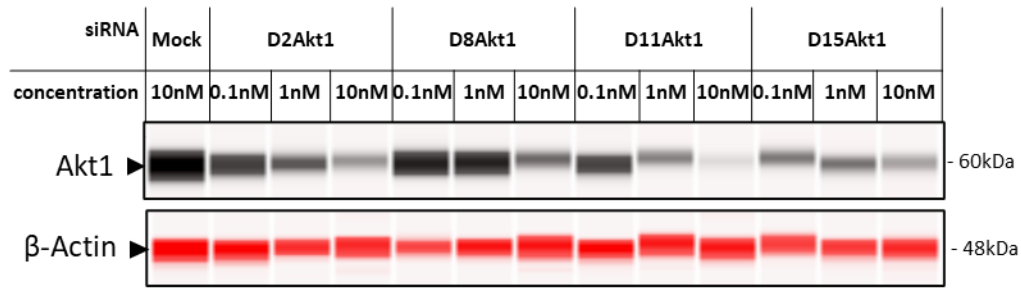
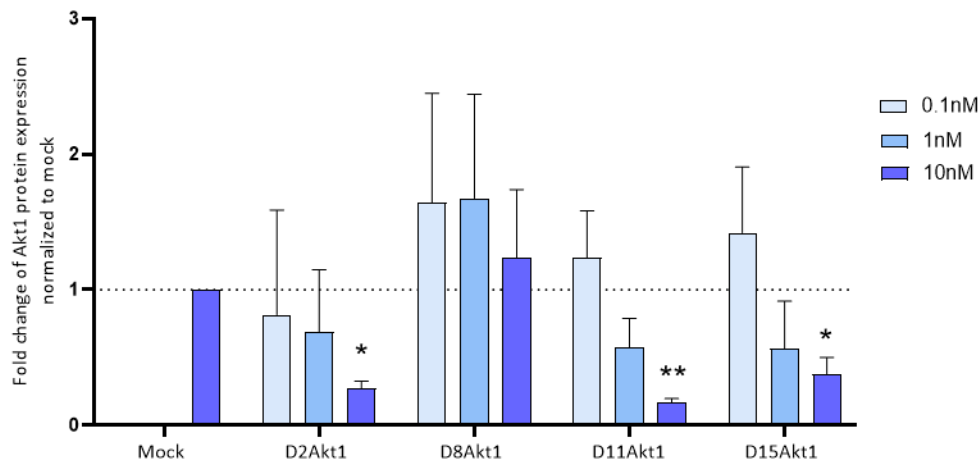
A**B**

Figure 16: Screening of Designed Akt1 siRNAs in cellulo. Efficiency of the chosen best 4 candidates of designed Akt1 siRNAs: D2Akt1, D8Akt1, D11Akt1 and D15Akt1 siRNAs (0.1, 1 and 10nM). (A) Representative protein immuno-detection by Jess 48 hours after transfection. β -Actin was used as a house keeping gene, the red color of β -Actin bands is due to their detection by NIR-coupled secondary antibody on Jess. (B) Quantification of the immuno-detection of Akt1 expression, represented as mean \pm SD (N = 3 independent experiments) of the ratio of Akt1/ β -Actin for each condition normalized to its corresponding mock concentration. Ordinary one-way ANOVA statistical analysis was done for every concentration versus the same concentration of the mock siRNA. The asterisks, in the order of their appearance on the graph from left to right, represent the following: $p=0.0115$, 0.0051 , and 0.0287 .

Given the variability of the efficiency between the tested siRNAs, and the significance being only present at the 10nM concentration, the results were again numerically represented. First, the weighed efficacy score calculated per siRNA candidate and attributed a rank. This was done by attributing a score for the mean inhibition at every concentration, followed by the calculation of the mean of all the inhibition efficiencies. The scores attributed were 1 for 10nM concentration inhibition, 2 for 1nM, and 3 for the 0.1nM concentration, see Table 10.

Table 10: Weighed *in cellulo* efficacy ranking of Akt1 siRNA candidates. The average of inhibition of Akt1 is representative of the mean inhibition in the 3 independent experiments. The red color indicates a degree of inhibition and the blue color indicates a degree of expression.

siRNA	Average % of inhibition of Akt1 at 10nM	Average % of inhibition of Akt1 at 1nM	Average % of inhibition of Akt1 at 0.1nM	Weighed efficacy score	Ranking
D2Akt1	73	31	18	32	1
D8Akt1	-23	-67	-64	-59	4
D11Akt1	83	43	-24	16	2
D15Akt1	62	44	-42	4	3

Next, in order to present numerically the *in silico* data, the mean number of off-targets in all the species together was calculated. And accordingly, each siRNA was attributed a rank. Finally, the combination of the *in silico* and the *in cellulo* ranking was done by summing up the ranking in both cases. The 2 siRNA candidates having the highest ranks, and thus the highest efficiency *in cellulo* and least predicted off-target effect *in silico*, were selected for further analysis. The chosen Akt1 siRNA candidates were **D2Akt1 and D11Akt1 siRNAs**, see Table 11.

Table 11: Combination of *in cellulo* and *in silico* data for Akt1 siRNA choice. Highlighted in green are the chosen Akt1 siRNA candidates.

siRNA	Weighed efficacy Score of Akt1 inhibition	Weighed Efficacy Rank	Number of off-target genes in <i>Homo sapiens</i>	Number of off-target genes in <i>Mus musculus</i>	Number of off-target genes in <i>Rattus norvegicus</i>	Mean number of off-target genes in all the species	<i>in silico</i> Rank	Sum of Ranks
D2Akt1	32%	1	2	4	16	7	2	3
D8Akt1	-59%	4	2	6	22	10	3	7
D11Akt1	16%	2	5	6	11	7	2	4
D15Akt1	4%	3	2	4	29	12	4	7

1.1.2. *In cellulo* assessment of the specificity and off-target effect of D2Akt1 and D11Akt1 siRNAs

Curation of the choice of the best Akt1 siRNA candidate necessitates its validation as a siRNA specifically targeting Akt1 – given the homology between Akt1 and Akt2 sequences – and showing no off-target effect to any of the *in silico* predicted genes. For that, HepG2 cells were pulse transfected for 6 hours by LipofectamineRNAiMAX coupled to D2Akt1 or D11Akt1 or mock siRNA at 10nM concentration. At the 48-hour time point, RT-qPCR was done assessing the expression level of Akt1, Akt2 and the respectively predicted off-target genes. Additionally, protein immuno-detection by Jess was done to assess Akt1 and Akt2 protein expression levels, *see Figure 17*.

The results for D2Akt1 siRNA candidate at the transcriptomic level showed a significant 10-fold decrease in the *AKT1 mRNA* expression however no change was seen with that of *AKT2* or the predicted off-target gene *MTNR1B*, upon comparison to the mock condition, *see Figure 17A*. On the other hand, D11Akt1 siRNA candidate showed a significant 2-fold decrease in the expression of Akt1 as well as Akt2, but without a change in the expression of other predicted off-target genes *SBNO2*, *MYCBP2* or *FUBP1*, at the transcriptomic level compared to mock siRNA, *see Figure 17B*. On another note, *INTS5* and *ZNF541* are also listed as predicted off-targets for D2Akt1 siRNA and D11Akt1 siRNA, respectively. However, due to very low expression of these genes in HepG2 cells, it could not be assessed. Furthermore, the protein immuno-detection for Akt1 and Akt2 protein expression upon transfection with either of the siRNA candidates showed similar results to those obtained at the transcriptomic level. The results showed a significant decrease of Akt1 upon the transfection with either D2Akt1 or D11Akt1, by 85% and 75%, respectively *see Figure 17C*., however a significant decrease in the expression of Akt2 was only shown in the case of D11Akt1 transfection. by 80%, when compared to the mock, *see Figure 17D*.

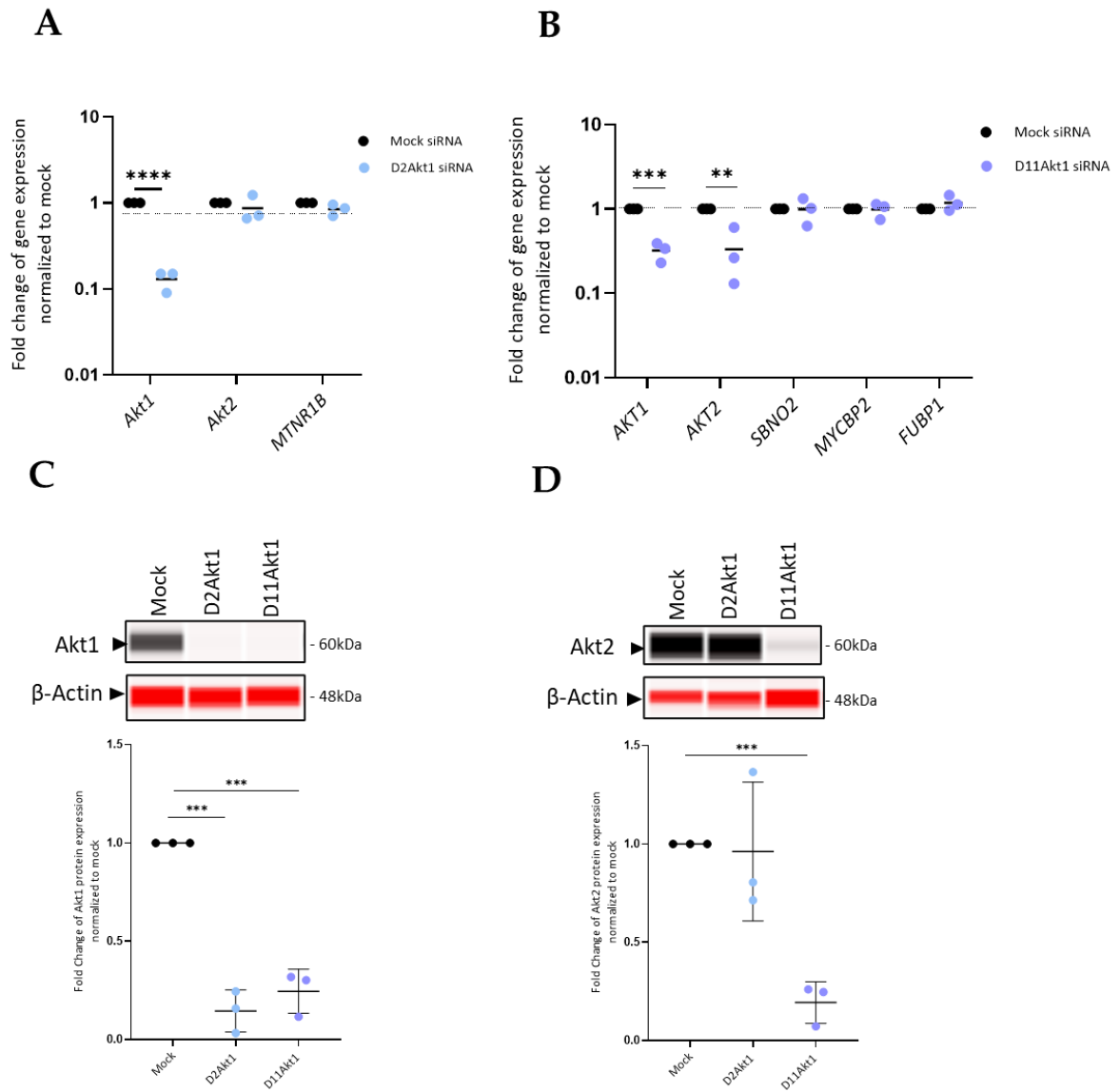


Figure 17: Specificity of D2Akt1 and D11Akt1 siRNAs. The transcriptomic analysis by RT-qPCR is presented at the top of panel, showing the mean \pm SD (N=3 independent experiment) of the fold change of mRNA expression normalized to the mock for Lipofectamine-mediated transfection using (A) D2Akt1 siRNA tested for the expression Akt1 ($p < 0.001$), Akt2, and the predicted off-target gene Melatonin Receptor 1B (MTNR1B); and (B) D11Akt1 siRNA tested for Akt1 ($p = 0.0001$), Akt2 (predicted off-target; $p = 0.0091$), and the other predicted off-target genes Strawberry Notch homologue 2 (SBNO2), MYC-Binding Protein 2 (MYCBP2), and Far Upstream Element Binding Protein 1 (FUBP1). Representative protein immuno-detection is presented on the bottom panel, showing (C) Akt1 expression and the corresponding quantification, represented as mean \pm SD (N=3 independent experiment) of the ratio of Akt1/ β -Actin normalized to that of the mock, in the case of D2Akt1 siRNA ($p = 0.0002$) and D11Akt1 siRNA ($p = 0.0003$); and (D) Akt2 expression and the corresponding quantification, represented as mean \pm SD of the ratio of Akt2/ β -Actin normalized to that of the mock, in the case of D2Akt1 siRNA and D11Akt1 siRNA ($p = 0.0002$). The statistical test used was unpaired t-test.

These results demonstrate that D2Akt1 siRNA is specific to Akt1 and does not show the off-target effect predicted *in silico*. However, D11Akt1 cross-reacts both human Akt isoforms, but shows no off-target effect for any of the other predicted genes.

1.1.3. *In cellulo* assessment of rodent cross-reactivity and specificity of D2Akt1 and D11Akt1 siRNAs

As the D2Akt1 and D11Akt1 candidates have been designed to cross the species barrier and target rodent Akt1 isoform as well as the human Akt1 isoform and not Akt2, the activity of the siRNAs was tested in rodents. The rodent cell line of choice was Hepa1.6 cell line. It is a mouse hepatocellular carcinoma cell line expressing Akt1 and Akt2. Hepa1.6 cells were pulse-transfected for 6 hours with LipofectamineRNAiMAX alone or coupled to D2Akt1 or D11Akt1 siRNAs. The expression of Akt1 and Akt2 was assessed on the protein level by Jess 48 hours later. The results of Akt1 protein expression, *see Figure 18A*, showed that both D2Akt1 and D11Akt1 siRNAs led to a decrease in the level of Akt1 by 75% and 82%, respectively. As far as Akt2 expression is concerned, it remained unchanged upon the transfection with D2Akt1 siRNA, however it showed a significant decrease by 52%, when compared to Lipofectamine alone, *see Figure 18B*. These results mirrored the results obtained on the human HepG2 cell line, thus proving the cross-reactivity of the siRNAs to the humans and mice. Moreover, the D11Akt1 is deemed non-specific to Akt1 in both humans and rodents.

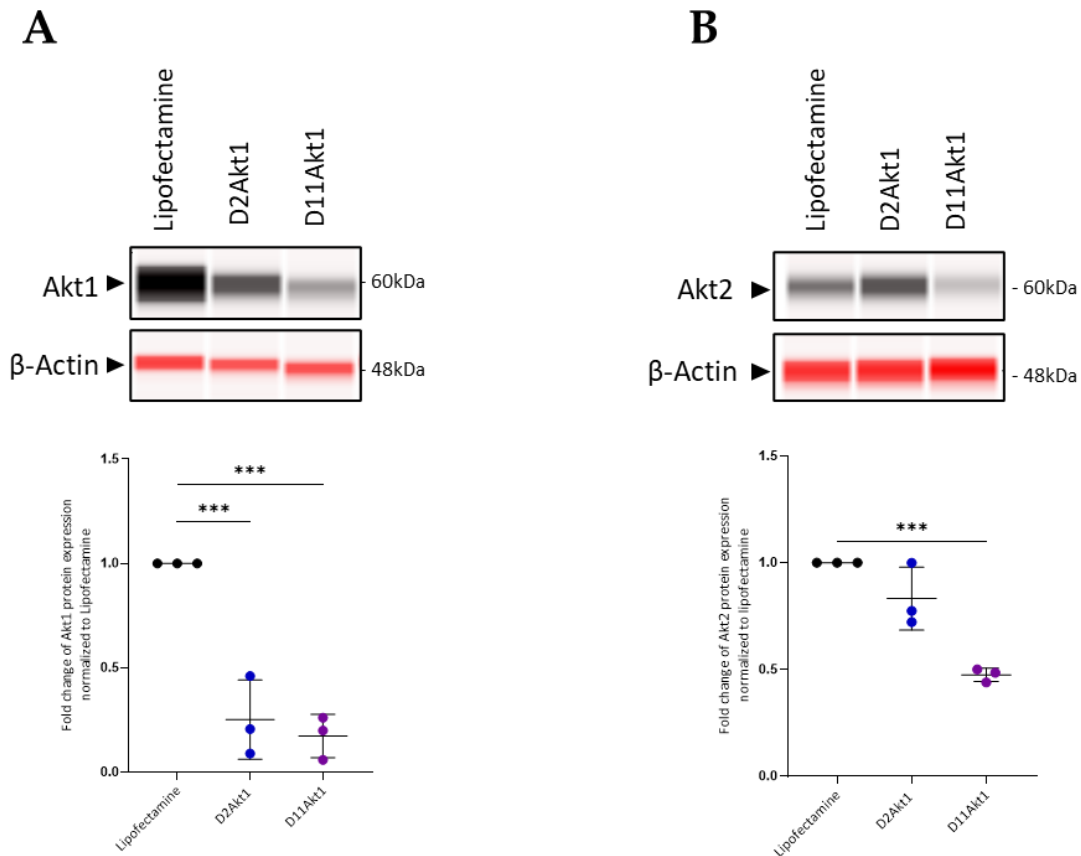


Figure 18: Rodent cross-reactivity and specificity of Akt1 siRNAs . Protein immuno-detection by Jess showing the expression of Akt1 and Akt2 isoforms in Hepa1.6 cell line, 48 hours following the transfection with D2Akt1 and D11Akt1 siRNAs. The top panel shows representative blots of. **(A)** the expression of Akt1, and its corresponding quantification represented as mean \pm SD (N=3 independent experiments) of the ratio of Akt1/ β -Actin for each condition normalized to LipofectamineRNAiMAX alone. The asterisks represent the p-value in their order of appearance from left to right: p=0.0008 and 0.005. **(B)** shows the expression of Akt2, and its corresponding quantification represented as mean \pm SD (N=3 independent experiments) of the ratio of Akt2/ β -Actin for each condition normalized to Lipofectamine alone. The asterisks represent the p-value: p=0.0008. The statistical test used is Ordinary one-way ANOVA.

The process of screening for the best Akt1 siRNA candidate starting with the 7 candidates: D2Akt1, D6Akt1, D7Akt1, D8Akt1, D10Akt1, D11Akt1, and D15Akt1, led to the diminution of the number of candidates into 2: D2Akt1 and D11Akt1 siRNAs. After taking into account the *in cellulo* efficiency, specificity, off-target effect and cross-reactivity to rodents, and the fact that D11Akt1 siRNA lacks the needed specificity for the Akt1 isoform in both humans and rodents; the **D2Akt1 siRNA** was chosen as the best candidate for further analysis.

1.2. Preliminary Akt2 siRNA design and screening

Similar to the workflow done for *Akt1* siRNA design and screening, as a first step, gene sequence of *Mus musculus Akt2* (NM_001110208.2) was used as a template for the generation of the 21-nucleotide siRNA sequences targeting *Akt2* mRNA. DSIR gave a list of 50 candidates for *Akt2* siRNA.

Then, the *in silico* analysis through NCBI blasting bioinformatics tool was done. Blasting each siRNA sequence (SS and AS strands) against the *Rattus norvegicus* and *Homo sapiens* genome in order to decipher the cross-reactivity, see Table 12. The siRNA sequences (AS and SS strands) showed that 11 candidates among the 50 siRNA sequence candidates cross the species barrier. The candidates were: **D2Akt2, D3Akt2, D7Akt2, D15Akt2, D16Akt2, D20Akt2, D27Akt2, D39Akt2, D41Akt2, D44Akt2, and D49Akt2** siRNAs.

Table 12: Inter-species reactivity of Akt2 siRNA candidates. The siRNA candidates in bold are the ones that show a cross reactivity to the three species. SS: sense strand; AS: anti-sense strand

siRNA	Sequence	<i>Mus musculus</i>		<i>Rattus norvegicus</i>		<i>Homo sapiens</i>	
		Query Cover	Identity	Query Cover	Identity	Query Cover	Identity
D1Akt2	SS sequence	100%	100%	100%	95.24%	-	-
	AS sequence	100%	100%	100%	95.24%	-	-
D2Akt2	SS sequence	100%	100%	90%	100%	90%	100%
	AS sequence	100%	100%	80%	100%	80%	100%
D3Akt3	SS sequence	100%	100%	100%	100%	100%	100%
	AS sequence	100%	100%	100%	100%	100.00%	100.00%
D4Akt2	SS sequence	100%	100%	-	-	-	-
	AS sequence	100%	100%	-	-	-	-
D5Akt2	SS sequence	100%	100%	-	-	-	-
	AS sequence	100%	100%	85%	94%	-	-
D6Akt2	SS sequence	100%	100%	100%	100%	-	-
	AS sequence	100%	100%	100%	100%	-	-
D7Akt2	SS sequence	100%	100%	100%	100.00%	100%	100%
	AS sequence	100%	100%	100%	100%	100%	100%
D8Akt2	SS sequence	100%	100%	-	-	-	-
	AS sequence	100%	100%	-	-	-	-

D9Akt2	SS sequence	100%	100%	-	-	-	-
	AS sequence	100%	100%	-	-	-	-
D10Akt2	SS sequence	100%	100%	-	-	-	-
	AS sequence	100%	100%	-	-	-	-
D11Akt2	SS sequence	100%	100%	-	-	-	-
	AS sequence	100%	100%	-	-	-	-
D12Akt2	SS sequence	100%	100%	-	-	-	-
	AS sequence	100%	100%	-	-	-	-
D13Akt2	SS sequence	100%	100%	-	-	-	-
	AS sequence	100%	100%	-	-	-	-
D14Akt2	SS sequence	100%	100%	100%	100%	-	-
	AS sequence	100%	100%	95%	100%	-	-
D15Akt2	SS sequence	100%	100%	100%	100%	100%	100%
	AS sequence	100%	100%	100%	100%	90%	100%
D16Akt2	SS sequence	100%	100%	85%	100%	71%	100%
	AS sequence	100%	100%	95%	100%	80%	100%
D17Akt2	SS sequence	100%	100%	100%	100%	-	-
	AS sequence	100%	100%	100%	100%	-	-
D18Akt2	SS sequence	100%	100%	-	-	-	-
	AS sequence	100%	100%	-	-	-	-
D19Akt2	SS sequence	100%	100%	-	-	-	-
	AS sequence	100%	100%	-	-	-	-
D20Akt2	SS sequence	100%	100%	80%	100%	71%	100%
	AS sequence	100%	100%	90%	100%	76%	100%
D21Akt2	SS sequence	100%	100%	-	-	-	-
	AS sequence	100%	100%	-	-	-	-
D22Akt2	SS sequence	100%	100%	-	-	-	-
	AS sequence	100%	100%	-	-	-	-
D23Akt2	SS sequence	100%	100%	-	-	-	-
	AS sequence	100%	100%	-	-	-	-
D24Akt2	SS sequence	100%	100%	90%	94.74%	-	-
	AS sequence	100%	100%	80%	94.12%	-	-
D25Akt2	SS sequence	100%	100%	-	-	-	-
	AS sequence	100%	100%	-	-	-	-
D26Akt2	SS sequence	100%	100%	-	-	-	-

	AS sequence	100%	100%	-	-	-	-
D27Akt2	SS sequence	100%	100%	100%	100%	100%	100%
	AS sequence	100%	100%	100%	100%	100%	100%
D28Akt2	SS sequence	100%	100%	100%	95.24%	-	-
	AS sequence	100%	100%	100%	95.24%	-	-
D29Akt2	SS sequence	100%	100%	-	-	-	-
	AS sequence	100%	100%	-	-	-	-
D30Akt2	SS sequence	100%	100%	100%	100%	-	-
	AS sequence	100%	100%	100%	100%	-	-
D31Akt2	SS sequence	100%	100%	-	-	-	-
	AS sequence	100%	100%	-	-	-	-
D32Akt2	SS sequence	100%	100%	-	-	-	-
	AS sequence	100%	100%	-	-	-	-
D33Akt2	SS sequence	100%	100%	100%	100%	-	-
	AS sequence	100%	100%	90%	100%	-	-
D34Akt2	SS sequence	100%	100%	-	-	-	-
	AS sequence	100%	100%	-	-	-	-
D35Akt2	SS sequence	100%	100%	80%	100%	-	-
	AS sequence	100%	100%	100%	95.24%	-	-
D36Akt2	SS sequence	100%	100%	76%	100%	-	-
	AS sequence	100%	100%	85%	100%	85%	94.44%
D37Akt2	SS sequence	100%	100%	100%	95.24%	-	-
	AS sequence	100%	100%	100%	95.24%	-	-
D38Akt2	SS sequence	100%	100%	71%	100%	-	-
	AS sequence	100%	100%	61%	100%	-	-
D39Akt2	SS sequence	100%	100%	100%	100%	100%	95.24%
	AS sequence	100%	100%	100%	100%	100%	95.24%
D40Akt2	SS sequence	100%	100%	100%	95.24%	-	-
	AS sequence	100%	100%	100%	95.24%	-	-
D41Akt2	SS sequence	100%	100%	100%	95.24%	100%	95.24%
	AS sequence	100%	100%	100%	95.24%	100%	95.24%
D42Akt2	SS sequence	100%	100%	-	-	-	-
	AS sequence	100%	100%	-	-	-	-
D43Akt2	SS sequence	100%	100%	-	-	-	-
	AS sequence	100%	100%	-	-	-	-

D44Akt2	SS sequence	100%	100%	100%	100%	80%	100%
	AS sequence	100%	100%	100%	100%	100%	95.24%
D45Akt2	SS sequence	100%	100%	61%	100%	-	-
	AS sequence	100%	100%	71%	100%	-	-
D46Akt2	SS sequence	100%	100%	85%	94.44%	-	-
	AS sequence	100%	100%	95%	95%	-	-
D47Akt2	SS sequence	100%	100%	-	-	-	-
	AS sequence	100%	100%	-	-	-	-
D48Akt2	SS sequence	100%	100%	-	-	-	-
	AS sequence	100%	100%	-	-	-	-
D49Akt2	SS sequence	100%	100%	95%	100%	100%	95.24%
	AS sequence	100%	100%	85%	100%	100%	95.24%
D50Akt2	SS sequence	100%	100%	85%	100%	-	-
	AS sequence	100%	100%	95%	100%	-	-

Further, deep *in silico* analysis was done to select the best 4 candidates of Akt2 targeting siRNAs to reveal the off-target effect and the degree of alignment to the seed sequence. See Table 13 for the off-target effect in *Homo sapiens*, Table 14 for that in *Mus musculus* and Table 15 for that in *Rattus norvegicus*. The *in silico* analysis of the off-target shows a varying degree of off-targets in each of the species, with varying degrees of alignment to the seed sequence.

Table 13: Off-target effect of Akt2 siRNA candidates in *Homo sapiens*. Seed sequence (from nucleotide 2 to nucleotide 7) is marked in red. Homology to the siRNA sequence is in bold.

siRNA	Gene name	Position on the siRNA sequence 5' -> 3'	Query Cover	Identities
D2Akt2	CASC1	UGAUGCUGAGGAAGAAUCUA	76%	16/16
D3Akt2	WDR7	UGUCUUU AUUGCUUGUACCGU	71%	15/15
	CSRNP3	UGUCUUU AUUGCUUGUACCGU	71%	15/15
D7Akt2	STAG2	UUUAUUG CUUGUACCGUACAA	66%	14/14
	CSRNP3	UUUAUUG CUUGUACCGUACAA	71%	15/15
D15Akt2	CEP70	UCUUGAU GUAUUCACCACGUU	66%	14/14
D16Akt2	LAMA5	UCAUGGA AGGUCCUCUCGAU	76%	16/16
D20Akt2	H2AZ2	UCACACG CUGUCACCUAGCUU	85%	17/18
	ZNF496	UCACACG CUGUCACCUAGCUU	66%	14/14
	IL16 TV3	UCACACG CUGUCACCUAGCUU	66%	14/14
	MRO TV8	UCACACG CUGUCACCUAGCUU	66%	14/14
	NKX6-2	UCACACG CUGUCACCUAGCUU	66%	14/14

	<i>ACE2 TVX1</i>	UCACACG CUGUCACCUAGCUU	66%	14/14
D27Akt2	<i>TCEAL6</i>	UGAGUGU CUUUU <u>AUUGCUUGUA</u>	76%	16/16
	<i>TAP1</i>	UGAGUGU CUUUU <u>AUUGCUUGUA</u>	90%	18/19
	<i>WDR7</i>	UGAGUGU CUUUU <u>AUUGCUUGUA</u>	71%	15/15
D39Akt2	<i>ATP2A1</i>	UUUGAUG ACAGAUACCUCAUU	71%	15/15
	<i>SHOC1</i>	UUUGAUG ACAGAUACCUCAUU	71%	15/15
D41Akt2	<i>ZSCAN25</i>	UCCAUCACAAAGCAU AGGCGG	66%	14/14
	<i>EYA2</i>	UCCAUCACAAAGCAU AGGCGG	66%	14/14
	<i>CYP3A5</i>	UCCAUCACAAAGCAU AGGCGG	66%	14/14
	<i>CD99</i>	UCCAUCACAAAGCAU AGGCGG	66%	14/14
	<i>ZFP92</i>	UCCAUCACAAAGCAU AGGCGG	66%	14/14
D44Akt2	<i>ATP2A1</i>	UUCUUUG AUGACAGAUACCUC	71%	15/15
D49Akt2	<i>MARCKS</i>	UUUGAGA UAAUCGAAGUCAUU	66%	14/14
	<i>BAG5</i>	UUUGAGA UAAUCGAAGUCAUU	61%	13/13
	<i>C3ORF14</i>	UUUGAGA UAAUCGAAGUCAUU	61%	13/13
	<i>GALNT5</i>	UUUGAGA UAAUCGAAGUCAUU	61%	13/13
	<i>SLC2A12</i>	UUUGAGA UAAUCGAAGUCAUU	61%	13/13
	<i>TAF1B</i>	UUUGAGA UAAUCGAAGUCAUU	80%	16/17
	<i>TBPL1</i>	UUUGAGA UAAUCGAAGUCAUU	61%	13/13

Table 14: Off-target effect of Akt2 siRNA candidates in *Mus musculus*. Seed sequence (from nucleotide 2 to nucleotide 7) is marked in red. Homology to the siRNA sequence is in bold.

siRNA	Gene name	Position on the siRNA sequence 5' -> 3'	Query Cover	Identities
D2Akt2	<i>Ttc29</i>	UGAUGC UGAGGAAGAAUCUA	71%	15/15
	<i>Nol9</i>	UGAUGC UGAGGAAGAAUCUA	71%	15/15
	<i>Symj1</i>	UGAUGC UGAGGAAGAAUCUA	71%	15/15
D3Akt2	<i>Wdr7</i>	UGUCUUU AUUGCUUGUACCGU	71%	15/15
	<i>Stag2</i>	UGUCUUU AUUGCUUGUACCGU	71%	15/15
	<i>Sall4</i>	UGUCUUU AUUGCUUGUACCGU	71%	15/15
	<i>Mst1</i>	UGUCUUU AUUGCUUGUACCGU	71%	15/15
D7Akt2	<i>Mst1</i>	UUUAUUG CUUGUACCGUACAA	71%	15/15
	<i>Stag2</i>	UUUAUUG CUUGUACCGUACAA	66%	14/14
	<i>Tafa2</i>	UUUAUUG CUUGUACCGUACAA	66%	14/14
	<i>Wdyf3</i>	UUUAUUG CUUGUACCGUACAA	85%	17/18
	<i>Syt10</i>	UUUAUUG CUUGUACCGUACAA	66%	14/14
D15Akt2	<i>Mroh3</i>	UCUUGAU GUAUUCACCACGUU	66%	14/14
D16Akt2	<i>Ank3</i>	UCAUGGA AAGGUCCUCUCGAU	71%	15/15
	<i>Pidd1</i>	UCAUGGA AAGGUCCUCUCGAU	66%	14/14
D20Akt2	<i>Cosp2</i>	UCACACG CUGUCACCUAGCUU	71%	15/15
	<i>Nisch</i>	UCACACG CUGUCACCUAGCUU	66%	14/14
	<i>Bdnf</i>	UCACACG CUGUCACCUAGCUU	66%	14/14

	A230072106Rik	UCACACG CUGUCACCUAGCUU	66%	14/14
	Rapgef2	UCACACG CUGUCACCUAGCUU	66%	14/14
	Trdmt1	UCACACG CUGUCACCUAGCUU	66%	14/14
	Atg2b	UCACACG CUGUCACCUAGCUU	66%	14/14
D27Akt2	Wdr7	UGAGUGU CUUAUUGCUUGUA	71%	15/15
	Sall4 Tvb	UGAGUGU CUUAUUGCUUGUA	71%	15/15
	B4galt1	UGAGUGU CUUAUUGCUUGUA	71%	15/15
D39Akt2	Ctdp1	UUUGAUG ACAGAUACCUCAUU	71%	15/15
	Dock9	UUUGAUG ACAGAUACCUCAUU	71%	15/15
	Cdh23	UUUGAUG ACAGAUACCUCAUU	71%	15/15
D41Akt2	-	-	-	-
D44Akt2	Dock9	UUCUUUGAUG ACAGAUACCUC	71%	15/15
	Cdh23	UUCUUUGAUG ACAGAUACCUC	71%	15/15
D49Akt2	Psmg2	UUUGAGA UAAUCGAAGUCAUU	61%	13/13
	Fam13c	UUUGAGA UAAUCGAAGUCAUU	61%	13/13
	Wdr3	UUUGAGA UAAUCGAAGUCAUU	61%	13/13

Table 15: Off-target effect of Akt2 siRNA candidates in *Rattus norvegicus*. Seed sequence (from nucleotide 2 to nucleotide 7) is marked in red. Homology to the siRNA sequence is in bold.

siRNA	Gene name	Position on the siRNA sequence 5' -> 3'	Query Cover	Identities
D2Akt2	Aplp2	UGAUGC CUGAGGAAGAAUCUA	71%	15/15
	Atcay	UGAUGC CUGAGGAAGAAUCUA	71%	15/15
	Zc3h18	UGAUGC CUGAGGAAGAAUCUA	71%	15/15
	Osmr	UGAUGC CUGAGGAAGAAUCUA	71%	15/15
	Olr 809	UGAUGC CUGAGGAAGAAUCUA	71%	15/15
	LOC686209	UGAUGC CUGAGGAAGAAUCUA	71%	15/15
	Pja1	UGAUGC CUGAGGAAGAAUCUA	66%	14/14
	LOC316124	UGAUGC CUGAGGAAGAAUCUA	66%	14/14
	Fam46a	UGAUGC CUGAGGAAGAAUCUA	66%	14/14
	Zfc3h1	UGAUGC CUGAGGAAGAAUCUA	66%	14/14
	LOC108351322	UGAUGC CUGAGGAAGAAUCUA	66%	14/14
	Galnt14	UGAUGC CUGAGGAAGAAUCUA	66%	14/14
	Galnt14	UGAUGC CUGAGGAAGAAUCUA	66%	14/14
	Arghap5	UGAUGC CUGAGGAAGAAUCUA	66%	14/14
	Gln2	UGAUGC CUGAGGAAGAAUCUA	66%	14/14
	Rb1cc1	UGAUGC CUGAGGAAGAAUCUA	66%	14/14
	Rbsn	UGAUGC CUGAGGAAGAAUCUA	66%	14/14
	Itch	UGAUGC CUGAGGAAGAAUCUA	66%	14/14
	LOC10834994	UGAUGC CUGAGGAAGAAUCUA	66%	14/14
	Cmya5	UGAUGC CUGAGGAAGAAUCUA	66%	14/14

	<i>Mcf2l</i>	UGAUGCUGAGGAAGAAUCUA	66%	14/14
	<i>Bod11l</i>	UGAUGCUGAGGAAGAAUCUA	66%	14/14
	<i>LOC100359816</i>	UGAUGCUGAGGAAGAAUCUA	66%	14/14
	<i>Tsc2</i>	UGAUGCUGAGGAAGAAUCUA	66%	14/14
	<i>Siglech</i>	UGAUGCUGAGGAAGAAUCUA	66%	14/14
	<i>Stra8</i>	UGAUGCUGAGGAAGAAUCUA	66%	14/14
D3Akt2	<i>Stag2</i>	UGUCUUUAUUGCUUGUACCGU	71%	15/15
	<i>Wdr7</i>	UGUCUUUAUUGCUUGUACCGU	71%	15/15
	<i>Mphosph9</i>	UGUCUUUAUUGCUUGUACCGU	66%	14/14
	<i>Pah</i>	UGUCUUUAUUGCUUGUACCGU	66%	14/14
	<i>Olr672</i>	UGUCUUUAUUGCUUGUACCGU	66%	14/14
	<i>Olr674</i>	UGUCUUUAUUGCUUGUACCGU	66%	14/14
	<i>Olr675</i>	UGUCUUUAUUGCUUGUACCGU	66%	14/14
	<i>Rab7b</i>	UGUCUUUAUUGCUUGUACCGU	66%	14/14
	<i>Luzp2</i>	UGUCUUUAUUGCUUGUACCGU	66%	14/14
	<i>Il36rn</i>	UGUCUUUAUUGCUUGUACCGU	66%	14/14
	<i>Casp8</i>	UGUCUUUAUUGCUUGUACCGU	61%	13/13
	<i>Ccdc38</i>	UGUCUUUAUUGCUUGUACCGU	61%	13/13
	<i>Smc2</i>	UGUCUUUAUUGCUUGUACCGU	61%	13/13
	<i>Tmem246</i>	UGUCUUUAUUGCUUGUACCGU	61%	13/13
	<i>Plag1</i>	UGUCUUUAUUGCUUGUACCGU	61%	13/13
	<i>Ube2k</i>	UGUCUUUAUUGCUUGUACCGU	61%	13/13
	<i>Sall4</i>	UGUCUUUAUUGCUUGUACCGU	61%	13/13
	<i>Ccdc54</i>	UGUCUUUAUUGCUUGUACCGU	80%	16/17
	<i>Fyco1</i>	UGUCUUUAUUGCUUGUACCGU	61%	13/13
	<i>Repin1</i>	UGUCUUUAUUGCUUGUACCGU	61%	13/13
D7Akt2	<i>Stag2</i>	UUUAUUGCUUGUACCGUACAA	66%	14/14
	<i>Ube2k</i>	UUUAUUGCUUGUACCGUACAA	61%	13/13
	<i>Mst1</i>	UUUAUUGCUUGUACCGUACAA	61%	13/13
	<i>Pah</i>	UUUAUUGCUUGUACCGUACAA	61%	13/13
	<i>Xrn2</i>	UUUAUUGCUUGUACCGUACAA	57%	12/12
	<i>Rab7b</i>	UUUAUUGCUUGUACCGUACAA	66%	14/14
	<i>Tmem246</i>	UUUAUUGCUUGUACCGUACAA	61%	13/13
	<i>Plag1</i>	UUUAUUGCUUGUACCGUACAA	61%	13/13
	<i>Nudt19</i>	UUUAUUGCUUGUACCGUACAA	61%	13/13
	<i>Apol11a</i>	UUUAUUGCUUGUACCGUACAA	61%	13/13
	<i>Ccdc88c</i>	UUUAUUGCUUGUACCGUACAA	61%	13/13
	<i>Akap8</i>	UUUAUUGCUUGUACCGUACAA	57%	12/12
	<i>Galnt16</i>	UUUAUUGCUUGUACCGUACAA	57%	12/12
	<i>Mmel1</i>	UUUAUUGCUUGUACCGUACAA	57%	12/12
	<i>Akap2</i>	UUUAUUGCUUGUACCGUACAA	57%	12/12

D15Akt2	<i>Tbck</i>	UCUUGAUGUAUUCACCACGUU	76%	16/16
	<i>Tor1aip2</i>	UCUUGAUGUAUUCACCACGUU	66%	14/14
	<i>Rnf145</i>	UCUUGAUGUAUUCACCACGUU	61%	13/13
	<i>Zdhhc20</i>	UCUUGAUGUAUUCACCACGUU	61%	13/13
	<i>Wdyhv1</i>	UCUUGAUGUAUUCACCACGUU	61%	13/13
	<i>Bdkrb2 tv1</i>	UCUUGAUGUAUUCACCACGUU	57%	12/12
	<i>Abi1</i>	UCUUGAUGUAUUCACCACGUU	61%	13/13
	<i>Uggt1</i>	UCUUGAUGUAUUCACCACGUU	66%	14/14
	<i>Dpysl3</i>	UCUUGAUGUAUUCACCACGUU	61%	13/13
	<i>kif1a</i>	UCUUGAUGUAUUCACCACGUU	61%	13/13
	<i>LOC100362216</i>	UCUUGAUGUAUUCACCACGUU	100%	19/21
	<i>Htr2c</i>	UCUUGAUGUAUUCACCACGUU	57%	12/12
	<i>Unc80</i>	UCUUGAUGUAUUCACCACGUU	57%	12/12
	<i>Ube2f</i>	UCUUGAUGUAUUCACCACGUU	57%	12/12
D16Akt2	<i>Mogs</i>	UACAUGGAAGGUCCUCUCGAU	66%	14/14
	<i>Ager</i>	UACAUGGAAGGUCCUCUCGAU	66%	14/14
	<i>Thsd1</i>	UACAUGGAAGGUCCUCUCGAU	66%	14/14
	<i>Pdlim1</i>	UACAUGGAAGGUCCUCUCGAU	61%	13/13
	<i>Mrpl38</i>	UACAUGGAAGGUCCUCUCGAU	61%	13/13
	<i>LOC100910838</i>	UACAUGGAAGGUCCUCUCGAU	71%	15/15
	<i>Nyap1</i>	UACAUGGAAGGUCCUCUCGAU	71%	15/15
	<i>Zfp335</i>	UACAUGGAAGGUCCUCUCGAU	66%	14/14
	<i>LOC103692171</i>	UACAUGGAAGGUCCUCUCGAU	66%	14/14
	<i>Sema7a tvX1</i>	UACAUGGAAGGUCCUCUCGAU	61%	13/13
	<i>Sfmbt2</i>	UACAUGGAAGGUCCUCUCGAU	61%	13/13
	<i>Tgm3</i>	UACAUGGAAGGUCCUCUCGAU	61%	13/13
	<i>Dok2</i>	UACAUGGAAGGUCCUCUCGAU	61%	13/13
	<i>Mpp2</i>	UACAUGGAAGGUCCUCUCGAU	61%	13/13
	<i>Eif5a</i>	UACAUGGAAGGUCCUCUCGAU	61%	13/13
	<i>LOC100911941</i>	UACAUGGAAGGUCCUCUCGAU	61%	13/13
	<i>Mro</i>	UACAUGGAAGGUCCUCUCGAU	61%	13/13
	<i>RGD1560281</i>	UACAUGGAAGGUCCUCUCGAU	61%	13/13
	<i>Vps37c</i>	UACAUGGAAGGUCCUCUCGAU	61%	13/13
	<i>Snx32</i>	UACAUGGAAGGUCCUCUCGAU	61%	13/13
<i>Cacnb4</i>	UACAUGGAAGGUCCUCUCGAU	61%	13/13	
D20Akt2	<i>Il16</i>	UCACACGCUGUCACCUAGCUU	71%	15/15
	<i>Dnajb6</i>	UCACACGCUGUCACCUAGCUU	66%	14/14
	<i>Rnf17</i>	UCACACGCUGUCACCUAGCUU	61%	13/13
	<i>Tada1</i>	UCACACGCUGUCACCUAGCUU	61%	13/13
	<i>Pnma8b</i>	UCACACGCUGUCACCUAGCUU	61%	13/13
	<i>Mpzl2</i>	UCACACGCUGUCACCUAGCUU	61%	13/13

	<i>Wnt7b</i>	UCACACGCUGUCACCUAGCUU	61%	13/13
	<i>Tfeb</i>	UCACACGCUGUCACCUAGCUU	66%	14/14
	<i>Trdmt1</i>	UCACACGCUGUCACCUAGCUU	66%	14/14
	<i>LOC103689927</i>	UCACACGCUGUCACCUAGCUU	85%	17/18
	<i>Bdp1</i>	UCACACGCUGUCACCUAGCUU	61%	13/13
	<i>Defb11</i>	UCACACGCUGUCACCUAGCUU	61%	13/13
	<i>LOC108352965</i>	UCACACGCUGUCACCUAGCUU	61%	13/13
	<i>Obscn</i>	UCACACGCUGUCACCUAGCUU	61%	13/13
	<i>Agbl3</i>	UCACACGCUGUCACCUAGCUU	61%	13/13
	<i>Tm9sf3</i>	UCACACGCUGUCACCUAGCUU	61%	13/13
	<i>Ms4a13-ps1</i>	UCACACGCUGUCACCUAGCUU	61%	13/13
	<i>Cep295</i>	UCACACGCUGUCACCUAGCUU	57%	12/12
D27Akt2	<i>Wdr7</i>	UGAGUGUCUUUAUUGCUUGUA	71%	15/15
	<i>Maea</i>	UGAGUGUCUUUAUUGCUUGUA	66%	14/14
	<i>Csrnp1</i>	UGAGUGUCUUUAUUGCUUGUA	66%	14/14
	<i>Stag2</i>	UGAGUGUCUUUAUUGCUUGUA	66%	14/14
	<i>Mphosph9</i>	UGAGUGUCUUUAUUGCUUGUA	66%	14/14
	<i>Olr672</i>	UGAGUGUCUUUAUUGCUUGUA	66%	14/14
	<i>Olr674</i>	UGAGUGUCUUUAUUGCUUGUA	66%	14/14
	<i>Olr675</i>	UGAGUGUCUUUAUUGCUUGUA	66%	14/14
	<i>Pah</i>	UGAGUGUCUUUAUUGCUUGUA	66%	14/14
	<i>Calr4</i>	UGAGUGUCUUUAUUGCUUGUA	66%	14/14
	<i>Rasl2</i>	UGAGUGUCUUUAUUGCUUGUA	66%	14/14
	<i>Luzp2</i>	UGAGUGUCUUUAUUGCUUGUA	66%	14/14
D39Akt2	<i>Dock9</i>	UUUGAUGACAGAUACCUCAUU	71%	15/15
	<i>Ctdp1</i>	UUUGAUGACAGAUACCUCAUU	71%	15/15
	<i>Rpgr tv2</i>	UUUGAUGACAGAUACCUCAUU	66%	14/14
	<i>Wnt2b</i>	UUUGAUGACAGAUACCUCAUU	66%	14/14
	<i>Cdh23</i>	UUUGAUGACAGAUACCUCAUU	66%	14/14
	<i>Atp2a1</i>	UUUGAUGACAGAUACCUCAUU	66%	14/14
	<i>LOC302586</i>	UUUGAUGACAGAUACCUCAUU	66%	14/14
	<i>Slc9a3r2</i>	UUUGAUGACAGAUACCUCAUU	66%	14/14
	<i>Serac1</i>	UUUGAUGACAGAUACCUCAUU	66%	14/14
	<i>Dlgap1</i>	UUUGAUGACAGAUACCUCAUU	80%	16/17
	<i>Inpp1</i>	UUUGAUGACAGAUACCUCAUU	61%	13/13
	<i>Arl13b</i>	UUUGAUGACAGAUACCUCAUU	61%	13/13
	<i>Irak4</i>	UUUGAUGACAGAUACCUCAUU	61%	13/13
	<i>Ptk2</i>	UUUGAUGACAGAUACCUCAUU	61%	13/13
	<i>Usp20</i>	UUUGAUGACAGAUACCUCAUU	61%	13/13
	<i>RGD1560883</i>	UUUGAUGACAGAUACCUCAUU	61%	13/13
	<i>Fbxl21</i>	UUUGAUGACAGAUACCUCAUU	61%	13/13

	<i>Pibf1</i>	UUUGAUGACAGAUACCUCAUU	61%	13/13
	<i>Peli2</i>	UUUGAUGACAGAUACCUCAUU	61%	13/13
	<i>Cdkn3</i>	UUUGAUGACAGAUACCUCAUU	61%	13/13
D41Akt2	<i>Pkn2</i>	UCCAUCAAAAAGCAUAGGCCGG	66%	14/14
	<i>Pkn1</i>	UCCAUCAAAAAGCAUAGGCCGG	66%	14/14
	<i>Prkcb</i>	UCCAUCAAAAAGCAUAGGCCGG	100%	19/21
	<i>Akt1</i>	UCCAUCAAAAAGCAUAGGCCGG	100%	19/21
	<i>LOC108351838</i>	UCCAUCAAAAAGCAUAGGCCGG	66%	14/14
	<i>Fbrs1</i>	UCCAUCAAAAAGCAUAGGCCGG	66%	14/14
	<i>LOC103690550</i>	UCCAUCAAAAAGCAUAGGCCGG	85%	17/18
	<i>Ap1s2</i>	UCCAUCAAAAAGCAUAGGCCGG	61%	13/13
	<i>Ccdc134</i>	UCCAUCAAAAAGCAUAGGCCGG	61%	13/13
	<i>Arl13b</i>	UCCAUCAAAAAGCAUAGGCCGG	61%	13/13
	<i>Tox</i>	UCCAUCAAAAAGCAUAGGCCGG	61%	13/13
	<i>Dnah9</i>	UCCAUCAAAAAGCAUAGGCCGG	61%	13/13
	<i>Leng8</i>	UCCAUCAAAAAGCAUAGGCCGG	61%	13/13
	<i>Fam155b</i>	UCCAUCAAAAAGCAUAGGCCGG	61%	13/13
	D44Akt2	<i>Rpgr</i>	UUCUUUGAUGACAGAUACCUC	71%
<i>Dock9</i>		UUCUUUGAUGACAGAUACCUC	71%	15/15
<i>Ezh2</i>		UUCUUUGAUGACAGAUACCUC	85%	17/18
<i>Ctdp1</i>		UUCUUUGAUGACAGAUACCUC	66%	14/14
<i>Sf3a</i>		UUCUUUGAUGACAGAUACCUC	85%	17/18
<i>Wnt9b</i>		UUCUUUGAUGACAGAUACCUC	66%	14/14
<i>Sdc1</i>		UUCUUUGAUGACAGAUACCUC	66%	14/14
<i>LOC302586</i>		UUCUUUGAUGACAGAUACCUC	71%	15/15
<i>Slc9a3r2</i>		UUCUUUGAUGACAGAUACCUC	66%	14/14
<i>LOC102547059</i>		UUCUUUGAUGACAGAUACCUC	66%	14/14
<i>Acat2l1</i>		UUCUUUGAUGACAGAUACCUC	66%	14/14
<i>Serac1</i>		UUCUUUGAUGACAGAUACCUC	66%	14/14
<i>Flr1</i>		UUCUUUGAUGACAGAUACCUC	66%	14/14
D49Akt2	<i>Muc16</i>	UUUGAGAUAAUCGAAGUCAUU	57%	12/12
	<i>Arghap20</i>	UUUGAGAUAAUCGAAGUCAUU	57%	12/12
	<i>Aste1</i>	UUUGAGAUAAUCGAAGUCAUU	57%	12/12
	<i>Dnah6</i>	UUUGAGAUAAUCGAAGUCAUU	57%	12/12
	<i>Csgalnact2</i>	UUUGAGAUAAUCGAAGUCAUU	57%	12/12
	<i>Uqcc1</i>	UUUGAGAUAAUCGAAGUCAUU	57%	12/12
	<i>Fermt1</i>	UUUGAGAUAAUCGAAGUCAUU	57%	12/12
	<i>Slitrk3</i>	UUUGAGAUAAUCGAAGUCAUU	57%	12/12
	<i>Maf</i>	UUUGAGAUAAUCGAAGUCAUU	57%	12/12
	<i>LOC102546698</i>	UUUGAGAUAAUCGAAGUCAUU	57%	12/12

<i>Wsb1</i>	UUUGAGAUAUCGAAGUCAUU	57%	12/12
<i>Lcor</i>	UUUGAGAUAUCGAAGUCAUU	76%	15/16
<i>Vasp</i>	UUUGAGAUAUCGAAGUCAUU	57%	12/12
<i>LOC103690502</i>	UUUGAGAUAUCGAAGUCAUU	76%	15/16
<i>Zfp952</i>	UUUGAGAUAUCGAAGUCAUU	57%	12/12
<i>Col25a1</i>	UUUGAGAUAUCGAAGUCAUU	76%	15/16
<i>Raet1e</i>	UUUGAGAUAUCGAAGUCAUU	57%	12/12
<i>Arap2</i>	UUUGAGAUAUCGAAGUCAUU	57%	12/12
<i>Tmem245</i>	UUUGAGAUAUCGAAGUCAUU	57%	12/12

Similar to the strategy used for Akt1 siRNA candidates, and due to the non-uniformity of the results between the species, a numerical representation of the results was done. The number of off-target genes predicted in every species was counted and the siRNA was attributed a rank accordingly. Then the ranks were summed up to give an indication about the siRNA candidates having the least off-target effect in the three species, *see Table 16*. The results unraveled the 4 best candidates having the least off-target effect in the three species, for further *in cellulo* analysis: **D15Akt2, D27Akt2, D41Akt2 and D44Akt2 siRNA sequences.**

Table 16: Off-target effect ranking of Akt2 siRNA candidates. In bold are the siRNAs having the least off-target effect in the three species.

siRNA	<i>Mus musculus</i>		<i>Rattus norvegicus</i>		<i>Homo sapiens</i>		All species
	Number of off-targets	Rank	Number of off-targets	Rank	Number of off-targets	Rank	Sum of Ranks
D2Akt2	3	4	25	9	1	1	14
D3Akt2	4	5	20	7	2	2	14
D7Akt2	5	6	15	4	2	2	12
D15Akt2	1	2	14	3	1	1	6
D16Akt2	2	3	21	8	1	1	12
D20Akt2	7	7	18	5	6	5	17
D27Akt2	3	4	12	1	3	3	8
D39Akt2	3	4	20	7	2	2	13
D41Akt2	0	1	14	3	5	4	8
D44Akt2	2	3	13	2	1	1	6
D49Akt2	3	4	19	6	7	6	16

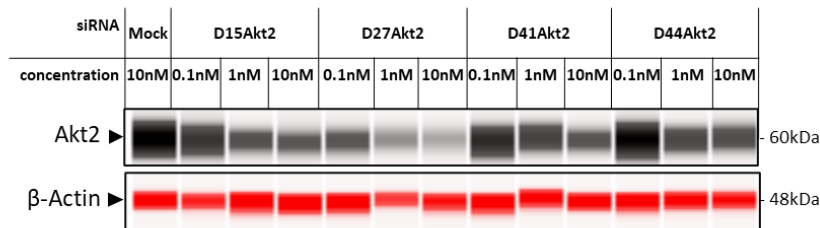
1.2.1. *In cellulo* assessment of the efficiency of the 4 candidates of Akt2 siRNA and choice of the best 2 candidates

The efficiency of Akt2 siRNA candidates was studied *in cellulo* in order to sort out the best among them. For that, human HepG2 cells, exhibiting a sustained level of expression of Akt2 were chosen for testing the efficiency of the candidates. HepG2 cells were pulse transfected for 6 hours with LipofectamineRNAiMAX coupled to D15Akt2, D27Akt2, D41Akt2 and D44Akt2 siRNAs at 3 concentrations (10, 1 and 0.1nM) with mock siRNA as a negative control. Protein analysis of the expression of Akt2 was done by Jess 48 hours later.

The results showed a dose-dependent decrease in the expression of Akt2 with varying efficiencies depending on the candidate when compared to mock siRNA, see Figure 20. D15Akt2 siRNA showed a 70%, 44%, and 11% decrease in the expression of Akt2 protein at 10nM, 1nM and 0.1nM siRNA concentrations, respectively. Similarly, D27Akt1 siRNA showed a decrease in the expression of Akt2 by 70% and 44% at the 10nM and 1nM concentrations, respectively. But, with

a higher decrease in the expression of Akt2 at the 0.1nM concentration by 45%, D41Akt2 and D44Akt2 siRNA sequences, showed lower efficiencies compared to the former two siRNA sequences. No decrease in the expression of Akt2 at the 0.1nM concentration in the case when compared to mock, but rather a slight non-significant increase in the expression was shown. At the 10nM and 1nM concentration, D41Akt2 siRNA showed a respective 60% and 10% decrease in the expression of Akt2. Whereas D44Akt2 siRNA showed no decrease of Akt2 protein expression at the 1nM concentration and a 23% decrease of Akt2 protein expression at the 10nM concentration, exhibiting the lowest efficiency compared to all the other candidates, *see Table 17*.

A



B

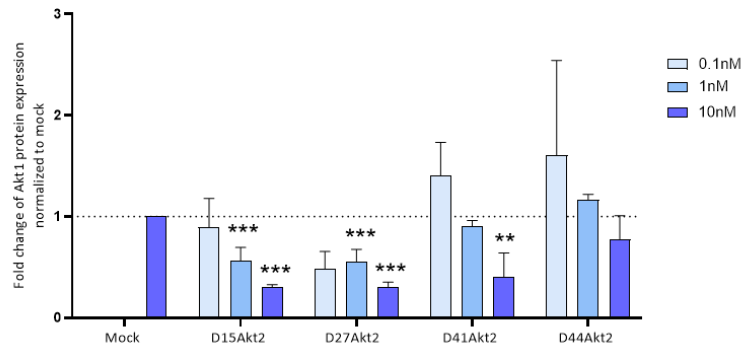


Figure 19: Screening of Designed Akt2 siRNAs in cellulo. Efficiency of the chosen best 4 candidates of designed Akt2 siRNAs: D15Akt2, D27Akt2, D41Akt2, and D44Akt2siRNAs, was tested in cellulo (0.1, 1, and 10nM). (A) Representative protein immune-detection by Jess 48 hours after transfection. β -Actin was used as a house keeping gene. (B) Quantification of the protein immune-detection data of Akt2 expression, represented as mean \pm SD (N = 3 independent experiments) of the ratio of Akt2/ β -Actin for each condition normalized to its corresponding mock concentration. Ordinary one-way ANOVA statistical analysis was done for every concentration versus the same concentration of the mock siRNA. The asterisks, in the order of their appearance on the graph from left to right, represent the following: $p = 0.0004$, 0.0008 , 0.0007 , 0.0004 , and 0.0023 .

Given the variability of the efficiency between the tested siRNAs, the weighed efficacy score was calculated and the Akt2 siRNA candidates were ranked accordingly, *see Table 17*.

Table 17: Weighed *in cellulo* efficacy ranking of Akt2 siRNA candidates. The average of inhibition of Akt1 is representative of the mean inhibition in the 3 independent experiments. The red color indicates a degree of inhibition and the blue color indicates a degree of expression.

siRNA	Average % of inhibition of Akt2 at 10nM	Average % of inhibition of Akt2 at 1nM	Average % of inhibition of Akt2 at 0.1nM	Weighed efficacy score	Rank
D15Akt2	70	44	11	32	2
D27Akt2	70	44	51	52	1
D41Akt2	60	9	-41	-7	3
D44Akt2	22	-17	-61	-32	4

Next, in order to present numerically the *in silico* data, the mean number of off-targets all the species together was calculated, and accordingly, each siRNA was attributed a rank. Finally, the combination of the *in silico* and the *in cellulo* ranking was done by summing up the ranking in both cases. The 2 siRNA candidates having the highest ranks, and thus the highest efficiency *in cellulo* and least predicted off-target effect *in silico*, were selected for further analysis, see Table 18. The chosen Akt2 siRNA candidates were **D15Akt2 and D27Akt2 siRNAs**.

Table 18: Combination of *in cellulo* and *in silico* data for Akt2 siRNA choice. Highlighted in green are the chosen Akt2 siRNA candidates.

siRNA	Weighed efficacy Score of Akt2 inhibition	Weighed Efficacy Rank	Number of off-target genes in <i>Homo sapiens</i>	Number of off-target genes in <i>Mus musculus</i>	Number of off-target genes in <i>Rattus norvegicus</i>	Mean number of genes in all the species	<i>in silico</i> Rank	Sum of Ranks
D15Akt2	32%	2	1	1	14	5	2	4
D27Akt2	52%	1	3	3	12	6	3	4
D41Akt2	-7%	3	5	0	14	6	4	7
D44Akt2	-32%	4	1	2	13	5	2	6

1.2.2. *In cellulo* assessment of the specificity and off-target effect of D15Akt2 and D27Akt2 siRNAs

After the validation of the efficiency, and similar to what was done for Akt1 siRNA candidates, the choice of the best Akt2 siRNA candidate necessitated its validation as a siRNA specifically targeting Akt2 and showing no off-target effect to any of the *in silico* predicted genes. For that, HepG2 cells were pulse transfected for 6 hours by LipofectamineRNAiMAX coupled D15Akt2 or D27Akt2 or mock siRNA at 10nM concentration. At the 48-hour time point, RT-qPCR was done assessing the expression level of *AKT2*, *AKT1* and the respectively predicted off-target genes, along with an immune-detection analysis assessing Akt2 and Akt1 protein expression levels, *see Figure 20*.

The results for D15Akt2 siRNA candidate transfection at the transcriptomic level showed a significant 10-fold decrease in the *AKT2* mRNA expression with no effect on the Akt1 expression, or the predicted off-target gene *CEP70*, compared to the mock condition, *see Figure 20A*. Similarly, D27Akt2 siRNA transfection resulted in a significant 10-fold decrease of *AKT2* mRNA expression, along with no significant change in the mRNA expression of Akt1 or any of the predicted off-target genes tested: *TAP3* and *WDR7*, *see Figure 20B*. On another note, *TCEAL6* is also listed as predicted off-target for D27Akt2 siRNA, however, due to very low expression of this gene in HepG2 cells, it could not be assessed. Furthermore, the protein immune-detection of Akt2 and Akt1 expression showed a decrease in the expression of Akt2 upon the transfection with either D15Akt2 or D27Akt2 siRNAs by 82% and 66%, respectively, when compared to the mock, *see Figure 20C*. On the other hand, the Akt1 expression showed no change in the case of transfection with D15Akt2 siRNA, but with a surprising 54% significant increase in its expression in the case of transfection with D27Akt2 siRNA, when compared to the mock, *see Figure 20D*.

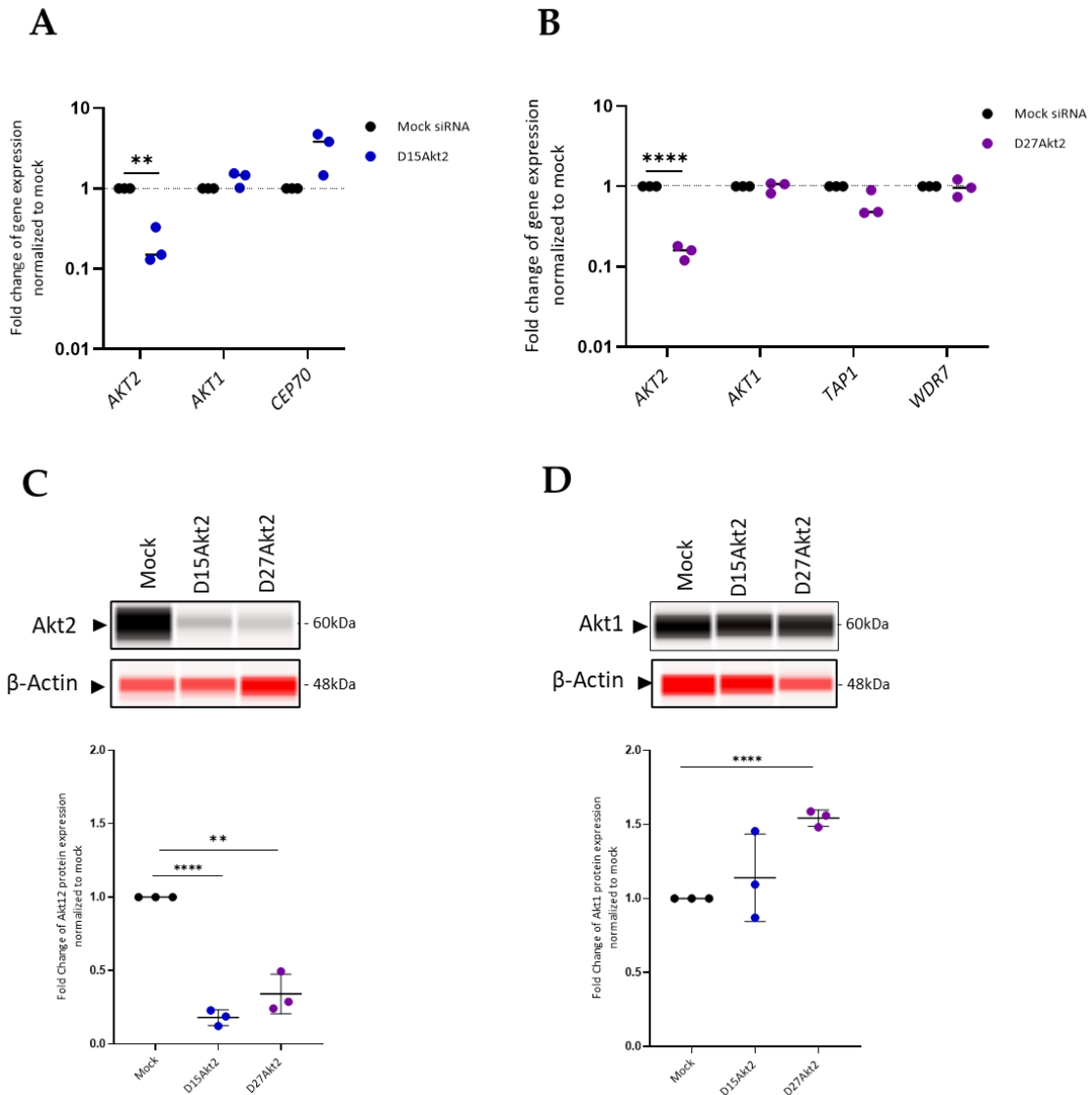


Figure 20: Specificity of D15Akt2 and D27Akt2 siRNAs. The transcriptomic analysis by RT-qPCR is presented at the top of panel, showing the mean \pm SD (N=3 independent experiments) of the fold change of mRNA expression normalized to the mock for LipofectamineRNAiMAX-mediated transfection using (A) D15Akt2 siRNA tested for the expression Akt2 ($p=0.0063$), Akt1, and the predicted off-target gene Centrosomal Protein 70 (CEP70); and (B) D27Akt2 siRNA tested for Akt2 ($p<0.0001$), Akt1 and the predicted off-target genes Transporter Associated with Antigen Processing 1 (TAP1), and WD Repeat Domain 7 (WDR7) Representative protein immuno-detection is presented on the bottom panel, showing (C) Akt2 expression and the corresponding quantification, represented as mean \pm SD (N=3 independent experiments) of the ratio of Akt2/ β -Actin normalized to that of the mock, in the case of D15Akt2 siRNA ($p<0.0001$) and D27Akt2 siRNA ($p=0.0011$); and (D) Akt1 expression and the corresponding quantification, represented as mean \pm SD of the ratio of Akt1/ β -Actin normalized to that of the mock, in the case of D15Akt2 siRNA and D27Akt2 siRNA ($p<0.0001$). The statistical test used was unpaired *t*-test.

1.2.3. *In cellulo* assessment of rodent cross-reactivity and specificity of D15Akt2 and D27Akt2 siRNAs

The overall strategy of designing siRNAs was to obtain candidates that cross the species barrier and be specific towards the designated isoform in both humans and rodents. As the cross-reactivity was verified for Akt1 siRNA candidates, the same was done for Akt2 siRNA candidates. For that, the mouse HCC cell line Hepa1.6 cell line was used. Cells were pulse-transfected for 6 hours with LipofectamineRNAiMAX alone or coupled to D15Akt2 or D27Akt2 siRNAs at a concentration of 10nM. The expression of Akt2 and Akt1 was assessed on the protein level by Jess immune-detection 48 hours later.

The results, *see Figure 21A*, showed that upon the transfection with either D15Akt2 or D27Akt2 siRNAs, a significant decrease of Akt2 was obtained (88% and 81%, respectively). Whereas, no change was observed in the Akt1 expression level following transfection, *see Figure 21B*. These results thus confirm the cross-reactivity and the specificity of both siRNAs to *Mus musculus*.

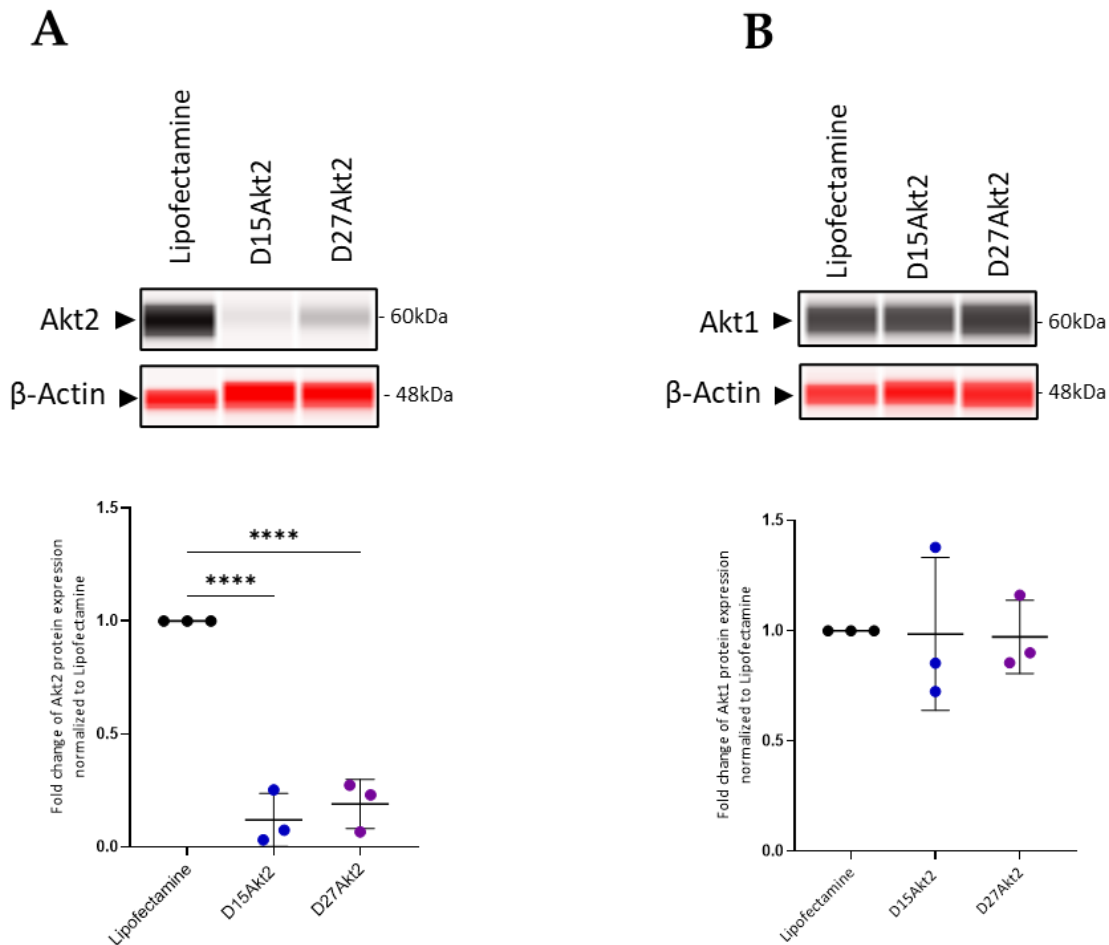


Figure 21: Rodent cross-reactivity and specificity of Akt2 siRNAs. Protein immuno-detection by Jess showing the expression of Akt2 and Akt1 isoforms in Hepa1.6 cell line, 48 hours following the transfection with D15Akt2 and D27Akt2 siRNAs. The top panel shows representative blots of (A) the expression of Akt2, and its corresponding quantification represented as mean ± SD (N=3 independent experiments) of the ratio of Akt2/β-Actin for each condition normalized to LipofectamineRNAiMAX alone. The asterisks represent the p-value: $P < 0.0001$ for both D15Akt2 and D27Akt2 siRNAs; (B) the expression of Akt1, and its corresponding quantification represented as mean ± SD (N=3 independent experiments) of the ratio of Akt1/β-Actin for each condition normalized to Lipofectamine alone. The statistical test used is Ordinary one-way ANOVA.

The process of screening for the best Akt1 siRNA candidate starting with the 11 candidates: D2Akt2, D3Akt2, D7Akt2, D15Akt2, D16Akt2, D20Akt2, D27Akt2, D39Akt2, D41Akt2, D44Akt2, and D49Akt2, led to the diminution of the number of candidates into 2: D15Akt2 and D27Akt2 siRNAs. After taking into account the *in cellulo* efficiency, specificity, off-target effect and cross-reactivity to rodents, and the fact that D11Akt1 siRNA lacks the needed specificity for the Akt1 isoform in both humans and rodents; the **D15Akt2 siRNA** was chosen as the best candidate for further analysis. based on the higher corrected score it has vs that of D27Akt2 siRNA. The corrected score is given by the DSIR algorithm upon the generation of

the siRNA sequences. It is the original efficacy score minored by the penalties from some intrinsic target features which have been shown to influence siRNA efficacy [310].

2. Long lasting effect of Akt1 and Akt2-targeting siRNAs

The efficiency of the siRNAs targeting Akt1 and Akt2 is not restricted with its ability to knockdown the respective proteins for a given time point, but rather the sustainability of such a knockdown over the span of time. For that, a kinetic study of the expression level of Akt1 and Akt2 over the span of 3 to 9 days was studied. HepG2 cells were pulse transfected for 6 hours with LipofectamineRNAiMAX coupled to D2Akt1 siRNA or D15Akt2 siRNA at 10nM concentration and the mRNA and protein expression level of Akt1 and Akt2 respectively were assessed. Since after 2 days of the pulse transfection the knockdown was evident, (demonstrated in the previous parts) the kinetic study began at day 3 and continued every two days: day 5,7 and 9.

Interestingly, the results demonstrated that D2Akt1 siRNA transfection led to a decrease in the mRNA expression of *AKT1* by 62% at day 3 which gradually increased until regaining the expression level as the mock siRNA and reaching a plateau at day 7 and day 9, *see Figure 22A*. The protein expression level of Akt1 followed the same trend by showing a 63% decrease at day 3, followed by a 35% decrease at day 5, until regaining an expression level that is the same as the mock at day 7 and 9, *see Figure 22B and C*.

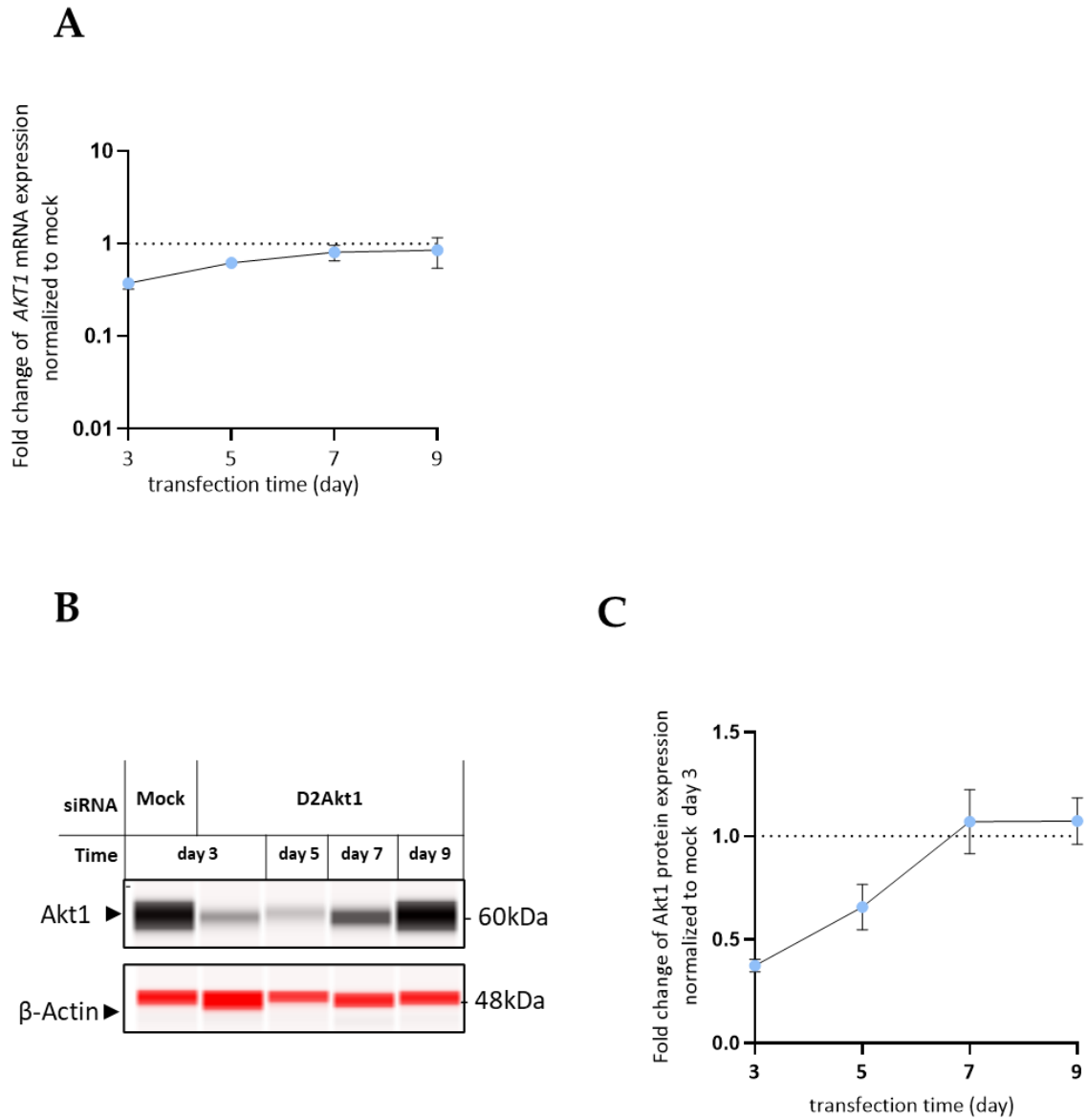


Figure 22: Long-lasting effect of D2Akt1 siRNA. Transcriptomic and proteomic analysis of the expression of Akt1 was done in HepG2 cells following the 6hour pulse transfection with LipofectamineRNAiMAX coupled to D2Akt1 siRNA. (A) The Akt1 mRNA expression evolution throughout 3 to 9 days is presented as mean +SD (N=3 independent experiments). of the fold change normalized to the mock at day 3 (B) A representative protein immunodetection by Jess throughout day 3-9. (C) The corresponding quantification of the protein immune-detection represented as mean \pm SD (N=3 independent experiments) of the ratio of Akt1/ β -Actin for each condition normalized to the mock condition at day 3.

More prominently, following the transfection with D15Akt2 siRNA the results showed a decrease in the *AKT2* mRNA level by 58% at day 3 which was maintained throughout day 5 (55%) and day 7 (40%), before regaining its an expression level equal to the mock condition at day 9, see *Figure 23A*. The protein expression of Akt2 followed the same trend as the mRNA expression levels. However, the decrease in the protein level remained drastic throughout day 3, 5 and 7 (92%, 83%, 77%, respectively), before spiking to the same level as the mock at day 9, see *Figure 23B and C*.

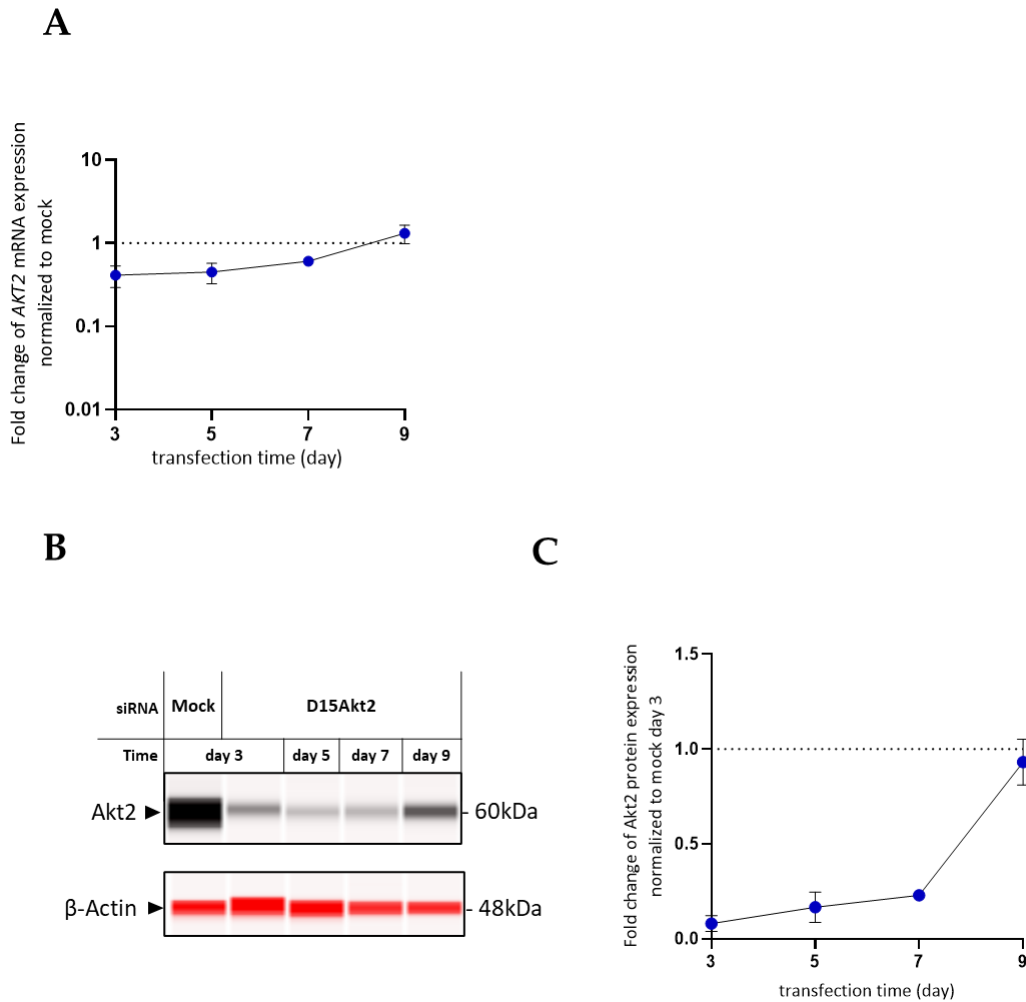


Figure 23: Long-lasting effect of D15Akt2 siRNA. Transcriptomic and proteomic analysis of the expression of Akt2 was done in HepG2 cells following the 6hour pulse transfection with LipofectamineRNAiMAX coupled to D15Akt2 siRNA. **(A)** the Akt2 mRNA expression evolution throughout 3 to 9 days is presented as mean +SD (N=3 independent experiments). of the fold change normalized to the mock at day 3. **(B)** A representative protein immunodetection by Jess throughout day 3-9 **(C)** the corresponding quantification represented as mean \pm SD (N=3 independent experiments) of the ratio of Akt2/ β -Actin for each condition normalized to the mock condition at day 3.

These results showed that the transfection of HepG2 cells for a short period of time (6 hours) with Akt1 or Akt2- targeting siRNAs was sufficient to mount not only a significant decrease in the expression of Akt1 and Akt2, but also a decrease that lasted for a long period of time. In conclusion, the designed siRNAs can be considered as specific, and long-lasting.

3. Efficiency of Akt1 and Akt2-targeting siRNAs

Following the results obtained with the kinetic study and since the 10nM was efficient to mount such a long-lasting effect, the next step in the characterization of the designed siRNAs was assessing their efficiency at lower concentrations. In order to test that, HepG2 cells were pulse transfected for 6 hours with D2Akt1 siRNA, D15Akt2 and mock siRNAs at varying concentrations stretching to the picomolar range (pM): 2.5, 5, 10, 20, 50, 70, 100, and 1000 pM. RT-qPCR and protein immuno-detection was done 48hours later.

The results of D2Akt1 siRNA transfection showed a dose-dependent decrease in the expression of *AKT1* at the mRNA level starting from 10% of decrease at 2.5 pM, to 70% at 1000 pM, when compared to the mock *see Figure 24A*. Additionally, the assessment of the expression of Akt1 at the protein level mirrored the scenario at the mRNA level, whilst the first signs of diminution in the expression appeared with 13% at 20 pM (13%), with a continued decrease reaching 65% at 1000 pM, *see Figure 24B and C*.

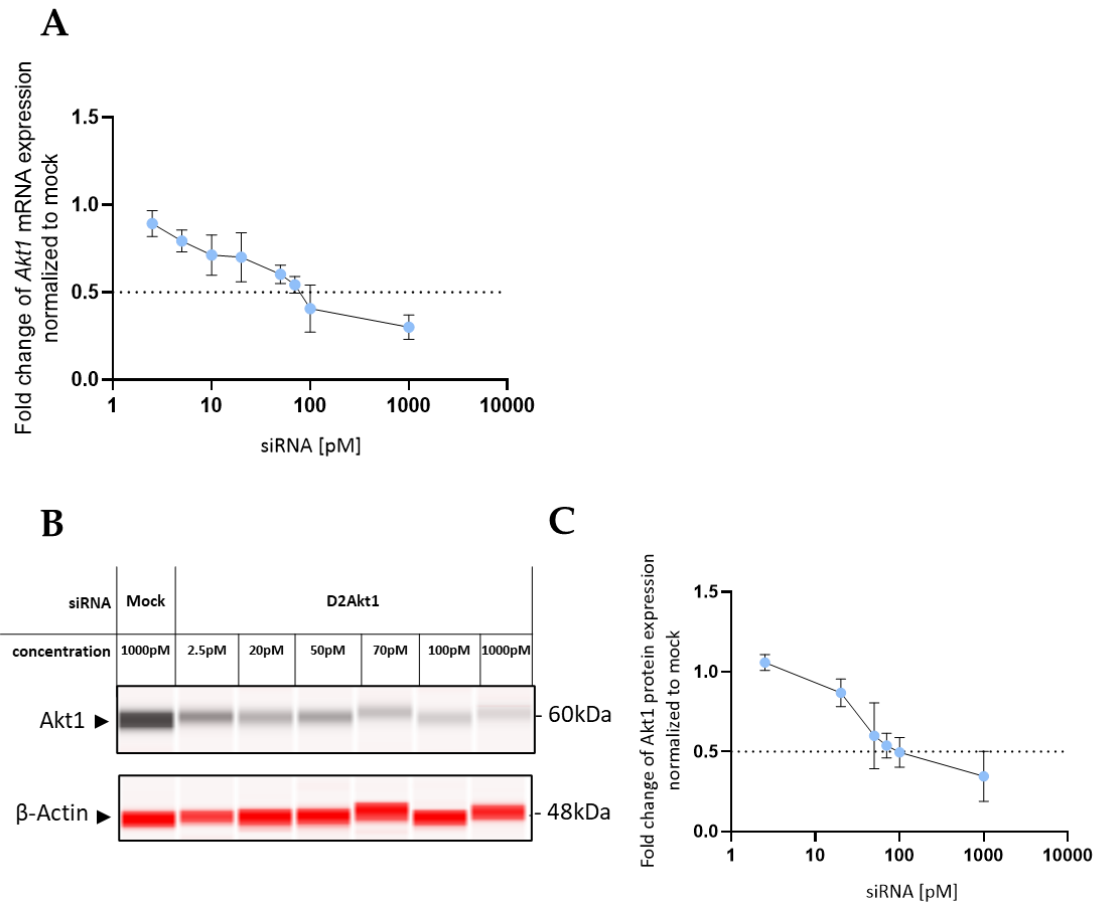


Figure 24: Efficiency of D2Akt1 siRNA. Transcriptomic and proteomic analysis of the expression of Akt1 was done in HepG2 cells following the 6hour pulse transfection with LipofectamineRNAiMAX coupled to D2Akt1 siRNA. at varying concentrations 48 hours after transfection. **(A)** the Akt1 mRNA expression evolution is presented as mean \pm SD (N=3 independent experiments) of the fold change at each concentration: 2.5, 5, 10, 20, 50, 70, 100, and 1000pM, normalized to the mock at 1000pM. **(B)** A representative protein immuno-detection by Jess **(C)** the corresponding quantification represented as mean \pm SD (N=3 independent experiments). of the ratio of Akt1/ β -Actin for each concentration (2.5, 20, 50, 70, 100 and 1000pM) normalized to the mock at 1000pM.

Similarly, the D15Akt2 siRNA transfection led to a dose-dependent decrease of AKT2 expression, compared to the mock, see Figure 25A at the mRNA level starting from 18% at 2.5pM. The expression further dropped by 30% at 20pM with a continued decrease reaching 51% at 1000pM concentration. The expression of Akt2 at the protein level however showed a better efficiency of the siRNA compared to that at the transcriptomic level. The first sign of decrease in the expression of Akt2 compared to the mock, was shown by 4% at 2.5pM with a continued decrease reaching 78% at 1000pM, see Figure 25B and C.

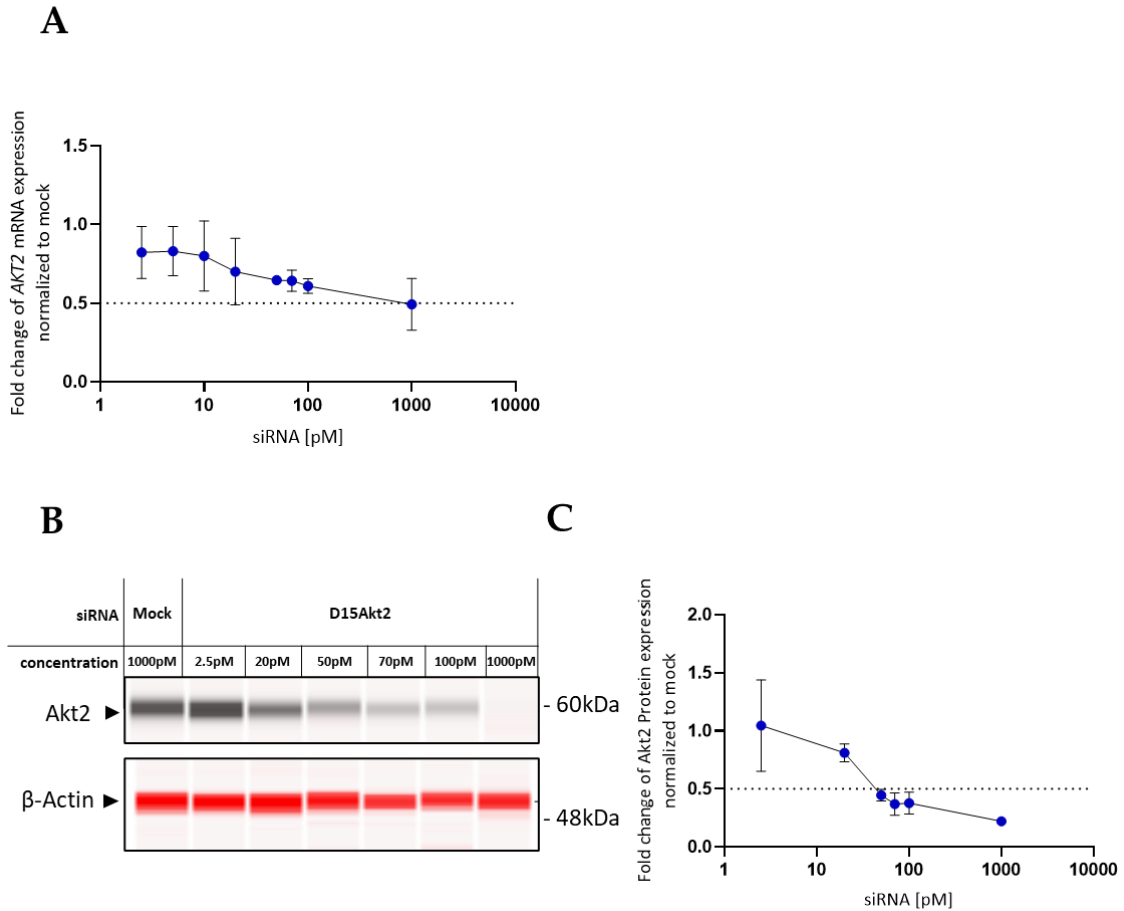


Figure 25: Efficiency of D15Akt2 siRNA. Transcriptomic and proteomic analysis of the expression of Akt2 was done in HepG2 cells following the 6hour pulse transfection with LipofectamineRNAiMAX coupled to D15Akt2 siRNA. at varying concentrations 48 hours after transfection. (A) the Akt2 mRNA expression evolution is presented as mean \pm SD of the fold change at each concentration: 2.5, 5, 10, 20, 50, 70, 100, and 1000pM, normalized to the mock at 1000pM (N=3 independent experiments). (B) A representative protein immuno-detection by Jess, (C) the corresponding quantification represented as mean \pm SD (N=3 independent experiments). of the ratio of Akt2/ β -Actin for each concentration (2.5, 20, 50, 70, 100 and 1000pM). normalized to the mock condition at 1000pM

The results demonstrate that the D2Akt1 siRNA is more efficient than the D15Akt2 siRNA, however both designed siRNAs display an Akt1 and Akt2 targeting activity in the pM range, following a short time of exposure: 6 hours. In conclusion, the designed siRNAs can be considered to be specific, long-lasting and efficient.

4. Inflammatory effect of Akt1 and Akt2-targeting siRNAs

RNA exposure may affect the immune/inflammatory response through a possible activation of the innate immune response signaling through Toll-like receptors (TLRs). Therefore, D2Akt1 and D15Akt2 siRNAs sequences were assessed. for activation of TLR using the NF κ B reporter cell line THP1-BlueTM-MD2-CD14 (further referred to as THP1-XBlue cells). It is a cell line derived from the human monocytic THP1 cells, which expressed all TLRs. THP1-XBlue cells were exposed for 24 hours to either D2Akt1 or D15Akt2 siRNA in their naked form (without any transfection reagent) at the following concentrations: 10nM, 20nM, 30nM and up to 100nM. Ligands of TLRs were used as positive controls: Pam3CSK4, HKLM, high molecular weight and low molecular weight poly (I:C), LPS-EK, FLA-ST, FSL-1, Imiquinone, ssRNA40, and ODN2006; which activate TLR1/2, TLR2, TLR3, TLR4, TLR5, TLR6/2, TLR7, TLR8 and TLR9, respectively. The activity of TLR is measured by the activity of alkaline phosphatase in a colorimetric assay.

The results showed no change in the absorbance at any of the used concentrations in both cases of exposure to D2Akt1 siRNA and D15Akt2 siRNA, *see Figure 26*. Thus, demonstrating no activation of the innate immune response via any of the TLR receptors.

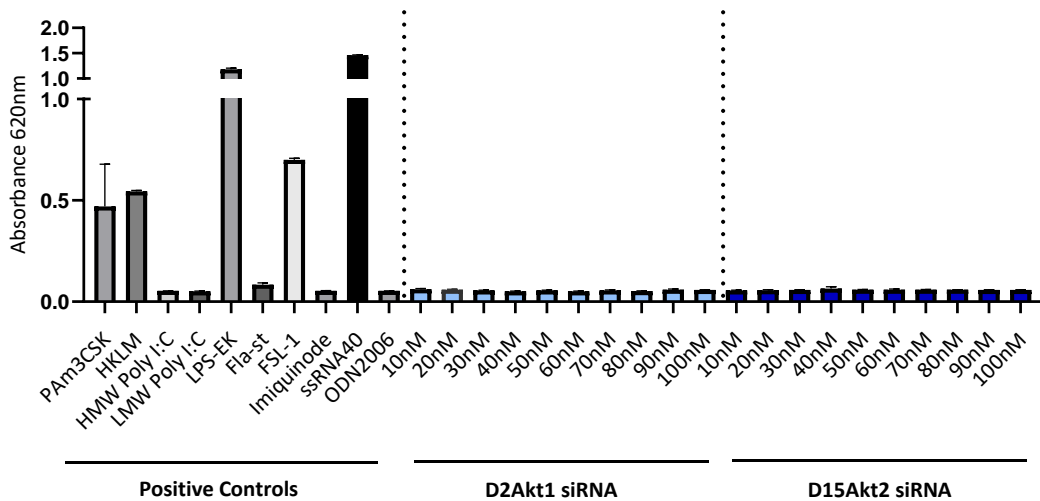


Figure 26: Pro-inflammatory effect of D2Akt1 and D15Akt2 siRNAs. Quantification of the Alkaline phosphatase activity of THP1-XblueTM MD2-CD14 cells, done by Quanti Blue and measured for the absorbance at 620nm (N=3 independent experiments). The exposure was done for 24 hours to the positive controls: 1 ng/ml Pam3CSK4 (TLR1/2), 10 ng/ml FSL-1 (TLR2/6), 107 cells/ml HKLM (TLR2), 10 mg/ml poly(I:C) (TLR3), 10 ng/ml LPS-EK (TLR4), 10 ng/ml RecFLA-ST (TLR5), 5 mg/ml imiquimod (TLR7), 5 mg/ml CL075 (TLR8), 10 mg/ml ODN2006 (TLR9); and D2Akt1 siRNA or D15Akt2 at 10, 20, 30, 40, 50, 60, 70, 80, 90, and 100nM. No sign

5. Phenotypic effect of the designed siRNA-mediated knockdown of Akt1 and Akt2

After verifying the efficiency of the designed siRNAs, the absence of any off-target effect on the genetic level and on the immune system, and further the long-lasting effect of the knockdown, the phenotypic effect of the siRNA-mediated knockdown of Akt1 and Akt2 was investigated in the cellular context. The designed siRNAs were tested for their effect on the various cellular processes: cell death, metabolism and cell proliferation. The previously mentioned processes were assessed whilst comparing to Sorafenib, as one of the current options of clinical treatment for HCC, and ARQ092 as a chemical inhibitor of both isoforms of Akt simultaneously.

5.1. Effect of the designed siRNA-mediated knockdown of *Akt1* and *Akt2* on cytotoxicity

As a first step, the effect of the designed siRNAs on cytotoxicity was assessed on the following human liver cell lines: PLCY/PRF/5, Huh7, Hep3B and HepG2. Upon cell death, many enzymes are released into the supernatant, among which is Lactase Dehydrogenase (LDH). Accordingly, the levels of LDH in the supernatant were measured by CytotoxOne kit, 24 after a 6hour pulse transfection of the cells with LipofectamineRNAiMAX coupled to D2Akt1 or D15Akt2 or both of the siRNAs at 10nM concentration, in addition mock siRNA as a control. A cytotoxic effect is considered to be evident when more than 20% of the cells are dead. The results showed no cytotoxic effect in any of the cell lines tested following the knockdown of Akt1, Akt2, or both isoforms simultaneously, *see Figure 27*. These results confirmed that the designed siRNAs did not elicit a cytotoxic effect on PLCY/PRF/5, Huh7, Hep3B and HepG2 cell lines.

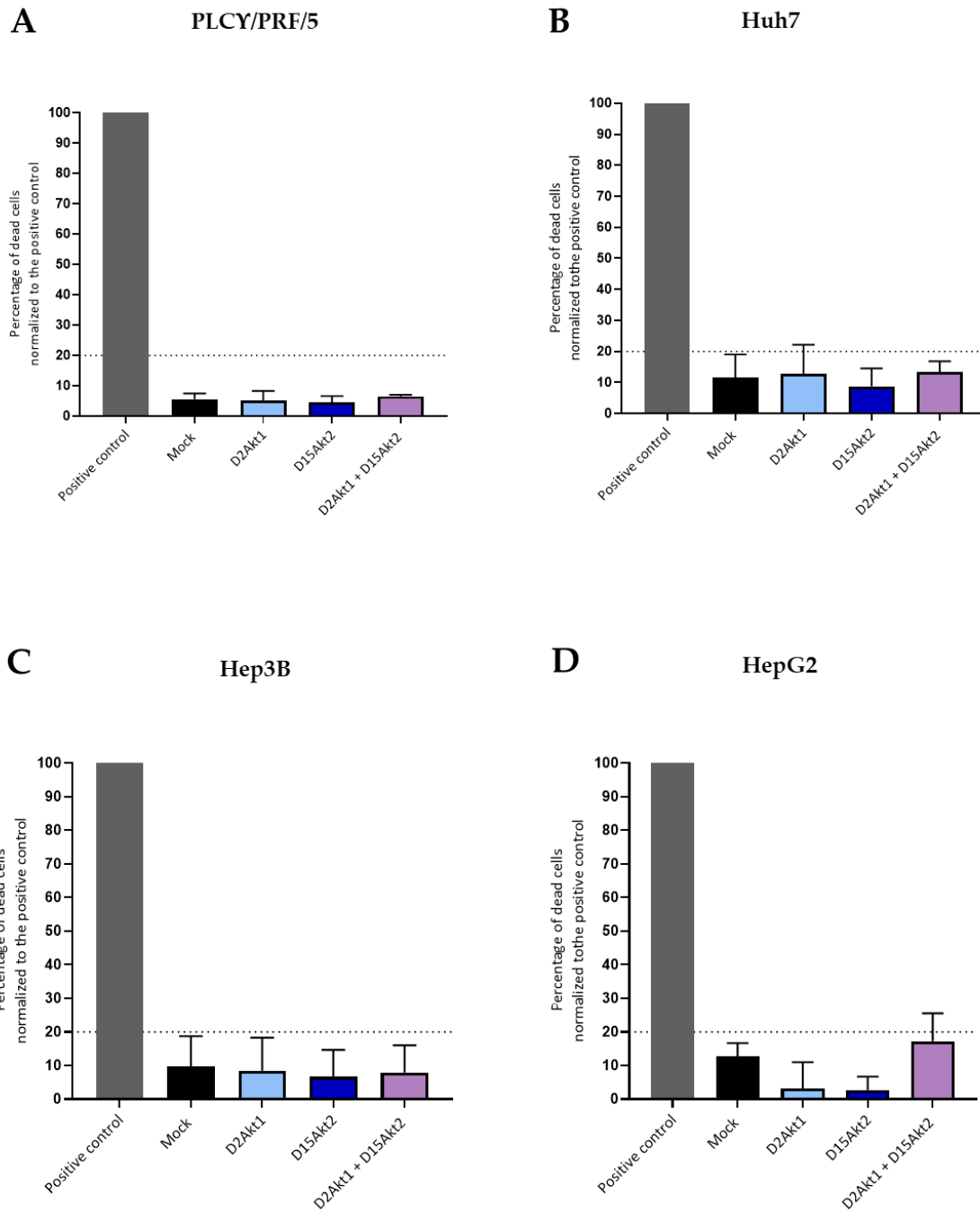


Figure 27: Effect of Akt1 and/or Akt2 knockdown on cytotoxicity. Measurement of the LDH levels in the supernatant 24 hours following the transfection, by LipofectamineRNAiMax coupled to D2Akt1, D15Akt2 siRNA or both simultaneously, of (A) PLCY/PRE/5 cell line, (B) Huh7 cell line, (C) Hep3B cell line, and (D) HepG2 cell line. The graphs represent the mean \pm SD (N=3 independent experiments) of the percentage of dead cells normalized to the positive control (lysis solution supplied with the Cytotoxone kit).

5.2. Effect of the designed siRNA-mediated knockdown of Akt1 and Akt2 on cell metabolism

Since the PI3K/Akt pathway is implicated in the regulation of the cell metabolism, the effect of targeting Akt1, Akt2, or both simultaneously by the designed siRNAs, on the production of ATP was tested on the 4 cell lines: PLCY/PRF/5, Huh7, Hep3B and HepG2. For that, the cells were subject to a 6hour pulse transfection by LipofectamineRNAiMAX coupled to D2Akt1, D15Akt2 or both siRNAs simultaneously at 10nM concentration, or treated for 6 hours with Sorafenib at 1 μ M and 10 μ M concentration and ARQ092 at 1 μ M, 10 μ M and 100 μ M. The ATP production rate in was measured 24 hours later.

The results of PLCY/PRF/5, *see Figure 28A*, upon the single knockdown of Akt1 or Akt2, or both simultaneously, showed a general elevated ATP production rate compared to the untreated cells. However, no significant change in the ATP activity was observed when compared to the mock siRNA, On the other hand, the ATP activity when the cells were treated with Sorafenib and ARQ092 showed no significant effect at the 1 μ M concentration of both, a significant decrease was shown with Sorafenib 10 μ M treatment by 44%, and ARQ092 treatments at 10 μ M (44%) and 100 μ M (98%); when compared to the control DMSO 1 μ M. The decrease observed is correlated to the concentration.

Huh7 cells, did not show the same results, *see Figure 28B*. In this cell line, aside from the general increase in the activity of ATP in all the transfection conditions compared to the untreated cells, only the single knockdown of Akt1 showed a significant decrease in the ATP activity when compared to the mock siRNA by 38%. Additionally, treatment with Sorafenib 1 μ M showed a significant decrease in the ATP production rate and with a more pronounced decrease at the 10 μ M concentration (71% and 91%, respectively). However, the treatment with ARQ092 10 μ M and 100 μ M showed a significant, concentration-dependent decrease in the ATP activity (72% and 95%, respectively), when compared to DMSO 1 μ M.

Hep3B cell line, *see Figure 28C*, and HepG2 cell line, *see Figure 28D* showed a pattern of ATP production rate quite similar to that of PLCY/PRF/5 cell line. Namely, a general increase in the ATP activity with all the transfected conditions compared to the untreated cells, with no significant change upon comparison to the internal control (mock siRNA); versus a decrease in the case of the chemical inhibitors upon the comparison to the internal control (DMSO 1 μ M). In the case of Hep3B cells, Sorafenib 10 μ M showed a decrease in ATP activity by 72%, whereas

ARQ092 10 μ M and 100 μ M showed a significant decrease by 64% and 93%, respectively. Whereas HepG2 cell line showed a decrease summarized by 64% when treated with Sorafenib 10 μ M, and 84% and 97% when treated with ARQ092 10 μ M, and 100 μ M, respectively.

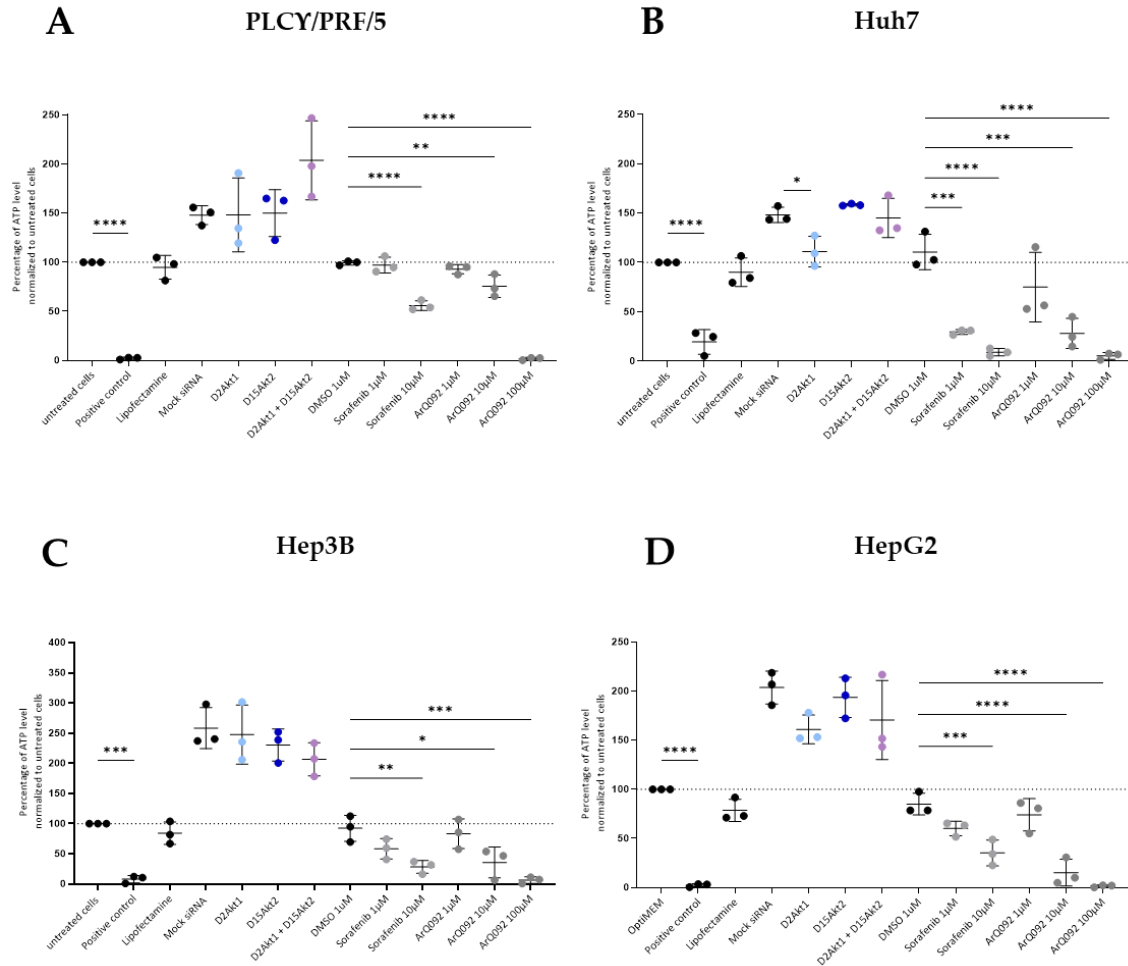


Figure 28: Effect of Akt1 and/or Akt2 knockdown on cell metabolism. Measurement of the ATP levels 24 hours following the transfection, by LipofectamineRNAiMAX coupled to D2Akt1, D15Akt2 siRNA or both simultaneously (10nM); or treated with Sorafenib (1 μ M and 10 μ M) and ARQ092 (1 μ M, 10 μ M and 100 μ M). ATP activity was measured by ViaLight® Plus Cell Proliferation and Cytotoxicity Bioassay kit. Where the control for transfection was the mock siRNA whilst that of the chemical inhibitors was DMSO at 1 μ M. A positive control was introduced as well to kill the cells (DMSO 1000 μ M). The results are presented as mean \pm SD (N=3 independent experiments) of the percentage of ATP level normalized to the untreated cells. Ordinary one-way ANOVA statistical analysis was done for every condition versus its control. (A) ATP levels in PLCY/PRE/5 cell line, the asterisks present the p-values for: positive control ($p < 0.0001$), Sorafenib 10 μ M ($p < 0.0001$), ARQ092 10 μ M ($p = 0.0029$), ARQ092 100 μ M ($p < 0.0001$). (B) ATP levels in Huh7 cell line, the asterisks present the p-values for: positive control ($p < 0.0001$), Sorafenib 1 μ M ($p = 0.0005$), Sorafenib 10 μ M ($p < 0.0001$), ARQ092 10 μ M ($p = 0.0004$), ARQ092 100 μ M ($p < 0.0001$), D2Akt1 siRNA ($p = 0.0212$). (C) ATP levels in Hep3B cell line, the asterisks present the p-values for: positive control ($p = 0.0008$), Sorafenib 10 μ M ($p = 0.0056$), ARQ092 10 μ M ($p = 0.0130$), ARQ092 100 μ M ($p = 0.0006$). (D) ATP levels in HepG2 cell line, the asterisks present the p-values for: positive control ($p < 0.0001$), Sorafenib 10 μ M ($p = 0.0009$), ARQ092 10 μ M ($p < 0.0001$), ARQ092 100 μ M ($p < 0.0001$).

Altogether, the results imply a general increase in the metabolic activity of the ATP metabolism in all siRNAs the transfections but not with that of the Lipofectamine alone, which could be attributed to an over-drive of the cells upon the addition of siRNAs. Of note, once compared to the internal control of transfection, namely mock siRNA, no change in the metabolic activity was observed, except in the case of Huh7 cell line which shows a slight decrease in the metabolic activity upon the single knockdown of Akt1, while sustaining an activity that is higher than that of the untreated cells. Thus, such an effect cannot be consolidated as an effect of the knockdown of Akt1 and/or Akt2. Hence, the knockdown mediated by the designed siRNAs shows no effect on the mitochondrial metabolism of the cells. This was not the case with Sorafenib and ARQ092 where a prominent decrease in the mitochondrial cell metabolism was observed in the 4 cell lines.

5.3. Effect of the siRNA-mediated knockdown of Akt1 and Akt2 on cell proliferation

Cell proliferation is also among the cellular processes that could be affected by targeting Akt1 and Akt2 due to the implication of the PI3K/Akt pathway in cell proliferation. Similarly, to what was done in the previous sections, the 4 cell lines: PLCY/PRF/5, Huh7, Hep3B and HepG2, were assessed for their proliferation rate, following the transfection with the designed siRNAs D2Akt1 or D15Akt2 or both of them simultaneously at 10nM concentration, or the treatment with the chemical inhibitors: Sorafenib (1 μ M and 10 μ M) and ARQ092 (1 μ M, 10 μ M, and 100 μ M).

The results for the PLCY/PRF/5 cell line, *see Figure 29A* show that following the siRNA-mediated single knockdown of Akt1 or Akt2 or the simultaneous knockdown of both by the designed siRNAs, no significant change in the proliferation rate was obtained when compared to the untreated cells, mock siRNA, or Lipofectamine alone conditions. Moreover, no significant change in the proliferation rate was obtained upon the treatment with Sorafenib or ARQ092 at 1 μ M, however, a significant decrease was shown with Sorafenib 10 μ M (70%), and ARQ092 at 10 μ M (46%) and 100 μ M (98%), when compared to DMSO 1 μ M.

Huh7 cell line, *see Figure 29B* showed a significant decrease in the proliferation rate when compared to the untreated cells upon the treatment with Lipofectamine (40%). The treatment with the chemical inhibitors, showed a similar pattern to that of the PLCY/PRF/5 cell line. The results show a significant decrease upon the

treatment with Sorafenib 10 μ M (96%) which was more prominent than that seen in the PLCY/PRF/5 cell line. Similarly, a significant decrease in the proliferation rate was shown in the case of ARQ092 10 μ M (95%) and 100 μ M (97%), when compared to DMSO 1 μ M.

Hep3B cell line, *see Figure 29C*, showed a pattern of change in the proliferation rate similar to that seen with Huh7 cell line. A significant decrease in the proliferation rate, when compared to untreated cells, was obtained, upon the treatment with Lipofectamine alone (45%). The chemical inhibitors' effect on the proliferation rate showed the same aspect as the previous cell lines, when compared to DMSO 1 μ M, summarized by a decrease in the proliferation rate upon treatment with: Sorafenib 10 μ M (89%), ARQ092 10 μ M (49%) and ARQ092 100 μ M (100%). However, unlike the other cell lines, a significant decrease in the proliferation rate was shown in the case of Sorafenib 1 μ M (38%).

Finally, the HepG2 cell line, *see Figure 29D*, demonstrated a significant decrease in the proliferation rate upon the treatment with Lipofectamine alone (52%). A significant decrease in the proliferation was also evident in the case of the treatment with the chemical inhibitors, when comparing to DMSO 1 μ M. Numerically the observed decrease was: 90% for Sorafenib 10 μ M, 95% for ARQ092 10 μ M, and 99% for ARQ092 100 μ M treatments.

Altogether, the results showed a varying pattern between the 4 cell lines. Interestingly, in the case of Huh7, Hep3B and HepG2 cell lines, when comparing to the internal controls, namely, Lipofectamine alone or the mock siRNA, no significant change in the cell proliferation was observed, despite its significant decrease when compared to the untreated cells. Thus, implying that the shown drop in the proliferation rate is due to the stress implicated by Lipofectamine on the cells rather than a specific effect of the knockdown. On the other hand, ARQ092 and Sorafenib show a prominent effect on the cell proliferation in all the tested cell lines with varying efficiencies.

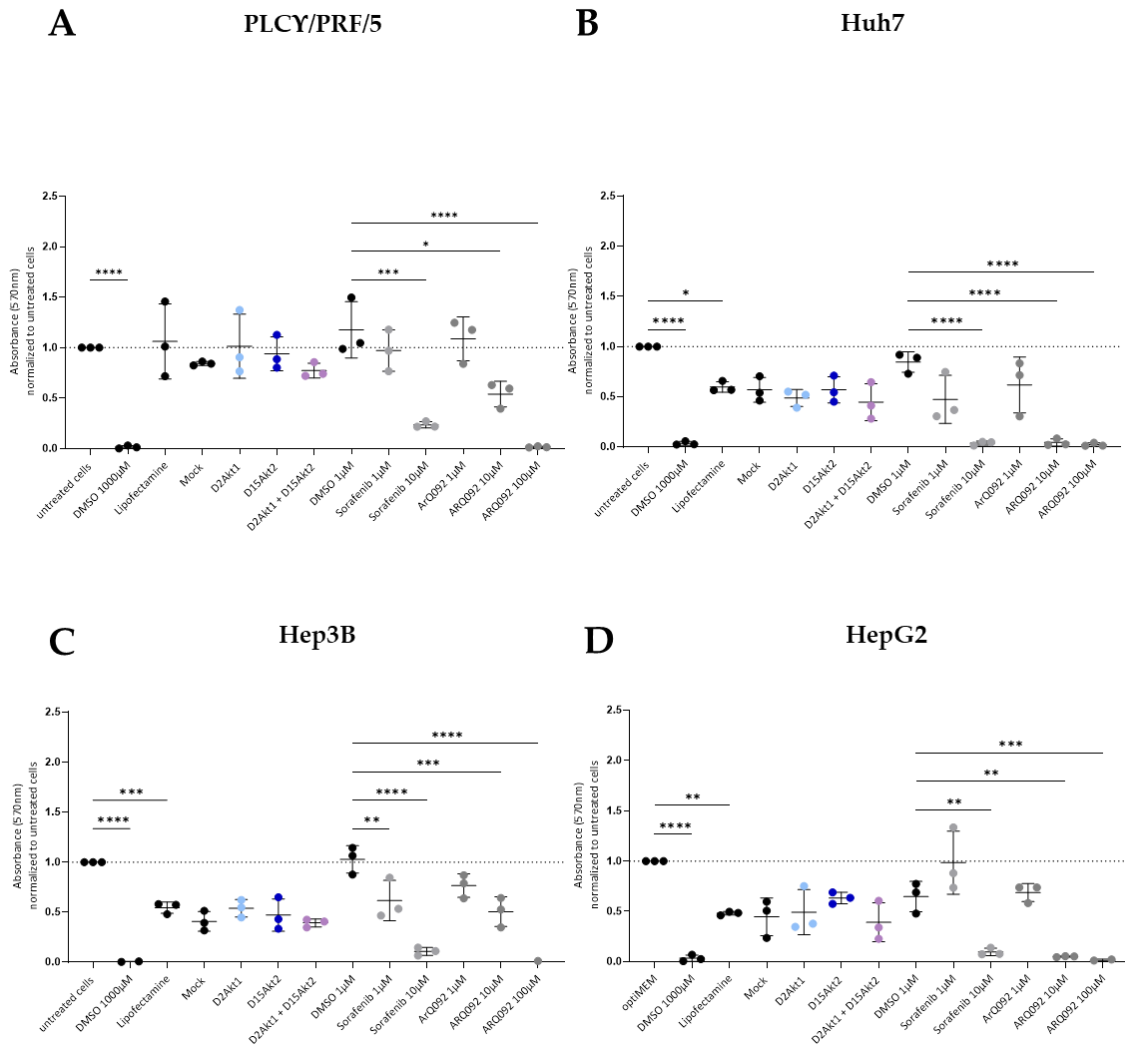


Figure 29: Effect of Akt1 and/or Akt2 knockdown on cell proliferation. Measurement of the formazon levels in the supernatant 48 hours following the transfection, by LipofectamineRNAiMAX coupled to D2Akt1, D15Akt2 siRNA or both simultaneously (10nM); or treated with Sorafenib (1 μ M and 10 μ M) and ARQ092 (1 μ M, 10 μ M and 100 μ M). Formazon levels were measured by CellTiter 96® Non-Radioactive Cell Proliferation Assay. Where the internal control for transfection was the LipofectamineRNAiMAX alone and the mock siRNA whilst that of the chemical inhibitors was DMSO at 1 μ M. A positive control was introduced as well to kill the cells (DMSO 1000 μ M). The results are presented as mean \pm SD (N=3 independent experiments) of absorbance at 570nm normalized to the untreated cells. Ordinary one-way ANOVA statistical analysis was done for every condition and the indicated control on the graph. **(A)** Absorbance at 577 nm in (A) PLCY/PREF/5 cell line, the asterisks present the p-values for: positive control ($p < 0.0001$), Sorafenib 10 μ M ($p = 0.0001$), ARQ092 10 μ M ($p = 0.153$), ARQ092 100 μ M ($p < 0.0001$). **(B)** Absorbance at 577 nm in Huh7 cell line, the asterisks present the p-values for: positive control ($p < 0.0001$), Lipofectamine ($p = 0.0373$), Sorafenib 10 μ M ($p < 0.0005$), ARQ092 10 μ M ($p < 0.0001$), ARQ092 100 μ M ($p < 0.0001$). **(C)** Absorbance at 577 nm in Hep3B cell line, the asterisks present the p-values for: positive control ($p < 0.0001$), Lipofectamine ($p = 0.0010$), Sorafenib 1 μ M ($p = 0.0034$), Sorafenib 10 μ M ($p < 0.0001$), ARQ092 10 μ M ($p = 0.0001$), ARQ092 100 μ M ($p < 0.0001$). **(D)** Absorbance at 577 nm in HepG2 cell line, the asterisks present the p-values for: positive control ($p < 0.0001$), Lipofectamine ($p = 0.0064$), Sorafenib 10 μ M ($p = 0.0033$), ARQ092 10 μ M ($p = 0.0012$), ARQ092 100 μ M ($p = 0.0005$). l

6. Vectorization of the designed Akt1 and Akt2 siRNAs using AD

So far, the designed siRNAs: D2Akt1 and D15Akt2, have been shown to be specific, long-lasting, and efficient. Moreover, they have been shown to cross the species barrier whilst having no inflammatory effect by themselves and no effect on the main cellular processes *in cellulo*. Despite their potency, the siRNAs show no significant effect on tumoral cell lines. We further investigated potential antitumoral actions in a more complex context by the mean of an *in vivo*. Actually, the choice of a vector suitable for use *in vivo* is essential. The vector of choice was the amphiphilic dendrimer (AD) due to its validated use as a delivery vector for siRNAs, and its ability to not only elicit its function in primary cells but also has been proven to be used *in vivo* [308].

The AD is a hybrid between a branched polymer and a lipid, which takes from the advantages of both traits to have a better delivery efficiency. Moreover, it retains its highly branched form and self-assembly aspect and thus gives it a greater advantage in binding to the siRNA, *see Figure 30A*. The AD-to-siRNA ratio serves an important factor in the complexation of the AD to siRNA and is termed as N/P ratio. According to the guidelines provided for cell transfection [306], the N/P used was 5 and concentrations 50 and 70nM. For that, HepG2 cells were selected to test the efficiency of the AD (N/P 5) as a delivery vector for D2Akt1 and D15Akt2 designed siRNAs. The transfection was done by a 6 hour pulse transfection and the readout of the expression of Akt1 and Akt2 at the protein level change was done 48 hours later, whilst monitoring the cytotoxicity after 6 hours, 24 hours and 48 hours by LDH assay.

The LDH results, showed no cytotoxic effect of the AD N/P 5 alone or coupled to either of the siRNAs at both 50nM and 70nM at the 6-hour, 24-hour or 48-hour time point *see Figure 30B*. Further, upon the AD N/P 5 – D2Akt1 siRNA-mediated transfection, the expression of Akt1, *see Figure 30C*, significantly decreased by 68% and 63% at 50nM and 70nM concentrations, respectively, when compared to the mock siRNA condition. Similarly, upon the AD N/P 5 – D15Akt2 siRNA-mediated transfection, the expression of Akt2, *see Figure 30D*, significantly decreased by 79% and 76%, at 50nM and 70nM concentrations, respectively. Moreover, the results showed that the treatment with the AD N/P 5 alone had no effect on the expression of either Akt1 or Akt2.

These results demonstrated a successful delivery of the siRNAs by the AD N/P 5, with equal efficiencies at both of the tested concentrations with no cytotoxicity.

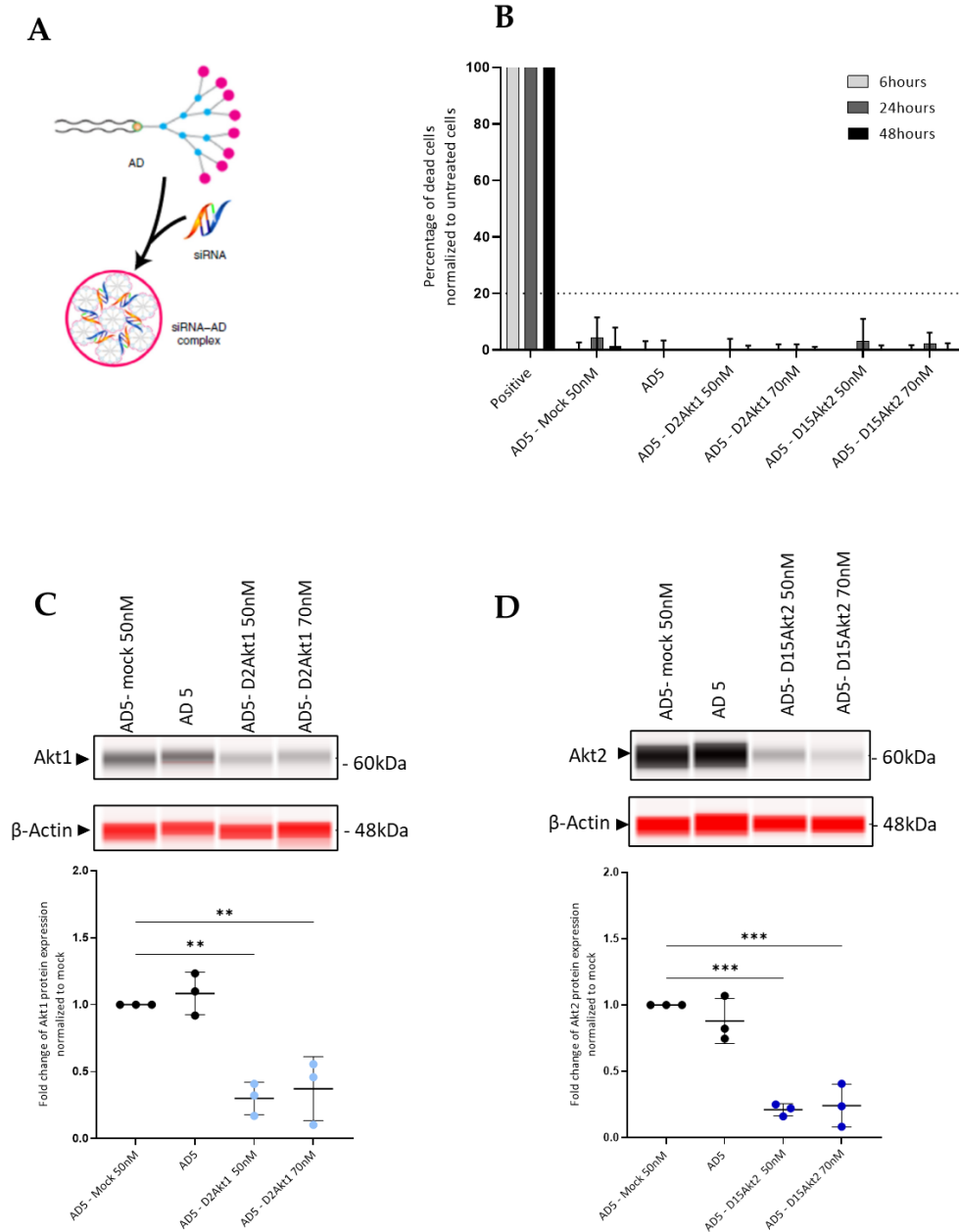


Figure 30: AD-mediated vectorization of siRNAs. (A) Scheme showing the structure of the AD, its self-assembly and complexation with the siRNAs. Adapted from Chen et al. Nature Protocols [306] (B) Measurement of the LDH levels in the supernatant 6, 24, and 48hours after 6hour pulse treatment of HepG2 cells with the AD alone, or coupled with the mock, D2Akt1, or D15Akt2 at the designated concentrations 50 or 70nM. The graph represents the mean \pm SD (N=3 independent experiments) of the percentage of dead cells normalized to untreated cells. (C) A representative protein immuno-detection by Jess of Akt1 protein expression and its corresponding quantification presented as mean \pm SD (N=3 independent experiments) of the ratio of Akt1/ β -Actin for each condition normalized to the AD5-mock siRNA 50nM condition. Ordinary one-way ANOVA statistical test was used, and the asterisks represent the p-value for AD5 – D2Akt1 siRNA 50nM ($p=0.0025$) and AD5 – D2Akt1 siRNA 70nM ($p=0.0050$). (D) A representative protein immuno-detection by Jess of Akt2 protein expression and its corresponding quantification presented as mean \pm SD (N=3 independent experiments) of the ratio of Akt2/ β -Actin for each condition normalized to the AD5-mock siRNA 50nM condition. Ordinary one-way ANOVA statistical test was used, and the asterisks represent the p-value for AD5 – D15Akt2 siRNA 50nM ($p=0.0002$) and AD5 – D15Akt2 siRNA 70nM ($p=0.0002$). AD5: Amphiphilic dendrimer N/P ratio 5.

7. *In ovo* assessment of the cytotoxicity and tumor growth of AD-designed siRNA-mediated knockdown of Akt1 and Akt2

Following the optimization of the delivery of D2Akt1 and D15Akt2 siRNAs by the AD N/P 5, the next step was to apply it to an *in vivo* context to assess the antitumorigenic effect of the designed siRNAs in a more physiological context. For that, the effect of the AD- siRNA-mediated knockdown of Akt1 and Akt2 on cytotoxicity and tumor growth was first tested in an *in ovo* model.

As innovative as that sounds, the egg model has been found to be the perfect middle ground between the *in cellulo* setup and the complex preclinical models of rodents. The *in ovo* model in this study was established by a company situated in Grenoble called “Inovotion” (<https://www.inovotion.com/>). This company had already established models of eggs harboring tumor grafts and exploited the physiological aspect of the growing embryo inside the egg to test the cytotoxicity of the applied drug – or in this case the complex of AD N/P 5-designed siRNA – while simultaneously being able to visualize and quantify the effect on the tumor growth on the surface. The added advantage versus the *in cellulo* is that there exists a whole physiological system of a living organism with an immune system that can unravel a new dimension of the effect of the treatment. Two models of choice were exploited in this study: the HepG2 and MV4-11 cell line models, *i.e.*, eggs that were either grafted with HepG2 cells or MV4-11 cells. The HepG2 cells were selected due to their compatibility to what was previously done *in cellulo* to represent the HCC tumor. The MV4-11 cell line on the other hand is a macrophage cell line. The notion behind its use was to assess the effect of the siRNA-mediated knockdown not only on the tumor itself but also on the tumor microenvironment which encompasses macrophages as a component.

The study was carried out AD N/P ratio 5 coupled to either mock, D2Akt1 or D15Akt2 siRNAs at a concentration of 50nM. The AD coupled to either of the designed siRNAs was administered in two doses: 0.025 mg/kg termed as “[1]” and 0.05 mg/kg termed as “[2]”. Whereas the mock siRNA was administered at only 0.05 mg/kg, *i.e.*, dose [2], and considered as the “negative control” throughout the study. The eggs were injected 4 times throughout the study, the first one being 2 days following the graft implantation (day E11, E signifies Embryo and thus the day is the age of the embryo in day) and then followed by another injection every 2 days. Every group included 15 eggs at the beginning of the study. Throughout the experiment, the embryos are monitored for their viability and dead embryos

were recorded. Further, at the end point of the experiment, day E18, the final surveillance of the dead/alive embryos was done to have the final score of the cytotoxicity of the AD-designed siRNA complex treatment. In addition, tumors were excised, fixed and weighed to ascertain for an anti-tumorigenic effect of the AD-designed siRNA-mediated knockdown of *Akt1* and *Akt2* in both HepG2 and MV4-11 cell line *in ovo* models.

7.1.HepG2 *in ovo* graft model

The results in the HepG2 cells in *in ovo* graft model showed no significant cytotoxic effect on the chick embryos throughout the experiment upon the treatment with AD N/P 5 coupled to either of the siRNAs at any of the doses [1] and [2], *see Figure 31A*, compared to the negative control group. The percentage of dead embryos did not surpass 29% (group of D15Akt2 [2]). Furthermore, the Kaplan-Meyer diagram, *see Figure 31B*, showed no significant difference in the probability of the survival between the different treatment groups. Unexpectedly, the tumor weight analysis at the end point, *see Figure 31C*, showed that at any of the tested doses the knockdown of *Akt1* or *Akt2*, by the AD N/P 5 coupled to either of the siRNAs (50nM), was not able to elicit a significant decrease in the tumor weight. However, although not significant, the knockdown of *Akt1* by AD N/P 5-D2Akt1 siRNA 50nM [1] shows the highest tendency of a decrease with tumor weight by a percentage of regression of 27% compared to the negative control, *see Table 19*.

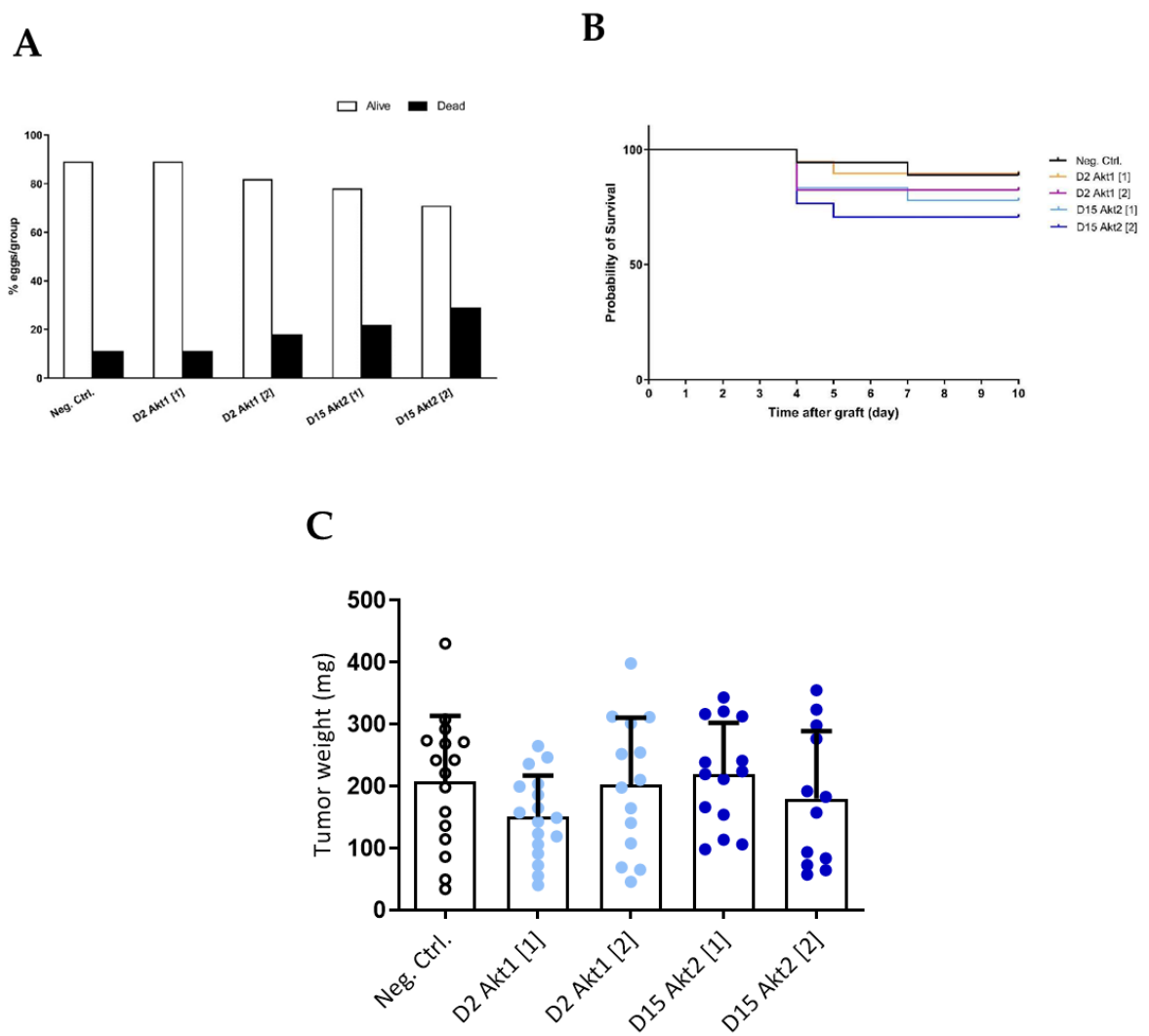


Figure 31: Effect of designed siRNAs in HepG2 in ovo graft model. The effect of AD-siRNA-mediated targeting of Akt1 and Akt2, on HepG2 tumor growth and chick toxicity. **(A)** Percentage of dead and surviving embryos at the end point. **(B)** Kaplan-Meier diagram showing the evolution of the chick toxicity throughout the study. **(C)** Graph representing the mean \pm SD (N is indicated in each condition by a circle) of the surviving chick embryos at the end point. The statistical test done is an ordinary one-way ANOVA. Neg. Ctrl: negative control; D2Akt1: AD N/P 5 – D2Akt1 siRNA 50nM; D15Akt2: AD N/P 5 – D15Akt2 50nM; [1]: dose 0.025 mg/kg; [2]: dose 0.05 mg/kg.

Table 19: End-point tumor weight analysis of HepG2 in ovo graft model. Gr.#: group number; n: number of eggs; Weight (mg): mean of the tumor weights at the end-point; SD: standard deviation; SEM: standard error of the mean; % Reg: percentage of regression.

Gr. #	Group Description	Tumor Analysis					p value vs Group #			
		n	Weight (mg)	SD	SEM	% Reg.	1	2	3	4
1	Neg. Ctrl.	16	208.21	105.7077	26.4269	/	/	/	/	/
2	D2 Akt1 [1]	17	150.80	66.6312	16.1604	27.57	0.4198	/	/	/
3	D2 Akt1 [2]	14	202.52	108.3616	28.9609	2.74	0.9998	0.5607	/	/
4	D15 Akt2 [1]	14	219.32	83.4521	22.3035	-5.33	0.9977	0.2778	0.9899	/
5	D15 Akt2 [2]	12	180.07	109.4359	31.5914	13.51	0.9368	0.9245	0.9745	0.8309

7.2.MV4-11 in ovo graft model

Similarly, the MV4-11 *in ovo* graft model showed no significant cytotoxic effect on the chick embryos following any of the previously mentioned treatments, *see Figure 32A*, when compared to the negative control group. The percentage of dead embryos did not surpass 12% (group of D2Akt1 [1]). Furthermore, the Kaplan-Meyer diagram, *see Figure 32B*, showed no significant difference in the survival probability between any of the treatment groups. Unexpectedly, and similar to the results obtained with the HepG2 *in ovo* graft model; the knockdown of Akt1 or Akt2, by the AD N/P 5 coupled to either of the siRNAs (50nM) did not elicit any significant decrease in the tumor weight, compared to the negative control, *see Figure 32C*. However, the AD N/P 5-D15Akt2 siRNA 50nM treatment showed a tendency of a decrease by 14% and 18% at doses [1] and [2] respectively, *see Table 20*.

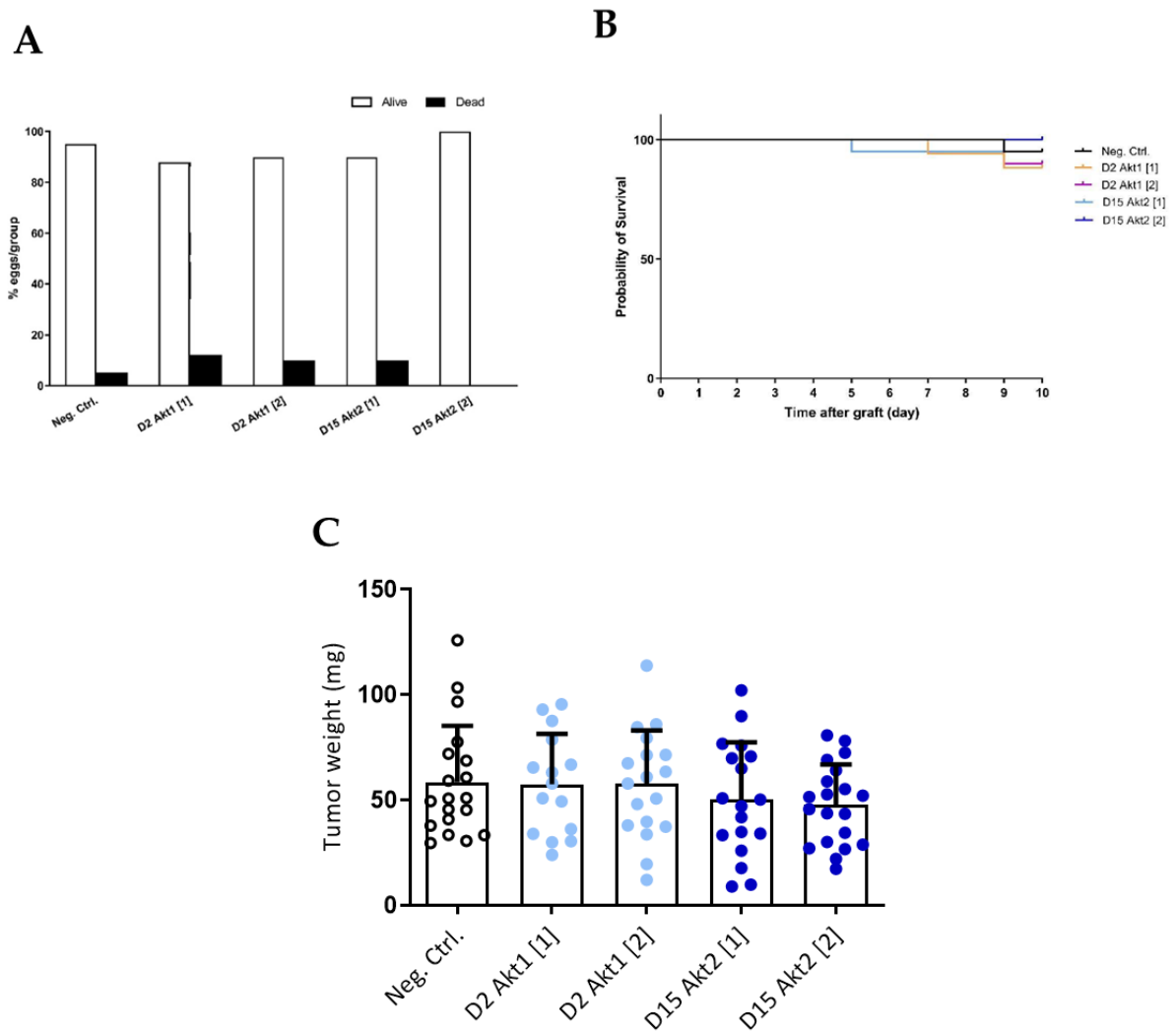


Figure 32: Effect of designed siRNAs in MV4-11 in ovo graft model. The effect of AD-siRNA-mediated targeting of Akt1 and Akt2, on HepG2 tumor growth and chick toxicity. **(A)** Percentage of dead and surviving embryos at the end point. **(B)** Kaplan-Meier diagram showing the evolution of the chick toxicity throughout the study. **(C)** Graph representing the mean \pm SD (N is indicated in each condition by a circle) of the surviving chick embryos at the end point. The statistical test done is an ordinary one-way ANOVA. Neg. Ctrl: negative control; D2Akt1: AD N/P 5 – D2Akt1 siRNA 50nM; D15Akt2: AD N/P 5 – D15Akt2 50nM; [1]: dose 0.025 mg/kg; [2]: dose 0.05 mg/kg.

Table 20: End-point tumor weight analysis of MV4-11 in ovo graft model. Gr.#: group number; n: number of eggs; Weight (mg): mean of the tumor weights at the end-point; SD: standard deviation; SEM: standard error of the mean; % Reg: percentage of regression.

Gr. #	Group Description	Tumor Analysis					p value vs Group #			
		n	Weight (mg)	SD	SEM	% Reg.	1	2	3	4
1	Neg. Ctrl.	19	58.62	26.6923	6.1236	/	/	/	/	/
2	D2 Akt1 [1]	15	57.62	23.8562	6.1596	1.70	>0.9999	/	/	/
3	D2 Akt1 [2]	18	57.63	25.4932	6.0088	1.69	>0.9999	>0.9999	/	/
4	D15 Akt2 [1]	18	50.36	27.0834	6.3836	14.08	0.8443	0.9153	0.9006	/
5	D15 Akt2 [2]	20	47.82	19.0683	4.2638	18.43	0.6462	0.7686	0.7339	0.9977

The overall results clearly demonstrate the absence of a cytotoxic effect of the AD N/P 5-D2Akt1 or D15Akt2 siRNA (50nM) transfection system at any of the doses 0.025 mg/kg or 0.05 mg/kg in the *in ovo* models of HepG2 and MV4-11 grafted cells. However, unexpectedly, no antitumorigenic effect was elicited in any of the models upon the treatment. Despite the statistical insignificance of the results, the tendency of the decrease observed in the 2 models remains interesting. The tendency of decrease in the case of Akt1 knockdown in HepG2 *in ovo* graft model, and Akt2 knockdown in the MV4-11 *in ovo* graft model suggests an isoform-dependent response based on the cell line origin: tumor versus TME, respectively.

8. Effect of Akt1 and/or Akt2 knockdown on the kinase activity

In light of the unexpected results obtained following the knockdown of Akt1 and/or Akt2 by the designed siRNAs, summarized by the absence of a significant effect on cell fate (survival, proliferation and metabolism) and on tumor growth *in ovo*. The consequences of the knockdown were investigated at the level of the activity of the PI3K/Akt pathway.

8.1. Effect of D2Akt1 and/or D15Akt2 siRNAs on the activity of Akt1 and Akt2

First, the effect on the phosphorylation levels of Akt1 and Akt2 following the respective single and double knockdown of the isoforms was assessed on PLCY/PRF/5, Huh7 and HepG2 cell lines. For this, cells were transfected for 6 hours by LipofectamineRNAimax coupled to D2Akt1 siRNA, D15Akt2 siRNA, or both siRNAs simultaneously, at 10nM concentration; then the proteins and their

phosphorylations were analyzed after 24 hours by immuno-detection. The phosphorylation events are known to occur at different Serine (Ser) and Threonine (Thr) residues, depending on the isoform. However, the phosphorylation at the Ser residue is recognized to be indicative of an active Akt isoform.

PLCY/PRF/5 cell line

Results of the protein immuno-detection by Jess on the PLCY/PRF/5 cell-line, *see Figure 33A and B*, show that following the single knockdown of Akt1, a 65% significant decrease in the Akt1 isoform expression was obtained, accompanied by a 72% significant decrease in the phosphorylated Akt1 (Ser473), when compared to the mock siRNA. Similarly, the double knockdown of Akt1 and Akt2, led to a significant 60% decrease in the protein expression of Akt1 along with a significant 48% decrease in the phosphorylated Akt1 (Ser473). However, no significant effect has been shown on the Akt1 expression level or its corresponding phosphorylated level following the single knockdown of Akt2.

Concerning the expression of Akt2 and its phosphorylation, *see Figure 33C and D*, the results showed a similar pattern to that obtained with Akt1. The single knockdown of Akt2 and the double knockdown of Akt1 and Akt2, led to a significant decrease in the expression level of Akt2 by 62% and 57%, respectively. Accompanied by a decrease of the phosphorylated Akt2 (Ser474) levels by 33% and 41%, respectively. In addition, no significant effect on the Akt2 or phosphorylated Akt2 levels has been shown upon the single knockdown of Akt1.

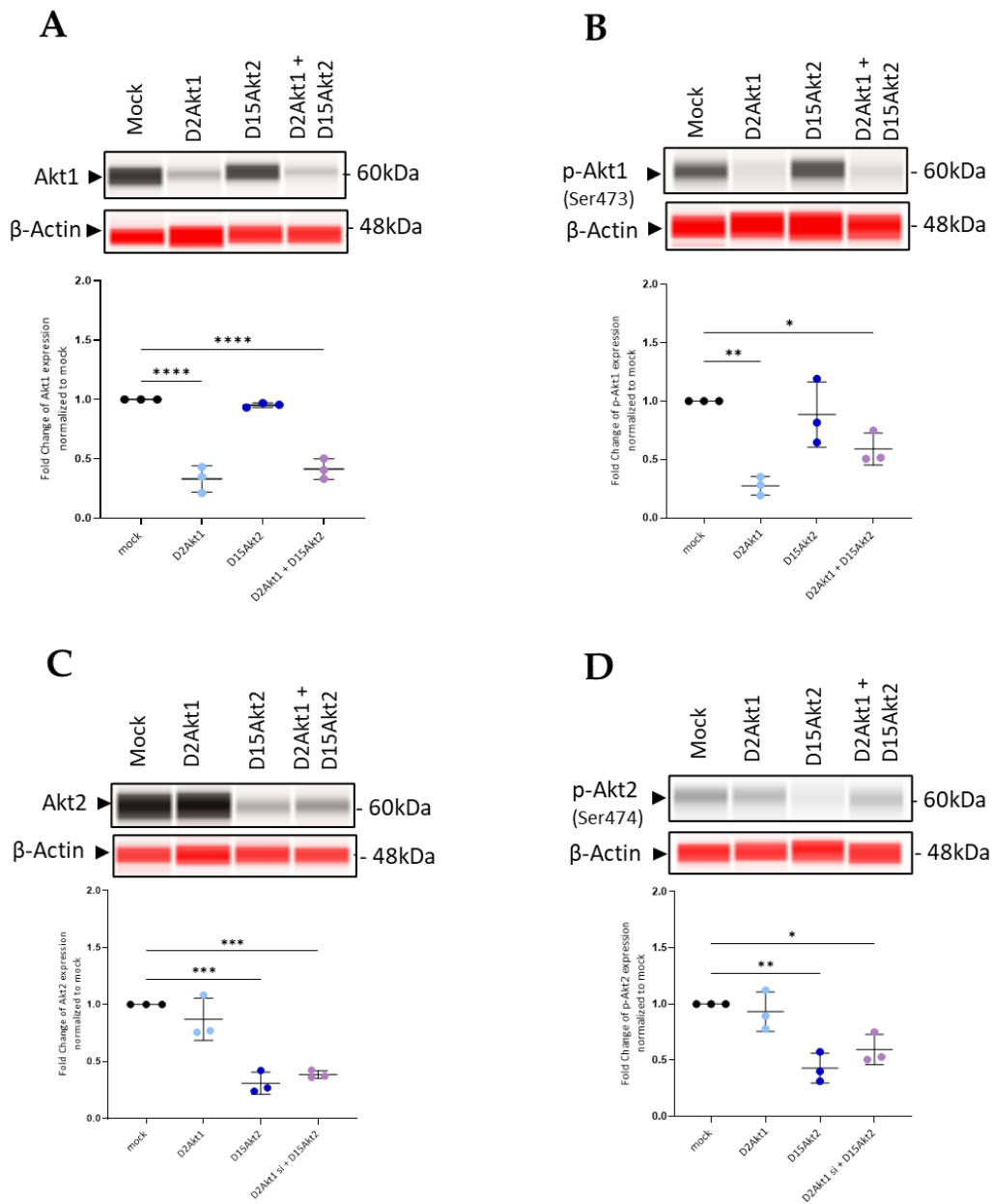


Figure 33: Phospho-Akt1/Akt2 after knockdown in PLC γ /PRF/5 cell line. Protein immuno-detection by Jess showing the expression of Akt1, p-Akt1 (Ser473), Akt2 and p-Akt2 (Ser474) in PLC γ /PRF/5, 24 hours after transfection with LipofectamineRNAiMAX coupled to D2Akt1 or D15Akt2 siRNAs. The top part of each set shows a representative immuno-detection with the corresponding quantification below it, represented as mean \pm SD (N=3 independent experiments) of (A) the ratio of Akt1/ β -Actin for each condition normalized to the mock. The asterisks represent the p-values ($p < 0.0001$); (B) the ratio of p-Akt1/ β -Actin for each condition normalized to the mock. The asterisks represent the p-values: D2Akt1 ($p = 0.0014$) and D2Akt1 + D15Akt2 ($p = 0.0345$); (C) the ratio of Akt2/ β -Actin for each condition normalized to the mock. The asterisks represent the p-values for: D15Akt2 siRNA ($p = 0.0001$) and D2Akt1 + D15Akt2 ($p = 0.0003$). (D) the ratio of p-Akt2/ β -Actin for each condition normalized to the mock. The asterisks represent the p-values: D15Akt2 ($p = 0.0016$) and D2Akt1 + D15Akt2 ($p = 0.0124$). The statistical test used in all the cases was ordinary one-way ANOVA.

Huh7 cell line

Results of the protein immuno-detection by Jess on the Huh7 cell-line, *see Figure 34A and B*, show that following the single knockdown of Akt1, a 44% significant decrease in the Akt1 isoform expression was obtained accompanied by a 62% significant decrease in its phosphorylated form, when compared to the mock. Similarly, double knockdown of Akt1 and Akt2, led to a 44% decrease in the protein expression of Akt1 along with a 40% decrease in the phosphorylated Akt1 (Ser473), when compared to the mock. However, no significant effect has been shown on the Akt1 expression level or its corresponding phosphorylated level following the single knockdown of Akt2.

Concerning Akt2 and its phosphorylated levels, the results, *see Figure 34C and D*, showed that the single knockdown of Akt2 and the double knockdown of Akt1 and Akt2, led to a decrease in the expression level of Akt2 by 60% and 53%, respectively. In addition, a decrease of the phosphorylated Akt2 (Ser474) was observed with single knockdown of Akt2 (45%) and the double knockdown of Akt1 and Akt2 (30%, respectively). In addition, no significant effect on the Akt2 or phosphorylated Akt2 levels has been shown upon the single knockdown of Akt2.

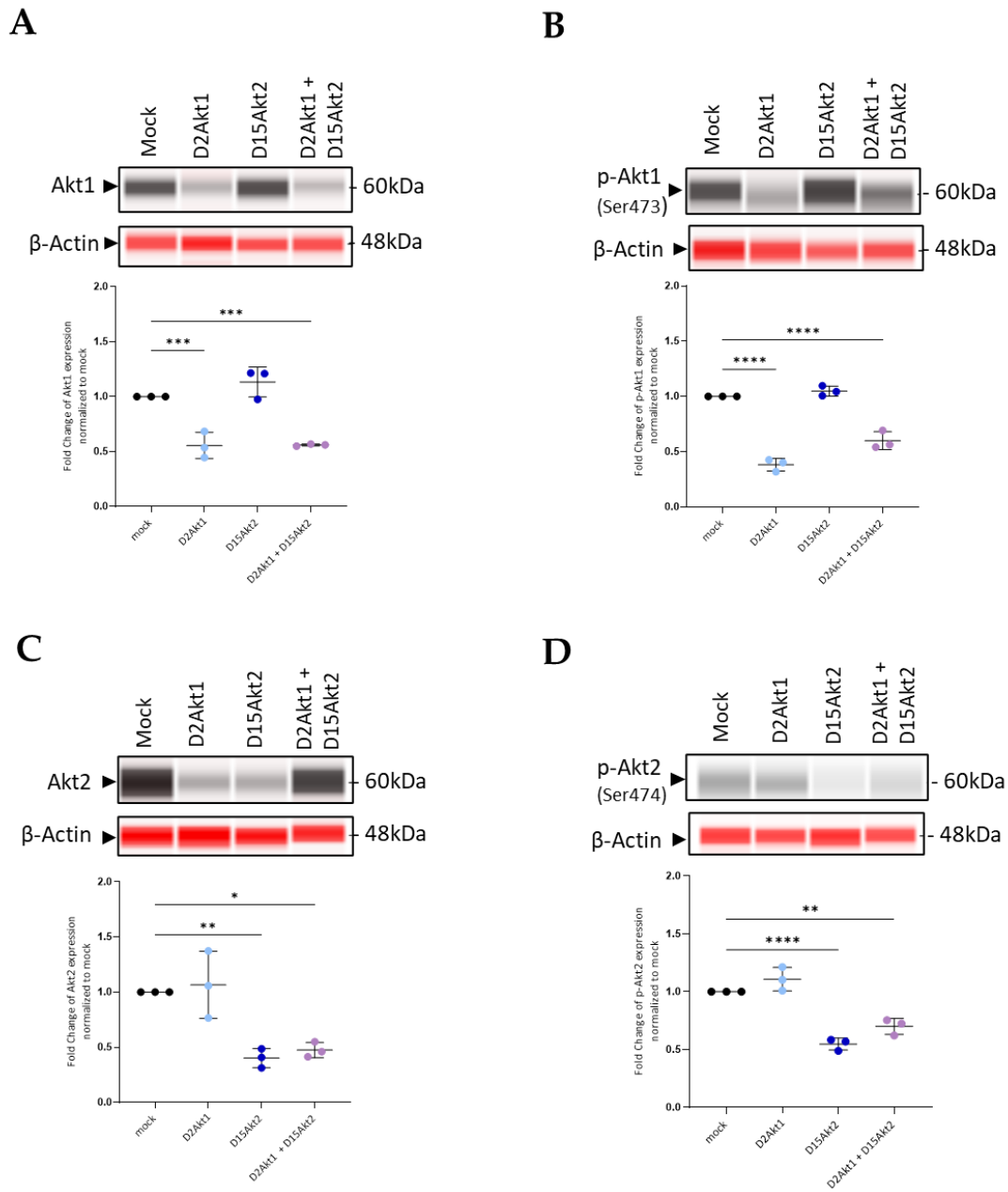


Figure 34: Phospho-Akt1/Akt2 after knockdown in Huh7 cell line. Protein immuno-detection by Jess showing the expression of Akt1, p-Akt1 (Ser473), Akt2 and p-Akt2 (Ser474) in Huh7 cell line, 24 hours after with LipofectamineRNAiMAX coupled to D2Akt1 or D15Akt2 siRNAs. The top part of each set shows a representative protein blot with the corresponding quantification below it, represented as mean \pm SD ($N=3$ independent experiments) of (A) the ratio of Akt1/ β -Actin for each condition normalized to the mock. The asterisks represent the p -values ($p=0.0009$). (B) the ratio of p-Akt1/ β -Actin for each condition normalized to the mock. The asterisks represent the p -values ($p<0.0001$). (C) the ratio of Akt2/ β -Actin for each condition normalized to the mock. The asterisks represent the p -values for: D15Akt2 siRNA ($p=0.0050$) and D2Akt1+D15Akt2 ($p=0.0104$). (D) the ratio of p-Akt2/ β -Actin for each condition normalized to the mock. The asterisks represent the p -values: D15Akt2 ($p<0.0001$) and D2Akt1 + D15Akt2 ($p=0.0015$). The statistical test used in all the cases was ordinary one-way ANOVA.

HepG2 cell line

Results of the protein immuno-detection by Jess on the HepG2 cell-line, *see Figure 35A and B*, showed that following the single knockdown of Akt1, a 53% significant decrease in the Akt1 isoform expression was obtained accompanied by a 69% significant decrease in the phosphorylated Akt1 (Ser473), when compared to the mock siRNA. Similarly, double knockdown of Akt1 and Akt2, led to a 44% decrease in the protein expression of Akt1 along with a 63% decrease in the phosphorylated Akt1 (Ser473), when compared to the mock. Importantly, a significant increase in the Akt1 expression level by 40% was demonstrated upon the single knockdown of Akt2, however no significant change was seen in the case of the phosphorylated form

For the expression of Akt2 and its phosphorylated levels, *see Figure 35C and D*, the single knockdown of Akt2 and the double knockdown of Akt1 and Akt2, led to a decrease in the expression level of Akt2 by 62% and 57%, respectively. In addition, the phosphorylated levels followed the same trend and exhibited a decrease by 68% and 73%, respectively. Moreover, no significant effect on the Akt2 or phosphorylated Akt2 levels was shown upon the single knockdown of Akt1.

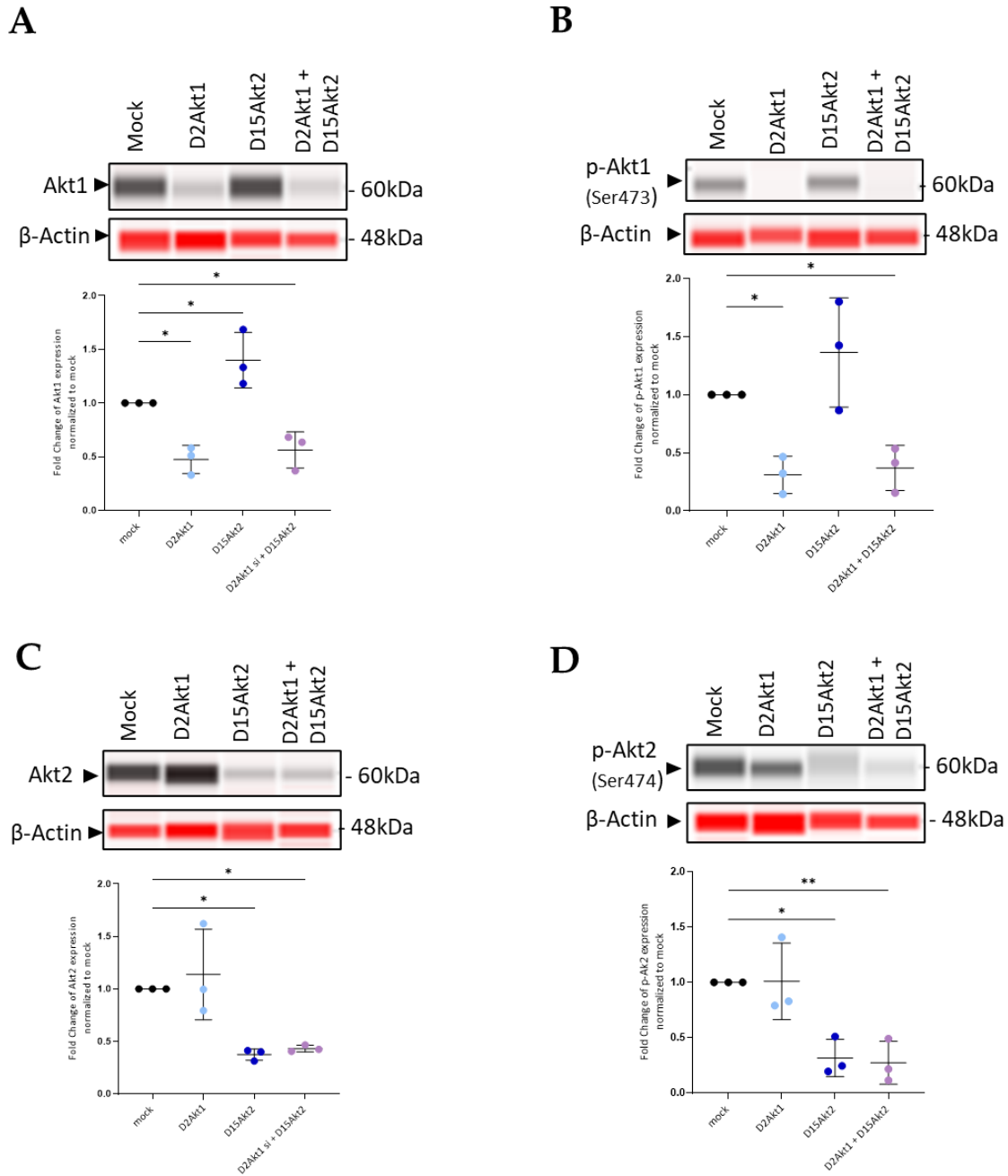


Figure 35: Phospho-Akt1/Akt2 after knockdown in HepG2 cell line. Protein immuno-detection by Jess showing the expression of Akt1, p-Akt1 (Ser473), Akt2 and p-Akt2 (Ser474) in HepG2 cell line, 24 hours after with LipofectamineRNAiMAX coupled to D2Akt1 or D15Akt2 siRNAs. The top part of each set shows a representative protein blot with the corresponding quantification below it, represented as mean \pm SD (N=3 independent experiments) of (A) the ratio of Akt1/ β -Actin for each condition normalized to the mock. The asterisks represent the p-values for: D2Akt1 ($p=0.0124$), D15Akt2 ($p=0.0470$), and D2Akt1+D15Akt2 ($p=0.0310$); (B) the ratio of p-Akt1/ β -Actin for each condition normalized to the mock. The asterisks represent the p-values for: D2Akt1 ($p=0.0329$) and D2Akt1 + D15Akt2 ($p=0.0487$); (C) the ratio of Akt2/ β -Actin for each condition normalized to the mock. The asterisks represent the p-values for: D15Akt2 siRNA ($p=0.0199$) and D2Akt1+D15Akt2 ($p=0.0316$); (D) the ratio of p-Akt2/ β -Actin for each condition normalized to the mock. The asterisks represent the p-values: D15Akt2 ($p=0.0119$) and D2Akt1 +D15Akt2 ($p=0.0084$). The statistical test used in all the cases was ordinary one-way ANOVA.

Altogether, the results suggest that upon exposure to the designed siRNAs D2Akt1 and/or D15Akt2, a decrease in the phosphorylated and thus activated forms of Akt1 and Akt2 is obtained. The range of decrease of activated Akt1 form was 48-69% and that of Akt2 was 30-63%, depending on the cell lines. Furthermore, the data support the specificity of action of the Akt1 and Akt2 siRNAs. The question that was yet to be answered was whether such a degree of a decrease in the activity of the isoforms was sufficient to be translated as a global effect on the downstream effectors of the PI3K/Akt pathway.

8.2. Effect of D2Akt1 and/or D15Akt2 siRNAs on the PI3K/Akt pathway

Akt pathway is a master regulator, regulating various cellular processes through different effector molecules. For that, and after validating the diminution in the activity of Akt1 and Akt2 following the targeting of either Akt1 or Akt2, and of both, the downstream effects on the Akt pathway were analyzed. For this purpose, the 2 cell lines Huh7 and HepG2 were exposed for 6 hours to either of the designed siRNAs, and to both siRNAs simultaneously, through Lipofectamine RNAiMAX-mediated transfection. Then, 24 hours later, the level of phosphorylation of 40 proteins known to be under control by the PI3K/Akt pathway was assessed in comparison to the mock in terms of fold change. This approach would give an insight about the effect of the designed-siRNAs-mediated knockdown Akt1 and/or Akt2, on two levels: i) the global activity of the PI3K/Akt pathway and ii) the preferential regulation of downstream effectors of PI3K/Akt by either of the Akt isoforms. The phospho-profiling was done using Proteome Profiler Human Phospho-Kinase Array Kit.

The heatmap in *Figure 36* provides an overview of the fold change in the target proteins tested relative to the mock. It reveals that the overall aspect differs between one Huh7 cell line and the HepG2 cell line, proving the first clues of cell-dependent response of Akt1 and/or Akt2 modulation. Furthermore, the clustering based on the condition tested shows that within the Huh7 cell line the single Akt2 knockdown condition clusters with that of the double knockdown of Akt1 and Akt2. Which is not the case in HepG2 cell line where the single knockdown conditions cluster with each other. The results will be further explained in the following sections.

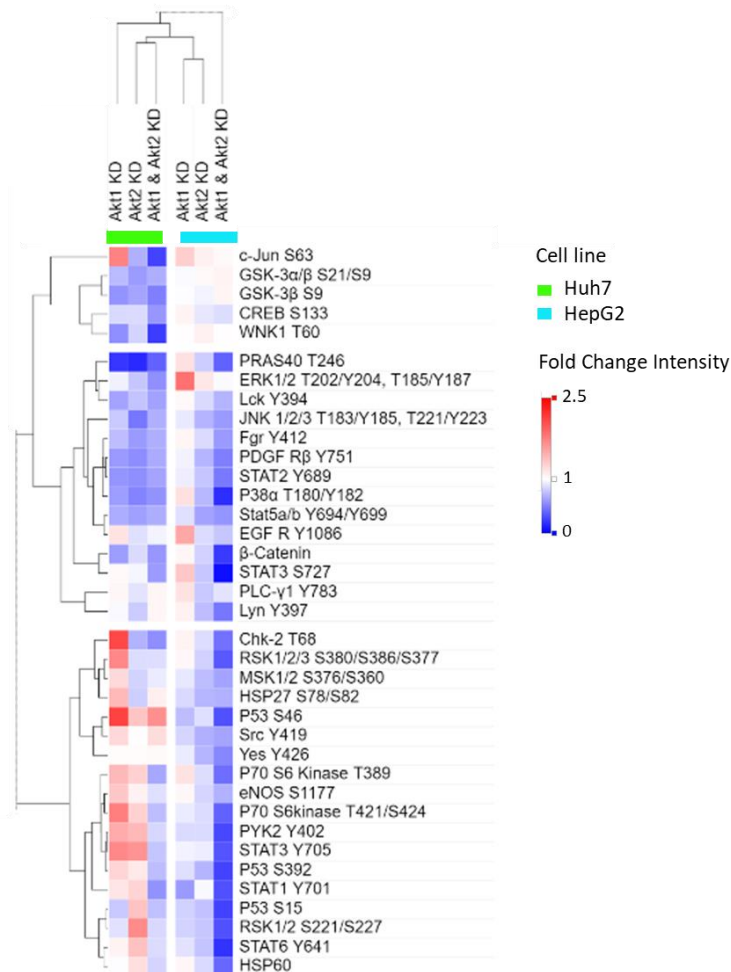


Figure 36: Heatmap of protein modulations in Huh7 and HepG2 cell lines upon the knockdown of Akt1 and/or Akt2. The heatmap displays the mean fold change, relative to the mock, in the target proteins tested in both Huh7 and HepG2 cell lines (N=2 replicates), along with the Euclidean clustering done based on the rows (target proteins) and the columns (conditions of knockdown (KD)).

The results of the effect of the knockdown of Akt1 and/or Akt2 on the various tested proteins were divided into 2 groups:

- iii) Direct effect group: demonstrating the effect on the proteins prone to a direct phosphorylation by Akt.
- iv) Indirect effect: demonstrating the effect on the proteins that are further downstream and are one grade or more farther away from Akt itself. Meaning that the effect seen on the phosphorylation level is a subsequent effect of masked events that led up to it.

In this section, the phosphorylated residues have the following abbreviations: S corresponds to a Serine residue, T corresponds to a Threonine residue, and Y corresponds to a Tyrosine residue.

The direct effect group encompasses the following proteins with their designated phosphorylation sites: CREB S133, endothelial nitric oxide synthase (eNOS) S1177, GSK-3 α/β S21/S9, GSK-3 β S9, and PRAS40 T246 and Lysine deficient protein kinase 1(WNK1) T60.

CREB is prone to an activating phosphorylation at the S133 by the kinase activity of Akt and are involved in the regulation of cell survival [314]. GSK3 α/β , as its name suggests exists in 2 isoforms α and β Both isoforms are subject to an inhibitory phosphorylation at the S21 and S9. It is involved in both cell cycle progression and cell metabolism [315]. Concerning eNOS, it is subject to an activating phosphorylation at the S1117, and is involved in the conversion of arginine into nitric oxide, and plays a role in cell proliferation, angiogenesis and DNA repair [316]. PRAS40, is inhibited upon its phosphorylation at the T246 by Akt. It is involved in regulating the metabolic functions of the cell. It interacts with the MTORC1 exerts an inhibitory constraint on it. Upon the phosphorylation of PRAS40 by Akt, mTORC1 is activated [317]. Finally, WNK1 is subject to an activating phosphorylation, at the T60 residue, and exerts a role in the inhibition of the insulin-stimulated mitogenesis [318].

The indirect effect includes: P70 S6 Kinase T389, P70 S6kinase T421/S424, EGF R Y1086, ERK1/2 T202/Y204, T185/Y187, Chk-2 T68, c-Jun S63, Fgr Y412, HSP27 S78/S82, P53 S15, P53 S46, P53 S392, JNK 1/2/3 T183/Y185, T221/Y223, Lck Y394, Lyn Y397, MSK1/2 S376/S360, PDGF R β Y751, PLC- γ 1 Y783, Src Y419, PYK2 Y402, RSK1/2 S221/S227, RSK1/2/3 S380/S386/S377, STAT2 Y689, Stat5a/b Y694/Y699, Yes Y426, STAT1 Y701, STAT3 Y705, STAT3 S727, β -Catenin, STAT6 Y641, P38 α T180/Y182, and HSP60.

These proteins are not subject to a direct phosphorylation by Akt. For instance, the effect seen on the phosphorylation of P53 at its various, serine and threonine residues, is inhibited by MDM2 which in turn is regulated (activated) by Akt [319]. On the other hand, the effect seen on the P70S6K is preceded by an inhibitory phosphorylation of TSC1/2 by Akt, thus activating Rheb, which in turn activates mTORC1 which lastly phosphorylates P70S6K. The effect of the knockdown of Akt1 and/or Akt2 in the cells was also assessed for its ability to affect other signaling pathways. Namely, the JAK/STAT, JNK/c-Jun, RAS/RAF/MEK/ERK, P38/MAPK, among others.

Huh7 cell line

The effect of the knockdown is presented in *Figure 37* and in *Table 21*, showing the different changes in the level of phosphorylation of the proteins upon Akt1 and/or Akt2 knockdown.

The analysis of the direct effect showed, *see Figure 37A and Table 21 (direct effect)*, that upon the simultaneous knockdown of both isoforms a decrease in the level of phosphorylation of all the tested proteins, in varying degrees and most prominently in the case of WNK1 T60 (76%) and PRAS40 T246 (62%), when compared to the mock. Knocking down Akt1 led to a decrease in the level of 5 out of 6 of the tested proteins, and most prominently in the case of PRAS40 T246 (79%), in contrast, eNOS S1117 showed a 32% increase in its phosphorylation level. Similarly, knocking down Akt2 showed a decrease in the level of 5 out of the 6 proteins tested compared to the mock, and PRAS40 T246 showed the most drastic decrease (83%), however eNOS S1117 showed no change.

Concerning the indirect effect on Huh7 cell line, *see Figure 37B and Table 21 (indirect effect)*, showed different changes in the phospho-protein levels depending on the Akt knockdown.

The simultaneous knockdown of Akt1 and Akt2, showed a decrease in the phospho-protein levels of 23 out of the 31 proteins tested, compared to the mock, with the most prominent decrease obtained in the case of c-Jun S63 (73%). Simultaneously some of the phospho-protein levels showed an increase when compared to the mock, namely, P53 S46 (65%), and Src Y419 (20%). However, some of the proteins showed no change in their levels, namely, EGF R Y1086, HSP27 S78/S82, Lyn Y397, MSK1/2 S376/S360, PLC- γ 1 Y783, and Yes Y426.

The single knockdown of Akt1, showed a similar pattern of effect. The results show that 10 out of the 31 tested phospho-protein levels were decreased when compared to the mock, and STAT2 Y689 (42%) showed the most prominent decrease. As for the rest of the tested phospho-proteins, an increase in the level of the following proteins was observed: EGF R Y1086 (16%), Chk-2 T68 (108%), c-Jun S63 (73%), HSP27 S78/S82 (41%), P53 S46 (111%), P53 S392 (24%), MSK1/2 S376/S360 (22%), P70S6K T389 (41%) and P70S6K T421/S424 (75%), Src Y419 (22%), PYK2 Y402 (49%), RSK1/2/3 S380/S386/S377 (70%), STAT1 Y701 (15%), and STAT3 Y705 (69%); and no change has been shown in the phospho-protein levels of ERK1/2 T202/Y204, T185/Y187, Lyn Y397, PLC- γ 1 Y783, Yes Y426, STAT3 S727, STAT6 Y641, and HSP60 when compared to the mock.

In the case of the single knockdown of Akt2, the fluctuation of the phospho-protein levels showed also a decrease, increase and no change. The phospho-protein level was decreased in 17 out of the 31 proteins tested, where the most eminent decreased was shown in: JNK 1/2/3 T183/Y185, T221/Y223 (53%). A contradictory increase in the level of the following proteins was observed when compared to the mock: P53 S15 (35%), P53 S46 (34%), P53 S392 (13%), P70 S6 Kinase T389 (26%), P70 S6kinase T421/S424 (26%), PYK2 Y402 (41%), RSK1/2 S221/S227 (68%), STAT1 Y701 (25%), STAT3 Y70 (63%), STAT6 Y641 (36%), and HSP60 (18%). Whereas no change was observed in the level of any of the following phospho-proteins: Src Y419, Yes Y426, STAT3 S727.

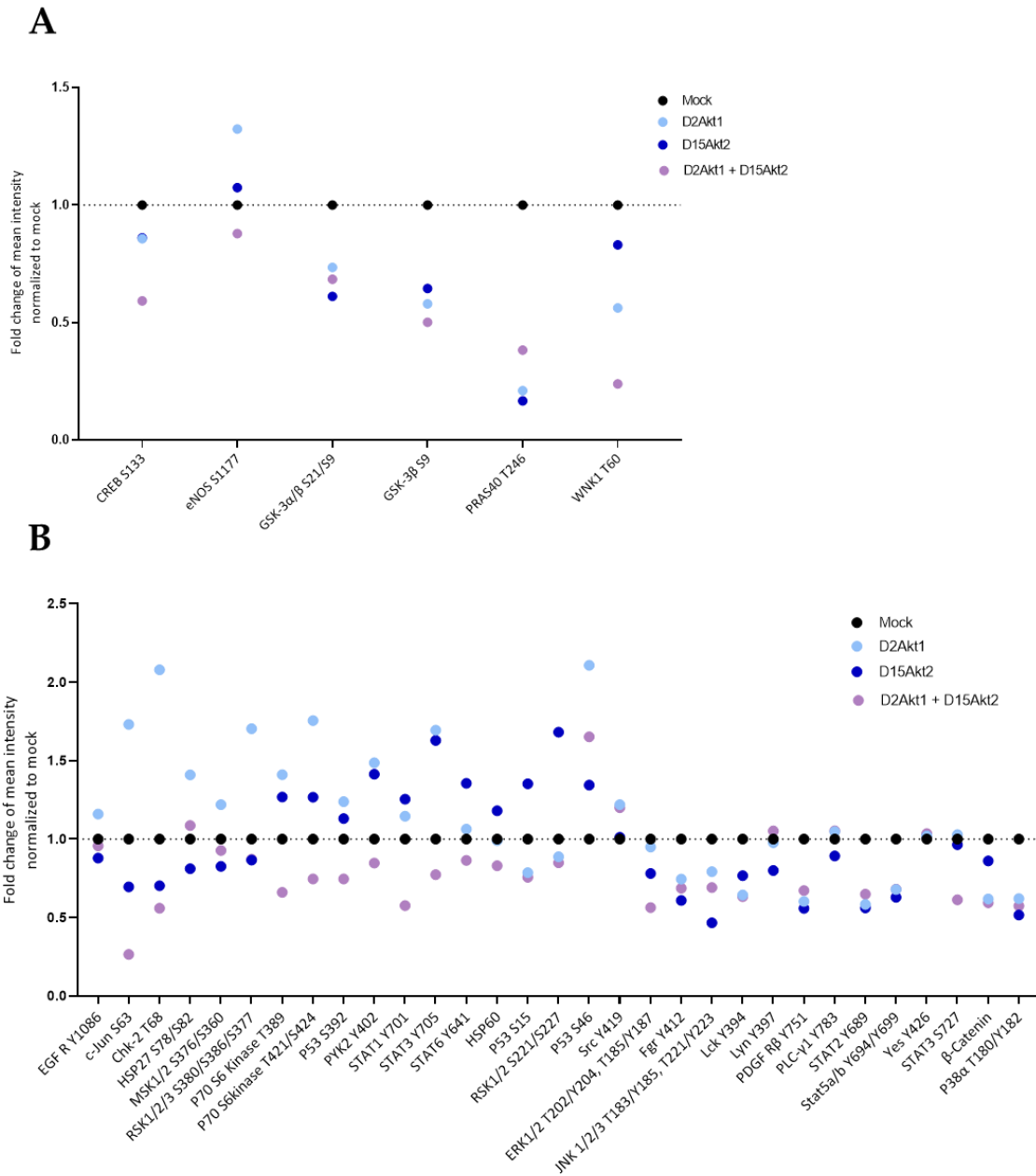


Figure 37: Effect of the knockdown of Akt1 and/or Akt2 in Huh7 cell line. Graphs showing the mean intensity (N=2 replicates) normalized to the mock of the (A) direct effect of the knockdown of Akt1 and/or Akt2, and (B) the indirect effect of the knockdown of Akt1 and/or Akt2, in Huh7 cell line. S: Serine, T: Threonine, and Y: Tyrosine.

Table 21: Effect of Akt1 and/or Akt2 knockdown in Huh7 cell line. Table showing the percentage of decrease (red arrow) and increase (green arrow) of the -proteins tested, compared to the mock siRNA condition. The proteins are categorized into direct and indirect effect. "/" signifies no change.

Effect	Target protein	Knockdown		
		AKT1	AKT2	AKT1 and AKT2
Direct effect	CREB S133	↓ 14%	↓ 14%	↓ 41%
	eNOS S1177	↑ 32%	/	↓ 12%
	GSK-3 α / β S21/S9	↓ 27%	↓ 39%	↓ 32%
	GSK-3 β S9	↓ 42%	↓ 35%	↓ 50%
	PRAS40 T246	↓ 79%	↓ 83%	↓ 62%
	WNK1 T60	↓ 44%	↓ 17%	↓ 76%
Indirect effect	EGF R Y1086	↑ 16%	↓ 12%	/
	ERK1/2 T202/Y204, T185/Y187	/	↓ 22%	↓ 44%
	Chk-2 T68	↑ 108%	↓ 30%	↓ 44%
	c-Jun S63	↑ 73%	↓ 30%	↓ 73%
	Fgr Y412	↓ 26%	↓ 39%	↓ 31%
	HSP27 S78/S82	↑ 41%	↓ 19%	/
	P53 S15	↓ 21%	↑ 35%	↓ 24%
	P53 S46	↑ 111%	↑ 34%	↑ 65%
	P53 S392	↑ 24%	↑ 13%	↓ 25%
	JNK 1/2/3 T183/Y185, T221/Y22	↓ 21%	↓ 53%	↓ 31%
	Lck Y394	↓ 36%	↓ 23%	↓ 37%
	Lyn Y397	/	↓ 20%	/
	MSK1/2 S376/S360	↑ 22%	↓ 17%	/
	P70 S6 Kinase T389	↑ 41%	↑ 27%	↓ 34%
	P70 S6kinase T421/S424	↑ 75%	↑ 27%	↓ 25%
	P38 α T180/Y182	↓ 38%	↓ 48%	↓ 43%
	PDGF R β Y751	↓ 40%	↓ 44%	↓ 33%
	PLC- γ 1 Y783	/	↓ 11%	/
	Src Y419	↑ 22%	/	↑ 20%
	PYK2 Y402	↑ 49%	↑ 41%	↓ 15%
	RSK1/2 S221/S227	↓ 11%	↑ 68%	↓ 15%
	RSK1/2/3 S380/S386/S377	↑ 70%	↓ 13%	↓ 13%
	STAT2 Y689	↓ 42%	↓ 44%	↓ 35%
	Stat5a/b Y694/Y699	↓ 32%	↓ 37%	↓ 32%
	Yes Y426	/	/	/
	STAT1 Y701	↑ 15%	↑ 25%	↓ 42%
	STAT3 Y705	↑ 69%	↑ 63%	↓ 23%
	STAT3 S727	/	/	↓ 39%
	β -Catenin	↓ 38%	↓ 14%	↓ 41%
	STAT6 Y641	/	↑ 36%	↓ 14%
HSP60	/	↑ 18%	↓ 17%	

HepG2 cell line

The effect of the knockdown is presented in *Figure 38* and in

Table 22, showing the different changes in the level of phosphorylation of the proteins upon Akt1 and/or Akt2 knockdown

At the level of the direct effect, *see Figure 38A and*

Table 22 (direct effect), the results showed, in the case of the double knockdown of Akt1 and Akt2 a decrease in 3 out of the 6 tested phospho-protein, when compared to the mock, and the most evident decrease was shown in the case of PRAS40 T246 (61%), with no change in all the other proteins. On the other hand, the single knockdown of Akt1 showed no change in the level of any of tested proteins except for PRAS40 T246 which was increased by 18% when compared to the mock. Additionally, the single knockdown of Akt2 showed a decrease only in the proteins eNOS S1117 and PRAS40 T246 by 16% and 20%, respectively. However, no change in the level of CREB S133, GSK3 α/β S21/S9, GSK3 β S9 and WNK1 T60 was observed.

At the level of the indirect effect, the single or double knockdown of Akt1 and/or *AKT2*, see *Figure 38B and*

Table 22 (indirect effect), revealed a variety of fluctuations depending on the phospho-protein tested and the condition of the knockdown.

Upon the simultaneous knockdown of Akt1 and Akt2 29 out of 31 of the tested proteins showed a decrease in their levels when compared to the mock, with the most drastic decrease in the case of STAT3 S727 by 94%. Whereas ERK1/2 T202/Y204, T185/Y187 and c-Jun S63 showed no change.

On the other hand, the single knockdown of Akt1 showed a decrease in the level of 10 proteins out of the 31 tested, the most prominent decrease was shown in the case of STAT1 Y701 by 39%. The other proteins that did not show a decrease showed either no change or an increase. More explicitly, Chk-2 T68, Fgr Y412, JNK 1/2/3 T183/Y185, T221/Y223, Lck Y394, Lyn Y397, MSK1/2 S376/S360, P70 S6kinase T421/S424, PDGF R β Y751, RSK1/2/3 S380/S386/S377, STAT2 Y689, Yes Y426, STAT3 Y705, β -Catenin and HSP60, showed no change in their levels compared to the mock. Whereas the following proteins an increase in their level: EGF R Y1086 (51%), ERK1/2 T202/Y204, T185/Y187 (83%), c-Jun S63 (28%), P70 S6 Kinase T389 (16%), and P38 α T180/Y182 (18%) PLC- γ 1 Y783 (17%) and STAT3 S727 (33%).

However, following the single knockdown of Akt2, 27 out of the 31 tested proteins showed a decrease in their level compared to the mock, and the most eminent decrease was in the case of Stat5a/b Y694/Y699 (36%). Moreover, an increase was shown in the case of ERK1/2 T202/Y204, T185/Y187 (14%) and no change was seen in the level of the following phospho-proteins, when compared to the mock, c-Jun S63, STAT1 Y701, and STAT3 Y705.

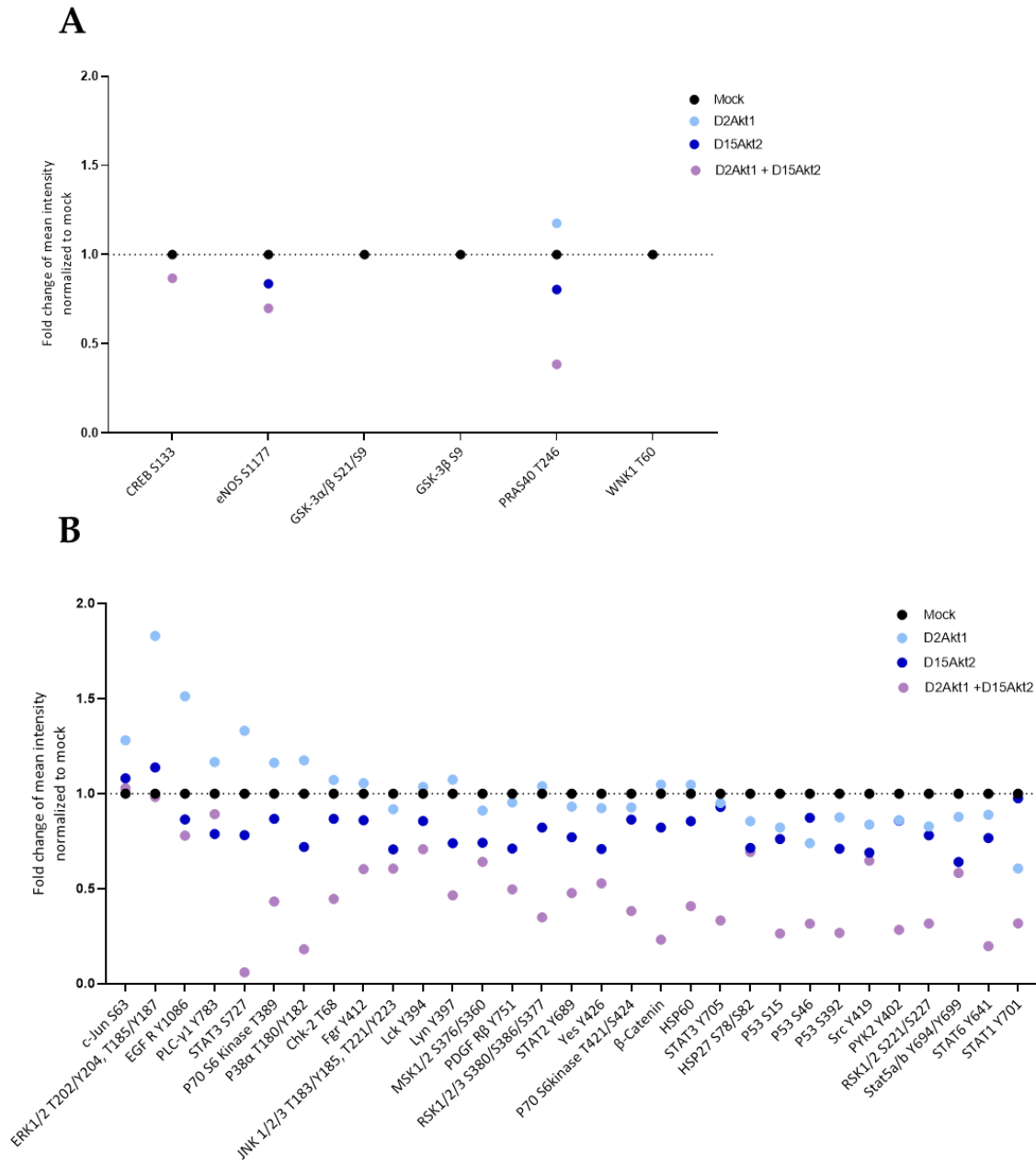


Figure 38: Effect of the knockdown of Akt1 and/or Akt2 in HepG2 cell line. Graphs showing the mean intensity (N=2 replicates) normalized to the mock of the (A) direct effect of the knockdown of Akt1 and/or Akt2, and (B) the indirect effect of the knockdown of Akt1 and/or Akt2, in HepG2 cell line. Abbreviations: S: Serine, T: Threonine, and Y: Tyrosine.

Table 22: Effect of the knockdown of Akt1 and/or Akt2 in HepG2 cell line. Table showing the percentage of decrease (red arrow) and increase (green arrow) of the -proteins tested, compared to the mock siRNA condition. The proteins are categorized into direct and indirect effect. "/" signifies no change.

Effect	Target protein	Knockdown		
		Akt1	Akt2	Akt1 and Akt2
Direct effect	CREB S133	/	/	↓ 13%
	eNOS S1177	/	↓ 16%	↓ 30%
	GSK-3 α / β S21/S9	/	/	/
	GSK-3 β S9	/	/	/
	PRAS40 T246	↑ 18%	↓ 20%	↓ 61%
	WNK1 T60	/	/	/
Indirect effect	EGF R Y1086	↑ 51%	↓ 14%	↓ 22%
	ERK1/2 T202/Y204, T185/Y187	↑ 83%	↑ 14%	/
	Chk-2 T68	/	↓ 13%	↓ 55%
	c-Jun S63	↑ 28%	/	/
	Fgr Y412	/	↓ 14%	↓ 40%
	HSP27 S78/S82	↓ 14%	↓ 29%	↓ 31%
	P53 S15	↓ 18%	↓ 24%	↓ 74%
	P53 S46	↓ 26%	↓ 13%	↓ 68%
	P53 S392	↓ 12%	↓ 29%	↓ 73%
	JNK 1/2/3 T183/Y185, T221/Y223	/	↓ 29%	↓ 39%
	Lck Y394	/	↓ 14%	↓ 29%
	Lyn Y397	/	↓ 26%	↓ 54%
	MSK1/2 S376/S360	/	↓ 26%	↓ 36%
	P70 S6 Kinase T389	↑ 16%	↓ 13%	↓ 57%
	P70 S6kinase T421/S424	/	↓ 14%	↓ 62%
	P38 α T180/Y182	↑ 18%	↓ 28%	↓ 82%
	PDGF R β Y751	/	↓ 29%	↓ 50%
	PLC- γ 1 Y783	↑ 17%	↓ 21%	↓ 11%
	Src Y419	↓ 16%	↓ 31%	↓ 35%
	PYK2 Y402	↓ 14%	↓ 14%	↓ 72%
	RSK1/2 S221/S227	↓ 17%	↓ 22%	↓ 68%
	RSK1/2/3 S380/S386/S377	/	↓ 18%	↓ 65%
	STAT2 Y689	/	↓ 23%	↓ 52%
	Stat5a/b Y694/Y699	↓ 12%	↓ 36%	↓ 42%
	Yes Y426	/	↓ 29%	↓ 47%
	STAT1 Y701	↓ 39%	/	↓ 68%
	STAT3 Y705	/	/	↓ 67%
	STAT3 S727	↑ 33%	↓ 22%	↓ 94%
	β -Catenin	/	↓ 18%	↓ 77%
	STAT6 Y641	↓ 11%	↓ 23%	↓ 80%
HSP60	/	↓ 15%	↓ 59%	

Altogether, these results demonstrated a modulation of the activity of the Akt pathway upon the single and double knockdown of Akt1 and Akt2 by the designed siRNAs. The modulations of the phosphorylation were cell line-dependent, phospho-protein dependent, and Akt isoform-dependent.

8.2.1. Comparative Analysis

The next step was to compare the profile of decreased proteins between the different knockdown conditions within the same cell line to infer isoform-specific roles. And on another level, to compare the profile of decreased proteins in each condition between the two tested cell lines, to infer cell-dependent roles of each isoform.

Within cell line

First, the comparative analysis was done using Venn Diagram, and categorized according to their position in it. See Figure 39 for the definition of the categories in the case of comparisons within the same cell line.

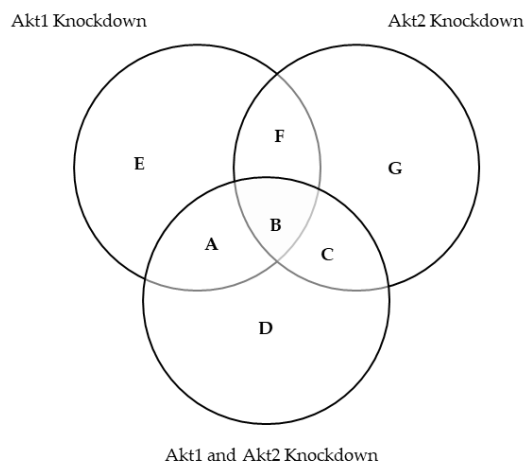


Figure 39: Categories of “within cell lines” comparative analysis. Venn diagram showing the different categories upon the comparative analysis of the different knockdown conditions within the same cell line: the different categories represent proteins that, compared to the mock, decrease : “A”: in both single Akt1 knockdown and double knockdown of Akt1 and Akt2; “B”: in all the conditions; “C”: in both single knockdown of Akt2 and double knockdown of Akt1 and Akt2; “D”: exclusively in the double knockdown of Akt1 and Akt2; “E”: exclusively in Akt1 knockdown; “F”: in the single knockdown of Akt1 and the single knockdown of Akt2; “G”: exclusively in the single Akt2 knockdown.

The categories depend on the position on the Venn Diagram:

- Category "A" shows proteins decreased upon the knockdown of Akt1 and the double knockdown of Akt1 and Akt2. Thus, are phosphorylated by the activity of Akt1 only.
- Category "B" shows proteins decreased upon the single knockdown of Akt1 or Akt2 and the double knockdown of Akt1 and Akt2. Thus, are phosphorylated by the activity of Akt1 or Akt2.
- Category "C" shows proteins decreased upon the knockdown of Akt2 and the double knockdown of Akt1 and Akt2. Thus, are phosphorylated by the activity of Akt2 only.
- Category "D" shows proteins decreased only in the case of the double knockdown of Akt1 and Akt2. Thus, it shows an additive compensatory effect in their phosphorylation by the Akt isoforms.
- Categories "E", "F", "G" are considered to be outliers and not taken into account.

Huh7 cell line

The comparative analysis in Huh7 cell line of the decreased level of phospho-proteins, between the different knockdown conditions, *see Ven Diagram in Figure 40*, allowed the stratification of the proteins as follows:

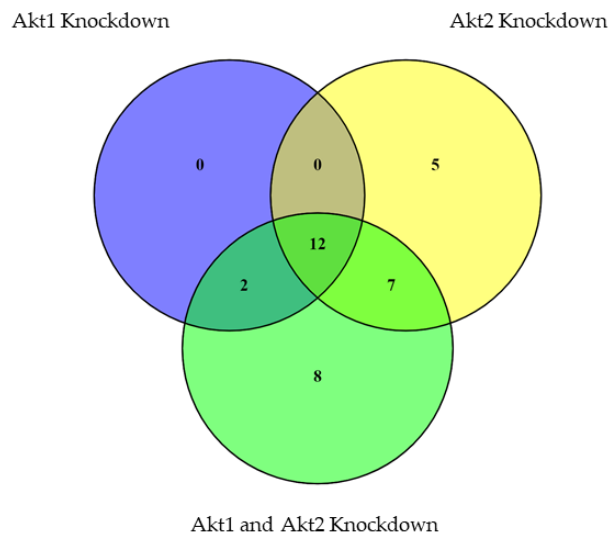


Figure 40: Comparative analysis in Huh7 cell line. Venn diagram showing the comparative analysis of the decreased phospho-proteins, compared to the mock in the knockdown of Akt1 and/or Akt2 in Huh7 cell line. The numbers represent the number of proteins in each category.

- Category A “proteins under the control of Akt1” included 2 phospho-proteins: P53 S15 and RSK1/2 S221/S227.
- Category B “proteins under the control of Akt1 or Akt2”, included 12 phospho-proteins: CREB S133, GSK-3 α / β S21/S9, GSK-3 β S9, Fgr Y412, JNK 1/2/3 T183/Y185, T221/Y223, Lck Y394, P38 α T180/Y182, PDGF R β Y751, STAT2 Y689, Stat5a/b Y694/Y699, WNK1 T60 and β -Catenin.
- Category C “proteins under the control of Akt2 only” included 7 phospho-proteins: PRAS40 T246, P70 S6 Kinase T389, P70 S6kinase T421/S424, ERK1/2 T202/Y204, T185/Y187, Chk-2 T68, c-Jun S63 and RSK1/2/3 S380/S386/S377.
- Category D “proteins under the control of Akt1 and Akt2”, included 8 phospho-proteins: eNOS S1177, P53 S392, PYK2 Y402, STAT1 Y701, STAT3 Y705, STAT3 S727, STAT6 Y641, and HSP60.

HepG2 cell line

Similarly, the comparative analysis in Huh7 cell line of the decreased level of phospho-proteins, between the different knockdown conditions, see Venn Diagram in Figure 41, allowed the stratification of the proteins as follows:

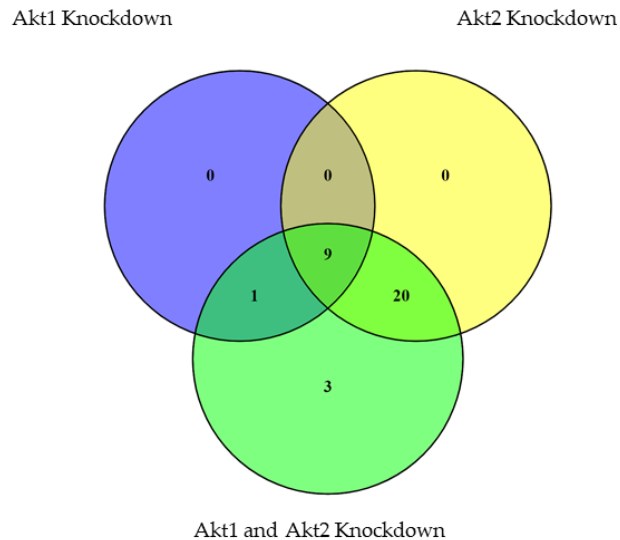


Figure 41: Comparative analysis of in HepG2 cell line. Venn diagram showing the comparative analysis of the decreased phospho-proteins, compared to the mock in the knockdown of Akt1 and/or Akt2 in HepG2 cell line. The numbers represent the number of phospho-proteins in each category.

- Category A: “proteins under the control of Akt1” included 1 phospho-protein STAT1 Y701.
- Category B: “proteins under the control of Akt1 or Akt2”, included 9 phospho-proteins: HSP27 S78/S82, P53 S15, P53 S46, P53 S392, Src Y419, PYK2 Y402, RSK1/2 S221/S227, Stat5a/b Y694/Y699, and STAT6 Y641.
- Category C: “proteins under the control of Akt2 only” included 20 phospho-proteins: eNOS S1177, PRAS40 T246, EGF R Y1086, Chk-2 T68, Fgr Y412, JNK 1/2/3 T183/Y185, T221/Y223, Lck Y394, Lyn Y397, MSK1/2 S376/S360, P70 S6 Kinase T389, P70 S6kinase T421/S424, P38 α T180/Y182., PDGF R β Y751, PLC- γ 1 Y783, RSK1/2/3 S380/S386/S377, STAT2 Y689, Yes Y426, STAT3 S727, β -Catenin, and HSP60
- Category D: “proteins under the control of Akt1 and Akt2”, included 3 phospho-proteins: CREB S133, ERK1/2 T202/Y204, T185/Y187 and STAT3 Y705.

Inter-cell lines

In addition, on a second level, the comparative analysis of the decreased proteins in every condition between Huh7 and HepG2 cell lines was done. See Venn diagram in Figure 42, for the definition of the categories.

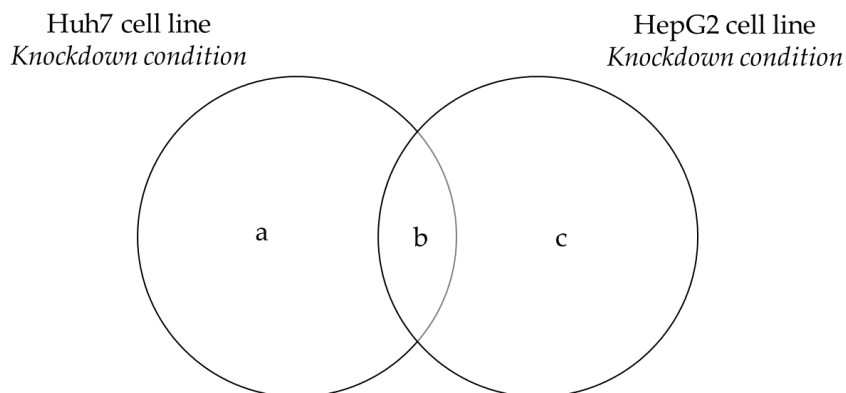


Figure 42: Categories of “inter-cell line” comparative analysis . Venn diagram showing the different categories upon the comparative analysis of each knockdown condition between Huh7 and HepG2 cell lines. The categories represent proteins that, when compared to the mock, decrease: “a”: exclusively in Huh7 cell line; “b”: in both Huh7 and HepG2 cell lines; “c”: exclusively in HepG2 cell line.

- Category “a” shows proteins that are exclusively decreased in Huh7 cell line in the knockdown condition compared. And are considered to be Huh7 cell-dependent function of the isoform.
- Category “b” shows proteins that are decreased in Huh7 and HepG2 cell lines in the knockdown condition compared. And are considered to be under the control of the isoform in both cell lines.
- Category “c” shows proteins that are exclusively decreased in HepG2 cell line in the knockdown condition compared. And are considered to be Huh7 cell-dependent function of the isoform

Akt1 and Akt2 knockdown

First, the comparative analysis of the proteins decreased in the case of the simultaneous knockdown of Akt1 and Akt2 between Huh7 and HepG2 cell lines, see Venn diagram in Figure 43, to decipher the difference in the activation of the pathway between the 2 cell lines. The comparison allowed the stratification of the proteins in the previously defined categories as follows:

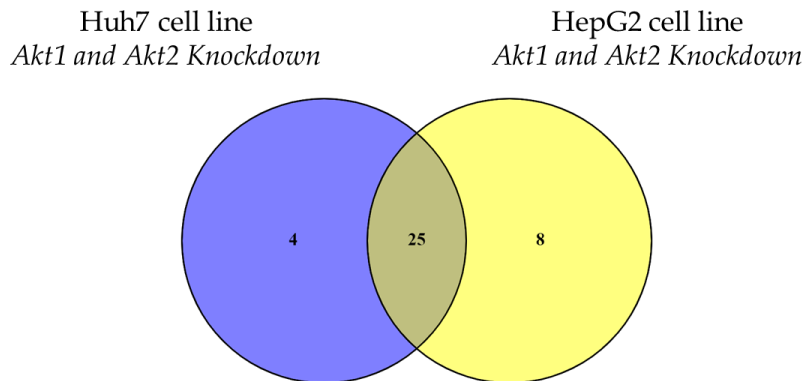


Figure 43: Inter-cell line comparative analysis of Akt1 and Akt2 knockdown. Venn diagram showing the comparative analysis of the decreased Huh7 cell line vs that of HepG2 cell line upon the double knockdown of Akt1 and Akt2. The numbers represent the number of proteins in each category.

- Category a: “Huh7-exclusive function of Akt pathway” includes 4 phospho-proteins: GSK-3 α/β S21/S9, GSK-3 β S9, c-Jun S63 and WNK1 T60
- Category b: “non-cell dependent function of Akt pathway” includes 25 phospho-proteins: CREB S133, eNOS S1177, PRAS40 T246, ERK1/2 T202/Y204, T185/Y18, Chk-2 T68, Fgr Y412, P53 S15, P53 S392, JNK 1/2/3 T183/Y185, T221/Y223, Lck Y394, P70 S6 Kinase T389, P70 S6kinase T421/S424, P38 α T180/Y182, PDGF R β Y751, PYK2 Y402, RSK1/2 S221/S227, RSK1/2/3 S380/S386/S377, STAT2 Y689, Stat5a/b Y694/Y699, STAT1 Y701, STAT3 Y705, STAT3 S727, β -Catenin, STAT6 Y641 and HSP60.
- Category c: “HepG2-exclusive Akt pathway function” includes 8 proteins: EGF R Y1086, HSP27 S78/S82, P53 S46, Lyn Y397, MSK1/2 S376/S360, PLC γ 1 Y783, Src Y419 and Yes Y426.

Single Akt1 knockdown

The comparative analysis of the proteins decreased in the case of Akt1 knockdown between Huh7 and HepG2 cell lines, *see Venn diagram in Figure 44*, allowed the stratification of the proteins in the previously defined categories as follows

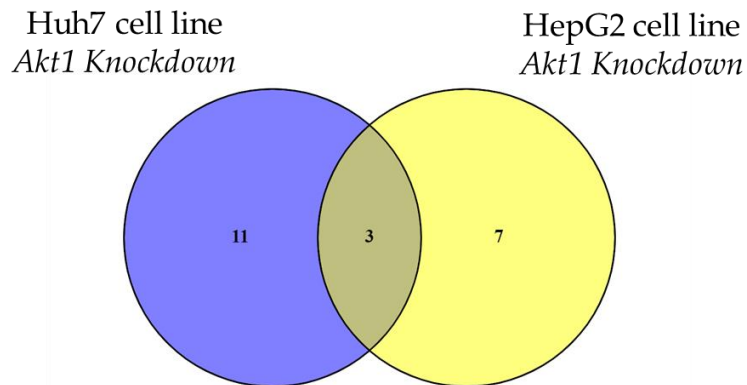


Figure 44: Inter-cell line comparative analysis of Akt1 knockdown. Venn diagram showing the comparative analysis of the decreased proteins in Huh7 cell line vs that of HepG2 cell line upon the single knockdown of Akt1. The numbers represent the number of proteins in each category.

- Category a: “Huh7-exclusive Akt1 function” includes 11 proteins: CREB S133, GSK-3 α / β S21/S9, GSK-3 β S9, Fgr Y412, JNK 1/2/3 T183/Y185, T221/Y223, Lck Y394, P38 α T180/Y182, PDGF R β Y751, STAT2 Y689, WNK1 T60, and β -Catenin.
- Category b: “non-cell dependent function of Akt1” includes 3 proteins: P53 S15, RSK1/2 S221/S227 and Stat5a/b Y694/Y699
- Category c: “HepG2-exclusive Akt1 function” includes 7 proteins: HSP27 S78/S82, P53 S46, P53 S392, Src Y419, PYK2 Y402, STAT1 Y701 and STAT6 Y641.

Single Akt2 knockdown

The comparative analysis of the proteins decreased in the case of Akt1 knockdown between Huh7 and HepG2 cell lines, *see Venn diagram in Figure 45*, allowed the stratification of the proteins in the previously defined categories as follows

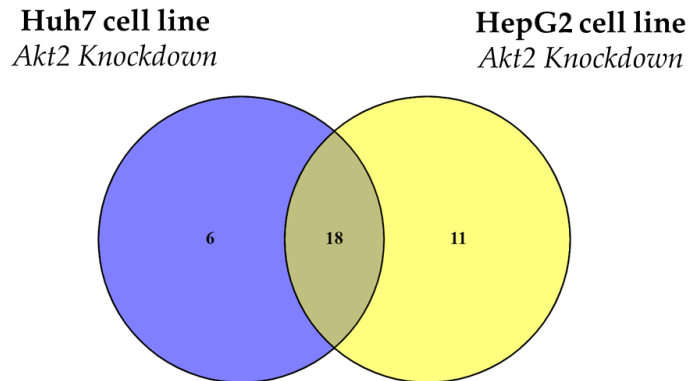


Figure 45: Inter-cell line comparative analysis of Akt2 knockdown. Venn diagram showing the comparative analysis of the decreased proteins in Huh7 cell line vs that of HepG2 cell line upon the single knockdown of Akt2. The numbers represent the number of proteins in each category.

- Category a: “Huh7-exclusive Akt2 function” includes 6 proteins: CREB S133, GSK-3 α / β S21/S9, GSK-3 β S9, ERK1/2 T202/Y204, T185/Y18, c-Jun S63, and WNK1 T60
- Category b: “non-cell dependent function of Akt2” includes 18 proteins: PRAS40 T246, P70 S6 Kinase T389, P70 S6kinase T421/S424, EGF R Y1086, Chk-2 T68, Fgr Y412, HSP27 S78/S82, JNK 1/2/3 T183/Y185, T221/Y223, Lck Y394, Lyn Y397, MSK1/2 S376/S360, P38 α T180/Y182, PDGF R β Y751, PLC- γ 1 Y783, RSK1/2/3 S380/S386/S377, STAT2 Y689, Stat5a/b Y694/Y699 and β -Catenin
- Category c: “HepG2-exclusive Akt2 function” includes 11 proteins: eNOS S1177, P53 S15, P53 S46, P53 S392, Src Y419, PYK2 Y402, RSK1/2 S221/S227, Yes Y426, STAT3 S727, STAT6 Y641 and HSP60.

All in all, the compiled comparative analysis revealed a unique profile of isoform specific roles in the different cell lines as well as within the same cell line. These results need to be further confirmed by protein immuno-detection.

9. Kinase fingerprint of Akt1 and/or Akt2 knockdown and their chemical inhibition

The modulations seen on the Akt pathway upon single or double knockdown of Akt1 and/or Akt2 by the designed siRNAs, ascertain that the designed siRNAs are not only able to knockdown Akt1/2 isoforms and decrease their corresponding phosphorylation, but also lead to fluctuations in the direct and indirect downstream effectors of the PI3K/Akt pathway. Consequently, a wider scope of the effect of the knockdown on the cellular pathways was needed whilst comparing to the treatment with Sorafenib and ARQ092. Such a comparative assessment of the overall changes in the kinase activity of the cell would establish a fingerprint of each of the treatments and thus allow the unraveling of distinctive pathway activation or inactivation. Which, in turn, could explain the unexpected absence of an antitumorigenic effect upon the targeted knockdown of Akt1 or Akt2 by the designed siRNAs and its presence in the case of Sorafenib and ARQ092. For that, analysis was done on the different Ser/Thr kinase activity of PLC γ /PRF/5, Huh7 and HepG2 cells, upon the knockdown of double and single knockdown of Akt1 and/or Akt2, and treatment with ARQ092. For that, cells were exposed for 6hours to either to LipofectamineRNAiMAX coupled to the designed siRNAs D2Akt1 and/or D15Akt1 at 10nM concentration with mock siRNA as a negative control. Furthermore, the cells were treated for 6hours to ARQ092 at the corresponding Inhibitory Concentration 20 (IC₂₀) concentrations with untreated cells as a negative control. Then, 24 hours later, analysis of the Serine/Threonine kinases fingerprint was analyzed.

The kinase fingerprint analysis was performed on Pamstation12, which is a technology developed by Pamgene (<https://pamgene.com/>). The basis of this technology is the presence of immobilized peptide motifs on a chip., called PamChip. Each sequence corresponds to a putative sequence of one or more known protein and prone to phosphorylation by the different kinases. Upon the incubation with the different protein lysates, harboring kinases in their active form, a series of phosphorylation events takes place on the chip, which are later detected by capture antibodies coupled to fluorescent molecules. Two levels of analysis of the detected phosphorylation events are then done: i) the analysis of the phosphorylation events on the chip and calculation of the fold change compared to the respective control termed “phosphosite analysis” and ii) the bioinformatic analysis done according to an “in-house” procedure from Pamgene termed “upstream kinase analysis” (UKA). First the phosphosite analysis is done

to distinguish the difference in the phosphorylation state of every peptide on the chip – increased or decreased when compared to the control – then a list of the phosphosites *i.e.*, proteins, with their accession number on UniprotKB, are generated. The UKA uses the set of the phosphosites and their changes, whether significant or not, in order to generate fact-based predictions about the different activated kinase pathways in every scenario. The analysis generates a “mean specificity score”. This score is based on a combined sensitivity score (difference between “Treatment” and “Control” groups) and specificity score (for a set of peptides to kinase relationship derived from current databases). The cutoff used in this study is 1.2.

The heatmap in *Figure 46* shows an overview about the different changes in the phosphosites on the PamChip following the transfection with the mock or the designed siRNAs and the subsequent single or double knockdown of Akt1 and/or Akt2 in PLC γ /PRF/5, Huh7 and HepG2 cells. The results reveal a similar clustering pattern between the different conditions and between the different cell lines tested. The phosphosite changes were further analyzed to decipher the exact modulations in the upcoming sections.

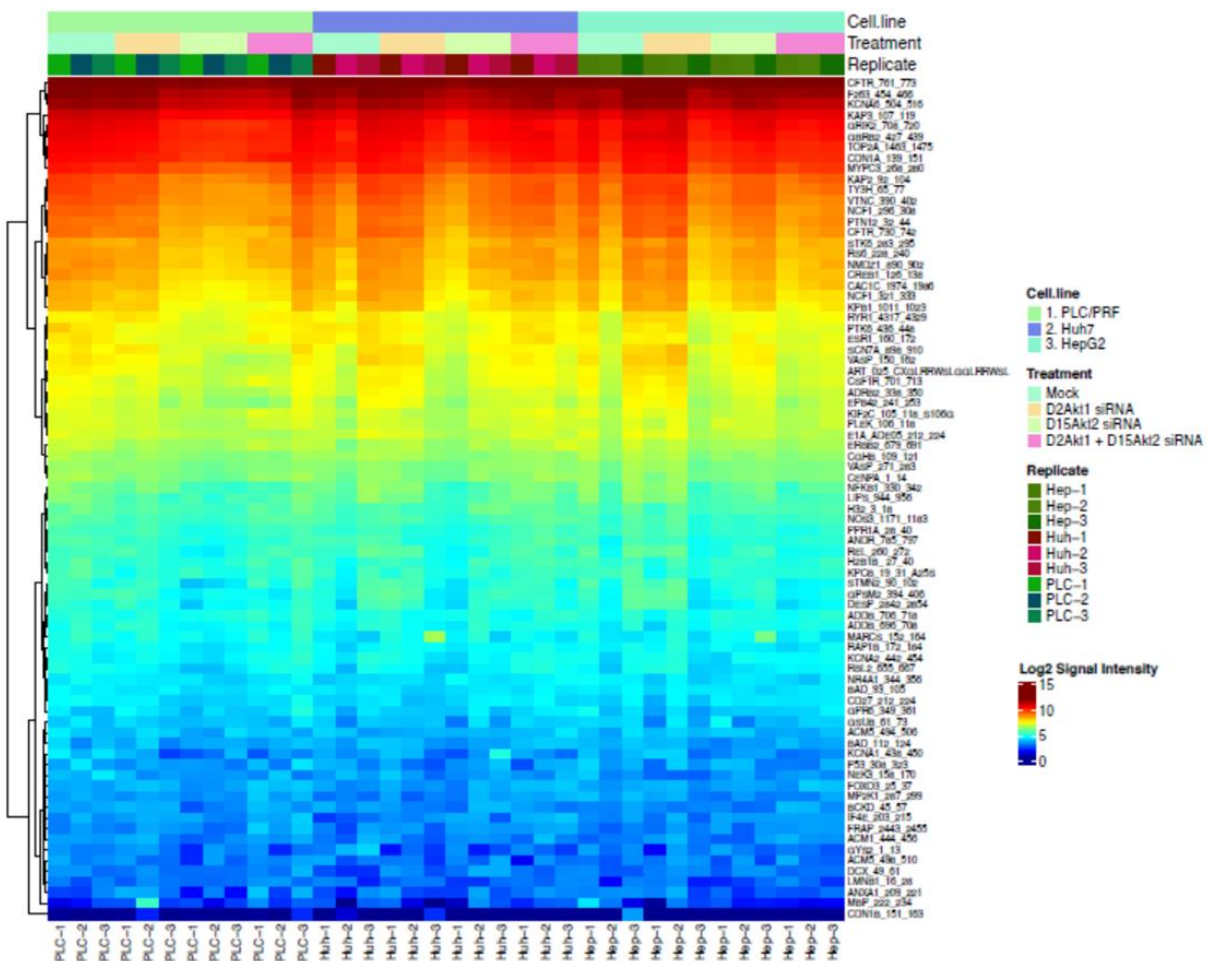


Figure 46: Heatmap of phosphosites upon the siRNA knockdown. of Akt1 and/or Akt2 in PLC/PRE/5, Huh7, and HepG2 cell lines. Heat map representation of the log₂ signal intensity of the changes in the phosphosites (N=3 independent experiments per cell line) normalized to the mock condition in every cell line, along with the Euclidean clustering based on the rows (phosphosites). The right panel includes the legend of the used colors.

Similarly, the heatmap in Figure 47 also shows an overall view of the different changes in the phosphosites in the 3 tested cell lines following the exposure to ARQ092. The patterns also seem to have a conserved overall clustering between the different cell lines. However, the patterns are not exactly the same, thus a further detailed analysis was done, and is presented in later sections.

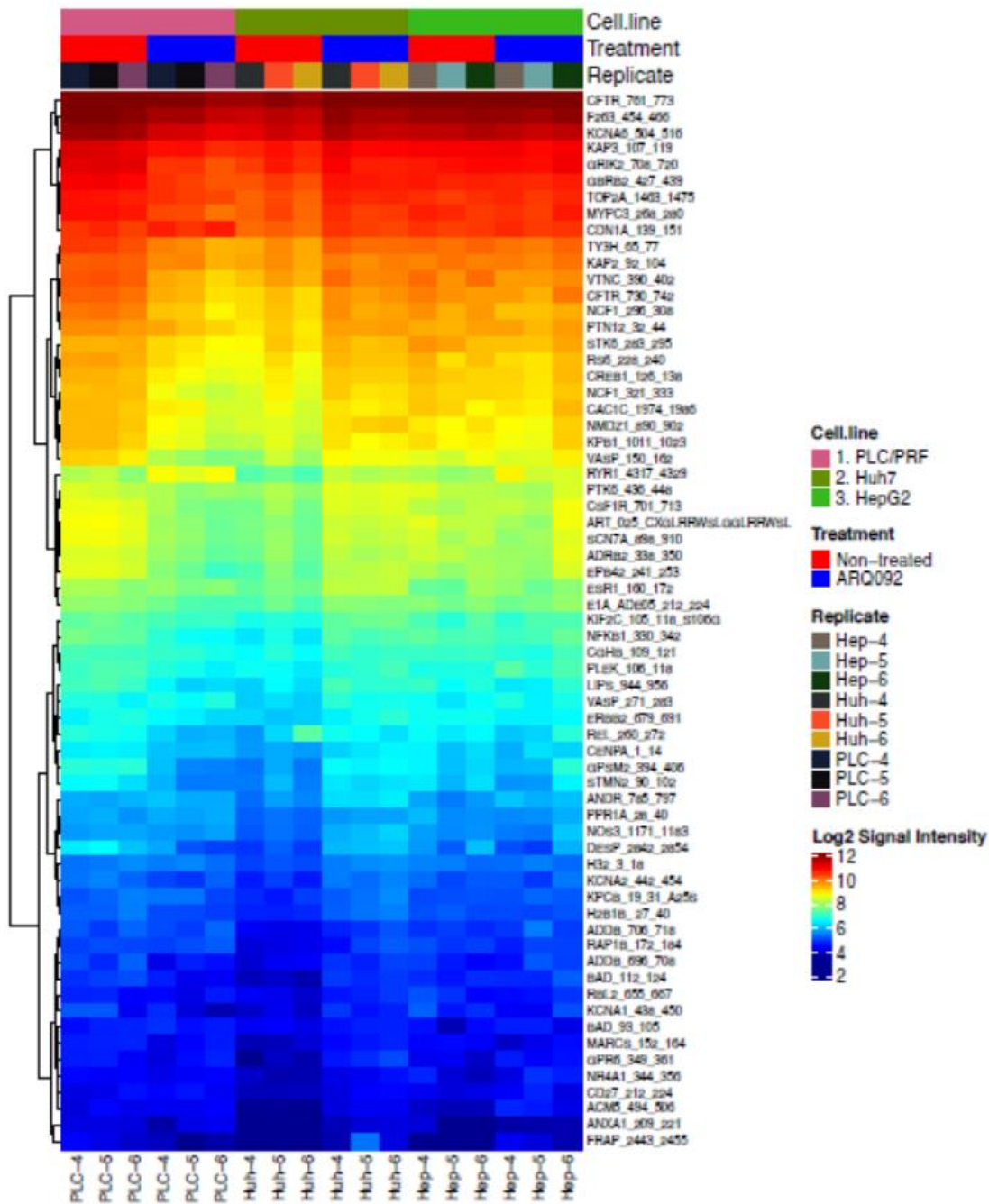


Figure 47: Heatmap of phosphosites ARQ092 treatment . in PLCγ/PRF/5, Huh7, and HepG2 cell lines. Heat map representation of the log₂ signal intensity of the changes in the phosphosites (N=3 independent experiments per cell line) normalized to the mock condition in every cell line, along with the Euclidean clustering based on the rows (phosphosites). The right panel includes the legend of the used colors.

Below are the detailed phosphosite and UKA results classified according to the cell line and explained upon the designed siRNA-mediated targeting of Akt1 and/or Akt2 and the treatment with ARQ092. Of note, the ARQ092 is an inhibitor which targets the three isoforms of Akt: Akt1, Akt2 and Akt3.

9.1. PLC γ /PRF/5 cell line

The knockdown of Akt1 and/or Akt2 in PLC γ /PRF/5 by the designed siRNAs cell line showed a different pattern of kinase activity in the different conditions. Primarily, the phosphosite analysis displayed in the volcano plot, *see Figure 48A*, shows the different increase and decrease in the phosphorylation of the tested peptides when compared to the mock condition. The Akt1 knockdown profile shows a general significant decrease in the phosphorylation of the peptides. The most drastic decrease in the phosphorylation was seen in the case of the Akt2 knockdown. Unexpectedly, the simultaneous knockdown of both Akt1 and Akt2 did not exhibit a profile of decrease in the phosphorylation as prominent as the one seen in the case of the single knockdown of Akt2.

The UKA analysis done on the different conditions, expectedly, predicted a unique activation and inhibition of Ser/Thr kinases.

The Akt1 knockdown, *see Figure 48B*, predicted an increase in the kinase activity of PCTRAIRE2(also known as CDK16: Cyclin-Dependent Kinase 16), Ribosomal Protein S6 Kinase-Like 2 (RSKL2), Serine/threonine-protein kinase (SGK1) and Cyclin-Dependent Kinase 5 (CDKL5), accompanied by a decrease in the kinase activity of Aurora Kinase B (AurB/Aur1), Calcium/calmodulin-dependent protein kinase type IV (CAMK4), Aurora Kinase A (AurA/Aur2), Protein Kinase-C (PKC) (alpha), PKC (theta)and PKC (delta).

On the other hand, the knockdown of Akt2, *see Figure 48C*, predicted only a decrease in the activity of the following kinases: PKG1, PKA (alpha), CAMK4, cAMP-dependent protein kinase catalytic subunit PRKX (PRKX), PKC (theta), PKC (alpha), PKC (delta), Proviral Integration site for Moloney murine leukemia virus (Pim)1 and Pim2.

Finally, and upon the simultaneous knockdown of Akt1 and Akt2, *see Figure 48D*, the results predicted a decrease in the serine/threonine kinase activity of PKG2, PKG1, PKA (alpha), CAMK4, PKC (alpha) and PKD1.

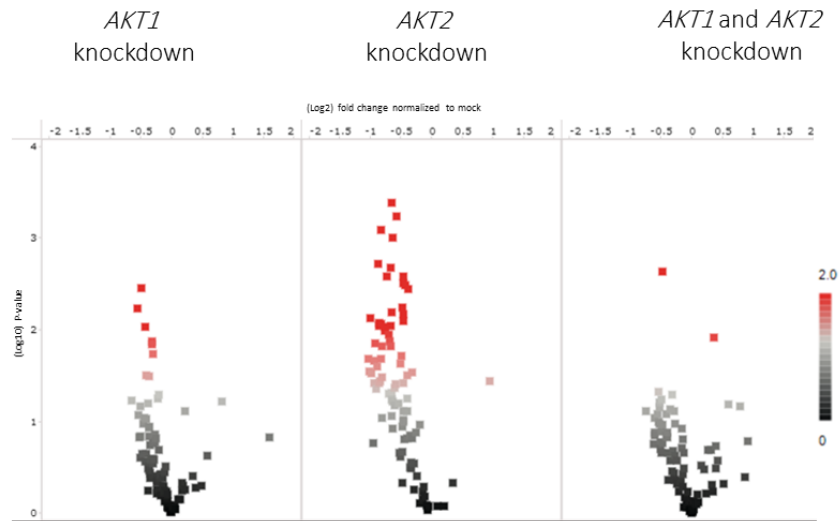
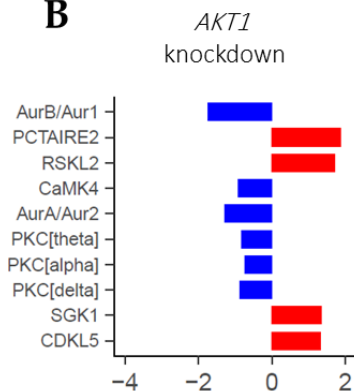
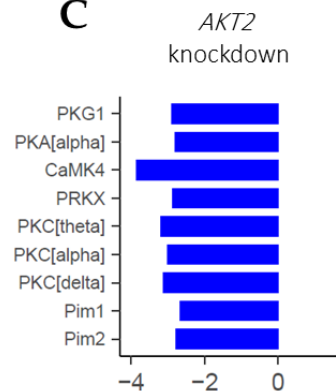
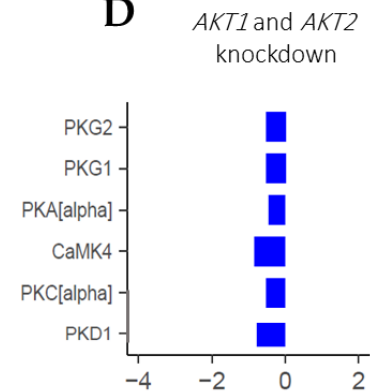
A**B****C****D**

Figure 48: Kinase fingerprint of PLC γ /PRF/5 cells upon siRNA knockdown of Akt1 and/or Akt2. (A) Volcano plots visualizing the results of the different knockdown conditions indicated plotting the log fold change of the phosphorylation of the peptides on the PamChip (x-axis) vs the log p-value (y-axis). Red spots correspond to the proteins having a significant change ($p < 0.05$). The statistical test used was the ordinary one-way ANOVA. The lower panel shows a graphical representation of the Upstream Kinase Analysis (UKA) of the changes in the phosphorylation of the peptides on the PamChip in the case of (A) Akt1 knockdown, (B) Akt2 knockdown and (C) Akt1 and Akt2 knockdown. Represented are the Ser/Thr kinases predicted to be inhibited (blue), or activated (red), compared to the mock, along with their degree of inhibition (x-axis), and having a mean specificity score of 1.2 or higher.

Following the treatment of the cells with ARQ092, first, the volcano plot, *see Figure 49A*, showed a general significant decrease in the profile of the phosphorylated peptides, with a significant increase in the phosphorylation of one peptide. The UKA analysis, *see Figure 49B*, predicted that ARQ092 leads to the decrease in the serine/threonine kinase activity of PKG2, PKC (alpha), P70S6K(beta), PKG1, PKA (alpha), and AurB/Aur1.

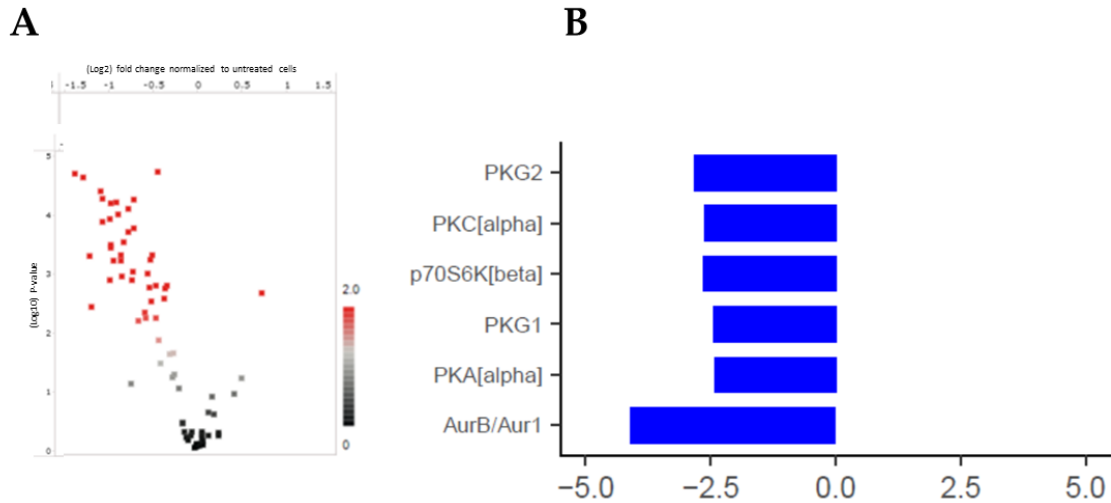


Figure 49: Kinase fingerprint of PLCY/PRF/5 cells upon ARQ092 treatment . (A) Volcano plots visualizing the results of the treatment with ARQ092, plotting the log fold change of the phosphorylation of the peptides on the PamChip (x-axis) versus the log p-value (y-axis). Red spots correspond to the proteins having a significant change ($p < 0.05$). The statistical test used was the ordinary one-way ANOVA. **(B)** Graphical representation of the Upstream Kinase Analysis (UKA) of the changes in the phosphorylation of the peptides on the PamChip. Represented are the Ser/Thr kinases that are predicted to be inhibited (blue), compared to the mock along with their degree of inhibition (x-axis), and having a mean specificity score of 1.2 or higher

9.2. Huh7 cell line

On the other hand, the knockdown of Akt1 and/or Akt2 by the designed siRNAs in Huh7 cell line revealed a general profile of phosphorylation of the different peptides that is less eminent than the one shown with the PLC γ /PRF/5 as shown in the volcano plot, *see Figure 50A*. The profile of decrease in the phosphorylation of peptides was most visible in the case of Akt2 knockdown (significant decrease in the phosphorylation of 6 peptides) when compared to Akt1 or the simultaneous knockdown of Akt1 and Akt2. The former showed a significant decrease of phosphorylation of one peptide whereas the latter showed a significant increase in the phosphorylation of 2 peptides

Furthermore, the UKA analysis translated the profiles of the peptide phosphorylation into predicted kinase activity in each condition.

The Ser/Thr kinase activity profile in the case of Akt1 knockdown, *see Figure 50B*, predicted a decrease in kinase activity of NUA family SNF1-like kinase 1 (NuaK1), AurA/Aur2, Pim2 and MAPK-Associated Protein 2 (MAPKAP2) when compared to the mock.

Whereas, that of Akt2 knockdown, *see Figure 50C*, in comparison to the mock, foresaw a decrease in the activity of CAMK4, NuaK1 and Casein Kinase -1 (CK1) (epsilon).

Finally, the simultaneous knockdown of Akt1 and Akt2, *see Figure 50D*, predicted an increase in the activity of RSKL2, ERK2, Rho-associated protein kinase 1 (ROCK1), ERK5, ERK1, GSK 3(alpha), GSK3 (beta), CDKL5, AarF Domain-Containing Protein Kinase 3 (ADCK3), RAF1, JNK3, JNK2, p38(beta) and JNK1.

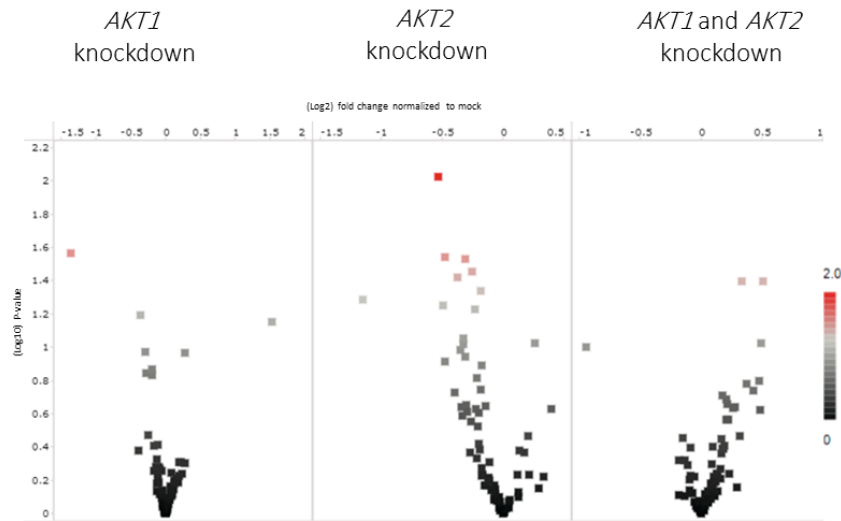
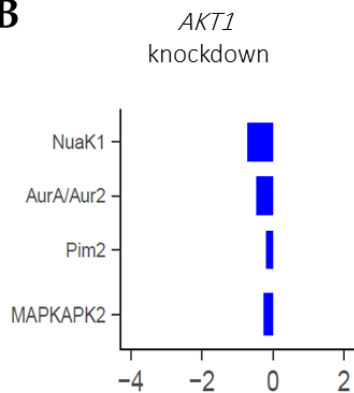
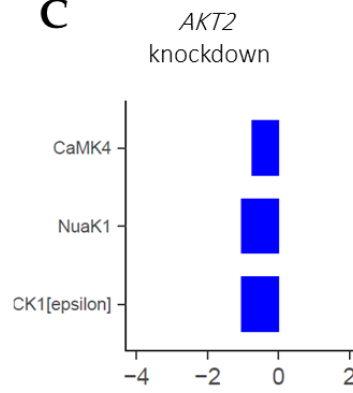
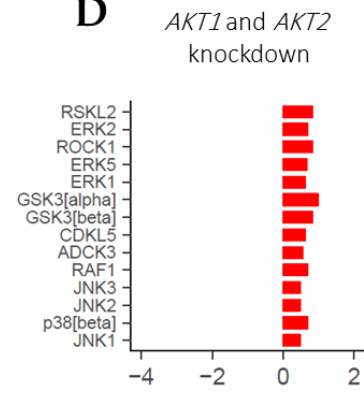
A**B****C****D**

Figure 50: Kinase fingerprint of Huh7 cells upon siRNA knockdown Akt1 and/or Akt2. (A) Volcano plots visualizing the results of the different knockdown conditions indicated plotting the log fold change of the phosphorylation of the peptides on the PamChip (x-axis) vs the log p-value (y-axis). Red spots correspond to the proteins having a significant change ($p < 0.05$). The statistical test used was the ordinary one-way ANOVA. The lower panel shows a graphical representation of the Upstream Kinase Analysis (UKA) of the changes in the phosphorylation of the peptides on the PamChip in the case of (A) Akt1 knockdown, (B) Akt2 knockdown and (C) Akt1 and Akt2 knockdown. Represented are the Ser/Thr kinases predicted to be inhibited (blue), or activated (red), compared to the mock, along with their degree of inhibition (x-axis), and having a mean specificity score of 1.2 or higher.

Results upon the treatment with ARQ092, unexpectedly, revealed a profile of activation when compared to untreated cells as shown in the volcano plot, *see Figure 51A*. The translation of the profile of the increase in the phosphorylation of the peptides at the level of the serine/threonine kinase activity, *see Figure 51B*, predicted the increase in the activity of P70S6K, IKK(epsilon), P70S6K(beta), SGK2, CK2(alpha)1, and RSK1/p90RSK.

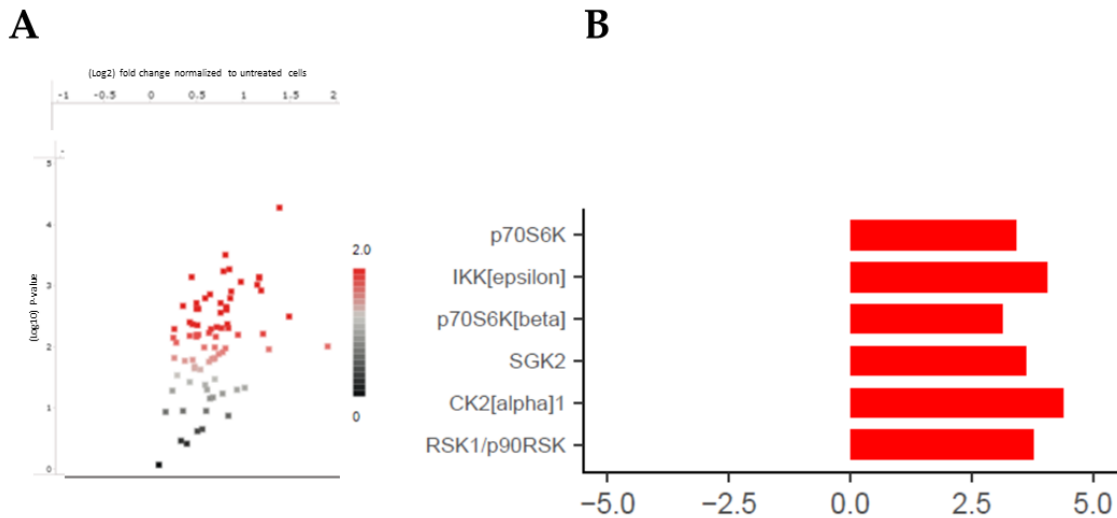


Figure 51: Kinase fingerprint of Huh7 cells upon ARQ092 treatment. (A) Volcano plots visualizing the results of the treatment with ARQ092, plotting the log fold change of the phosphorylation of the peptides on the PamChip (x-axis) versus the log p-value (y-axis). Red spots correspond to the proteins having a significant change ($p < 0.05$). The statistical test used was the ordinary one-way ANOVA. (B) Graphical representation of the Upstream Kinase Analysis (UKA) of the changes in the phosphorylation of the peptides on the PamChip. Represented are the Ser/Thr kinases that are predicted to be inhibited (blue), compared to the mock along with their degree of inhibition (x-axis), and having a mean specificity score of 1.2 or higher.

9.3. HepG2 cell line

Furthermore, the effect of the knockdown of Akt1 and/or Akt2 on HepG2 cells showed a phosphosite profile less drastic than the one shown with PLC γ /PRF/5 and Huh7, as shown in the volcano plot in *Figure 52A*. The knockdown of Akt1 showed a significant decrease in the phosphorylation of 2 peptides, similar to that shown in the case of Akt2 knockdown. However, the simultaneous knockdown of both Akt1 and Akt2 showed a significant decrease in the phosphorylation of 3 peptides, when compared to the mock.

Altogether the decrease in the respective peptides, revealed different fluctuations in the Ser/Thr kinase activity by UKA analysis.

The Akt1 knockdown, *see Figure 52B*, predicted a decrease in the activity of ERK2, p21-Activated Kinase 1 (PAK1), ERK1, ICK, JNK2, p38beta, and JNK1.

In parallel, in the case of Akt2 knockdown, *see Figure 52C*, the Ser/Thr kinase activity of BRAF, PKG1, PKA (alpha), PAK1, IKKalpha, RAF1 and PKD1 was predicted to be decreased when compared to the mock.

Furthermore, and in the case of the simultaneous knockdown of Akt1 and Akt2, the serine/threonine kinase activity profile, *see Figure 52D*, predicted the decrease in the activity of PKG2, PKG1, p70S6K(beta), PKA (alpha), CAMK4, PRKX and PKC (delta).

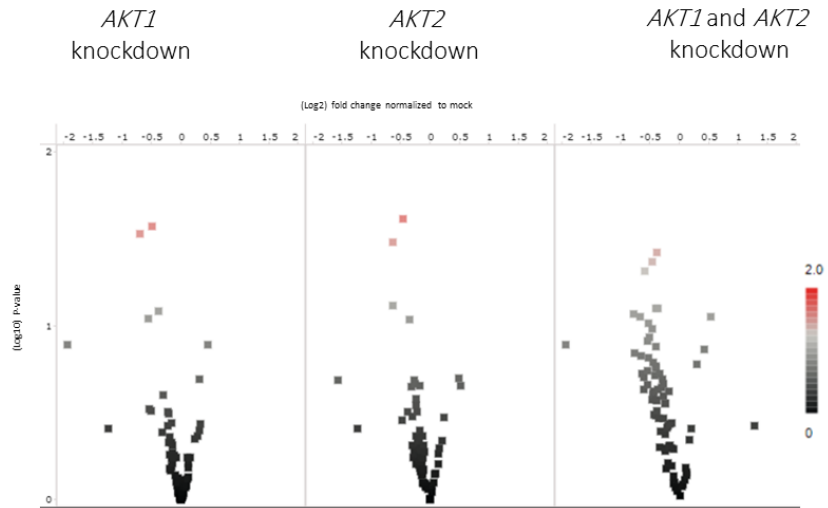
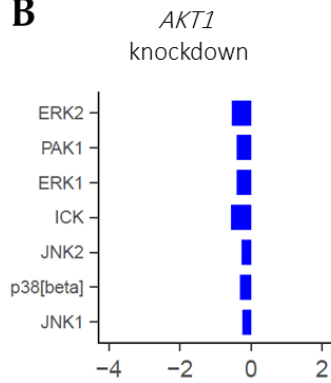
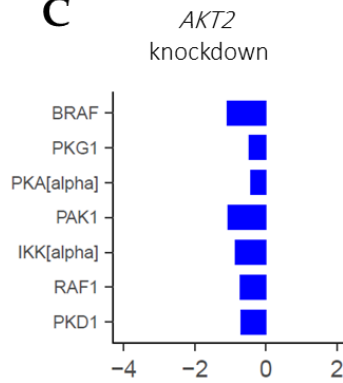
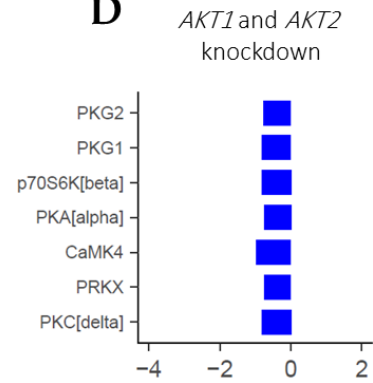
A**B****C****D**

Figure 52: Kinase fingerprint of HepG2 cells upon siRNA knockdown of Akt1 and/or Akt2. (A) Volcano plots visualizing the results of the different knockdown conditions indicated plotting the log fold change of the phosphorylation of the peptides on the PamChip (x-axis) vs the log p-value (y-axis). Red spots correspond to the proteins having a significant change ($p < 0.05$). The statistical test used was the ordinary one-way ANOVA. The lower panel shows a graphical representation of the Upstream Kinase Analysis (UKA) of the changes in the phosphorylation of the peptides on the PamChip in the case of (A) Akt1 knockdown, (B) Akt2 knockdown and (C) Akt1 and Akt2 knockdown. Represented are the Ser/Thr kinases predicted to be inhibited (blue), or activated (red), compared to the mock, along with their degree of inhibition (x-axis), and having a mean specificity score of 1.2 or higher.

Comparatively, the treatment of HepG2 cells with ARQ092 showed a general profile of partitioned changes between an increase and a decrease in the phosphorylation, as shown in the volcano plot, *see Figure 53A*. Even though, none of the fluctuations were significant, the UKA analysis was done, *see Figure 53B*, and predicted a decrease in the activity of PKG2, ADCK3 and PKA (alpha) when compared to the untreated cells.

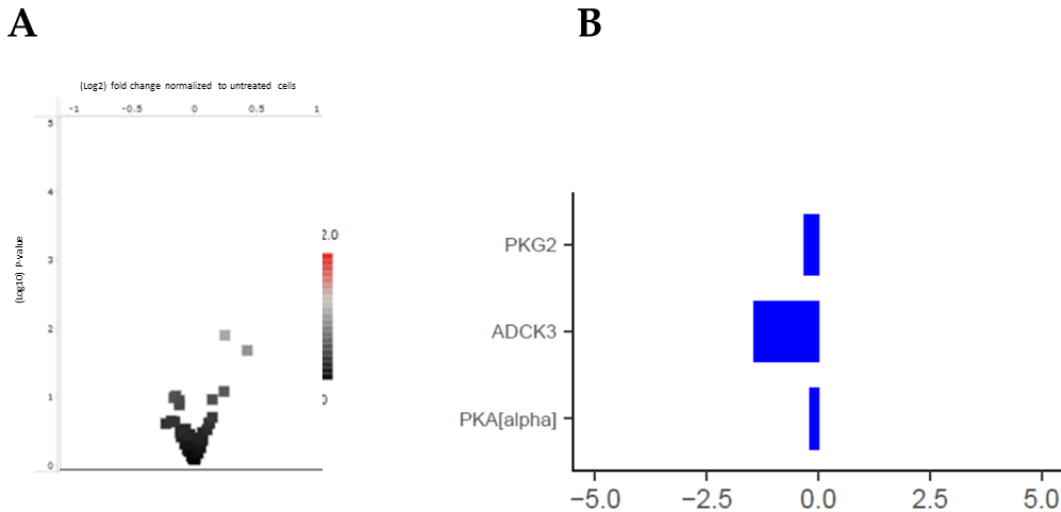


Figure 53: Kinase fingerprint of HepG2 cells upon ARQ092 treatment . (A) Volcano plots visualizing the results of the treatment with ARQ092, plotting the log fold change of the phosphorylation of the peptides on the PamChip (x-axis) versus the log p-value (y-axis). Red spots correspond to the proteins having a significant change ($p < 0.05$). The statistical test used was the ordinary one-way ANOVA. **(B)** Graphical representation of the Upstream Kinase Analysis (UKA) of the changes in the phosphorylation of the peptides on the PamChip. Represented are the Ser/Thr kinases that are predicted to be inhibited (blue), compared to the mock along with their degree of inhibition (x-axis), and having a mean specificity score of 1.2 or higher.

The results revealed different predictive profiles of the Ser/Thr kinase activity, in every condition and between the different cell lines. Interestingly, major differences were revealed in the predicted pattern of Ser/Thr kinase activity between the siRNA-mediated double knockdown of the isoforms, and the pan Akt inhibition by ARQ092 in all the cell lines, except for that in PLC γ /PRF/5. In this cell line the pattern was exactly the same except for an additional inhibited kinase in the siRNA-mediated double knockdown. Further analysis is needed to decipher the differences; however, the preliminary results convey a different mode of action of ARQ092 compared to the siRNAs, despite the fact that both strategies target Akt.

IX. DISCUSSION

Background and objective

HCC is one of the most common causes of cancer-related deaths worldwide, and its incidence is rising. Its development, almost always, is prerequisite to a chronic inflammation in the liver. The etiology behind the chronic inflammation can be due to chronic alcohol consumption, consumption of toxins, metabolic disorders leading to NASH and NAFLD, or viral hepatitis (hepatitis B and C) [6]. The dangerous aspect of hepatocellular carcinogenesis is that its incidence is correlated to lifestyle habits including an unhealthy diet and chronic alcohol consumption, which is translated by the changes in its incidence rate geographically in the world [1]. The treatment options for HCC were first restricted to Sorafenib which failed to extend the patient life by more than 3 months and faced the problem of Sorafenib-resistance. However, recently, immune-based therapies have been introduced [320]. Unfortunately, their use is restricted to a defined cohort of patients. Those eligible for immune based therapies should possess a specific tumor immune profile, which depends on the etiology and the liver status. Based on the immune profile of the tumors, they are classified as “hot tumors” and “cold tumors”. On the one hand, the “hot tumors” are immune-therapy responsive and are characterized by an intra-tumoral infiltration of lymphocytes, and an expression of immune checkpoint molecules like PD-1/PDL-1 which is crucial for immune checkpoint targeting. On the other hand, the “cold tumors” lack the intra-tumoral infiltration of lymphocytes, mainly CD8⁺ T-cells, along with the lack of expression of immune checkpoint molecules, rendering them non-responsive to immune-based treatments [321, 322].

As HCC still faces difficulties for diagnosis at an early stage, the best approach to combat HCC is to unravel the underlying molecular changes which drive its carcinogenesis properties. Upon carcinogenesis, a cascade of molecular changes at the transcriptional and proteomic level leads to a change in the phenotypic and secretory profile of the cells. The transcriptional and proteomic changes often result in the dysregulation of the different signaling pathways in the cell, disrupting its homeostasis and resulting in an overdrive of the crucial cellular process and, more often than not, a change in the whole identity of the cell giving it carcinogenic properties, *e.g.*, highly proliferative, migrating and resistant to apoptosis. Among the dysregulated pathways is the PI3K/Akt pathway.

The PI3K/Akt pathway is a central hub in the cell, regulating various cellular processes including cell proliferation, cell survival, translation and metabolism, among others... Recently, Akt has been receiving a lot of attention as a target for therapy in HCC, mainly through chemical inhibitors, *see Table 1*. Nevertheless, the chemical inhibitors fail to display a specificity to the different Akt isoforms: Akt1

(constitutively expressed in the human body), Akt2 (mainly expressed in insulin sensitive tissues) and Akt3 (mainly expressed in the brain and the testes). In this study, we investigated the roles played by Akt1 and Akt2 in HCC, and further the plausibility of targeting one isoform or the other as a treatment for HCC. In order to do that, a tool that specifically targets one of the isoforms without affecting the other was needed. Thus, we exploited the technology of RNAi and more specifically siRNAs.

Differential Activity of AKT isoforms

The notion of differential isoform roles in HCC is not farfetched. Although the different isoforms show an overlap in their activity: inhibition of Bcl-2 family proteins (regulating apoptosis), GSK3 isoforms (regulating metabolism), and TSC2 (tumor suppressor); the substrate-specificities of Akt1/2/3 exist. These are dependent on several parameters such as the distribution of the Akt isoforms in the tissues, the differential activation of Akt by external stimuli (amplitude and timing of activation), the preferential intrinsic catalytic activity of the different isoforms, and the specific cell-context factors (subcellular localization and substrate proximity) [323]. The theory of differential activity of Akt isoforms stemmed from the fact that in some cancers one isoform showed gene amplification and not the other; in gastric adenocarcinomas Akt1 gene exhibited gene amplifications [324]. On the other hand, Akt2 gene amplification was shown in ovarian and pancreatic cancers [325, 326]. Furthermore, several studies of Akt knockout mice backed up the notion:

- *Akt1*^{-/-} mice show embryonic lethality, and those which survive exhibit impaired body growth;
- *Akt2*^{-/-} mice manifest severe diabetic phenotypes;
- *Akt3*^{-/-} mice on the other hand have reduced brain sizes while maintaining cognitive abilities [327], [328].

The study of the non-redundant roles is still an ongoing process and is difficult to distinguish. Akt1 has been shown to play a role in angiogenesis. This is mainly due to the preferential expression in endothelial cells associated with the increase in vascular permeability and decreased vessel maturation upon the knockdown of Akt1 *in vivo* [329]. On the other hand, Akt2 plays a role in the regulation of glucose in the body. Insulin is among the external stimuli that fire up the Akt pathway. Insulin regulates the glucose homeostasis in the whole body – uptake of glucose into fat and muscle- and inhibits the hepatic glucose secretion. The relocalization of GLUT4 glucose transporter from the cytoplasm to the plasma membrane is crucial for the import of glucose into the fat and muscle in a concentration-

dependent manner. Consistent with the phenotype displayed by Akt2 knockdown mice, the siRNA-mediated downregulation of Akt2 caused an aberration in the GLUT4 trafficking in 3T3-L1 adipocytes. Interestingly, the overexpression of Akt1 did not rescue the phenotype, thus further asserting the specific role of Akt2 in GLUT4 redistribution and glucose homeostasis due to the preferential accumulation of Akt2 at the plasma membrane in these cells [330]. Furthermore, the preferential activation of either of the isoforms is, in some instances, regulated by the class of PI3Ks activated; p110 α preferentially activated Akt1 while p110 β preferentially activated Akt2 [331]. In carcinogenesis, studies showed differential roles of Akt in the various pro-tumorigenic processes. A series of *in vitro* and *in vivo* studies showed that cell migration is inhibited by Akt1 while being enhanced by Akt2 [332]. On the contrary, Akt1 enhanced migration in non-transformed cells, which further confirms that the control of cellular processes is cell-context dependent [333]. Concerning the subcellular localization of the different isoforms one example is the study done by Santi and Lee [334]. In that study, MDA-MB-231 human breast cancer cells demonstrated that Akt1 localized into the cytoplasm, Akt2 in the mitochondria, and Akt3 in the nucleus. Because of oncogenic mutations and the preferential accumulation of Akt1 at the plasma membrane in cancerous cells, Akt1 can take over the GLUT4 mediated import of glucose into the cells [334].

Thus, the literature strongly implies the differential roles played by the different Akt isoforms in various cellular contexts. Which made the study of the differential roles of Akt1 and Akt2 in HCC a very interesting aspect. This unraveling could be of crucial use in the future for customized therapies for HCC patients.

RNAi

RNAi as a tool for the specific targeting of Akt1 and Akt2 was the backbone of this study. Despite the recent advances in clinical application of RNAi, the avoidance of nonspecific toxicity is a major critical challenge in the development of RNAi therapeutics. The toxicity and activity of RNAi drugs depend largely on sequences present or absent in the transcriptome. Thus, a siRNA that has no off-target effects in rodents could induce intolerable off-target-related toxicity in humans; a siRNA that induces well silencing in animals may have insufficient activity against the human gene. Therefore, the careful preclinical development process is required. Unlike gene therapy, which is based on the modification of the genomic content within the nucleus, siRNAs act directly in the cytoplasm of cells and do not require a nuclear import. Therefore, siRNA-based therapies raise a much lower threat of introducing mutations that can lead to cancer. In addition, specificity of gene targeting, intracellular enzymatic degradation, stability and the kinetics of

RNAi molecules in circulation and their local distribution are among the important parameters to be developed and optimized [335, 336] For that, in our study, we designed, *in silico*, siRNA sequences targeting the human and the rodent (mouse and rat) Akt1 and Akt2 isoforms, simultaneously. The screening of the best 4 candidates for testing *in cellulo* was done on the basis of cross-reactivity and lowest predicted off-target effect in the three species (human, rat and mouse). Following their validation *in cellulo* on HepG2 cells, the 2 best candidates showing the highest efficiency *in cellulo* and the lowest combined off-target effect *in silico* in the three species (human, rat, mouse) were selected for further analysis. They were verified for their specificity, *in cellulo*, in terms of isoform-targeting, *i.e.*, the Akt1 targeting siRNA does not influence the Akt2 isoform, neither on the transcriptomic nor on the proteomic level, and vice versa, in both human and mouse cell line (HepG2 and Hepa1.6 cell lines, respectively). Further, the designed siRNAs were validated for their specificity to solely target the Akt1 or the Akt2 isoforms and not any of the other off-target genes predicted by the *in silico* tools.

The screening of the off-target effect was not restricted to the gene level, but rather surpassed it to study the possible off-target effect on the immune system. siRNA sequences are known to cause unwanted inflammatory effects resulting from the activation of the TLRs expressed by the innate immune cells *e.g.*, macrophages and dendritic cells and by non-immune cells such as fibroblast cell, epithelial and endothelial cells. They are said to be fired upon the recognition of conserved structural molecules, encompassing nucleic acid motifs, and elicit an inflammatory response [337]. The designed siRNAs were assessed for their ability to activate TLRs, and the results showed no activation of any of the TLRs: TLR1, TLR2, TLR3, TLR4, TLR5, TLR6, TLR7, TLR8, TLR9, at any of the concentrations ranging between 10nM – 100nM. Thus, the obtained siRNAs surpass the species barrier, and have no “off-target” effect, which could otherwise mask or generate consequences that would not necessarily be attributed to the knockdown of either isoform. The designed siRNAs were additionally analyzed for their long-lasting effect and their dose efficiency. The results show that the exposure of HepG2 cells to the designed siRNAs for a small period of time (6 hours), was sufficient to decrease the expression level of Akt1 and Akt2 for up to 5 and 7 days, respectively, on the transcriptomic and proteomic level. Commercially available siRNAs’ use in rapidly dividing tumor cells have a standard peaking time of action of 2-3 days after transfection, lasting until day 5, after which it begins to decline [338]. Our designed siRNAs depict the same timeline of action, with a boost of durability in the case of Akt2 siRNA (lasting until day 7).

Interestingly, the designed siRNAs were shown to have an activity at low concentration. The siRNA concentration used often in the literature is in the nM range [339], and that of the chemical inhibitors stretches to the μ M range (*studies in*

Table 1). However, in our case the designed siRNAs following a short time of transfection (6 hours), elicited a decrease the expression of Akt1 or Akt2 in HepG2 cells, starting from the pM range. Such a decrease was seen on the transcriptomic as well as the proteomic level. Signs of decrease appeared at concentrations as low as 5 pM and were prominent at 20 pM (see Figure 22 and Figure 23).

In conclusion, the RNAi tool in hand is designed siRNAs: D2Akt1 siRNA and D15Akt2 siRNA, which are specific, targeting uniquely Akt1 and Akt2, respectively, whilst crossing the human-rodent species barrier, have no inflammatory effect, have a long-lasting effect, and are efficient at low doses. All of these factors make them good candidates for RNAi therapeutic approach for HCC.

Phenotypic consequences of siRNA-mediated knockdown of Akt1 and Akt2

To be considered as candidates for a therapeutic approach, the designed siRNAs needed to be further consolidated. First, by demonstrating whether or not the designed siRNAs and their subsequent knockdown of either or both of the Akt1 and Akt2 isoforms could elicit an effect on the major driving carcinogenic processes in HCC: cell death, metabolism and cell proliferation. For that, the next step for us was to do deep *in cellulo* analysis on 4 human liver cancer cell lines, namely, PLCY/PRF/5, Huh7, Hep3B, and HepG2 cell lines, to address the effect depending on the heterogeneity of tumors harboring unique genetic landscapes and etiologies. Furthermore, the *in cellulo* assays allowed the comparison to the treatment with Sorafenib (a tyrosine kinase inhibitor used in clinics for the treatment of HCC) and ARQ092 (an allosteric pan Akt inhibitor), in order to level the effect to be seen with the designed siRNAs. The conditions that were tested were a single knockdown of Akt1 through D2Akt1 siRNA, a single knockdown of Akt2 by D15Akt2 siRNA and the simultaneous knockdown of Akt1 and Akt2 by the simultaneous exposure of the cells to D2Akt1 and D15Akt2 siRNAs. The introduction of the last condition was to mimic the scenario of the chemical inhibitor which targets both Akt isoforms and to further ascertain any effect seen in the case of the single knockdown. Walking through the results *in cellulo*: no effect was seen neither on cell-death, metabolism, or cell proliferation in any of the tested cell lines and in any of the conditions where the designed siRNAs were used whereas Sorafenib and ARQ092 induced effects. These results were unexpected and puzzling. The most intriguing question was why the double targeting of Akt1 and Akt2 by the specific designed siRNAs did not mimic the scenario with ARQ092. This will be discussed later below.

In an attempt to confirm the results of the designed siRNAs *in cellulo* and to better understand the effect of the single knockdown of Akt1 and Akt2 in a more physiological environment, we moved to a model *in ovo*. The model encompasses a growing embryo on which a tumoral cell line is grafted. And this time, the effect of the single knockdown of Akt1 and Akt2 was tested with HepG2 cell line and MV4-11 cell line. The introduction of the MV4-11 cell line graft model, which is a macrophage carcinoma cell line, was to assess the effect of the knockdown of Akt1 or Akt2 by the designed siRNAs on the TME, a major player in HCC.

The *in ovo* use of the designed siRNAs necessitates a replacement of the transfection agent used *in cellulo* (LipofectamineRNAiMAX). An important issue of RNAi-based therapeutics is the possible dose-limiting toxicity of carriers, related to their heterogeneity in complexity, uniformity and stability, as reviewed recently [176]. There are still major barriers to systemic delivery to target cells. For instance, the plasma membrane remains the major barrier of an RNAi molecules due to its hydrophilic nature, global negative charge and high molecular weight that reduces its uptake efficiency. For that, the designed siRNAs were first vectorized, *in cellulo* on HepG2 cell line, and verified for the knockdown of Akt1 and Akt2, by Amphiphilic Dendrimer (AD). It is a potent vector, which takes into account all of the previously mentioned parameters, through its hybrid trait between the lipid and polymer entities. Thus, rendering it, as its name suggests, amphiphilic, favoring its uptake by the cells. Furthermore, its use for the delivery of siRNAs was validated both *in vitro* on primary immune cells [306] and *in vivo* [308]. Once used *in ovo*, the results did not display cytotoxicity of the complex AD-designed siRNA complex. Thus, further asserting its safe use *in ovo*.

The knockdown of Akt1 or Akt2 did not provoke a significant decrease in the tumor weight in both cell-line models. Despite that, trends of a decrease in the tumor weight were displayed with Akt1 knockdown in the case of HepG2 cells and Akt2 in the case of MV4-11 cells. The dichotomy of the isoforms between the tumor cell line and the macrophage cell line is interesting. It reflects upon the cell-dependent role of Akt isoforms. And it suggests that upon the targeting of one isoform over the other, the cell identity is a factor to be taken into account. In the literature, siRNA targeting of Akt1 or Akt2 or Akt3 in the context of prostate cancer showed prominent antitumorigenic effects [340]. However, the siRNAs used were not validated for their off-target effect. Which raises the question of specificity of the siRNAs? Other studies that target Akt by siRNAs stress on the necessity of knocking down the 3 isoforms of Akt simultaneously to elicit an effect on apoptosis *in vitro* [341]. Or else, knocking down Akt was in the interest of combination therapy, like in the case of breast cancer where knocking down Akt

was for the purpose of sensitizing the cancer cell to chemotherapy, rather than to elicit an antitumorigenic function by itself [342].

However, the absence of a strong antitumorigenic effect in this model can be explained by:

i) the dose of the administered complex of AD-designed siRNA was not sufficient to mount a significant effect.

The doses administered in the *in ovo* model were 0.025 mg/kg and 0.05 mg/kg of the complex of the AD at N/P ratio 5 and siRNA concentration of 50nM. Since no cytotoxicity has been shown throughout the study and in both cell lines, the speculation about the dose administered complex is valid and perhaps upon the increase in the dose administered, the system would be pushed to show a significant antitumorigenic effect.

ii) the knockdown efficiency was not sufficient to decrease the activity of the PI3K/Akt pathway enough to drive the antitumorigenic effect of the system. The knockdown efficiency was demonstrated to be up to a 10-fold decrease at the transcriptomic level and met by a 90% decrease at the protein level upon the use of LipofectamineRNAiMAX and the AD. Supposedly, the efficiency of the knockdown seen in the *in cellulo* context was the same as the one seen in the *in ovo* graft model, the effect is thus, not cell-line dependent (the 4 liver cell lines studied and the macrophage cell line), or physiologically dependent (*in cellulo* and *in ovo*), it is at the molecular level.

Molecular consequences of siRNA-mediated knockdown of Akt1 and Akt2

Following the compiled data of the *in cellulo* and *in ovo* studies, we raised the following question: what is the effect of the decrease in the expression level of Akt1 or Akt2, at the transcriptomic and proteomic level, on the activity of the isoforms and further the PI3K/Akt pathway?

To answer the question, first we assessed the phosphorylation level of the different isoforms after the single or the double knockdown of Akt1 and/or Akt2 by the designed siRNAs. In the case of the single knockdown of Akt1 in HepG2, Huh7, Hep3B and PLCY/PRF/5 cell lines the phosphorylation level of Akt1 decreased up to 73%. And in the case of the knockdown of Akt2, the corresponding phosphorylation of dropped by up to 70%. The compensation of one of the Akt isoforms by the other was only evident in HepG2 cells upon the knockdown of Akt2, where a subsequent increase in the expression of Akt1 was shown at the protein level. Despite that, the level of phosphorylated Akt1 remained unchanged compared to the mock. Of note, the knockdown of Akt1/2 was 90%. In this setting,

it could be established that the remaining 10% of each expressed isoform results in a 30% level of phosphorylation. Moreover, in the case of the simultaneous knockdown of both isoforms, the phosphorylation of both isoforms decreased also by 70%. This signifies no additive effect on the activated Akt of either isoform when compared to the single knockdown conditions. Thus, implying that the cells tend to compensate the loss of the expression by increasing the phosphorylation, and thus the activation, of the remaining Akt isoform.

The most plausible scenario, explaining the observed maintained activity of Akt isoforms, despite the single or double knockdown, is that the cells tend to maintain a basal activated state of the Akt isoforms regardless of the level of their expression.

The effect of the decrease of the phosphorylation was further assessed on the PI3K/Akt pathway, using 2 cell lines (Huh7 and HepG2). The tested targets were divided into two categories: the direct effect and the indirect effect, explicitly explained in the results section. The data demonstrate that the effect of the single knockdown of either of the isoforms or the knockdown of both simultaneously yield a prominent effect on the various downstream effectors of the PI3K/Akt pathway in a cell-dependent and isoform-dependent manner. Thus, conveying that despite the persisting basal activation of the Akt isoforms following the knockdown, the activity of the pathway overall was diminished in an isoform-dependent and cell line-dependent manner.

Consequently, the idea of compensatory mechanisms upon the single knockdown of either of the isoforms spurred, which could explain the absence of an antitumorigenic effect both *in cellulo* and *in ovo*. Moreover, an insight was needed as to why the knockdown and subsequent inhibition of both isoforms by the designed siRNAs did not mimic the effect seen by the chemical pan Akt inhibitor, ARQ092. For that, we set out to get an insight about the overall kinase activity of the different Ser/Thr kinases in Huh7, HepG2, and PLC γ /PRF/5 cells following the knockdown of Akt1 and/or Akt2, in addition to the treatment with the chemical inhibitor ARQ092. The overall kinase activity analysis revealed a Ser/Thr kinase fingerprint for each of the different conditions in each cell line. The study was done in three independent experiments per cell line. The reproducibility of the results was evident within each cell line, however the kinase fingerprint of every condition between the cell lines was different.

Taking into consideration the PLC γ /PRF/5 cell line in the case of the knockdown of Akt1, the predicted activity of the Ser/Thr kinases showed a mix of ones that were activated and others that were inhibited. This could account for the compensatory effect of the single knockdown of Akt1, and the absence of an anti-tumorigenic effect. Explicitly, the predicted decrease in the kinase activity of AurB/Aur1, PKC delta, AuraA/Aur2, PKC alpha and theta, was also met by an increase in the activity of PCTAIRE2, RSKL2, and CDKL5. The kinases that were predicted to show an increase or a decrease in their activity are implicated in the control of cell proliferation. Hence, implying a neutralizing effect by the counter-activation of the mentioned kinases. The Akt2 condition, however, predicted only a decrease in the activity of kinases without an evident increase in any particular kinase. Moreover, the same pattern was obtained in the case of the simultaneous knockdown of both isoforms. Interestingly, the ARQ092 treatment predicted a decrease in the Ser/Thr kinase activity of the same kinases in the case of the simultaneous knockdown of Akt1 and Akt2. Surprisingly, an additional inhibited kinase, CAMK4, was shown in the case of the double knockdown when compared to the ARQ092 condition.

As far as Huh7 is concerned, the single knockdown of Akt1 or Akt2 predicted only a decrease in the Ser/Thr kinase activity. Thus, no suggestive evidence of a compensatory mechanism. Surprisingly, the simultaneous knockdown of both isoforms predicted activated pattern of the Ser/Thr kinases, and so did the ARQ092. However, there were no similarities between any of the activated kinases in the two conditions.

On the other hand, the results with the HepG2 cell line in the case of the single knockdown of Akt1 or Akt2 and the simultaneous knockdown of both, predicted a decrease in the activity of the Ser/Thr kinases with no predicted increase in the activity of any serine/threonine kinase. The pattern of decrease was the same in the three conditions, however the Ser/Thr kinases predicted were different among the three. Similarly, the ARQ092 shows a decrease in a different set of serine/threonine kinases as well when compared to the single or the double knockdown conditions.

Altogether, the overall kinase activity provides large number of parameters which remain to be integrated in precise scenario to become conclusive. On the one hand, the suggestive **compensatory effect** was evident with one cell line (PLC γ /PRF/5) in the Akt1 single knockdown condition.

On the other hand, the drastic difference in the kinase profile between the ARQ092 treatment and the double knockdown suggests a different mode of action of the chemical inhibitors versus that of the siRNAs, which is intriguing. However, the high degree of inter-cell line variability hinders the possibility of having a grand

overview of the mode of action of either. Such a difference in the predicted kinases among the cell lines is justified when taking into consideration the different features of the cell lines: etiology, genetics, grade

The data needs further deep analysis taking into consideration each kinase activity and the action behind it in every condition. Because, as the cellular pathways are complex and intertwining, the inactivation of a given Ser/Thr kinase could further result in the activation of different pathways downstream and *vice versa*. Moreover, the effect seen with this approach is merely on the Ser/Thr kinase family, however the effect of the knockdown by the designed siRNAs and/or the treatment with the chemical inhibitors, could extend into the tyrosine kinase family which, in this case, are not visualized.

X. CONCLUSIONS AND PERSPECTIVES

We have developed a powerful tool for targeting Akt1 and Akt2, specifically, being able to decrease the expression of the different isoforms by up to 90% and their subsequent activity by up to 70%. Furthermore, the knockdown *in cellulo* was shown to downmodulate the activity PI3K/Akt pathway and its cross-talk partners, in an isoform and cell-dependent fashion. However, the specific targeting of Akt1 or Akt2 displayed no antitumorigenic effect, *in cellulo* and displayed trends of antitumorigenic activity *in ovo*. Contradictory to the pan-Akt targeting ARQ092, which displayed a prominent antitumorigenic activity in a cirrhotic rat model, mimicking HCC [162].

The difference between the two strategies of targeting Akt through the two lies in the fact that:

- i) the siRNAs are more specific than the ARQ092.

The consequences seen upon the treatment with the designed siRNAs are due to the **sole action** on one of the Akt isoforms or on both isoforms exclusively. This is a fact proven by the assessment of the predicted off-target activity of the designed siRNAs. However, the effect seen with ARQ092 has not been demonstrated to be exclusive to the Akt pathway. On that note, it has been shown that multiple cancer drug candidates kill tumor cells through off-target effects rather than by interacting with their intended molecular targets. The comparative efficiency of some drugs in wild type cells was shown to be the same as that in cells where the intended target of the drug was deleted by regularly interspaced short palindromic repeats (CRISPR)-Cas9 technology [343]. Thus, suggesting that the cytotoxic effect of the drug is not an “on-target” but rather an “off-target” effect. Which unravels how little is known about the specific mode of action of drugs. The unseen interactions could be the real mechanism by which small-molecule drugs block cancer growth. The difference in the specificity of action between siRNAs and inhibitors could explain their different antitumorigenic effects

- ii) the siRNAs decrease the physical presence of the protein whereas in the case of ARQ092 the protein levels remain intact.

The dynamic property of the cell relies on the most intricate processes from transcription to translation of the designated proteins, up until their ultimate activity. It could be inferred that a change in the amount of a protein in the cell could tip the scale of dynamic activity of the cell in a manner that is different than when the protein is solely inactivated. The scenario with the designed siRNA approach disrupts the transcriptional activity dynamic leading to a less protein expression. However, in the case of the ARQ092 treatment, the transcriptional and translational dynamic remains intact, and the effect is seen only at the level of the

activity. Which could be a playing factor in the different phenotypic and molecular consequences seen between the two approaches.

- iii) the degree of the inactivation of Akt in the case of ARQ092 is up to 100% [162], whereas the remaining 10% of Akt protein support 30% of activity.

The use of the chemical inhibitor ARQ092 ensures a total inactivation of the Akt isoforms, which is not the case with the designed siRNAs. The kinase activity serves a role in the overall dynamic of the cell. Therefore, the consequence of a total inactivation of the pathway would not be the same as in the case where there is a remaining basal activity. In our case, and upon the use of the designed siRNAs for single or double targeting of the Akt isoforms, a 30% of basal Akt activity remains evident. This could explain the fact that the system was not inhibited enough to display the antitumorigenic activity attained with the chemical inhibitor.

Given the compiled results obtained in our study, further studies remain to be done to reach the full understanding of the designed siRNAs' activity *vs* that of the inhibitor and the preferential roles of Akt1 and Akt2 in HCC carcinogenesis. First, a deep analysis of the data given by the Pamgene and the predicted state of the Ser/Thr kinases is to be done to ascertain in detail the consequences of the predicted activation/inactivation of each kinase in every condition. Furthermore, the integration of these data with that of the consequences seen on the PI3K/Akt pathway will be valuable in order to validate the predictions.

Second, to assess the effect of the specific complete inactivation of the Akt isoforms, the Crisper-Cas9 technology would permit the complete deletion of the different Akt isoforms from the cell. However, such an approach still modulates the dynamic of the cell. For that, another approach would be the directed mutagenesis toward the Ser473 and Ser474 in the Akt1 and Akt2 isoforms, respectively, which could better mimic the chemical inhibitor scenario, by displaying a total inactivation of the isoforms without affecting the translational machinery of the cell and thus its dynamics. Such an approach would also ascertain the specific effect of the designed siRNAs versus the pleotropic effect of chemical inhibitor.

Third, the combination of different treatment strategies could be beneficial in terms of HCC treatment. This has already been established in the case with the combination of ARQ092 (Akt chemical inhibitor) and Sorafenib (a clinical treatment option for HCC) [163], and more interestingly, the combination of the RNAi strategy with immune checkpoint inhibitors [344] the combination therapy would take advantage of the specificity of the RNAi therapy to tweak the

expression of a specific protein, which is needed to boost the activity of its partner treatment.

Finally, despite the lack of the designed siRNAs' ability to elicit an antitumorigenic effect in the context of HCC, they keep their potency as tools to modulate the expression of Akt1 and Akt2 isoforms. Thus, it is empirical to assess their use in other fields where the effect of solely targeting Akt could be more pronounced. The tumor itself is not the sole player in the carcinogenesis of HCC. The TME plays a crucial role in the early stages of HCC as well as its continuous thriving [6]. For that, it is crucial that we assess the effect of the designed siRNAs and the fine tuning of the Akt isoforms on effectors of the TME, specifically immune cells. As demonstrated in the introduction the Akt isoforms display their dichotomy in regulating the different roles of the different immune cells. Thus, modulating the activity of the different Akt isoforms, without the need of their complete inactivation, and taking into advantage their ability to compensate each other in these cells, could tip the scale towards an anti-tumorigenic TME rather than a pro-tumorigenic TME.

The show must go on...

XI. REFERENCES

1. Chidambaranathan-Reghupaty, S., P.B. Fisher, and D. Sarkar, *Hepatocellular carcinoma (HCC): Epidemiology, etiology and molecular classification*. Adv Cancer Res, 2021. 149: p. 1-61.
2. Fitzmaurice, C., et al., *Global, Regional, and National Cancer Incidence, Mortality, Years of Life Lost, Years Lived With Disability, and Disability-Adjusted Life-Years for 29 Cancer Groups, 1990 to 2017: A Systematic Analysis for the Global Burden of Disease Study*. JAMA Oncol, 2019. 5(12): p. 1749-1768.
3. Kulik, L. and H.B. El-Serag, *Epidemiology and Management of Hepatocellular Carcinoma*. Gastroenterology, 2019. 156(2): p. 477-491 e1.
4. Bray, F., et al., *Global cancer statistics 2018: GLOBOCAN estimates of incidence and mortality worldwide for 36 cancers in 185 countries*. CA Cancer J Clin, 2018. 68(6): p. 394-424.
5. Yang, J.D., et al., *A global view of hepatocellular carcinoma: trends, risk, prevention and management*. Nat Rev Gastroenterol Hepatol, 2019. 16(10): p. 589-604.
6. Ogunwobi, O.O., et al., *Mechanisms of hepatocellular carcinoma progression*. World J Gastroenterol, 2019. 25(19): p. 2279-2293.
7. Villanueva, A. and T. Luedde, *The transition from inflammation to cancer in the liver*. Clin Liver Dis (Hoboken), 2016. 8(4): p. 89-93.
8. Liang, T.J., *Hepatitis B: the virus and disease*. Hepatology, 2009. 49(5 Suppl): p. S13-21.
9. Tu, T., et al., *HBV DNA Integration: Molecular Mechanisms and Clinical Implications*. Viruses, 2017. 9(4).
10. Cheng, A.S., et al., *COX-2 mediates hepatitis B virus X protein abrogation of p53-induced apoptosis*. Biochem Biophys Res Commun, 2008. 374(2): p. 175-80.
11. Lee, Y.I., S. Kang-Park, and S.I. Do, *The hepatitis B virus-X protein activates a phosphatidylinositol 3-kinase-dependent survival signaling cascade*. J Biol Chem, 2001. 276(20): p. 16969-77.
12. Kuo, T.C. and C.C. Chao, *Hepatitis B virus X protein prevents apoptosis of hepatocellular carcinoma cells by upregulating SATB1 and HURP expression*. Biochem Pharmacol, 2010. 80(7): p. 1093-102.
13. Shen, L., et al., *Hepatitis B virus X (HBx) play an anti-apoptosis role in hepatic progenitor cells by activating Wnt/beta-catenin pathway*. Mol Cell Biochem, 2013. 383(1-2): p. 213-22.
14. Hyams, K.C., *Risks of chronicity following acute hepatitis B virus infection: a review*. Clin Infect Dis, 1995. 20(4): p. 992-1000.
15. Lumley, S.F., et al., *Hepatitis B Virus Adaptation to the CD8+ T Cell Response: Consequences for Host and Pathogen*. Front Immunol, 2018. 9: p. 1561.

16. Kanwal, F., et al., *HCV genotype 3 is associated with an increased risk of cirrhosis and hepatocellular cancer in a national sample of U.S. Veterans with HCV*. *Hepatology*, 2014. 60(1): p. 98-105.
17. Mattos, A.A., et al., *Hepatocellular Carcinoma in a Non-Cirrhotic Patient with Sustained Virological Response after Hepatitis C Treatment*. *Rev Inst Med Trop Sao Paulo*, 2015. 57(6): p. 519-22.
18. Janjua, N.Z., et al., *Long-term effect of sustained virological response on hepatocellular carcinoma in patients with hepatitis C in Canada*. *J Hepatol*, 2017. 66(3): p. 504-513.
19. Kim, H., et al., *Hepatitis C virus suppresses C9 complement synthesis and impairs membrane attack complex function*. *J Virol*, 2013. 87(10): p. 5858-67.
20. Kramer, J.R., et al., *The effect of HIV viral control on the incidence of hepatocellular carcinoma in veterans with hepatitis C and HIV coinfection*. *J Acquir Immune Defic Syndr*, 2015. 68(4): p. 456-62.
21. Levy, P.L., et al., *Hepatitis C virus infection triggers a tumor-like glutamine metabolism*. *Hepatology*, 2017. 65(3): p. 789-803.
22. Syed, G.H., Y. Amako, and A. Siddiqui, *Hepatitis C virus hijacks host lipid metabolism*. *Trends Endocrinol Metab*, 2010. 21(1): p. 33-40.
23. Takaki, A. and K. Yamamoto, *Control of oxidative stress in hepatocellular carcinoma: Helpful or harmful?* *World J Hepatol*, 2015. 7(7): p. 968-79.
24. Takaki, A., et al., *Cellular immune responses persist and humoral responses decrease two decades after recovery from a single-source outbreak of hepatitis C*. *Nat Med*, 2000. 6(5): p. 578-82.
25. Koike, K., *Hepatitis C virus contributes to hepatocarcinogenesis by modulating metabolic and intracellular signaling pathways*. *J Gastroenterol Hepatol*, 2007. 22 Suppl 1: p. S108-11.
26. Korenaga, M., et al., *Hepatitis C virus core protein inhibits mitochondrial electron transport and increases reactive oxygen species (ROS) production*. *J Biol Chem*, 2005. 280(45): p. 37481-8.
27. Machida, K., et al., *Hepatitis C virus triggers mitochondrial permeability transition with production of reactive oxygen species, leading to DNA damage and STAT3 activation*. *J Virol*, 2006. 80(14): p. 7199-207.
28. Kanda, T., et al., *Molecular Mechanisms Driving Progression of Liver Cirrhosis towards Hepatocellular Carcinoma in Chronic Hepatitis B and C Infections: A Review*. *Int J Mol Sci*, 2019. 20(6).
29. Ganne-Carrie, N. and P. Nahon, *Hepatocellular carcinoma in the setting of alcohol-related liver disease*. *J Hepatol*, 2019. 70(2): p. 284-293.
30. Gao, B. and R. Bataller, *Alcoholic liver disease: pathogenesis and new therapeutic targets*. *Gastroenterology*, 2011. 141(5): p. 1572-85.

31. Schuppan, D., et al., *Liver fibrosis: Direct antifibrotic agents and targeted therapies*. Matrix Biol, 2018. 68-69: p. 435-451.
32. Szabo, G. and S. Bala, *Alcoholic liver disease and the gut-liver axis*. World J Gastroenterol, 2010. 16(11): p. 1321-9.
33. Maurice, J. and P. Manousou, *Non-alcoholic fatty liver disease*. Clin Med (Lond), 2018. 18(3): p. 245-250.
34. Pierantonelli, I. and G. Svegliati-Baroni, *Nonalcoholic Fatty Liver Disease: Basic Pathogenetic Mechanisms in the Progression From NAFLD to NASH*. Transplantation, 2019. 103(1): p. e1-e13.
35. Buzzetti, E., M. Pinzani, and E.A. Tsochatzis, *The multiple-hit pathogenesis of non-alcoholic fatty liver disease (NAFLD)*. Metabolism, 2016. 65(8): p. 1038-48.
36. Kumar, P., et al., *Aflatoxins: A Global Concern for Food Safety, Human Health and Their Management*. Front Microbiol, 2016. 7: p. 2170.
37. Turkez, H. and T. Sisman, *The genoprotective activity of resveratrol on aflatoxin B(1)-induced DNA damage in human lymphocytes in vitro*. Toxicol Ind Health, 2012. 28(5): p. 474-80.
38. Peng, X.M., W.W. Peng, and J.L. Yao, *Codon 249 mutations of p53 gene in development of hepatocellular carcinoma*. World J Gastroenterol, 1998. 4(2): p. 125-127.
39. Stockley, R.A., *The multiple facets of alpha-1-antitrypsin*. Ann Transl Med, 2015. 3(10): p. 130.
40. Perlmutter, D.H., *Pathogenesis of chronic liver injury and hepatocellular carcinoma in alpha-1-antitrypsin deficiency*. Pediatr Res, 2006. 60(2): p. 233-8.
41. Liberal, R., et al., *Pathogenesis of autoimmune hepatitis*. Best Pract Res Clin Gastroenterol, 2011. 25(6): p. 653-64.
42. !!! INVALID CITATION !!!
43. Radford-Smith, D.E., E.E. Powell, and L.W. Powell, *Haemochromatosis: a clinical update for the practising physician*. Intern Med J, 2018. 48(5): p. 509-516.
44. Kew, M.C., *Hepatic iron overload and hepatocellular carcinoma*. Liver Cancer, 2014. 3(1): p. 31-40.
45. ElMBERG, M., et al., *Cancer risk in patients with hereditary hemochromatosis and in their first-degree relatives*. Gastroenterology, 2003. 125(6): p. 1733-41.
46. Derks, T.G. and M. van Rijn, *Lipids in hepatic glycogen storage diseases: pathophysiology, monitoring of dietary management and future directions*. J Inherit Metab Dis, 2015. 38(3): p. 537-43.
47. Jang, H.J., et al., *Development of Hepatocellular Carcinoma in Patients with Glycogen Storage Disease: a Single Center Retrospective Study*. J Korean Med Sci, 2020. 35(1): p. e5.

48. Ramanujam, V.S. and K.E. Anderson, *Porphyria Diagnostics-Part 1: A Brief Overview of the Porphyrias*. *Curr Protoc Hum Genet*, 2015. 86: p. 17 20 1-17 20 26.
49. Lang, E., et al., *Occurrence of Malignant Tumours in the Acute Hepatic Porphyrias*. *JIMD Rep*, 2015. 22: p. 17-22.
50. Bergeron, A., et al., *Structural and functional analysis of missense mutations in fumarylacetoacetate hydrolase, the gene deficient in hereditary tyrosinemia type 1*. *J Biol Chem*, 2001. 276(18): p. 15225-31.
51. Tanguay, R.M., F. Angileri, and A. Vogel, *Molecular Pathogenesis of Liver Injury in Hereditary Tyrosinemia 1*. *Adv Exp Med Biol*, 2017. 959: p. 49-64.
52. Kim, E. and P. Viatour, *Hepatocellular carcinoma: old friends and new tricks*. *Exp Mol Med*, 2020. 52(12): p. 1898-1907.
53. Macek-Jilkova, Z., et al., *Clinical and Experimental Evaluation of Diagnostic Significance of Alpha-Fetoprotein and Osteopontin at the Early Stage of Hepatocellular Cancer*. *Bull Exp Biol Med*, 2021. 170(3): p. 340-344.
54. Llovet, J.M., et al., *Sorafenib in advanced hepatocellular carcinoma*. *N Engl J Med*, 2008. 359(4): p. 378-90.
55. Fan, G., X. Wei, and X. Xu, *Is the era of sorafenib over? A review of the literature*. *Ther Adv Med Oncol*, 2020. 12: p. 1758835920927602.
56. Faivre, S., L. Rimassa, and R.S. Finn, *Molecular therapies for HCC: Looking outside the box*. *J Hepatol*, 2020. 72(2): p. 342-352.
57. Finn, R.S., et al., *Atezolizumab plus Bevacizumab in Unresectable Hepatocellular Carcinoma*. *N Engl J Med*, 2020. 382(20): p. 1894-1905.
58. Macek Jilkova, Z., C. Aspod, and T. Decaens, *Predictive Factors for Response to PD-1/PD-L1 Checkpoint Inhibition in the Field of Hepatocellular Carcinoma: Current Status and Challenges*. *Cancers (Basel)*, 2019. 11(10).
59. Cheng, A.L., et al., *Efficacy and safety of sorafenib in patients in the Asia-Pacific region with advanced hepatocellular carcinoma: a phase III randomised, double-blind, placebo-controlled trial*. *Lancet Oncol*, 2009. 10(1): p. 25-34.
60. Wilhelm, S.M., et al., *Preclinical overview of sorafenib, a multikinase inhibitor that targets both Raf and VEGF and PDGF receptor tyrosine kinase signaling*. *Mol Cancer Ther*, 2008. 7(10): p. 3129-40.
61. Zhai, B. and X.Y. Sun, *Mechanisms of resistance to sorafenib and the corresponding strategies in hepatocellular carcinoma*. *World J Hepatol*, 2013. 5(7): p. 345-52.
62. Kudo, M., *Extremely High Objective Response Rate of Lenvatinib: Its Clinical Relevance and Changing the Treatment Paradigm in Hepatocellular Carcinoma*. *Liver Cancer*, 2018. 7(3): p. 215-224.

63. Bruix, J., et al., *Regorafenib for patients with hepatocellular carcinoma who progressed on sorafenib treatment (RESORCE): a randomised, double-blind, placebo-controlled, phase 3 trial*. *Lancet*, 2017. 389(10064): p. 56-66.
64. Finn, R.S., et al., *Outcomes of sequential treatment with sorafenib followed by regorafenib for HCC: Additional analyses from the phase III RESORCE trial*. *J Hepatol*, 2018. 69(2): p. 353-358.
65. Abou-Alfa, G.K., et al., *Cabozantinib in Patients with Advanced and Progressing Hepatocellular Carcinoma*. *N Engl J Med*, 2018. 379(1): p. 54-63.
66. Kudo, M., *Cabozantinib as a Second-Line Agent in Advanced Hepatocellular Carcinoma*. *Liver Cancer*, 2018. 7(2): p. 123-133.
67. Yau, T., et al., *Efficacy and Safety of Nivolumab Plus Ipilimumab in Patients With Advanced Hepatocellular Carcinoma Previously Treated With Sorafenib: The CheckMate 040 Randomized Clinical Trial*. *JAMA Oncol*, 2020. 6(11): p. e204564.
68. Zhu, A.X., et al., *Pembrolizumab in patients with advanced hepatocellular carcinoma previously treated with sorafenib (KEYNOTE-224): a non-randomised, open-label phase 2 trial*. *Lancet Oncol*, 2018. 19(7): p. 940-952.
69. Zhu, A.X., et al., *Ramucirumab versus placebo as second-line treatment in patients with advanced hepatocellular carcinoma following first-line therapy with sorafenib (REACH): a randomised, double-blind, multicentre, phase 3 trial*. *Lancet Oncol*, 2015. 16(7): p. 859-70.
70. Mroweh, M., et al., *Targeting Akt in Hepatocellular Carcinoma and Its Tumor Microenvironment*. *Int J Mol Sci*, 2021. 22(4).
71. Mroweh, M., et al., *Modulating the Crosstalk between the Tumor and Its Microenvironment Using RNA Interference: A Treatment Strategy for Hepatocellular Carcinoma*. *Int J Mol Sci*, 2020. 21(15).
72. Nault, J.C. and J. Zucman-Rossi, *Genetics of hepatocellular carcinoma: the next generation*. *J Hepatol*, 2014. 60(1): p. 224-6.
73. Gollob, J.A., et al., *Role of Raf kinase in cancer: therapeutic potential of targeting the Raf/MEK/ERK signal transduction pathway*. *Semin Oncol*, 2006. 33(4): p. 392-406.
74. Newell, P., et al., *Ras pathway activation in hepatocellular carcinoma and anti-tumoral effect of combined sorafenib and rapamycin in vivo*. *J Hepatol*, 2009. 51(4): p. 725-33.
75. Bouattour, M., et al., *Recent developments of c-Met as a therapeutic target in hepatocellular carcinoma*. *Hepatology*, 2018. 67(3): p. 1132-1149.
76. Dimri, M. and A. Satyanarayana, *Molecular Signaling Pathways and Therapeutic Targets in Hepatocellular Carcinoma*. *Cancers (Basel)*, 2020. 12(2).
77. Gonzalez, M.N., et al., *HGF potentiates extracellular matrix-driven migration of human myoblasts: involvement of matrix metalloproteinases and MAPK/ERK pathway*. *Skelet Muscle*, 2017. 7(1): p. 20.

78. Pascale, R.M., F. Feo, and D.F. Calvisi, *An infernal cross-talk between oncogenic beta-catenin and c-Met in hepatocellular carcinoma: Evidence from mouse modeling*. *Hepatology*, 2016. 64(5): p. 1421-1423.
79. Garajova, I., et al., *c-Met as a Target for Personalized Therapy*. *Transl Oncogenomics*, 2015. 7(Suppl 1): p. 13-31.
80. Garcia-Lezana, T., J.L. Lopez-Canovas, and A. Villanueva, *Signaling pathways in hepatocellular carcinoma*. *Adv Cancer Res*, 2021. 149: p. 63-101.
81. Zhang, L., et al., *VEGF is essential for the growth and migration of human hepatocellular carcinoma cells*. *Mol Biol Rep*, 2012. 39(5): p. 5085-93.
82. Chiang, D.Y., et al., *Focal gains of VEGFA and molecular classification of hepatocellular carcinoma*. *Cancer Res*, 2008. 68(16): p. 6779-88.
83. Morse, M.A., et al., *The Role of Angiogenesis in Hepatocellular Carcinoma*. *Clin Cancer Res*, 2019. 25(3): p. 912-920.
84. Zheng, N., W. Wei, and Z. Wang, *Emerging roles of FGF signaling in hepatocellular carcinoma*. *Transl Cancer Res*, 2016. 5(1): p. 1-6.
85. Harimoto, N., et al., *The significance of fibroblast growth factor receptor 2 expression in differentiation of hepatocellular carcinoma*. *Oncology*, 2010. 78(5-6): p. 361-8.
86. Chen, J., J.A. Gingold, and X. Su, *Immunomodulatory TGF-beta Signaling in Hepatocellular Carcinoma*. *Trends Mol Med*, 2019. 25(11): p. 1010-1023.
87. Wang, H., et al., *Distinct functions of transforming growth factor-beta signaling in c-MYC driven hepatocellular carcinoma initiation and progression*. *Cell Death Dis*, 2021. 12(2): p. 200.
88. Chen, J., et al., *Analysis of Genomes and Transcriptomes of Hepatocellular Carcinomas Identifies Mutations and Gene Expression Changes in the Transforming Growth Factor-beta Pathway*. *Gastroenterology*, 2018. 154(1): p. 195-210.
89. Komposch, K. and M. Sibilica, *EGFR Signaling in Liver Diseases*. *Int J Mol Sci*, 2015. 17(1).
90. Liu, Z., et al., *EGF is highly expressed in hepatocellular carcinoma (HCC) and promotes motility of HCC cells via fibronectin*. *J Cell Biochem*, 2018. 119(5): p. 4170-4183.
91. Huang, P., et al., *The role of EGF-EGFR signalling pathway in hepatocellular carcinoma inflammatory microenvironment*. *J Cell Mol Med*, 2014. 18(2): p. 218-30.
92. Kasprzak, A., et al., *Insulin-like growth factor (IGF) axis in cancerogenesis*. *Mutat Res Rev Mutat Res*, 2017. 772: p. 78-104.
93. Martinez-Quetglas, I., et al., *IGF2 Is Up-regulated by Epigenetic Mechanisms in Hepatocellular Carcinomas and Is an Actionable Oncogene Product in Experimental Models*. *Gastroenterology*, 2016. 151(6): p. 1192-1205.
94. Levy, D.E. and J.E. Darnell, Jr., *Stats: transcriptional control and biological impact*. *Nat Rev Mol Cell Biol*, 2002. 3(9): p. 651-62.

95. Calvisi, D.F., et al., *Ubiquitous activation of Ras and Jak/Stat pathways in human HCC*. *Gastroenterology*, 2006. 130(4): p. 1117-28.
96. Martinez-Chantar, M.L., et al., *Loss of the glycine N-methyltransferase gene leads to steatosis and hepatocellular carcinoma in mice*. *Hepatology*, 2008. 47(4): p. 1191-9.
97. Parikh, N., et al., *Effects of TP53 mutational status on gene expression patterns across 10 human cancer types*. *J Pathol*, 2014. 232(5): p. 522-33.
98. Kancherla, V., et al., *Genomic Analysis Revealed New Oncogenic Signatures in TP53-Mutant Hepatocellular Carcinoma*. *Front Genet*, 2018. 9: p. 2.
99. He, S. and S. Tang, *WNT/beta-catenin signaling in the development of liver cancers*. *Biomed Pharmacother*, 2020. 132: p. 110851.
100. Khalaf, A.M., et al., *Role of Wnt/beta-catenin signaling in hepatocellular carcinoma, pathogenesis, and clinical significance*. *J Hepatocell Carcinoma*, 2018. 5: p. 61-73.
101. Satoh, S., et al., *AXIN1 mutations in hepatocellular carcinomas, and growth suppression in cancer cells by virus-mediated transfer of AXIN1*. *Nat Genet*, 2000. 24(3): p. 245-50.
102. Wang, Q., X. Chen, and N. Hay, *Akt as a target for cancer therapy: more is not always better (lessons from studies in mice)*. *Br J Cancer*, 2017. 117(2): p. 159-163.
103. Ferrín, G., et al., *Activation of mTOR Signaling Pathway in Hepatocellular Carcinoma*. *Int J Mol Sci*, 2020. 21(4).
104. Son, M.K., et al., *HS-173, a Novel PI3K Inhibitor, Attenuates the Activation of Hepatic Stellate Cells in Liver Fibrosis*. *Scientific Reports*, 2013. 3(1): p. 3470.
105. Cai, C.X., et al., *Activation of Insulin-PI3K/Akt-p70S6K Pathway in Hepatic Stellate Cells Contributes to Fibrosis in Nonalcoholic Steatohepatitis*. *Dig Dis Sci*, 2017. 62(4): p. 968-978.
106. Schmitz, K.J., et al., *Activation of the ERK and AKT signalling pathway predicts poor prognosis in hepatocellular carcinoma and ERK activation in cancer tissue is associated with hepatitis C virus infection*. *J Hepatol*, 2008. 48(1): p. 83-90.
107. Zhang, Y., et al., *Identification of AKT kinases as unfavorable prognostic factors for hepatocellular carcinoma by a combination of expression profile, interaction network analysis and clinical validation*. *Mol Biosyst*, 2014. 10(2): p. 215-22.
108. Bellacosa, A., et al., *A retroviral oncogene, akt, encoding a serine-threonine kinase containing an SH2-like region*. *Science*, 1991. 254(5029): p. 274-7.
109. Martelli, A.M., et al., *The emerging multiple roles of nuclear Akt*. *Biochim Biophys Acta*, 2012. 1823(12): p. 2168-78.
110. Chan, T.O., S.E. Rittenhouse, and P.N. Tsichlis, *AKT/PKB and other D3 phosphoinositide-regulated kinases: kinase activation by phosphoinositide-dependent phosphorylation*. *Annu Rev Biochem*, 1999. 68: p. 965-1014.

111. Nitulescu, G.M., et al., *Akt inhibitors in cancer treatment: The long journey from drug discovery to clinical use (Review)*. *Int J Oncol*, 2016. 48(3): p. 869-85.
112. Chen, R., et al., *Regulation of Akt/PKB activation by tyrosine phosphorylation*. *J Biol Chem*, 2001. 276(34): p. 31858-62.
113. Hanada, M., J. Feng, and B.A. Hemmings, *Structure, regulation and function of PKB/AKT--a major therapeutic target*. *Biochim Biophys Acta*, 2004. 1697(1-2): p. 3-16.
114. Garcia-Echeverria, C. and W.R. Sellers, *Drug discovery approaches targeting the PI3K/Akt pathway in cancer*. *Oncogene*, 2008. 27(41): p. 5511-26.
115. Xu, Z., et al., *The mTORC2-Akt1 Cascade Is Crucial for c-Myc to Promote Hepatocarcinogenesis in Mice and Humans*. *Hepatology*, 2019. 70(5): p. 1600-1613.
116. Zhao, J.X., et al., *Aldose reductase interacts with AKT1 to augment hepatic AKT/mTOR signaling and promote hepatocarcinogenesis*. *Oncotarget*, 2017. 8(40): p. 66987-67000.
117. Dai, F., et al., *Extracellular polyamines-induced proliferation and migration of cancer cells by ODC, SSAT, and Akt1-mediated pathway*. *Anticancer Drugs*, 2017. 28(4): p. 457-464.
118. Delogu, S., et al., *SKP2 cooperates with N-Ras or AKT to induce liver tumor development in mice*. *Oncotarget*, 2015. 6(4): p. 2222-34.
119. Zhu, L., et al., *Real-time imaging nuclear translocation of Akt1 in HCC cells*. *Biochem Biophys Res Commun*, 2007. 356(4): p. 1038-43.
120. Wang, X.H., et al., *Wnt/ β -catenin signaling regulates MAPK and Akt1 expression and growth of hepatocellular carcinoma cells*. *Neoplasia*, 2011. 58(3): p. 239-44.
121. Xu, X., et al., *Akt2 expression correlates with prognosis of human hepatocellular carcinoma*. *Oncol Rep*, 2004. 11(1): p. 25-32.
122. Xie, Y., J. Li, and C. Zhang, *STAT3 promotes the proliferation and migration of hepatocellular carcinoma cells by regulating AKT2*. *Oncol Lett*, 2018. 15(3): p. 3333-3338.
123. Wang, C., et al., *Activated mutant forms of PIK3CA cooperate with RasV12 or c-Met to induce liver tumour formation in mice via AKT2/mTORC1 cascade*. *Liver Int*, 2016. 36(8): p. 1176-86.
124. Chew, T.W., et al., *Crosstalk of Ras and Rho: activation of RhoA abates Kras-induced liver tumorigenesis in transgenic zebrafish models*. *Oncogene*, 2014. 33(21): p. 2717-27.
125. Zhang, Y., et al., *miR-582-5p inhibits proliferation of hepatocellular carcinoma by targeting CDK1 and AKT3*. *Tumour Biol*, 2015. 36(11): p. 8309-16.
126. Ma, Y., et al., *MicroRNA-144 suppresses tumorigenesis of hepatocellular carcinoma by targeting AKT3*. *Mol Med Rep*, 2015. 11(2): p. 1378-83.
127. Okkenhaug, K., M. Graupera, and B. Vanhaesebroeck, *Targeting PI3K in Cancer: Impact on Tumor Cells, Their Protective Stroma, Angiogenesis, and Immunotherapy*. *Cancer Discov*, 2016. 6(10): p. 1090-1105.

128. Kumar, B.V., T.J. Connors, and D.L. Farber, *Human T Cell Development, Localization, and Function throughout Life*. Immunity, 2018. 48(2): p. 202-213.
129. Kouidhi, S., A.B. Elgaaied, and S. Chouaib, *Impact of Metabolism on T-Cell Differentiation and Function and Cross Talk with Tumor Microenvironment*. Front Immunol, 2017. 8: p. 270.
130. Waickman, A.T. and J.D. Powell, *mTOR, metabolism, and the regulation of T-cell differentiation and function*. Immunol Rev, 2012. 249(1): p. 43-58.
131. Pollizzi, K.N., et al., *Asymmetric inheritance of mTORC1 kinase activity during division dictates CD8(+) T cell differentiation*. Nat Immunol, 2016. 17(6): p. 704-11.
132. Powell, J.D., C.G. Lerner, and R.H. Schwartz, *Inhibition of cell cycle progression by rapamycin induces T cell clonal anergy even in the presence of costimulation*. J Immunol, 1999. 162(5): p. 2775-84.
133. Delgoffe, G.M., et al., *The kinase mTOR regulates the differentiation of helper T cells through the selective activation of signaling by mTORC1 and mTORC2*. Nat Immunol, 2011. 12(4): p. 295-303.
134. Chi, H., *Regulation and function of mTOR signalling in T cell fate decisions*. Nat Rev Immunol, 2012. 12(5): p. 325-38.
135. Parry, R.V., et al., *CTLA-4 and PD-1 receptors inhibit T-cell activation by distinct mechanisms*. Mol Cell Biol, 2005. 25(21): p. 9543-53.
136. Sinclair, L.V., et al., *Phosphatidylinositol-3-OH kinase and nutrient-sensing mTOR pathways control T lymphocyte trafficking*. Nat Immunol, 2008. 9(5): p. 513-21.
137. Ouyang, S., et al., *Akt-1 and Akt-2 Differentially Regulate the Development of Experimental Autoimmune Encephalomyelitis by Controlling Proliferation of Thymus-Derived Regulatory T Cells*. J Immunol, 2019. 202(5): p. 1441-1452.
138. DuBois, J.C., et al., *Akt3-Mediated Protection Against Inflammatory Demyelinating Disease*. Front Immunol, 2019. 10: p. 1738.
139. Beutler, B., *Innate immunity: an overview*. Mol Immunol, 2004. 40(12): p. 845-59.
140. DeNardo, D.G. and B. Ruffell, *Macrophages as regulators of tumour immunity and immunotherapy*. Nat Rev Immunol, 2019. 19(6): p. 369-382.
141. Vergadi, E., et al., *Akt Signaling Pathway in Macrophage Activation and M1/M2 Polarization*. J Immunol, 2017. 198(3): p. 1006-1014.
142. Weichhart, T. and M.D. Saemann, *The PI3K/Akt/mTOR pathway in innate immune cells: emerging therapeutic applications*. Ann Rheum Dis, 2008. 67 Suppl 3: p. iii70-4.
143. Martin, M., et al., *Role of the phosphatidylinositol 3 kinase-Akt pathway in the regulation of IL-10 and IL-12 by Porphyromonas gingivalis lipopolysaccharide*. J Immunol, 2003. 171(2): p. 717-25.

144. Rocher, C. and D.K. Singla, *SMAD-PI3K-Akt-mTOR pathway mediates BMP-7 polarization of monocytes into M2 macrophages*. PLoS One, 2013. 8(12): p. e84009.
145. Rauh, M.J., et al., *SHIP represses the generation of alternatively activated macrophages*. Immunity, 2005. 23(4): p. 361-74.
146. Araki, K., A.H. Ellebedy, and R. Ahmed, *TOR in the immune system*. Curr Opin Cell Biol, 2011. 23(6): p. 707-15.
147. Mercalli, A., et al., *Rapamycin unbalances the polarization of human macrophages to M1*. Immunology, 2013. 140(2): p. 179-90.
148. Jiang, Z., et al., *CD14 is required for MyD88-independent LPS signaling*. Nat Immunol, 2005. 6(6): p. 565-70.
149. Strassheim, D., et al., *Phosphoinositide 3-kinase and Akt occupy central roles in inflammatory responses of Toll-like receptor 2-stimulated neutrophils*. J Immunol, 2004. 172(9): p. 5727-33.
150. Schaeffer, V., et al., *Role of the mTOR pathway in LPS-activated monocytes: influence of hypertonic saline*. J Surg Res, 2011. 171(2): p. 769-76.
151. Arranz, A., et al., *Akt1 and Akt2 protein kinases differentially contribute to macrophage polarization*. Proc Natl Acad Sci U S A, 2012. 109(24): p. 9517-22.
152. Zhou, S.-L., et al., *Tumor-Associated Neutrophils Recruit Macrophages and T-Regulatory Cells to Promote Progression of Hepatocellular Carcinoma and Resistance to Sorafenib*. Gastroenterology, 2016. 150(7): p. 1646-1658.e17.
153. Chen, J., et al., *Akt isoforms differentially regulate neutrophil functions*. Blood, 2010. 115(21): p. 4237-4246.
154. Chen, Y., et al., *Infiltrating mast cells promote renal cell carcinoma angiogenesis by modulating PI3K→AKT→GSK3β→AM signaling*. Oncogene, 2017. 36(20): p. 2879-2888.
155. Brown, J.S. and U. Banerji, *Maximising the potential of AKT inhibitors as anti-cancer treatments*. Pharmacology & Therapeutics, 2017. 172: p. 101-115.
156. Landel, I., et al., *Spotlight on AKT: Current Therapeutic Challenges*. ACS Medicinal Chemistry Letters, 2020. 11(3): p. 225-227.
157. Lin, J., et al., *Targeting Activated Akt with GDC-0068, a Novel Selective Akt Inhibitor That Is Efficacious in Multiple Tumor Models*. Clinical Cancer Research, 2013. 19(7): p. 1760-1772.
158. Zhai, B., et al., *Inhibition of Akt reverses the acquired resistance to sorafenib by switching protective autophagy to autophagic cell death in hepatocellular carcinoma*. Mol Cancer Ther, 2014. 13(6): p. 1589-98.
159. Doi, T., et al., *Phase I study of ipatasertib as a single agent and in combination with abiraterone plus prednisolone in Japanese patients with advanced solid tumors*. Cancer Chemotherapy and Pharmacology, 2019. 84(2): p. 393-404.

160. Zhang, Y., et al., *A novel AKT inhibitor, AZD5363, inhibits phosphorylation of AKT downstream molecules, and activates phosphorylation of mTOR and SMG-1 dependent on the liver cancer cell type*. *Oncology Letters*, 2016. 11(3): p. 1685-1692.
161. Dean, E., et al., *A Phase 1, open-label, multicentre study to compare the capsule and tablet formulations of AZD5363 and explore the effect of food on the pharmacokinetic exposure, safety and tolerability of AZD5363 in patients with advanced solid malignancies: OAK*. *Cancer Chemotherapy and Pharmacology*, 2018. 81(5): p. 873-883.
162. Roth, G.S., et al., *Efficacy of AKT Inhibitor ARQ 092 Compared with Sorafenib in a Cirrhotic Rat Model with Hepatocellular Carcinoma*. *Mol Cancer Ther*, 2017. 16(10): p. 2157-2165.
163. Jilkova, Z.M., et al., *Combination of AKT inhibitor ARQ 092 and sorafenib potentiates inhibition of tumor progression in cirrhotic rat model of hepatocellular carcinoma*. *Oncotarget*, 2018. 9(13): p. 11145-11158.
164. Kurma, K., et al., *Effect of novel AKT inhibitor ARQ 751 as single agent and its combination with sorafenib on hepatocellular carcinoma in a cirrhotic rat model*. *Journal of Hepatology* 2017. 66(1): p. S459-S460.
165. Wilson, J.M., et al., *MK2206 inhibits hepatocellular carcinoma cellular proliferation via induction of apoptosis and cell cycle arrest*. *Journal of Surgical Research*, 2014. 191(2): p. 280-285.
166. Ahn, D.H., et al., *Results of an abbreviated phase-II study with the Akt Inhibitor MK-2206 in Patients with Advanced Biliary Cancer*. *Scientific Reports*, 2015. 5(1).
167. Davies, B.R., et al., *Preclinical Pharmacology of AZD5363, an Inhibitor of AKT: Pharmacodynamics, Antitumor Activity, and Correlation of Monotherapy Activity with Genetic Background*. *Molecular Cancer Therapeutics*, 2012. 11(4): p. 873-887.
168. Patra, T., et al., *A combination of AZD5363 and FH5363 induces lethal autophagy in transformed hepatocytes*. *Cell Death & Disease*, 2020. 11(7).
169. Carnevalli, L.S., et al., *PI3K α/δ inhibition promotes anti-tumor immunity through direct enhancement of effector CD8⁺ T-cell activity*. *Journal for ImmunoTherapy of Cancer*, 2018. 6(1): p. 158.
170. Abu-Eid, R., et al., *Selective Inhibition of Regulatory T Cells by Targeting the PI3K–Akt Pathway*. *Cancer Immunology Research*, 2014. 2(11): p. 1080-1089.
171. Searle, E.J., et al., *Akt inhibition improves long-term tumour control following radiotherapy by altering the microenvironment*. *EMBO Mol Med*, 2017. 9(12): p. 1646-1659.
172. Macek Jilkova, Z., K. Kurma, and T. Decaens, *Animal Models of Hepatocellular Carcinoma: The Role of Immune System and Tumor Microenvironment*. *Cancers (Basel)*, 2019. 11(10).
173. Marks, D.K., et al., *Akt Inhibition Is Associated With Favorable Immune Profile Changes Within the Tumor Microenvironment of Hormone Receptor Positive, HER2 Negative Breast Cancer*. *Frontiers in Oncology*, 2020. 10(968).

174. Fire, A., et al., *Potent and specific genetic interference by double-stranded RNA in *Caenorhabditis elegans**. *Nature*, 1998. 391(6669): p. 806-11.
175. Mansoori, B., S. Sandoghchian Shotorbani, and B. Baradaran, *RNA interference and its role in cancer therapy*. *Adv Pharm Bull*, 2014. 4(4): p. 313-21.
176. Setten, R.L., J.J. Rossi, and S.P. Han, *Publisher Correction: The current state and future directions of RNAi-based therapeutics*. *Nat Rev Drug Discov*, 2020. 19(4): p. 291.
177. Wang, Q. and G.G. Carmichael, *Effects of length and location on the cellular response to double-stranded RNA*. *Microbiol Mol Biol Rev*, 2004. 68(3): p. 432-52, table of contents.
178. Mahmoodi Chalbatani, G., et al., *Small interfering RNAs (siRNAs) in cancer therapy: a nano-based approach*. *Int J Nanomedicine*, 2019. 14: p. 3111-3128.
179. Guo, J., X. Jiang, and S. Gui, *RNA interference-based nanosystems for inflammatory bowel disease therapy*. *Int J Nanomedicine*, 2016. 11: p. 5287-5310.
180. Olena, A.F. and J.G. Patton, *Genomic organization of microRNAs*. *J Cell Physiol*, 2010. 222(3): p. 540-5.
181. O'Brien, J., et al., *Overview of MicroRNA Biogenesis, Mechanisms of Actions, and Circulation*. *Front Endocrinol (Lausanne)*, 2018. 9: p. 402.
182. Khatri, N., et al., *In vivo delivery aspects of miRNA, shRNA and siRNA*. *Crit Rev Ther Drug Carrier Syst*, 2012. 29(6): p. 487-527.
183. Burke, J.M., et al., *Expression of short hairpin RNAs using the compact architecture of retroviral microRNA genes*. *Nucleic Acids Res*, 2017. 45(17): p. e154.
184. Paddison, P.J., et al., *Short hairpin RNAs (shRNAs) induce sequence-specific silencing in mammalian cells*. *Genes Dev*, 2002. 16(8): p. 948-58.
185. Aagaard, L. and J.J. Rossi, *RNAi therapeutics: principles, prospects and challenges*. *Adv Drug Deliv Rev*, 2007. 59(2-3): p. 75-86.
186. Carthew, R.W. and E.J. Sontheimer, *Origins and Mechanisms of miRNAs and siRNAs*. *Cell*, 2009. 136(4): p. 642-55.
187. Matzke, M.A. and J.A. Birchler, *RNAi-mediated pathways in the nucleus*. *Nat Rev Genet*, 2005. 6(1): p. 24-35.
188. Sheu-Gruttadauria, J. and I.J. MacRae, *Structural Foundations of RNA Silencing by Argonaute*. *J Mol Biol*, 2017. 429(17): p. 2619-2639.
189. Adams, D., et al., *Patisiran, an RNAi Therapeutic, for Hereditary Transthyretin Amyloidosis*. *N Engl J Med*, 2018. 379(1): p. 11-21.
190. *Second RNAi drug approved*. *Nat Biotechnol*, 2020. 38(4): p. 385.
191. Thi, E.P., et al., *Lipid nanoparticle siRNA treatment of Ebola-virus-Makona-infected nonhuman primates*. *Nature*, 2015. 521(7552): p. 362-5.

192. Hnisz, D., et al., *Activation of proto-oncogenes by disruption of chromosome neighborhoods*. Science, 2016. 351(6280): p. 1454-1458.
193. Katoh, M., *FGFR2 and WDR11 are neighboring oncogene and tumor suppressor gene on human chromosome 10q26*. Int J Oncol, 2003. 22(5): p. 1155-9.
194. Nieth, C., et al., *Modulation of the classical multidrug resistance (MDR) phenotype by RNA interference (RNAi)*. FEBS Lett, 2003. 545(2-3): p. 144-50.
195. Liang, X., et al., *RNA-based pharmacotherapy for tumors: From bench to clinic and back*. Biomed Pharmacother, 2020. 125: p. 109997.
196. Chiu, Y.L. and T.M. Rana, *RNAi in human cells: basic structural and functional features of small interfering RNA*. Mol Cell, 2002. 10(3): p. 549-61.
197. Park, J., et al., *Pharmacokinetics and biodistribution of recently-developed siRNA nanomedicines*. Adv Drug Deliv Rev, 2016. 104: p. 93-109.
198. Zhang, Q.Y., et al., *Lipidation of polyethylenimine-based polyplex increases serum stability of bioengineered RNAi agents and offers more consistent tumoral gene knockdown in vivo*. Int J Pharm, 2018. 547(1-2): p. 537-544.
199. Wagner, M.J., et al., *Preclinical Mammalian Safety Studies of EPHARNA (DOPC Nanoliposomal EphA2-Targeted siRNA)*. Mol Cancer Ther, 2017. 16(6): p. 1114-1123.
200. Uchimura, K., et al., *HSulf-2, an extracellular endoglucosamine-6-sulfatase, selectively mobilizes heparin-bound growth factors and chemokines: effects on VEGF, FGF-1, and SDF-1*. BMC Biochem, 2006. 7: p. 2.
201. Filliol, A. and R.F. Schwabe, *Contributions of Fibroblasts, Extracellular Matrix, Stiffness, and Mechanosensing to Hepatocarcinogenesis*. Semin Liver Dis, 2019. 39(3): p. 315-333.
202. Montalbano, M., et al., *Role of Glypican-3 in the growth, migration and invasion of primary hepatocytes isolated from patients with hepatocellular carcinoma*. Cell Oncol (Dordr), 2018. 41(2): p. 169-184.
203. Sun, W., et al., *Codelivery of sorafenib and GPC3 siRNA with PEI-modified liposomes for hepatoma therapy*. Biomater Sci, 2017. 5(12): p. 2468-2479.
204. Vlodavsky, I. and Y. Friedmann, *Molecular properties and involvement of heparanase in cancer metastasis and angiogenesis*. J Clin Invest, 2001. 108(3): p. 341-7.
205. Jiang, G., et al., *Small RNAs targeting transcription start site induce heparanase silencing through interference with transcription initiation in human cancer cells*. PLoS One, 2012. 7(2): p. e31379.
206. Wang, X., et al., *Targeting of growth factors in the treatment of hepatocellular carcinoma: The potentials of polysaccharides*. Oncol Lett, 2017. 13(3): p. 1509-1517.
207. Fuchs, B.C., et al., *Epidermal growth factor receptor inhibition attenuates liver fibrosis and development of hepatocellular carcinoma*. Hepatology, 2014. 59(4): p. 1577-90.

208. Gao, J., et al., *EGFR-specific PEGylated immunoliposomes for active siRNA delivery in hepatocellular carcinoma*. *Biomaterials*, 2012. 33(1): p. 270-82.
209. Huang, Z., et al., *Low-molecular weight chitosan/vascular endothelial growth factor short hairpin RNA for the treatment of hepatocellular carcinoma*. *Life Sci*, 2012. 91(23-24): p. 1207-15.
210. Li, T., et al., *Multi-target siRNA: Therapeutic Strategy for Hepatocellular Carcinoma*. *J Cancer*, 2016. 7(10): p. 1317-27.
211. Wu, Y.Y., et al., *Inhibition of hepatocellular carcinoma growth and angiogenesis by dual silencing of NET-1 and VEGF*. *J Mol Histol*, 2013. 44(4): p. 433-45.
212. Huang, X.H., et al., *Small interfering RNA (siRNA)-mediated knockdown of macrophage migration inhibitory factor (MIF) suppressed cyclin D1 expression and hepatocellular carcinoma cell proliferation*. *Oncotarget*, 2014. 5(14): p. 5570-80.
213. Mazumder, S., E.L. DuPree, and A. Almasan, *A dual role of cyclin E in cell proliferation and apoptosis may provide a target for cancer therapy*. *Curr Cancer Drug Targets*, 2004. 4(1): p. 65-75.
214. Li, K., et al., *Use of RNA interference to target cyclin E-overexpressing hepatocellular carcinoma*. *Cancer Res*, 2003. 63(13): p. 3593-7.
215. Bai, T., C.C. Chen, and L.F. Lau, *Matricellular protein CCN1 activates a proinflammatory genetic program in murine macrophages*. *J Immunol*, 2010. 184(6): p. 3223-32.
216. Jia, Q., Q. Dong, and L. Qin, *CCN: core regulatory proteins in the microenvironment that affect the metastasis of hepatocellular carcinoma?* *Oncotarget*, 2016. 7(2): p. 1203-14.
217. Mizuno, H., et al., *Changes in adhesive and migratory characteristics of hepatocellular carcinoma (HCC) cells induced by expression of alpha3beta1 integrin*. *Biochim Biophys Acta*, 2008. 1780(3): p. 564-70.
218. Bogorad, R.L., et al., *Nanoparticle-formulated siRNA targeting integrins inhibits hepatocellular carcinoma progression in mice*. *Nat Commun*, 2014. 5: p. 3869.
219. Zhou, X., et al., *The function and clinical application of extracellular vesicles in innate immune regulation*. *Cell Mol Immunol*, 2020. 17(4): p. 323-334.
220. Roma-Rodrigues, C., A.R. Fernandes, and P.V. Baptista, *Exosome in tumour microenvironment: overview of the crosstalk between normal and cancer cells*. *Biomed Res Int*, 2014. 2014: p. 179486.
221. Becker, A., et al., *Extracellular Vesicles in Cancer: Cell-to-Cell Mediators of Metastasis*. *Cancer Cell*, 2016. 30(6): p. 836-848.
222. Maia, J., et al., *Exosome-Based Cell-Cell Communication in the Tumor Microenvironment*. *Front Cell Dev Biol*, 2018. 6: p. 18.
223. Xie, F., et al., *miRNA-320a inhibits tumor proliferation and invasion by targeting c-Myc in human hepatocellular carcinoma*. *Onco Targets Ther*, 2017. 10: p. 885-894.

224. Qu, Z., et al., *Exosomes derived from HCC cells induce sorafenib resistance in hepatocellular carcinoma both in vivo and in vitro*. J Exp Clin Cancer Res, 2016. 35(1): p. 159.
225. Wang, S., et al., *Exosomes released by hepatocarcinoma cells endow adipocytes with tumor-promoting properties*. J Hematol Oncol, 2018. 11(1): p. 82.
226. Wang, X., et al., *14-3-3zeta delivered by hepatocellular carcinoma-derived exosomes impaired anti-tumor function of tumor-infiltrating T lymphocytes*. Cell Death Dis, 2018. 9(2): p. 159.
227. He, M., et al., *Hepatocellular carcinoma-derived exosomes promote motility of immortalized hepatocyte through transfer of oncogenic proteins and RNAs*. Carcinogenesis, 2015. 36(9): p. 1008-18.
228. Zhao, Y., et al., *RNAi silencing of c-Myc inhibits cell migration, invasion, and proliferation in HepG2 human hepatocellular carcinoma cell line: c-Myc silencing in hepatocellular carcinoma cell*. Cancer Cell Int, 2013. 13(1): p. 23.
229. Haga, Y., et al., *Overexpression of c-Jun contributes to sorafenib resistance in human hepatoma cell lines*. PLoS One, 2017. 12(3): p. e0174153.
230. Patt, Y.Z., et al., *Hepatic arterial infusion of floxuridine, leucovorin, doxorubicin, and cisplatin for hepatocellular carcinoma: effects of hepatitis B and C viral infection on drug toxicity and patient survival*. J Clin Oncol, 1994. 12(6): p. 1204-11.
231. Lee, J.E., et al., *Epirubicin, cisplatin, 5-FU combination chemotherapy in sorafenib-refractory metastatic hepatocellular carcinoma*. World J Gastroenterol, 2014. 20(1): p. 235-41.
232. Ishikawa, T., et al., *Hepatic arterial infusion chemotherapy with cisplatin before radical local treatment of early hepatocellular carcinoma (JIS score 0/1) improves survival*. Ann Oncol, 2014. 25(7): p. 1379-1384.
233. Li, M., et al., *Biocompatible co-loading vehicles for delivering both nanoplatin cores and siRNA to treat hepatocellular carcinoma*. Int J Pharm, 2019. 572: p. 118769.
234. Conigliaro, A., et al., *CD90+ liver cancer cells modulate endothelial cell phenotype through the release of exosomes containing H19 IncRNA*. Mol Cancer, 2015. 14: p. 155.
235. Huang, K.W., et al., *Galactose Derivative-Modified Nanoparticles for Efficient siRNA Delivery to Hepatocellular Carcinoma*. Biomacromolecules, 2018. 19(6): p. 2330-2339.
236. Yao, Y., et al., *Co-delivery of sorafenib and VEGF-siRNA via pH-sensitive liposomes for the synergistic treatment of hepatocellular carcinoma*. Artif Cells Nanomed Biotechnol, 2019. 47(1): p. 1374-1383.
237. De Clercq, E., *AMD3100/CXCR4 Inhibitor*. Front Immunol, 2015. 6: p. 276.
238. Liu, J.Y., et al., *Delivery of siRNA Using CXCR4-targeted Nanoparticles Modulates Tumor Microenvironment and Achieves a Potent Antitumor Response in Liver Cancer*. Mol Ther, 2015. 23(11): p. 1772-1782.

239. Ishii, G., et al., *Bone-marrow-derived myofibroblasts contribute to the cancer-induced stromal reaction*. *Biochem Biophys Res Commun*, 2003. 309(1): p. 232-40.
240. Kalluri, R. and M. Zeisberg, *Fibroblasts in cancer*. *Nat Rev Cancer*, 2006. 6(5): p. 392-401.
241. Elenbaas, B. and R.A. Weinberg, *Heterotypic signaling between epithelial tumor cells and fibroblasts in carcinoma formation*. *Exp Cell Res*, 2001. 264(1): p. 169-84.
242. Tahmasebi Birgani, M. and V. Carloni, *Tumor Microenvironment, a Paradigm in Hepatocellular Carcinoma Progression and Therapy*. *Int J Mol Sci*, 2017. 18(2).
243. Yang, J.D., I. Nakamura, and L.R. Roberts, *The tumor microenvironment in hepatocellular carcinoma: current status and therapeutic targets*. *Semin Cancer Biol*, 2011. 21(1): p. 35-43.
244. Kumar, D.P., et al., *A Regulatory Role of Apoptosis Antagonizing Transcription Factor in the Pathogenesis of Nonalcoholic Fatty Liver Disease and Hepatocellular Carcinoma*. *Hepatology*, 2019. 69(4): p. 1520-1534.
245. Novikova, M.V., N.V. Khromova, and P.B. Kopnin, *Components of the Hepatocellular Carcinoma Microenvironment and Their Role in Tumor Progression*. *Biochemistry (Mosc)*, 2017. 82(8): p. 861-873.
246. Sun, F., et al., *Interleukin-8 promotes integrin beta3 upregulation and cell invasion through PI3K/Akt pathway in hepatocellular carcinoma*. *J Exp Clin Cancer Res*, 2019. 38(1): p. 449.
247. Quail, D.F. and J.A. Joyce, *Microenvironmental regulation of tumor progression and metastasis*. *Nat Med*, 2013. 19(11): p. 1423-37.
248. Liu, J., et al., *Cancer-associated fibroblasts promote hepatocellular carcinoma metastasis through chemokine-activated hedgehog and TGF-beta pathways*. *Cancer Lett*, 2016. 379(1): p. 49-59.
249. Baluk, P., et al., *Abnormalities of basement membrane on blood vessels and endothelial sprouts in tumors*. *Am J Pathol*, 2003. 163(5): p. 1801-15.
250. Santamato, A., et al., *Hepatic stellate cells stimulate HCC cell migration via laminin-5 production*. *Clin Sci (Lond)*, 2011. 121(4): p. 159-68.
251. Cho, Y., et al., *Tumor-Stroma Crosstalk Enhances REG3A Expressions that Drive the Progression of Hepatocellular Carcinoma*. *Int J Mol Sci*, 2020. 21(2).
252. Faouzi, S., et al., *Activation of cultured rat hepatic stellate cells by tumoral hepatocytes*. *Lab Invest*, 1999. 79(4): p. 485-93.
253. Amann, T., et al., *Activated hepatic stellate cells promote tumorigenicity of hepatocellular carcinoma*. *Cancer Sci*, 2009. 100(4): p. 646-53.
254. Carloni, V., T.V. Luong, and K. Rombouts, *Hepatic stellate cells and extracellular matrix in hepatocellular carcinoma: more complicated than ever*. *Liver Int*, 2014. 34(6): p. 834-43.

255. Mehdizadeh, A., et al., *Liposome-mediated RNA interference delivery against Erk1 and Erk2 does not equally promote chemosensitivity in human hepatocellular carcinoma cell line HepG2*. *Artif Cells Nanomed Biotechnol*, 2017. 45(8): p. 1612-1619.
256. Nathan, C. and A. Ding, *Nonresolving inflammation*. *Cell*, 2010. 140(6): p. 871-82.
257. Murray, P.J., *Macrophage Polarization*. *Annu Rev Physiol*, 2017. 79: p. 541-566.
258. Patel, P., S.E. Schutzer, and N. Pylsopoulos, *Immunobiology of hepatocarcinogenesis: Ways to go or almost there?* *World J Gastrointest Pathophysiol*, 2016. 7(3): p. 242-55.
259. Yeung, O.W., et al., *Alternatively activated (M2) macrophages promote tumour growth and invasiveness in hepatocellular carcinoma*. *J Hepatol*, 2015. 62(3): p. 607-16.
260. Dong, N., et al., *M2 macrophages mediate sorafenib resistance by secreting HGF in a feed-forward manner in hepatocellular carcinoma*. *Br J Cancer*, 2019. 121(1): p. 22-33.
261. Liu, A.W., et al., *ShRNA-targeted MAP4K4 inhibits hepatocellular carcinoma growth*. *Clin Cancer Res*, 2011. 17(4): p. 710-20.
262. Zhang, W., et al., *SENP1 regulates hepatocyte growth factor-induced migration and epithelial-mesenchymal transition of hepatocellular carcinoma*. *Tumour Biol*, 2016. 37(6): p. 7741-8.
263. Cho, S.B., et al., *Small interfering RNA-directed targeting of RON alters invasive and oncogenic phenotypes of human hepatocellular carcinoma cells*. *Oncol Rep*, 2011. 26(6): p. 1581-6.
264. Zhang, C., et al., *SIRT6 regulates the proliferation and apoptosis of hepatocellular carcinoma via the ERK1/2 signaling pathway*. *Mol Med Rep*, 2019. 20(2): p. 1575-1582.
265. Chen, J., et al., *ECT2 regulates the Rho/ERK signalling axis to promote early recurrence in human hepatocellular carcinoma*. *J Hepatol*, 2015. 62(6): p. 1287-95.
266. Wang, W., et al., *Inhibition of invasion and metastasis of hepatocellular carcinoma cells via targeting RhoC in vitro and in vivo*. *Clin Cancer Res*, 2008. 14(21): p. 6804-12.
267. Xu, Z.W., et al., *The influence of TNF-alpha and Ang II on the proliferation, migration and invasion of HepG2 cells by regulating the expression of GRK2*. *Cancer Chemother Pharmacol*, 2017. 79(4): p. 747-758.
268. Shirabe, K., et al., *Role of tumor-associated macrophages in the progression of hepatocellular carcinoma*. *Surg Today*, 2012. 42(1): p. 1-7.
269. Kuang, D.M., et al., *Activated monocytes in peritumoral stroma of hepatocellular carcinoma promote expansion of memory T helper 17 cells*. *Hepatology*, 2010. 51(1): p. 154-64.
270. Wan, S., et al., *Tumor-associated macrophages produce interleukin 6 and signal via STAT3 to promote expansion of human hepatocellular carcinoma stem cells*. *Gastroenterology*, 2014. 147(6): p. 1393-404.

271. Nicolas-Avila, J.A., J.M. Adrover, and A. Hidalgo, *Neutrophils in Homeostasis, Immunity, and Cancer*. *Immunity*, 2017. 46(1): p. 15-28.
272. Michaeli, J., et al., *Tumor-associated neutrophils induce apoptosis of non-activated CD8 T-cells in a TNFalpha and NO-dependent mechanism, promoting a tumor-supportive environment*. *Oncoimmunology*, 2017. 6(11): p. e1356965.
273. Ameratunga, M., et al., *Neutrophil-lymphocyte ratio kinetics in patients with advanced solid tumours on phase I trials of PD-1/PD-L1 inhibitors*. *Eur J Cancer*, 2018. 89: p. 56-63.
274. Jeyakumar, G., et al., *Neutrophil lymphocyte ratio and duration of prior anti-angiogenic therapy as biomarkers in metastatic RCC receiving immune checkpoint inhibitor therapy*. *J Immunother Cancer*, 2017. 5(1): p. 82.
275. Margetts, J., et al., *Neutrophils: driving progression and poor prognosis in hepatocellular carcinoma?* *Br J Cancer*, 2018. 118(2): p. 248-257.
276. Arai, K., et al., *Preoperative neutrophil-to-lymphocyte ratio as a predictor of survival after reductive surgery plus percutaneous isolated hepatic perfusion for hepatocellular carcinoma: a retrospective analysis*. *Surg Today*, 2017. 47(3): p. 385-392.
277. Koh, M.Y., et al., *A new HIF-1alpha/RANTES-driven pathway to hepatocellular carcinoma mediated by germline haploinsufficiency of SART1/HAF in mice*. *Hepatology*, 2016. 63(5): p. 1576-91.
278. Zhou, S.L., et al., *Tumor-Associated Neutrophils Recruit Macrophages and T-Regulatory Cells to Promote Progression of Hepatocellular Carcinoma and Resistance to Sorafenib*. *Gastroenterology*, 2016. 150(7): p. 1646-1658 e17.
279. Zhou, S.L., et al., *Overexpression of CXCL5 mediates neutrophil infiltration and indicates poor prognosis for hepatocellular carcinoma*. *Hepatology*, 2012. 56(6): p. 2242-54.
280. Ormandy, L.A., et al., *Direct ex vivo analysis of dendritic cells in patients with hepatocellular carcinoma*. *World J Gastroenterol*, 2006. 12(20): p. 3275-82.
281. Streba, L.A., et al., *Dendritic cells and hepatocellular carcinoma*. *Rom J Morphol Embryol*, 2014. 55(4): p. 1287-93.
282. Li, P., et al., *Interferon-gamma induces autophagy with growth inhibition and cell death in human hepatocellular carcinoma (HCC) cells through interferon-regulatory factor-1 (IRF-1)*. *Cancer Lett*, 2012. 314(2): p. 213-22.
283. Li, C., et al., *Interferon-stimulated gene 15 (ISG15) is a trigger for tumorigenesis and metastasis of hepatocellular carcinoma*. *Oncotarget*, 2014. 5(18): p. 8429-41.
284. Han, C., et al., *Natural killer cells involved in tumour immune escape of hepatocellular carcinomas*. *Int Immunopharmacol*, 2019. 73: p. 10-16.
285. Hasmim, M., et al., *Critical Role of Tumor Microenvironment in Shaping NK Cell Functions: Implication of Hypoxic Stress*. *Front Immunol*, 2015. 6: p. 482.

286. Yang, W., et al., *Hypoxia-inducible factor-1alpha downregulation by small interfering RNA inhibits proliferation, induces apoptosis, and enhances radiosensitivity in chemical hypoxic human hepatoma SMMC-7721 cells*. *Cancer Biother Radiopharm*, 2011. 26(5): p. 565-71.
287. Takahashi, Y., M. Nishikawa, and Y. Takakura, *Inhibition of tumor cell growth in the liver by RNA interference-mediated suppression of HIF-1alpha expression in tumor cells and hepatocytes*. *Gene Ther*, 2008. 15(8): p. 572-82.
288. Vujanovic, L., et al., *Tumor-Derived alpha-Fetoprotein Directly Drives Human Natural Killer-Cell Activation and Subsequent Cell Death*. *Cancer Immunol Res*, 2017. 5(6): p. 493-502.
289. Yamamoto, M., et al., *alpha-Fetoprotein impairs activation of natural killer cells by inhibiting the function of dendritic cells*. *Clin Exp Immunol*, 2011. 165(2): p. 211-9.
290. Langhans, B., et al., *Regulatory CD4+ T cells modulate the interaction between NK cells and hepatic stellate cells by acting on either cell type*. *J Hepatol*, 2015. 62(2): p. 398-404.
291. Li, T., et al., *Hepatocellular carcinoma-associated fibroblasts trigger NK cell dysfunction via PGE2 and IDO*. *Cancer Lett*, 2012. 318(2): p. 154-61.
292. Scaggiante, B., et al., *Improving siRNA bio-distribution and minimizing side effects*. *Curr Drug Metab*, 2011. 12(1): p. 11-23.
293. Lee, S.J., et al., *Delivery strategies and potential targets for siRNA in major cancer types*. *Adv Drug Deliv Rev*, 2016. 104: p. 2-15.
294. Xu, C., S.A. Lee, and X. Chen, *RNA interference as therapeutics for hepatocellular carcinoma*. *Recent Pat Anticancer Drug Discov*, 2011. 6(1): p. 106-15.
295. Babu, A., et al., *Nanoparticles for siRNA-Based Gene Silencing in Tumor Therapy*. *IEEE Trans Nanobioscience*, 2016. 15(8): p. 849-863.
296. Tomalia, D.A., L.A. Reyna, and S. Svenson, *Dendrimers as multi-purpose nanodevices for oncology drug delivery and diagnostic imaging*. *Biochem Soc Trans*, 2007. 35(Pt 1): p. 61-7.
297. Abbasi, E., et al., *Dendrimers: synthesis, applications, and properties*. *Nanoscale Res Lett*, 2014. 9(1): p. 247.
298. Chen, C.Z., et al., *Quaternary ammonium functionalized poly(propylene imine) dendrimers as effective antimicrobials: structure-activity studies*. *Biomacromolecules*, 2000. 1(3): p. 473-80.
299. Meyers, S.R., et al., *Anionic amphiphilic dendrimers as antibacterial agents*. *J Am Chem Soc*, 2008. 130(44): p. 14444-5.
300. Mintzer, M.A. and M.W. Grinstaff, *Biomedical applications of dendrimers: a tutorial*. *Chem Soc Rev*, 2011. 40(1): p. 173-90.
301. Hayder, M., et al., *Phosphorus-Based Dendrimer ABP Treats Neuroinflammation by Promoting IL-10-Producing CD4(+) T Cells*. *Biomacromolecules*, 2015. 16(11): p. 3425-33.

302. Ullas, P.T., et al., *Enhancement of immunogenicity and efficacy of a plasmid DNA rabies vaccine by nanoformulation with a fourth-generation amine-terminated poly(ether imine) dendrimer*. Int J Nanomedicine, 2014. 9: p. 627-34.
303. Halkes, S.B., et al., *Synthesis and biological activity of polygalloyl-dendrimers as stable tannic acid mimics*. Bioorg Med Chem Lett, 2002. 12(12): p. 1567-70.
304. Supattapone, S., K. Nishina, and J.R. Rees, *Pharmacological approaches to prion research*. Biochem Pharmacol, 2002. 63(8): p. 1383-8.
305. Battah, S.H., et al., *Synthesis and biological studies of 5-aminolevulinic acid-containing dendrimers for photodynamic therapy*. Bioconjug Chem, 2001. 12(6): p. 980-8.
306. Chen, J., et al., *Synthesis and use of an amphiphilic dendrimer for siRNA delivery into primary immune cells*. Nat Protoc, 2021. 16(1): p. 327-351.
307. Yu, T., et al., *An amphiphilic dendrimer for effective delivery of small interfering RNA and gene silencing in vitro and in vivo*. Angew Chem Int Ed Engl, 2012. 51(34): p. 8478-84.
308. Ellert-Miklaszewska, A., et al., *Efficient and innocuous delivery of small interfering RNA to microglia using an amphiphilic dendrimer nanovector*. Nanomedicine (Lond), 2019. 14(18): p. 2441-2458.
309. Dong, Y., et al., *A Dual Targeting Dendrimer-Mediated siRNA Delivery System for Effective Gene Silencing in Cancer Therapy*. J Am Chem Soc, 2018. 140(47): p. 16264-16274.
310. Filhol, O., et al., *DSIR: assessing the design of highly potent siRNA by testing a set of cancer-relevant target genes*. PLoS One, 2012. 7(10): p. e48057.
311. Kunter, I., et al., *Active form of AKT controls cell proliferation and response to apoptosis in hepatocellular carcinoma*. Oncol Rep, 2014. 31(2): p. 573-80.
312. Franke, T.F., *PI3K/Akt: getting it right matters*. Oncogene, 2008. 27(50): p. 6473-88.
313. Anderson, E.M., et al., *Experimental validation of the importance of seed complement frequency to siRNA specificity*. RNA, 2008. 14(5): p. 853-61.
314. Du, K. and M. Montminy, *CREB is a regulatory target for the protein kinase Akt/PKB*. J Biol Chem, 1998. 273(49): p. 32377-9.
315. Hermida, M.A., J. Dinesh Kumar, and N.R. Leslie, *GSK3 and its interactions with the PI3K/AKT/mTOR signalling network*. Adv Biol Regul, 2017. 65: p. 5-15.
316. Michell, B.J., et al., *The Akt kinase signals directly to endothelial nitric oxide synthase*. Curr Biol, 1999. 9(15): p. 845-8.
317. Wiza, C., E.B. Nascimento, and D.M. Ouwens, *Role of PRAS40 in Akt and mTOR signaling in health and disease*. Am J Physiol Endocrinol Metab, 2012. 302(12): p. E1453-60.
318. Jiang, Z.Y., et al., *Identification of WNK1 as a substrate of Akt/protein kinase B and a negative regulator of insulin-stimulated mitogenesis in 3T3-L1 cells*. J Biol Chem, 2005. 280(22): p. 21622-8.

319. Ogawara, Y., et al., *Akt enhances Mdm2-mediated ubiquitination and degradation of p53*. J Biol Chem, 2002. 277(24): p. 21843-50.
320. Llovet, J.M., et al., *Immunotherapies for hepatocellular carcinoma*. Nat Rev Clin Oncol, 2021.
321. Harding, J.J., et al., *Prospective Genotyping of Hepatocellular Carcinoma: Clinical Implications of Next-Generation Sequencing for Matching Patients to Targeted and Immune Therapies*. Clin Cancer Res, 2019. 25(7): p. 2116-2126.
322. Morita, M., et al., *Immunological Microenvironment Predicts the Survival of the Patients with Hepatocellular Carcinoma Treated with Anti-PD-1 Antibody*. Liver Cancer, 2021. 10(4): p. 380-393.
323. Gonzalez, E. and T.E. McGraw, *The Akt kinases: isoform specificity in metabolism and cancer*. Cell Cycle, 2009. 8(16): p. 2502-8.
324. Staal, S.P., *Molecular cloning of the akt oncogene and its human homologues AKT1 and AKT2: amplification of AKT1 in a primary human gastric adenocarcinoma*. Proc Natl Acad Sci U S A, 1987. 84(14): p. 5034-7.
325. Cheng, J.Q., et al., *Amplification of AKT2 in human pancreatic cells and inhibition of AKT2 expression and tumorigenicity by antisense RNA*. Proc Natl Acad Sci U S A, 1996. 93(8): p. 3636-41.
326. Cheng, J.Q., et al., *AKT2, a putative oncogene encoding a member of a subfamily of protein-serine/threonine kinases, is amplified in human ovarian carcinomas*. Proc Natl Acad Sci U S A, 1992. 89(19): p. 9267-71.
327. Garofalo, R.S., et al., *Severe diabetes, age-dependent loss of adipose tissue, and mild growth deficiency in mice lacking Akt2/PKB beta*. J Clin Invest, 2003. 112(2): p. 197-208.
328. Easton, R.M., et al., *Role for Akt3/protein kinase Bgamma in attainment of normal brain size*. Mol Cell Biol, 2005. 25(5): p. 1869-78.
329. Somanath, P.R., et al., *Akt1 in endothelial cell and angiogenesis*. Cell Cycle, 2006. 5(5): p. 512-8.
330. Gonzalez, E. and T.E. McGraw, *Insulin-modulated Akt subcellular localization determines Akt isoform-specific signaling*. Proc Natl Acad Sci U S A, 2009. 106(17): p. 7004-9.
331. Degan, S.E. and I.H. Gelman, *Emerging Roles for AKT Isoform Preference in Cancer Progression Pathways*. Mol Cancer Res, 2021. 19(8): p. 1251-1257.
332. Stambolic, V. and J.R. Woodgett, *Functional distinctions of protein kinase B/Akt isoforms defined by their influence on cell migration*. Trends Cell Biol, 2006. 16(9): p. 461-6.
333. Zhou, G.L., et al., *Opposing roles for Akt1 and Akt2 in Rac/Pak signaling and cell migration*. J Biol Chem, 2006. 281(47): p. 36443-53.

334. Santi, S.A. and H. Lee, *The Akt isoforms are present at distinct subcellular locations*. *Am J Physiol Cell Physiol*, 2010. 298(3): p. C580-91.
335. Xin, Y., et al., *Nano-based delivery of RNAi in cancer therapy*. *Mol Cancer*, 2017. 16(1): p. 134.
336. Ragelle, H., G. Vandermeulen, and V. Preat, *Chitosan-based siRNA delivery systems*. *J Control Release*, 2013. 172(1): p. 207-218.
337. Kariko, K., et al., *Exogenous siRNA mediates sequence-independent gene suppression by signaling through toll-like receptor 3*. *Cells Tissues Organs*, 2004. 177(3): p. 132-8.
338. Dykxhoorn, D.M., D. Palliser, and J. Lieberman, *The silent treatment: siRNAs as small molecule drugs*. *Gene Ther*, 2006. 13(6): p. 541-52.
339. Salguero-Aranda, C., et al., *Expression of Concern: STAT6 knockdown using multiple siRNA sequences inhibits proliferation and induces apoptosis of human colorectal and breast cancer cell lines*. *PLoS One*, 2021. 16(1): p. e0246415.
340. Sasaki, T., et al., *Knockdown of Akt isoforms by RNA silencing suppresses the growth of human prostate cancer cells in vitro and in vivo*. *Biochem Biophys Res Commun*, 2010. 399(1): p. 79-83.
341. Koseoglu, S., et al., *AKT1, AKT2 and AKT3-dependent cell survival is cell line-specific and knockdown of all three isoforms selectively induces apoptosis in 20 human tumor cell lines*. *Cancer Biol Ther*, 2007. 6(5): p. 755-62.
342. Fatemian, T., H.R. Moghimi, and E.H. Chowdhury, *Intracellular Delivery of siRNAs Targeting AKT and ERBB2 Genes Enhances Chemosensitization of Breast Cancer Cells in a Culture and Animal Model*. *Pharmaceutics*, 2019. 11(9).
343. Lin, A., et al., *Off-target toxicity is a common mechanism of action of cancer drugs undergoing clinical trials*. *Sci Transl Med*, 2019. 11(509).
344. Shao, L., et al., *Enhancing anti-tumor efficacy and immune memory by combining 3p-GPC-3 siRNA treatment with PD-1 blockade in hepatocellular carcinoma*. *Oncoimmunology*, 2022. 11(1).

XII. ANNEXES

Review 1


The COVID-19 outbreak and the deterioration of the sanitary situation in France and the world, took its toll on the experimental work that I could do. During the first confinement in 2020, I was not able to go to the Lab, so, I used the time to write a review about the crosstalk between the tumor and its TME, and the use of RNAi in HCC. The article was published later on the 24th of July 2020.

The article is attached below.



Review

Modulating the Crosstalk between the Tumor and Its Microenvironment Using RNA Interference: A Treatment Strategy for Hepatocellular Carcinoma

Mariam Mroweh ^{1,2,3}, Thomas Decaens ^{1,2,4}, Patrice N Marche ^{1,2}, Zuzana Macek Jilkova ^{1,2,4,*} and Flora Clément ^{1,2,*} 

¹ Institute for Advanced Biosciences, Research Center Inserm U 1209/CNRS 5309, 38700 La Tronche, France; mariam.mroweh@gmail.com (M.M.); tdecaens@chu-grenoble.fr (T.D.); patrice.marche@inserm.fr (P.N.M.)

² Université Grenoble Alpes, 38000 Grenoble, France

³ Laboratory of Cancer Biology and Molecular Immunology, Faculty of Sciences I, Lebanese University, Hadath Beirut 6573-14, Lebanon

⁴ Service d'hépatogastroentérologie, Pôle Digidune, CHU Grenoble Alpes, 38700 La Tronche, France

* Correspondence: zmacekjilkova@chu-grenoble.fr (Z.M.J.); flora.clement@inserm.fr (F.C.)

Received: 15 June 2020; Accepted: 22 July 2020; Published: 24 July 2020



Abstract: Hepatocellular carcinoma (HCC) is the most common primary liver malignancy with one of the highest mortality rates among solid cancers. It develops almost exclusively in the background of chronic liver inflammation, which can be caused by viral hepatitis, chronic alcohol consumption or an unhealthy diet. Chronic inflammation deregulates the innate and adaptive immune responses that contribute to the proliferation, survival and migration of tumor cells. The continuous communication between the tumor and its microenvironment components serves as the overriding force of the tumor against the body's defenses. The importance of this crosstalk between the tumor microenvironment and immune cells in the process of hepatocarcinogenesis has been shown, and therapeutic strategies modulating this communication have improved the outcomes of patients with liver cancer. To target this communication, an RNA interference (RNAi)-based approach can be used, an innovative and promising strategy that can disrupt the crosstalk at the transcriptomic level. Moreover, RNAi offers the advantage of specificity in comparison to the treatments currently used for HCC in clinics. In this review, we will provide the recent data pertaining to the modulation of a tumor and its microenvironment by using RNAi and its potential for therapeutic intervention in HCC.

Keywords: HCC; tumor microenvironment; RNAi; miRNA; shRNA; siRNA

1. Hepatocellular Carcinoma

Hepatocellular carcinoma (HCC) is the most common type of liver malignancy, comprising 75–85% of all liver cancers. It is a leading cause of cancer-related death, being estimated to be the fourth most common cause of cancer-related death overall worldwide [1]. The emergence of HCC is triggered by a chronic inflammation background. The typical stages of emergence can be summarized as follows: inflammation, fibrosis, cirrhosis and finally HCC. The risk factors implicated in favoring HCC, mainly through the induction of chronic inflammation, include viral hepatitis C (HCV), viral hepatitis B (HBV), chronic alcohol intake, metabolic disorders leading to non-alcoholic fatty liver diseases and non-alcoholic steatohepatitis (NASH), the consumption of toxins (such as aflatoxins) and hereditary diseases such as hemochromatosis [2]. The main problems that HCC treatment is facing are the delays in the diagnosis, recurrence and drug resistance. Some patients remain asymptomatic until the advanced stages of the disease; however, if detected at an early stage, HCC can be curable by surgical resection, percutaneous ablation or liver transplantation. Unfortunately, at an advanced stage, the treatment

options are limited. The current standard therapy option for advanced HCC treatment is Sorafenib [3]. Additionally, Lenvatinib (another first-line drug for treating HCC besides Sorafenib), Regorafenib and Cabozantinib, Nivolumab, Pembrolizumab and Atezolizumab plus Bevacizumab (second-line treatment after Sorafenib) were recently approved for HCC treatment [4], but these drugs show no additional improvement in survival compared to Sorafenib [5]. Thus, the search for a possible treatment with better efficacy continues, and currently, various immunotherapies and angiogenic inhibitors are under testing as candidates for HCC treatment, targeting the complex intrahepatic network. Noticeably, the search for a drug shifted from the conditional “direct tumor-targeting” tyrosine kinases to “neighboring effectors” targeting the immune and angiogenic network of the tumor. From this shift, one can infer that the players in HCC extend beyond the tumor into the tumor microenvironment and thus serve as certified targets for treatment [2]. Very recently, a new therapeutic option was published demonstrating the superiority of Atezolizumab—an anti-programmed death-ligand 1 (PDL-1) antibody—plus Bevacizumab, an anti-vascular endothelial growth factor (VEGF) antibody, compared to Sorafenib in the first line treatment of advanced HCC, and the FDA approved this treatment on 29 May 2020 [6].

2. RNA Interference (RNAi) Overview

The Nobel Prize in Physiology and Medicine was awarded in 2006 to RNAi discoverers, Andrew Z. Fire and Craig C. Mello [7]. RNAi involves a double-stranded ribonucleic acid that interferes with a specific messenger RNA (mRNA) and prevents its translation or leads to its degradation, therefore decreasing the expression levels of the corresponding protein. This mechanism censors the output of the genome and dictates the fate of a specific transcript, inhibiting its translation into the final active form, the protein. Due to the aberrant activities of a variety of proteins in cancers, RNAi represents a promising tool in cancer therapy. Moreover, as RNAi interrupts the gene of interest (and can be specific to a mutated version of a gene), mRNA, and protein flow, it can modulate the secretory profile of the cells, leading to disrupted crosstalk, which is essential for tumor progression [8].

RNAi is a regulatory mechanism involving small regulatory RNAs (belonging to non-coding RNAs—ncRNA) that are not translated into proteins. The RNAi mechanism is one way of inducing post-transcriptional gene silencing and can participate as a natural process of resistance to the presence of pathogenic exogenous double-stranded RNA (dsRNA) [9]. The presence of dsRNA in the cell is termed to be “abnormal”, and it is degraded by the cellular machinery upon recognition through Toll-like receptor (TLR) activities. dsRNAs can be of viral origin but can also be from endogenous genes such as transposons [10]. Therefore, by mimicking this process, i.e., the introduction of RNA molecules with the ability to bind to the target mRNA and thus labelling it for degradation, it is possible to control the expression of specific genes for treatment purposes. Diverse studies have shown, *in vitro*, the efficiency of this mechanism in numerous pathologies, specifically in inflammatory diseases as well as cancer [11,12]. RNAi comprises three different types of RNA molecules: microRNAs (miRNA), short hairpin RNAs (shRNA) and small interfering RNAs (siRNA) (Figure 1).

2.1. Biogenesis and Gene Silencing Mechanism of MicroRNA

A miRNA is an endogenous single-stranded RNA molecule of 19–22 nucleotides (nt) derived from a double-stranded region of a 60–70 nt RNA hairpin precursor. Sequences encoding miRNAs are dispersed in the genome and occur in the form of clusters. They can be intercalated between two genes, i.e., in intergenic regions, or within the intron sites of a specific gene [13]. The biogenesis of miRNAs takes place in both the nucleus and cytoplasm. Depending on the DNA region, the miRNA gene is transcribed by either RNA polymerase II or III (generally the latter). The resulting primary (pri-)miRNA is then processed to give the precursor (pre-)miRNA, which assumes a loop structure and is exported into the cytoplasm by the help of Exportin-5. Further maturation occurs in the cytosol to produce a mature miRNA that binds to the target mRNA. The silencing of the target mRNA is initiated by a partial hybridization of the miRNA-RNA induced silencing complex (RISC) on the

3'-untranslated region of the mRNA through base pairing [14]. The induction of miRNA, therefore, implies nucleus modification.

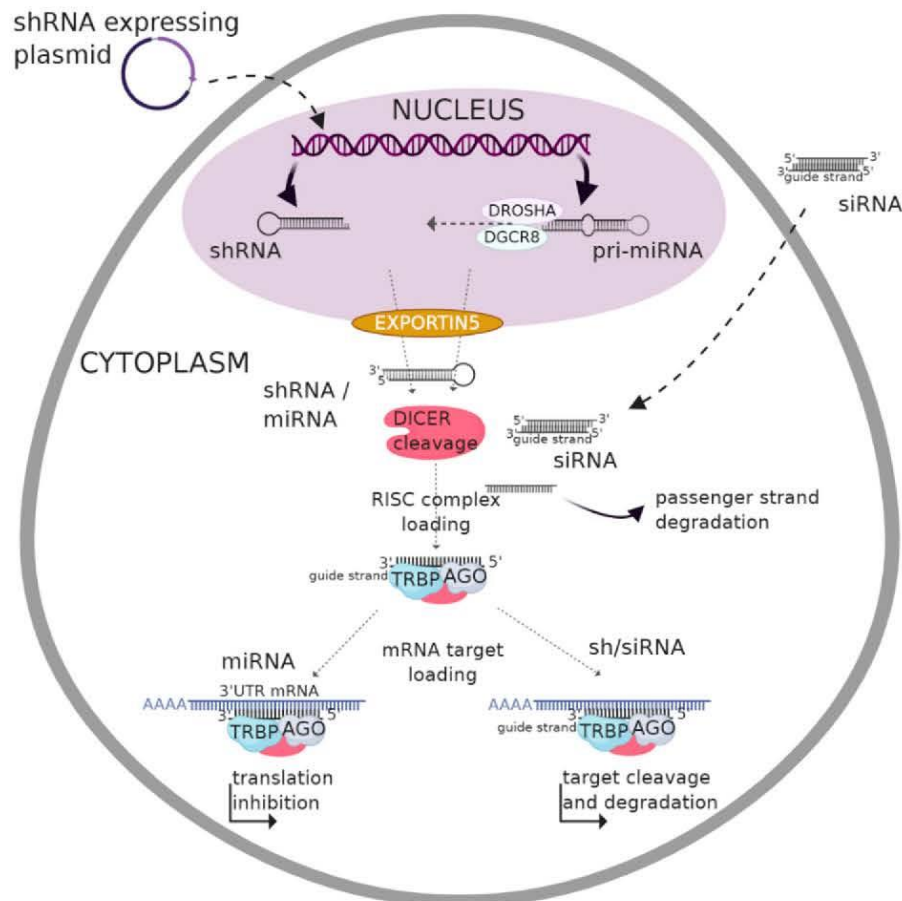


Figure 1. Scheme of three different RNA interference (RNAi) pathways: micro(mi)RNA, short hairpin (sh)RNA and small interfering (si)RNA. shRNA and miRNA mediated silencing are based on a modification of the genomic content within the nucleus whereas siRNAs act directly in the cytoplasm of cells and do not require nuclear import. shRNAs and miRNAs are introduced into the cell in the form of DNA, and it is essential that they are transported into the nucleus to be transcribed into dsRNAs with a hairpin-like structure and are thus termed pri-shRNAs and pri-miRNAs, respectively, which are further cleaved in the nucleus by the DROSHA enzyme. The resulting transcripts are termed pre-shRNAs and pre-miRNAs, respectively, and are exported to the cytoplasm via Exportin 5. siRNAs, on the other hand, are introduced in the form of dsRNA sequences and are not delimited by a nuclear transport step; they are cleaved by DICER enzyme to attain their final form. In the cytoplasm, the three pathways converge as they are all loaded to the RNA induced silencing (RISC) complex. After that, they diverge again in their mechanism of action to silence a target gene: a miRNA-RISC complex inhibits translation, whereas sh/siRNA-RISC complexes bind to mRNA sequences resulting in their degradation.

2.2. Biogenesis and Gene Silencing Mechanism of shRNA

Another form of RNAi is shRNA. shRNAs are engineered RNA sequences that can be produced within the cell from a DNA vector. The transfection of DNA that expresses shRNA into the nucleus of the target cell can be achieved by using different vectors such as lentivirus, adenovirus, plasmids, polymerase chain reaction amplicons or small circular DNA sequences [15,16]. The first transcripts of shRNAs known as pri-shRNAs with hairpin-like structures are transcribed within the nucleus [17] and then processed to give pre-shRNAs of 50–70 nt in length, which are then exported to the cytosol through Exportin-5. After cytosolic maturation, the pre-shRNA is then cleaved to generate

double-stranded fragments of 21–22 nt shRNAs. Finally, the silencing mechanism is similar to that of siRNAs, as described below [15]. The strong expression of shRNA may be less beneficial as it can alter the endogenous RNAi pathway, thus increasing the saturation of the miRNA pathway. In addition to the off-targets, the lack of an efficient delivery system poses a major challenge for shRNA-based therapy [18]. Additionally, the nonspecific binding of RNAi molecules to cellular components, such as non-targeted mRNAs, can increase the immune- and toxicity-related responses. Moreover, the use of viral vectors for delivery forces a margin of toxicity, insertional mutagenesis and immunogenicity, thus limiting their clinical application [18].

2.3. Biogenesis and Gene Silencing Mechanism of siRNA

RNAi technology has evolved over time, with the easiest approach being delivering chemically synthesized siRNAs. Primarily, siRNAs were thought to be exogenous in origin; however, several studies have identified endogenous siRNAs arising from genomic loci [19]. siRNAs are conserved among eukaryotes and involved in gene expression regulation and cell proliferation [8,20]. siRNAs are produced from a long double-stranded RNA (200–500 bp) precursor that is cleaved by Dicer via two RNase III domains. The resulting dsRNA fragments are unwound by helicase enzymes, and the antisense strand known as the guide strand is associated with a RISC to form a siRNA-RISC. This complex is then directed to the target mRNA, and the cleavage of the latter is induced by the active site residues in the P-element Induced Wimpy testis (PIWI) domain of the argonaute (AGO) protein [21].

3. Clinical Application of RNAi

Despite the recent advances in the clinical application of RNAi, the avoidance of nonspecific toxicity is a major critical challenge in the development of RNAi therapeutics. The toxicity and activity of RNAi drugs depend largely on sequences present or absent in the transcriptome. Thus, a siRNA that has no off-target effects in rodents could induce intolerable off-target-related toxicity in humans, and a siRNA that induces good silencing in animals may have insufficient activity against the human gene. Therefore, a careful preclinical development process is required. Another important issue in RNAi-based therapeutics is the possible dose-limiting toxicity of carriers, related to their heterogeneity in terms of complexity, uniformity and stability, as reviewed recently [9].

Unlike gene therapy, which is based on the modification of the genomic content within the nucleus, siRNAs act directly in the cytoplasm of cells and do not require nuclear import. Therefore, siRNA-based therapies raise a much lower threat of introducing mutations that can lead to cancer. The first RNAi-based therapeutics have been introduced into clinical practice recently. Indeed, Patisiran, the first-ever therapeutic based on RNAi, was approved by the FDA in August 2018. This siRNA specifically blocks the expression of an abnormal form of the transthyretin protein in patients with hereditary transthyretin amyloidosis [22]. The next-ever drug that was developed based on RNAi, Givlaari, was approved by the FDA in November 2019 for the treatment of acute hepatic porphyria [23]. Both drugs were developed by Alnylam Pharmaceuticals, the RNAi pioneer company that managed to encase its synthetic siRNA in a lipid-based nanoparticle and deliver it into the liver. Moreover, many studies have validated the use of siRNA to treat various viral infections, including Ebola, in non-human primates in a very specific way, as siRNAs can be tailored for each epidemic strain [24]. These studies highlight the therapeutic potential of siRNAs, a potential that is currently exploited to propose innovative solutions to target the crosstalk between the tumor cell and its environment.

3.1. RNAi and Cancer

To date, there is no RNAi-based drug approved for anticancer therapy, but several therapeutics are currently undergoing clinical trials. Originally, RNAi-based anticancer therapy was proposed to target oncogenes. In fact, proto-oncogene activation can occur through genetic alterations including gene fusion, translocation, mutation or chromosomal rearrangement [25]. Therefore, an imbalance between

proto-oncogenes and tumor suppressor genes can sustain cancer development [26]. RNAi could be used to inhibit the mRNA translation of oncogenic genes and improve chemotherapy efficiency by reducing the activity of multidrug resistance-related genes within cancer cells [27,28]. However, there are still major barriers to the systemic delivery of these macromolecules to target cells. For instance, the plasma membrane remains the major barrier to RNAi molecules due to its hydrophilic nature, global negative charge and high molecular weight, which reduces its uptake efficiency. In addition, the specificity of gene targeting, intracellular enzymatic degradation, stability and the kinetics of RNAi molecules in circulation and their local distribution are among the important parameters to be developed and optimized [29,30]. Recently, non-viral vectors, especially nanoparticle carriers such as polymers (polyethylene glycol, polyethylenimine (PEI), poly l-lysine and chitosan), lipids (lipid nanoparticles, liposomes, micelles, etc.) or inorganic nanoparticles (carbon nanotubes, gold and mesoporous silica nanoparticles), have shown multiple advantages concerning RNAi delivery [31]. In fact, nanoparticles have received considerable attention due to their ability to protect RNAi molecules from enzymatic degradation and their capacity to be associated with specific peptides, increasing their selectivity for tumor cells [32,33]. In addition, chemical modifications involving sugar and phosphate and chemical structure modifications in the oligonucleotide backbone of RNAi have been proven to be efficient as they considerably reduce toxicity, off-target effects and degradation by nucleases [34,35]. Clinical trials of RNAi-based therapeutics for solid tumors including HCC are listed in Table 1.

Table 1. Clinical trials of RNAi-based therapeutics for solid tumors including hepatocellular carcinoma (HCC). EPHA2: ephrin type-A receptor 2, PLK1: polo-like kinase 1, STMN: stathmin, EGF: epidermal growth factor, KSP: kinesin spindle protein, GMSF: granulocyte-macrophage colony-stimulating factor.

Drug Name	Target	Phase	Company	NCT Reference	Status
siRNA-EphA2-DOP C	EPHA2	Phase I	MD Anderson	NCT01591356	ongoing
TKM-PLK1/TKM-080301	PLK1	Phase I/II	Arbutus	NCT02191878	completed
pbi-shRNA STMN	STMN	Phase Ib/2	Gradalis	NCT01505153	completed
ALN-VSP02	VEGF and KSP	Phase I	Alnylam	NCT01158079	completed
Fang	Furin and GMSF	Phase I	Gradalis	NCT01061840	completed
DCR-MYC	MYC	Phase I	Dicema	NCT02314052	terminated
MRX34	miR-32 mimic	Phase I	Mirna Therapeutics	NCT01829971	terminated

3.2. RNAi-Mediated Therapeutic Intervention in the Context of HCC

The potential anticancer effects of RNAi technology show that the gene silencing of overexpressed genes in tumor cells—involved in tumor growth, proliferation, signaling pathways, drug resistance or tumor metastasis—could provide curative benefits and reduce HCC development [36]. Moreover, RNAi could target other cells in the liver and thereby modify the crosstalk between the tumor and its surrounding microenvironment to limit the potentiation effects of either of the cells on each other [37].

The use of RNAi in treating HCC comprises the RNAi molecule and its vector, and the success of such an intervention is dependent on the efficiency of the delivery system along with the RNAi efficiency, e.g., many studies have been done on the carrier to maximize the siRNA delivery. For instance, a study showed that the lipidation of a PEI-based polyplex increases the stability of the complex in vivo and results in better accumulation in the liver and knockdown in orthotopic HCC xenografts [38]. A clinical trial, NCT01591356, involving siRNA-mediated therapy in solid tumors is currently ongoing for HCC patients. It was launched by the MD Anderson Cancer Center and is expected to be completed by June 2020. This trial evaluates the effect of ephrin type-A receptor 2 (EphA2)-targeting siRNA in patients

with advanced or recurrent solid tumors using neutral liposomal delivery [39]. Furthermore, the FDA granted in 2020 an orphan drug designation to the therapeutic candidate, STP705, a siRNA targeting both the transforming growth factor (TGF)- β and cyclooxygenase-2 genes for the treatment of HCC [40].

4. Tackling the Crosstalk between the Tumor and Its Microenvironment Using RNA Interference

The tumor microenvironment is a crucial player in the progression of the tumors in all cancers, and HCC is no exception. The key to cancer progression and thriving is the presence of a milieu that sustains the cancer's multiplication and helps in combating the various stresses that come its way; among them are hypoxia and the immune response that attempts to combat the cancer. The microenvironment status is a key player in evading these stresses and creating coping mechanisms for the cancer to thrive. As explained above, inflammation drives HCC development. This suggests the key role of immune cells in the vicinity of the tumor before the emergence of HCC. A change in the status of the tumor microenvironment from a "combating" one to a "permissive" one is crucial. This is established by changes in the tumor microenvironment of the liver including many effectors: extracellular matrix (ECM) components, cancer-associated fibroblasts (CAFs), endothelial cells, hepatic stellate cells (HSCs) and immune cells (migratory and resident) (Figure 2). All of these mediate a crosstalk with the tumor via a profile of secretome ranging from chemokines, cytokines and growth factors to extracellular vesicles (e.g., exosomes) harboring effector molecules (nucleic acids and/or proteins) that aid in the tumor progression and the conversion of the milieu into a pro-tumorigenic one. This back-and-forth communication serves as a feedback loop to ensure a sustained adaptation according to the tumor status [41].

4.1. Targeting Communication with Extracellular Components

4.1.1. Extracellular Matrix (ECM)

The ECM is a mesh of an interstitial matrix and basal membrane composed of proteoglycans and hyaluronic acid that hold the organ together. However, this mesh is not only a matrix witnessing the evolution of the tumor in HCC; rather, it facilitates the interactions between the effectors and their corresponding effectors. It acts as a bridge in the crosstalk between the tumor and the different cells in the tumor's vicinity and faces many changes due to hepatocarcinogenesis [42].

Heparin sulfate (HS) plays an important role in HCC and mediates the binding of the growth factors to their respective receptor tyrosine kinases. Heparin-degrading endosulfatases sulfatase 1 and sulfatase 2 in the ECM regulate such a process [43]. As crosstalk mediators and potentiators of HCC, RNAi approaches have been developed to target the different growth factors in the vicinity of HCC.

Besides heparin sulfate, a heparan sulphate proteoglycan glypican 3 (GPC3) is located at the extracellular side of the cell membrane through a glycosylphosphatidylinositol anchor. It has recently emerged as a potential biomarker and/or therapeutic target for HCC. Silencing GPC3 in hepatocytes from proximal liver tissue and human HCC cells, with a targeted siRNA, was shown to decrease proliferation and boost apoptosis, along with a decrease in the invasive profile [44]. Furthermore, another study exploited the synergistic effect of the siRNA-mediated knockdown of GPC3 along with Sorafenib to combat HCC. Liposomes harboring GPC3 siRNA along with Sorafenib were delivered to HepG2 cells. The results showed a hindered proliferation, possibly due to the decrease in Cyclin D1 expression following GPC3 knockdown and Sorafenib administration, along with an increase in the apoptosis rate. In vivo subcutaneous xenografts of HepG2 cells in nude mice yielded results consistent with those obtained in vitro [45].

Heparanase, another important component of the ECM, plays a prominent role in tumorigenesis [46]. It contributes to the cleavage of the HS side chains of heparin sulfate proteoglycans, releasing sequestered bioactive molecules. In the context of HCC, heparanase has been shown to promote metastasis by two means: the degradation of the ECM components and a non-enzymatic

alteration of the adhesive properties of HCC [47]. Reducing the heparanase expression utilizing siRNA could efficiently inhibit tumor metastasis [48].

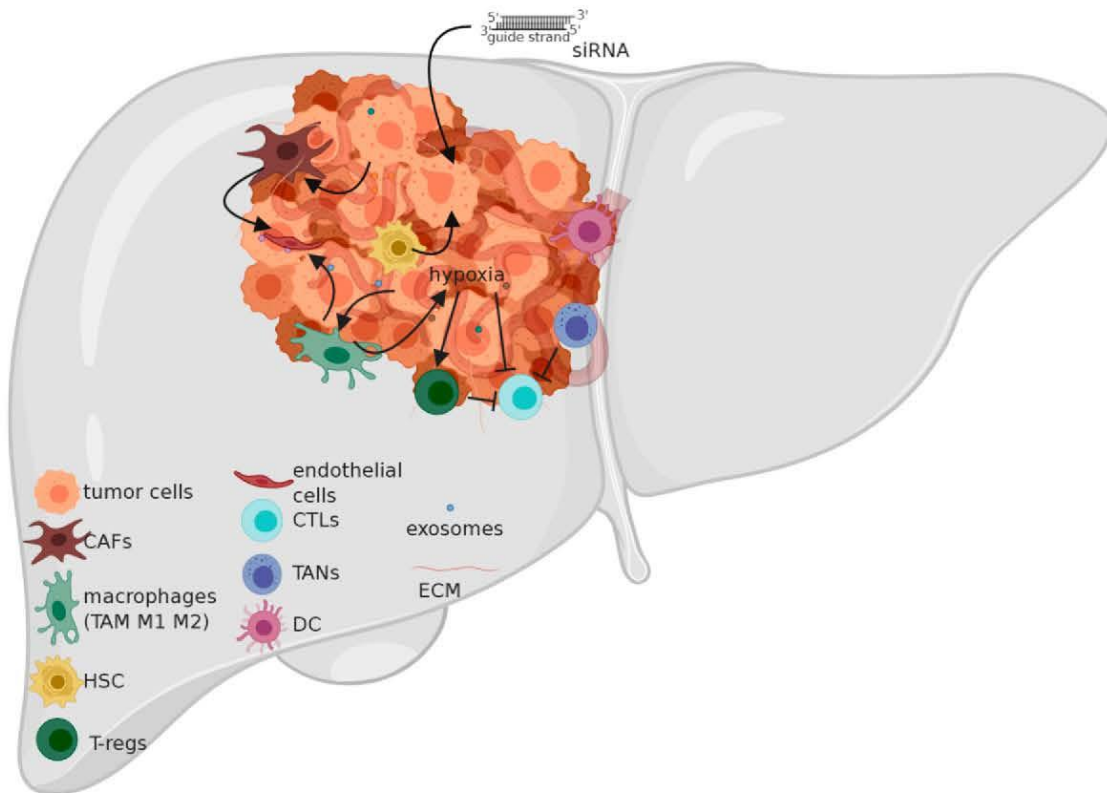


Figure 2. Tumor microenvironment in hepatocellular carcinoma (HCC). CAFs: Cancer associated fibroblasts; TAM: tumor associated macrophages; HSC: hepatic stellate cell; T-regs: T-regulatory cells; CTLs: cytotoxic T-Lymphocytes; TANs: tumor associated neutrophils; DC: dendritic cell; ECM: extracellular matrix; siRNA: small interfering ribonucleic acid. The cellular and non-cellular components of the tumor microenvironment of HCC are modulated by the tumor–tumor microenvironment communication and help the cancer to thrive by reciprocal communication. siRNAs can serve as a communication barrier by targeting the effector molecules exchanged. CAFs arise from resident cells in the tumor microenvironment and support tumor growth, survival and metastasis. TAMs are a macrophage subset that exhibits a tumor-supporting role. HSCs are modulated by the tumor to sustain its invasiveness and growth. T-regs depotentiate the immune response against the tumor. CTLs aim to combat the tumor but are often depotentiated. TANs recruit TAMs and T-regs to the tumor’s vicinity. DCs impair the T-cell response against the tumor. The ECM acts as a mediator of communication between the various cells. Exosomes shuttle effector molecules (proteins and/or nucleic acids) between the tumor and the cell of origin and vice versa.

Growth factors such as VEGF and hepatocyte growth factor (HGF), and epidermal growth factor receptor (EGFR) have been observed to be overexpressed in many cancers including HCC, as they play a crucial role in different mechanisms involving tumor proliferation, metastasis and angiogenesis [49–51]. A shRNA targeting VEGF was designed to inhibit VEGF expression in HCC cells and liver tumor tissues. The latter was administrated intratumorally or via intravenous injection into orthotopic allograft liver tumor-bearing mice. The results demonstrated a more effective suppression of tumor angiogenesis and tumor growth in the different HCC models studied [52]. Moreover, a study designed a multiple targeting siRNA which could simultaneously suppress three genes: NET-1, EMS1 and VEGF. This co-silencing reduced tumor proliferation and growth and induced tumor cell death [53,54]. Similarly, the simultaneous silencing of VEGF and KSP using a siRNA cocktail in Hep3B cells inhibited

cell proliferation, migration and invasion and also promoted tumor apoptosis [48]. In another study, a siRNA was used to suppress migration inhibitory factor (MIF) cytokines that play an important role in HCC proliferation. Upon MIF knockdown, the tumor growth rate was reduced in both HCC cell lines and in an *in vivo* xenograft model, along with an increased expression of apoptosis-related proteins [55]. As growth factors have an impact on the proliferation of HCC, RNAi targeting proliferation mediators in HCC have been utilized. Cyclin E and cyclin-dependent kinase 2 are essential actors in the cell cycle and initiation of DNA replication [56], and overexpression of cyclin E has been found in 70% of HCC cases. Accordingly, a siRNA targeting the coding region of cyclin E was designed, this showed a suppression of cyclin E expression up to 90% in HCC cell lines and also inhibited HCC tumor growth in nude mice [57].

Another group of matricellular proteins involved in HCC is cellular communication network factors (CCN), core regulatory proteins—including cysteine-rich angiogenic protein 61 (CYR61 or CCN1), connective tissue growth factor (CTGF or CCN2), nephroblastoma overexpressed (NOV or CCN3) and Wnt1-Inducible Signaling pathway proteins (WISP-1 or CCN4)—that modulate cell–matrix interactions to modify the cellular phenotype. CCNs play a role in differentiation, adhesion, migration, mitogenesis, chemotaxis and angiogenesis. The first four members of this family are shown to play a role in HCC: CCN1 to 4. CCNs induce the secretion of chemokines and cytokines to establish an inflammatory milieu and orchestrate the recruitment of immune cells to the tumor microenvironment. For instance, platelet-derived CCN1 increases the percentage of reactive oxygen species in hepatocytes, leading to macrophage activation and immunosuppression. CCN1 has also been shown to increase the expression of several proinflammatory signals through the activation of integrin–nuclear factor κ B (NF κ B) signaling in macrophages [58,59]. Moreover, fibronectin, laminin, collagen and elastin in the ECM are involved in chemotaxis and cell–cell interactions. Additionally, the laminin-5-dependent overexpression of integrins α 3 β 1 and α 6 β 4 positively correlates with the invasive and metastatic potentials of HCC cells. Changes are introduced in the adhesive and migratory characteristics of HCC cells by the α 3 β 1 integrin by the mediation of the interaction between the ECM and the cells [60]. Silencing β 1 and α v integrin subunits by the nanoparticle delivery of siRNAs in mouse liver reduced tumor proliferation and increased tumor cell death without harming the healthy liver tissue [61].

4.1.2. Extracellular Vesicles (Exosomes)

Exosomes are small membrane vesicles that are generated by many different cell types, in both normal and pathological conditions. These small nanoparticles are released by the fusion of multivesicular bodies with the plasma membrane [62]. Their role in crosstalk lies in the cargo they carry within them. Exosomes play important roles in the exchange of biological information as substance transport carriers and in the regulation of the cellular microenvironment by delivering a variety of biological molecules, including mRNAs, miRNAs and proteins. The shuttling of exosomes between the different effectors has been shown to reshape the tumor microenvironment in order to support carcinogenesis. Among the effects of exosomes are the suppression of the immune response, the favoring of angiogenesis, the remodeling of the ECM and changes in the stromal cells [63–65]. Exosomes have been shown to transfer genetic material from cancerous cells to normal ones, mediating tumor progression, traverse the blood stream to distant areas to elicit a metastatic site for the tumor, and modulate the anti-tumor immunity. On the level of the nucleic acid content of exosomes, extensive research has been done on the miRNA of HCC-derived exosomes. Studies over the years have provided a panel of miRs that are transported from the tumor to the adjacent cells, some of which are as follows: miR-584, miR-517c, miR-378, miR-520f, miR-142-5p, miR-451, miR-518d, miR-215, miR-376a, miR-133b and miR-367, miR-21, miR-192, miR-221, miR-122, miR-423-5p, miR-21-5, plet-7d-5p, let-7b-5p, let-7c-5p, miR-486-5p and miR-10b-5p, miR-519d and miR-1228. The different miRNAs modulate the gene expression in the recipient cells, favoring metastasis, tumor progression, drug resistance and recurrence [66]. Techniques to exploit miRNA to tackle the crosstalk between tumor cells and their environment have recently emerged. For instance, miR-320a, which is downregulated in several cancers,

was found to inhibit c-Myc expression in HCC tissues and cell lines. Therefore, the upregulation of miR-320a by transfecting the cells with miR-320a mimics inhibited tumor proliferation and invasion by decreasing the expression of c-Myc in HCC cells [67].

A study in 2016 described that exosomes alter drug sensitivity by releasing molecules such as mRNAs and miRNAs into neighboring cells. This study sheds the light on the activation of the HGF/c-Met/Akt signaling pathway via HCC-cell derived exosomes resulting in the inhibition of Sorafenib-induced apoptosis, thus emphasizing the role of exosomes in Sorafenib resistance in liver cancer [68]. Wang and colleagues in 2018 described that HCC cell line HepG2-derived exosomes could be actively internalized by adipocytes differentiated from mesenchymal stem cells (MSCs) and caused significant transcriptomic alterations, in particular induced inflammatory phenotypes in adipocytes [69]. Additionally, the 14-3-3 ζ protein high expression in CD8⁺ T cells induces their exhaustion. This was concluded by a comparative assessment of the expression level of programmed cell death protein-1 (PD-1), T-cell immunoglobulin and mucin domain-containing molecule-3 (TIM-3), lymphocyte-activation gene 3 (LAG3) and cytotoxic T-lymphocyte-associated protein-4 (CTLA-4) between 14-3-3 ζ ^{high} and 14-3-3 ζ ^{low} CD8⁺ T cells. Tumor-derived exosomes mediate the transfer of the 14-3-3 ζ protein to the tumor-infiltrating lymphocytes, leading to their exhaustion and/or their differentiation into T-regulatory cells (T-regs) [70].

Aside from miRNAs, exosomes have been shown to shuttle mRNAs and long ncRNAs. Many studies have shown that HCC cell lines with a great metastatic potential secrete exosomes carrying proto-oncogenes, in the form of mRNA, such as Met S100 family members and caveolin [71]. The oncogene c-Myc's abnormal expression boosts the proliferative, invasive and migrative capabilities of HCC HepG2 cells, and therefore, a plasmid-based polymerase III promoter system was used to deliver and express siRNA to silence c-Myc in HepG2 cells. The results showed that the siRNA-based knockdown of c-Myc significantly decreased its expression in HepG2 cells by up to 85%. Consequently, a significant decrease in the migration, invasion and proliferation of the HepG2 cells was recorded [72]. Another study demonstrated that the overexpression of c-Jun, a proto-oncogene involved in mitogen-activated protein kinases (MAPK) signaling, was associated with Sorafenib HCC resistance; hence, when using a siRNA tool, c-Jun downregulation was correlated with significantly enhanced Sorafenib-induced tumor apoptosis [73]. Another oncogene in HCC is polycomb complex protein BMI-1 (Bmi-1), which facilitates DNA repair and promotes survival. A recent study correlated the resistance to Cisplatin treatment with elevated Bmi-1 expression levels. Cisplatin treatment alone or in combination with other drugs is used to combat HCC, especially in non-resectable or Sorafenib-refractory HCC [74–76]. On that basis, Li and colleagues developed, in 2019, a nanoparticle delivery system incorporating both nanoplatine cores and a calcium phosphate-coated siRNA targeting Bmi-1. The efficiency of the delivery and the silencing was tested first in vitro on HepG2 cells and then in vivo on a mice xenograft model. The results showed the highest tumor inhibition in the mice treated with nanoparticles loaded with calcium phosphate coated Bmi-1 siRNA and nanoplatine cores in comparison to that in the control groups [77].

Furthermore, a study showed that CD90⁺ Huh7 cells (HCC cell line) secreted exosomes harboring H19, a lncRNA, and once in the target cells, it upregulated the expression and release of VEGF, thus stimulating angiogenesis and the adherence of CD90⁺ Huh7 cells to endothelial cells [78], further stressing the importance of VEGF as a target for RNAi. A study was conducted in 2018 utilizing a galactose-derivative-modified nanoparticle harboring VEGF siRNA for an attempted knockdown. The results showed that VEGF siRNA loaded in asialoglycoprotein receptor-targeted nanoparticles silenced VEGF both in vitro and in vivo, demonstrated potent anti-angiogenic activity in HCA-1 tumors and suppressed primary HCC growth and distal metastasis [79]. A more recent study focused on attaining a synergistic effect by co-loading pH-sensitive liposomes loaded with a siRNA targeting VEGF, and Sorafenib. The system was tested in two-dimensional cultured HepG2 cells, three-dimensional HepG2 tumor spheroids and tumor regions of H22 tumor-bearing mice. The results showed a successful uptake of the system and decreased VEGF expression in all models along with

an induction of apoptosis [80]. Moreover, and due to its role in drug resistance, a C-X-C chemokine receptor (CXCR) type-4-targeted lipid-based nanoparticle along with a modified antagonist of CXCR4, AMD3100, was designed to specifically deliver VEGF siRNA [81]. The results showed that the efficient downregulation of VEGF expression both in vitro and in vivo and together with Sorafenib led to synergistic tumor growth inhibition compared to Sorafenib only, suggesting that the use of siRNA in cancer therapy could increase drug efficacy [82].

4.2. Targeting Communication with Cellular Components

4.2.1. Cancer-Associated Fibroblasts (CAFs)

CAFs are cells that trans-differentiate from different resident cells in the liver, mainly fibroblasts, but they can also derive from epithelial cells, endothelial cells, local mesenchymal cells, smooth muscle cells, pre-adipocytes and bone-marrow-derived progenitors [83–86].

Their trans-differentiation can be mediated by the tumor necrosis factor (TNF)- α and platelet-derived growth factor (PDGF) secreted by the macrophages [87]. HCC derives from a cirrhotic background, which involves a strong activation of fibroblasts, the main precursor of CAFs [88,89]. TNF- α was shown to upregulate the expression of the transcription factor apoptosis-antagonizing transcription factor (AATF) via its regulatory element site of sterol regulatory element-binding protein-1 in both HepG2 and Huh-7 cell lines via the siRNA targeting of the formerly mentioned regulatory element site. Furthermore, the knockdown of AATF in the HCC cell line QGY-7703 inhibited proliferation, migration, anchorage-independent growth, invasion and colony formation. A decrease in the tumorigenicity was also shown in the QGY-7703 xenograft model of NSG mice (non-obese diabetic severe combined immunodeficiency (SCID) gamma mice) harboring AATF knockdown. This study stresses the importance of TNF- α in HCC thriving [90].

On the level of tumor microenvironment priming, CAFs intercalate in the ECM and secrete ECM components. Among these, it is worth mentioning type 1 collagen fibers, fibronectin, tenascin and secreted protein acidic and rich in cysteine. Immune modulation-wise, CAFs secrete cytokines (interleukin(IL)-1, IL-6 etc.) and chemokines (monocyte chemoattractant protein-1 (MCP-1), C-X-C motif ligand (CXCL)-12 etc.). By the secretion of CXCL-12, CAFs also recruit endothelial progenitor cells to the tumor's vicinity, thus supporting tumor vascularization [87]. To further support the tumor's growth, CAFs produce and secrete growth factors (EGF, fibroblast growth factor (FGF), HGF and TGF- β) [91,92]. In addition, CAFs have been shown to secrete C-C motif ligand-(CCL)-2, -5 and -7 and CXCL-16, which in turn promote metastasis to bone, brain and lung in SCID mice via the activation of the TGF- β pathway [93], thus stressing the wide array of pathways activated by the crosstalk between CAFs and the tumor. These pathways are the focus of RNAi interventions.

4.2.2. Endothelial Cells

Endothelial cells are important for the tumor as they are the nutrient and oxygen suppliers. In addition, they mediate crosstalk with the tumor via a change in the expression profile of receptors, rendering them responsive to signals derived from the tumor microenvironment and the tumor itself, while also secreting a variety of cytokines to communicate with the tumor [94]. The phenotype changes can be summarized by an upregulation of the expression of endoglin along with that of the various angiogenic receptors: VEGF receptor (VEGFR), EGFR, PDGF receptor (PDGFR) and CXCR [94]. RNAi-based gene silencing delivered by an optimized immunoliposome induced an effective EGFR gene knockdown in mice bearing orthotopic HCC, thereby showing the potential of this promising therapy [53]. The role of endoglin is prominent as it is activated by a variety of TGF- β superfamily members. It facilitates the extravasation of leukocytes into the site of inflammation and induces the "leaking" of chemotaxis factors into the bloodstream. Several studies have underlined the importance of IL-8-mediated inflammation in metastatic HCC through the activation of the transcription factor

forkhead box C1 or via integrin $\alpha v\beta 3$ [95]. The silencing of IL-8 with siRNA showed that it could be used to reduce the tumor metastasis mediated by IL-8 [96].

4.2.3. Hepatic Stellate Cells (HSCs)

HSCs are normally non-proliferating cells residing in the liver, ready to be activated upon injury. These cells are primarily activated by signals from injured Kupffer cells, injured platelets or any other type of injured cell in the vicinity. In the context of HCC, HSCs are activated during the fibrogenesis process that precedes the tumorigenesis and continue to secrete ECM components. HSCs can be activated by HBV, HCV, cathepsins B and D, PDGF, TGF- $\beta 1$, matrix metalloprotease (MMP)-9, JNK and insulin-like growth factor-binding protein 5 (IGFBP-5), and they can infiltrate into the HCC stroma. Once there, they stimulate tumor vascularization through the secretion of VEGF-A and MMP-2 [45]. They are known to secrete laminin-5, increase cytokine production, and exhibit liver-specific pericyte properties [97]. Various studies have been performed to stress the importance of the reciprocal crosstalk between HSCs and the tumor. A recent study showed that the crosstalk between HSCs and HCC via PDGF- β induced the increase in the expression of regenerating islet-derived protein 3 alpha (REG3A) in HCC cells. Furthermore, the silencing of REG3A via siRNA led to a decrease in the proliferation of LX-2 HCC cells when cocultured with the HSC cell line MH134. This is shown to be a result of the modulation of the p42/44 pathway [98].

A study showed an increase in the proliferation rate of rat HSCs following culturing with conditioned tumoral hepatocyte media, accompanied by an increase in α -smooth muscle actin expression and desmin, PDGFR and Gelatinase A secretion—markers of CAFs [99]. Another study showed the reciprocal priming of HSCs to the tumor. It showed that the conditioned media of HSCs increased the growth and invasiveness of HCC. Similar results were obtained upon the co-implantation of HSCs and HCC cells in nude mice, which appears to be as a result of activated NF κ B and extracellular signal-regulated kinase (Erk) signaling pathways [100,101]. In that context, silencing Erk1 and Erk2 using siRNAs enhanced Fluorouracil sensitivity and increased Fluorouracil-induced apoptosis in the HCC HepG2 cell line, thus promoting chemosensitivity [102].

4.2.4. Immune Cells

The landscape of the tumor microenvironment of HCC comprises a complex set of immune cells with their intricate cytokine and chemokine secretions. The immune responses sustained against HCC include the cytotoxic T-cells (CTLs), which produce perforin and granzymes to kill the cancer cells upon activation. The frequency of CTLs in the tumor's vicinity is positively correlated with survival. However, the crosstalk in the tumor's vicinity between the tumor and these cells, along with effector molecules and immunosuppressive cells, namely T-regs, hinders the function of CTLs [43]. The tumor microenvironment plays a pivotal role in the immune evasion by establishing an immunosuppressive profile. The preferential activation of subsets of immune cells and their subsequent secreted chemokines and cytokines are the means for such a process. The crosstalk mediated between the immune cells and the tumor via the different secretory components plays a major role in the tumor's progression.

Macrophages

As HCC is a result of chronic inflammation, the persistent inflammatory signal drives the constant recruitment of monocytes into the inflammatory site along with an alteration in the bone marrow signal to favor the increased output of myeloid cells [103]. Thus, the pool of macrophages in the tumor site results from the invasion of circulating macrophages added to the pre-existing macrophages in the liver, termed Kupffer cells. The pool is heterogenous in terms of macrophage subtypes: M1, M2 or Tumor Associated Macrophages (TAMs) [104]. It has been shown that macrophages display a plasticity between the two major types of M1 and M2 macrophages. However, the line for discriminating between the two subtypes is not yet crystal clear. Principally, M1 macrophages (classically activated) are pro-inflammatory and are associated with anti-tumorigenic activity, whilst M2 macrophages

(alternatively activated) are anti-inflammatory and favor tumorigenicity. The cell fate is decided by extrinsic factors ranging from growth factors, cytokines and chemokines to microenvironment stress. M1 macrophages are stimulated by interferon (IFN)- γ along with a TLR agonist such as lipopolysaccharide. M2 macrophages, on the other hand, are stimulated by IL-4, IL-10 and IL-13. The differentiation implicates phenotypical, genetic, epigenetic, metabolic and secretome changes. Of major importance in the context of cancer is the profile of the secretion of each macrophage subtype. On the level of M1 macrophages, they exhibit a typical pro-inflammatory cytokine and chemokine profile: TNF- α , IL-1, IL-6, IL-12, IL-18, IL-23, MCP-1, CXCL9 and CXCL10. As for M2 macrophages, they are known for the secretion of IL-10, IL-12^{low}, CCL17, CCL22 and CCL24 [104,105]. M2 macrophages are active effectors in the context of HCC. A clinical study in 2014 showed a poor prognosis for patients exhibiting an increased expression of CD-163 and Scavenger A macrophages (markers for M2 macrophages). This was accompanied by increased tumor nodules and venous infiltration in HCC, along with an increased epithelial–mesenchymal transition potential via M2 macrophage CCL22 secretion [106]. Another study showed that M2 macrophages accumulated more in Sorafenib-resistant HCC tumors than in Sorafenib-sensitive ones, and confer Sorafenib resistance by secreting HGF, which sustains tumor growth and metastasis by the activation of the HGF/c-Met, ERK1/2/MAPK and PI3K/AKT pathways in tumor cells [107].

Several targeting mediators of tumor cells are secreted by macrophages and have been studied in the development and progression of HCC. In the context of targeting MAPK signaling, which is overexpressed in HCC and associated with tumor growth, the downregulation of mitogen-activated protein kinase kinase kinase 4 (MAP4K4) using shRNA led to reduced cell proliferation, S-phase cell cycle blockade and increased tumor apoptosis [108]. Another signaling pathway targeted by RNAi is HGF/c-Met. A study showed that small ubiquitin-like modifier (SUMO) specific protease 1 silencing resulted in a downregulation of HGF-induced proliferation and migration of HCC cells through effects on the HGF/c-Met pathway [109]. Additionally, in order to inhibit the proliferation of HCC cell lines (HepG2 and Huh7), siRNA targeting a tyrosine kinase receptor known as macrophage-stimulating protein receptor was shown to efficiently suppress tumor cell migration and invasion and enhance apoptosis by activating cleaved caspase-3 and poly (ADP-ribose) polymerase through the modulation of the Akt, c-Raf and ERK signaling pathway [110]. A study in 2019 by Zhang and colleagues evaluated the expression of sirtuin 6 (SIRT6) in a variety of HCC cell lines and its effect on the Erk1/2 signaling pathway favoring proliferation and inhibiting apoptosis. The results showed an elevated expression of SIRT6 in nine HCC cell lines in comparison to in a normal liver cell line. Moreover, the knockdown of SIRT6 via a siRNA approach in the Huh-7 cell line resulted in a decrease in the proliferation rate along with an increase in the apoptosis rate, with a downregulation of B-cell lymphoma 2 (Bcl-2) and an upregulation of Bcl-2-associated X protein (Bax) and cleaved-caspase 3. This was accompanied by a decrease in the phosphorylation of Erk1/2 [111]. Epithelial cell transforming sequence 2 (ECT2) has been shown to be implicated in early HCC recurrence via the activation of Rho/Erk signaling. The downregulation of ECT2 by siRNA entailed the suppression of Erk, thereby enhancing apoptosis and reducing the metastatic ability of HCC cells [112]. Further focusing on Rho, Ras homolog family member C (RhoC) overexpression and the metastatic potential of HCC have been correlated with the enhanced invasion and migration of HCC cells. The inhibition of RhoC resulted in the inhibition of invasion and migration without reducing cell viability in HCCLM3 cells. In addition, the silencing of RhoC expression in an HCC metastatic mouse model significantly inhibited tumor metastasis [113].

Another subset of macrophages termed “TAMs” was found in the vicinity of HCC tumors. Studies have shown that the presence of TAMs in the tumor’s vicinity correlates with poor prognosis in HCC. These cells exhibit an M2-like phenotype and express both M1 and M2 macrophage hallmarks. They secrete pro-inflammatory cytokines, e.g., IL-1 β , IL-6, IL-23 and TNF- α . A recent study demonstrated that the interaction of TNF- α and angiotensin II in HCC cells could enhance tumor proliferation, migration and invasion via the regulation of G protein-coupled receptor kinase 2 (GRK2). Therefore, GRK2 siRNA was used to examine the molecular interactions of TNF- α in tumor growth,

and the obtained results suggested that TNF- α could serve as a new potential therapeutic target in HCC [114]. TAMs also secrete a variety of growth factors such as TGF- β , VEGF, FGF, PDGF, angiogenic factor thymidine phosphorylase, angiogenesis-modulating enzyme cyclooxygenase-2, MMP-9 and MMP-12 [105,115]. On the level of immune response modulation, TAMs have been shown to suppress CD4⁺CD25⁻ T cells, activate T-regs and contribute to the expansion of Th-17 cells, which, in turn, favor the expression of the immune-suppressing antigens PD-1, CTLA-4 and glucocorticoid-induced TNF receptor family-related (GITR) [116,117]. Moreover, TGF- β in the tumor microenvironment triggers the expression of TIM-3 on the surface of TAMs and subsequent IL-6 secretion; the TAM-derived IL-6 further activates the IL-6/signal transducer and activators of transcription (STAT3) pathway in the tumor, sustaining survival and proliferation [43,118]. When HCC cell lines (SMMC7721 and QGY-7703) were transfected with siRNA targeting STAT3 and AKT2, a significant decrease in the mRNA level of AKT2 and STAT3 was observed. Furthermore, nude mice were used to verify the correlation, and a decreased ability for HCC cell proliferation, migration and invasion has been since concluded [119].

Neutrophils

Neutrophils in the vicinity of a tumor are termed tumor-associated neutrophils (TANs). As is the case with macrophages, TANs in the tumor microenvironment exhibit two polarizations: N1 neutrophils that are said to be anti-tumorigenic and N2 neutrophils that are said to be pro-tumorigenic [120]. Their activation is governed by type 1 IFNs and TGF- β . Their main role in tumors is to suppress CD8⁺ T-cells, thus helping the tumor evade the immune response. Nitric oxide production by TANs, induced by TNF- α in the tumor microenvironment, promotes CD8⁺ T-cell apoptosis [121]. In the context of HCC, TANs exhibit the same role as in different cancers, associating with poor prognosis and driving tumor progression. The neutrophil-lymphocyte ratio (NLR) is of great significance in patients subject to immunotherapy (Programmed cell death 1 (PD-1)/PDL-1) and correlates with tumor progression [122,123]. On the clinical level, NLR has been shown to be an indicator of survival after hepatectomy [124,125]. Recent studies have shown that the accumulation of TANs via hypoxia-inducible factor (HIF)-1/CCL5 upregulation in NASH drives the initiation and progression into HCC [126]. While in the tumor's vicinity, TANs secrete chemokines such as CCL2 and CCL17, which, in turn, recruit TAMs and T-regs, thus contributing to HCC progression, metastasis and resistance to Sorafenib treatment [127]. Interestingly, the downregulation of CXCL5—a direct chemoattractant for neutrophils—by shRNA in HCC cells reduced tumor growth, metastasis and intratumoral neutrophil infiltration [128].

Dendritic Cells

Dendritic cells (DCs) in a healthy liver play the role of bridging the innate and adaptive immunity as antigen-presenting cells (APCs) as well as of instructing lymphocytes. The most prominent role of DCs in HCC is mediating immune tolerance. Thus, the crosstalk between DCs, the tumor and its tumor environment is mediated by the secretion of various cytokines, leading to immune tolerance and tumor progression. At first hand, the activation of DCs is mediated by IFN- γ secretion by the tumor or effector cells in the vicinity. Upon activation, DCs tend to secrete IL-10 and IL-12. IL-12 leads to the impaired activation of allogenic T-cells. IL-10 depotentiates the immune response against the tumor and excludes APCs from the tumor mass [129]. It is important to mention that the DCs are emerging targets for immune therapy in the context of HCC, thus further stressing the fact that the crosstalk between DCs, immune cells and the tumor is crucial for tumor progression [130]. A study demonstrated that the anti-tumor effect of IFN- γ , which mediates cell death by autophagy, can be regulated by the modulation of interferon regulatory factor (IRF)-1 by shRNA [131]. On another note, IFN-stimulated gene 15 (ISG15) is a ubiquitin-like molecule that has been identified as an intrinsic actor that elicits HCC tumorigenesis and metastasis; the former is overexpressed in HCC patients. Using cell lines and a xenograft model, the siRNA-mediated knockdown of ISG15 was shown to significantly inhibit tumor growth [132].

Natural Killer Cells

Natural killer (NK) cells are prominent in the liver and are the first responders against viral infections (HBV and HCV). NK cells are also in charge of maintaining proper immune function as they regulate the tuning of the immune response between the defensive and tolerance modes [105,133]. The inhibitory function of NK cells in HCC supports the tumor thriving. Growing evidence suggests that the hypoxic conditions inducing the activation of HIF-1 α along with immune modulators in the tumor microenvironment disrupt the regulating ability of NK cells, resulting in the exhaustion of the anti-tumor response and poor prognosis [134]. Interestingly, the RNAi-mediated suppression of HIF-1 α expression in the liver inhibited metastatic tumor growth in the hepatoma cell line (SMMC-7721) and tumor-bearing mouse liver [135,136]. NK cells can be inhibited by HCC cells as HCC cells express major histocompatibility complex (MHC) class I polypeptide-related sequence A, a specific NK cell ligand that inhibits NK cell interaction [91,105]. Another mechanism of the depotentiation of NK cells by HCC cells is the impairment of IL-12 secretion by DCs by HCC cell-derived α -fetoprotein (AFP). A more direct effect of AFP has been shown on NK cells and is dictated by the time frame [137,138]. T-regs play a role in the attenuation of the NK cell's function, either by the release of cytokines such as IL-8, TGF- β 1 and IL-10—which then decrease the expression of NK receptors' ligands on HSCs, preventing them from binding to the NK group 2D receptor on NK cells—or by their competition with NK cells for the available IL-2 in the tumor microenvironment [139]. Moreover, the attenuation of the production of TNF- α and IFN- γ by NK cells mediated by CAF-derived indoleamine-pyrrole 2,3-dioxygenase and prostaglandin E2 has been shown to be among the reasons for sustained fibrosis in HCC and immune cell evasion [140].

5. Challenges and Future Perspectives

HCC is a primary type of liver cancer with a high mortality rate and a poor prognosis. It has varying advancement and occurrence rates epidemiologically according to the environmental factors in each region of the world, stressing a vast group of risk factors [141]. To date, the treatment options for this type of cancer are Sorafenib, Lenvatinib, Regorafenib and Cabozantinib, which improve patient prognosis but with the cost of side effects and deterioration in the quality of life. Hence emerges the need for alternative treatment options. Research in this field has increased dramatically, with the search for other first-line and second-line treatment options exploiting various angles: immunotherapy, selective tyrosine kinase inhibitors, anti-angiogenic agents or combination therapy, among others. Aligned with these current developments, a first-in-human study of the small double-stranded activating RNA oligonucleotide MTL-CEBPA has shown that the pre-treatment of the HCC tumor microenvironment with MTL-CEBPA renders it more susceptible to the effects of established anti-HCC therapies, which shows the great potential of innovation in HCC treatment [142]. As extensive as the search for alternative treatments is, another approach is exploiting RNAi for a highly targeted therapy, targeting the impairments of the different molecular pathways in HCC exacerbated by the extensive crosstalk with the tumor microenvironment actors, as described in this review. However, such an approach faces many difficulties that need to be addressed. As previously explained, the definitive actor and director of such an approach is the nucleic acid composed of either an siRNA, shRNA or miRNA.

This tool confers the advantage of designing an intervention down to the gene level. si/sh/miRNA sequences can be customized to target a specific gene or even a gene corresponding to a specific isotype of the protein. Part of the equation in RNAi is the specificity of the effector molecule and its "exclusive" effect on the set target. An extended analysis should be done on the off-target effects of a given RNAi tool prior its use to provide a better picture of the biosafety. The off-targets of such an approach can be predicted by *in silico* methods, unlike those of small-molecule drugs, where the undesired effects often remain unraveled until further *in vitro* and *in vivo* testing. Moreover, a study published in 2019 showed that multiple cancer drug candidates kill tumor cells through off-target effects instead of by interacting with their intended molecular targets. They showed by the clustered

regularly interspaced short palindromic repeats (CRISPR)-Cas9 deletion of a target that small-molecule drugs kill the target-KO cells as efficiently as the wild-type cells, suggesting that not on-target but rather off-target interactions are frequently the real mechanism by which small-molecule drugs block cancer growth [143]. On the other hand, the *in silico* study of the sequences of RNAi, via “NCBI blasting” for instance, gives an overview of the possible off-target effects via a simple blasting of the sequence of interest against the whole genome of humans—or any other organism. The results show a list of the various annealing possibilities, which could be tested and controlled prior to functional assessment. One additional advantage is the possibility of designing sequences that cross-react among species. Exploiting the “NCBI blasting” *in silico* system and blasting the sequence of interest against rodent and human genomes could result in a candidate sequence that can be used in both. This is one of the great advantages of utilizing RNAi as a treatment option, as the molecule tested preclinically in an *in vivo* rodent model is exactly the same as the one that will be used in humans, which could minimize the variables to be controlled in clinical trials.

The effectiveness of RNAi is dictated by the ability of the si/sh/miRNAs to reach their targets. The obstacles faced in an *in vitro* system are mainly the cell membrane and the endosomal escape. The selectivity of the cell membrane hinders the internalization of the sequences introduced; thereafter, the endosome poses a great threat to the integrity of the sequences, as they could be degraded by endosomal enzymes. Moreover, in a complex *in vivo* system, the obstacles are exacerbated due to the complexity of the human body [144]. Great progress has been made during the past decade regarding the delivery of RNAi. There are still many challenges for extrahepatic organs, where RNAi delivery by oral or intravenous administration is still limited due to vascular barriers. However, the liver is the prime organ target for systemically delivered RNAi due to its relatively open vasculature. Furthermore, researchers are taking advantage of the expression of the asialoglycoprotein receptor on the surface of hepatocytes to ameliorate the delivery to the liver [145]. Recently, RNAi administration during liver machine preservation was proposed. This technique harbors many advantages as it can further increase the targeted delivery to the liver with lower RNAi doses and, subsequently, at a lower cost while avoiding side effects on other organs [146]. These approaches may open up novel possibilities for RNAi therapeutics in the HCC field.

Various studies in the RNAi field have focused on modulating the carrier to increase the efficiency of the delivery by regulating the variables of size, charge, pH, composition, etc. Additionally, the development of transport carriers capable of selective siRNA delivery is particularly important when targeting the tumor microenvironment. A liver with HCC tumors is known to contain an abundant population of immune cells with immunosuppressive functions in the tumor microenvironment. RNAi therapeutics that could restore the anti-tumor immune response in HCC are needed, but the development of transport carriers capable of the selective delivery of siRNA to specific immune cells remains challenging. The effect of a siRNA could be cell-dependent, as different cells would express different isoforms and/or amounts of the mRNA of a specific target. As reviewed in this article, the expression level of a given protein may have a drastic effect on the secretory profile of the cell—taking into account the different subpopulations of T-cells, macrophages and neutrophils, each with their own transcriptomic profile. Thus, the effect of an siRNA targeting a specific protein could be contradictory if it not delivered to the right cell population and/or subpopulation. Moreover, it is important to keep in mind that some carriers, without taking into account the siRNA carried, can modulate the immune system, especially the functions of APCs [147].

One carrier of natural origin, which could avoid the hindrances of synthetic nanoparticle carriers, is exosomes. As described in the article, these extracellular vesicles serve as shuttles of nucleic acids and proteins that are the means of intercellular communication between the various cell types. The notion of exosomes became clearer over time, as they were once said to be “waste disposal vehicles” before their crucial role in cell communication was unraveled. Exosomes are of particular interest in immune cells’ communication as they are naturally excreted from several immune cells including dendritic cells, T-cells, mastocytes and B-cells [148], and have been reported to be a key effector of

inflammation and tumor microenvironment communication [149]. Exosomes have been shown to activate or suppress innate immunity and regulate the TLR/NFκB signaling pathway. Interestingly, exosomes have been exploited as ways of administering epitopes for anticancer vaccination. Moreover, exosomes have become incorporated in theragnostic approaches and facilitated the access to biomarkers to follow the evolution of the disease through miRNAs carried in exosomes, especially in lung cancer, liver cancer, gastrointestinal cancer, pancreatic cancer, melanoma, breast cancer, ovarian cancer and prostate cancer [63]. During the past years, exosomes have been studied as a new natural vector for shuttling RNAi molecules due to their high biocompatibility for various reasons: (i) exosomes are delimited by a lipid bilayer, which confers a great advantage when fusing with other cell types; (ii) exosomes can utilize a receptor-mediated endocytosis mechanism for cell entry, thus conferring a specific cell targeting advantage; and (iii) exosomes have been shown to traverse the bloodstream easily, establishing metastatic niches for cancer, thus avoiding the hindrances of the vascular barriers facing other RNAi carrier particles [150,151]. In that context, Morishita and colleagues performed an *in vivo* study on the bioavailability of exosomes. The results showed that exosomes were mostly concentrated in the liver, spleen and pancreas in addition to other abdominal organs and the lungs [152], shedding light on a possible enhancement of liver targeting. However, loading cargo into exosomes remains challenging [149], and developing new strategies to vectorize RNAi molecules through exosomes could be rendered beneficial in exosome-RNAi therapy. In the meantime, new RNAi vectors developed based on natural exosomes are under investigation and have shown promising results for efficiently delivering RNAi molecules. This is highlighted by the study of Lunavat and colleagues where they delivered c-Myc specific siRNA into cancer cells through exosome-mimetic nanovesicles [153]. More recently, the study of Zhou and colleagues has shown that the delivery of Kirsten Rat Sarcoma viral oncogene homolog siRNA with internalizing arginylglycylaspartic acid (RGD) exosomes efficiently inhibits tumor growth in a mouse model of lung cancer [154].

As complex as the optimization process is, RNAi still serves as a source of hope and a valid candidate for a treatment option for HCC. We are optimistic that with the advancements in the scientific approaches and the continuous unraveling of the molecular impairments that drive HCC, an RNAi approach with the correct combination of a carrier and a nucleic acid component will one day significantly improve the outcomes of HCC patients.

Author Contributions: Conceptualization, M.M., F.C. and Z.M.J.; methodology, M.M. and F.C.; writing—original draft preparation, M.M. and F.C.; writing—review and editing, M.M., F.C., T.D., Z.M.J. and P.N.M.; supervision, F.C. and Z.M.J.; project administration, T.D. and P.N.M.; funding acquisition, T.D. and P.N.M. All authors have read and agreed to the published version of the manuscript.

Funding: This research was funded by “Dotation Agir pour les Maladies Chroniques”, France. This project has received funding from the European Union’s Horizon 2020 research and innovation program H2020 “NEWDEAL” (grant agreement No. 720905). F.C. was supported by a fellowship from the H2020 NEWDEAL project; M.M. was supported by a fellowship from the Lebanese University, Lebanon. This publication reflects only the author’s view, and the Commission is not responsible for any use that may be made of the information it contains.

Acknowledgments: M.M. acknowledges the Lebanese University in Lebanon and, namely, Bassam Badran and Nader Hussein for their support. Additionally, we thank Bertin Ndayishimiye and Nazareth Carigga-Gutierrez for helping to build a library of published studies.

Conflicts of Interest: The authors declare no conflict of interest.

Abbreviations

HCC	hepatocellular carcinoma
RNAi	RNA interference
HCV	viral hepatitis C
HBV	viral hepatitis B
NASH	non-alcoholic steatohepatitis
PDL-1	anti-programmed death-ligand1
VEGF	anti-vascular endothelial growth factor

mRNA	messenger RNA
ncRNA	non coding RNA
dsRNA	double-stranded RNA
TLR	Toll-like receptor
miRNA	microRNA
shRNA	short hairpin RNA
siRNA	small interfering RNA
nt	nucleotide
pri-miRNA/shRNA/siRNA	primary-miRNA/shRNA/siRNA
pre-miRNA/shRNA/siRNA	precursor-miRNA/shRNA/siRNA
RISC	RNA induced silencing complex
PEI	polyethylenimine
EPHA2	ephrin type-A receptor 2
PLK1	polo-like kinase 1
STMN	stathmin
KSP	kinesin spindle protein
GMSF	granulocyte-macrophage colony-stimulating factor
TGF	transforming growth factor
ECM	extracellular matrix
CAFs	cancer associated fibroblasts
HSCs	hepatic stellate cells
TAMs	tumor associated macrophages
TANs	tumor-associated neutrophils
DCs	dendritic cells
T-regs	T-regulatory cells
HS	heparin Sulfate
GPC3	glypican 3
EGF	epidermal growth factor
HGF	hepatocyte growth factor
EGFR	epidermal growth factor receptor
NET-1	neuroepithelial cell transforming-1
EMS1	<i>gene encoding protein: leucine-rich repeat receptor protein kinase EMS1</i>
MIF	migration inhibition factor
CCN	cellular communication network factor
CYR61	cysteine-rich angiogenic protein 61
CTGF	connective tissue growth factor
NOV	nephroblastoma overexpressed
WISP-1	Wnt1-Inducible Signaling pathway proteins
NFκB	nuclear factor kappa B
MSCs	mesenchymal stem cells
TIM-3	T-cell immunoglobulin and mucin domain-containing molecule-3
LAG3	lymphocyte-activation gene 3
CTLA-4	cytotoxic T-lymphocyte-associated protein-4
MAPK	microtubule associated protein kinase
Bmi-1	polycomb complex protein
CXCR	C-X-C chemokine receptor type
TNF	tumor necrosis factor
PDGF	platelet-derived growth factor
AATF	apoptosis-antagonizing transcription factor
NSG	non-obese diabetic severe combined immunodeficiency gamma mice
SCID	severe combined immunodeficiency
IL	interleukin
MCP-1	monocyte chemoattractant protein-1
CXCL	C-X-C motif ligand
FGF	fibroblast growth factor

CCL	chemokine C-C motif ligand
VEGFR	vascular endothelial growth factor receptor
PDGFR	platelet-derived growth factor receptor
MMP	matrix metalloprotease
GTIR	glucocorticoid-induced TNF receptor family-related
IGFBP-5	insulin-like growth factor-binding protein 5
REG3A	regenerating islet-derived protein 3 alpha
Erk	extracellular signal-regulated kinases
CTLs	cytotoxic T-cells
IFN	interferon
MAP4K4	mitogen-activated protein kinase kinase kinase kinase 4
SUMO	small ubiquitin-like modifier
SIRT6	sirtuin 6
Bcl-2	B-cell lymphoma 2
Bax	Bcl-2-associated X protein
ECT2	epithelial cell transforming sequence 2
RhoC	Ras homolog family member C
GRK2	G protein-coupled receptor kinase 2
GTIR	glucocorticoid-induced tumor necrosis factor receptor
STAT3	Signal Transducer and Activators of Transcription
NLR	neutrophil–lymphocyte ratio
PD-1	programmed cell death protein-1
HIF-1	hypoxia-inducible factor
APCs	antigen-presenting cells
IRF	interferon regulatory factor
ISG15	IFN-stimulated gene 15
NK	natural killer
AFP	α -fetoprotein
CRISPR	clustered regularly interspaced short palindromic repeats
RGD	arginylglycylaspartic acid

References

1. Fitzmaurice, C.; Allen, C.; Barber, R.M.; Barregard, L.; Bhutta, Z.A.; Brenner, H.; Dicker, D.J.; Chimed-Orchir, O.; Dandona, R.; Dandona, L.; et al. Global, Regional, and National Cancer Incidence, Mortality, Years of Life Lost, Years Lived with Disability, and Disability-Adjusted Life-years for 32 Cancer Groups, 1990 to 2015: A Systematic Analysis for the Global Burden of Disease Study. *JAMA Oncol.* **2017**, *3*, 524–548. [[CrossRef](#)] [[PubMed](#)]
2. Ogunwobi, O.; Harricharran, T.; Huaman, J.A.; Galuza, A.; Odumuwaqun, O.J.; Tan, Y.; Ma, G.X.; Nguyen, M.T. Mechanisms of hepatocellular carcinoma progression. *World J. Gastroenterol.* **2019**, *25*, 2279–2293. [[CrossRef](#)] [[PubMed](#)]
3. Llovet, J.M.; Ricci, S.; Mazzaferro, V.; Hilgard, P.; Gane, E.; Blanc, J.-F.; de Oliveira, A.C.; Santoro, A. Sorafenib in Advanced Hepatocellular Carcinoma. *N. Engl. J. Med.* **2008**, *359*, 378–390. [[CrossRef](#)] [[PubMed](#)]
4. Medavaram, S.; Zhang, Y. Emerging therapies in advanced hepatocellular carcinoma. *Exp. Hematol. Oncol.* **2018**, *7*, 17. [[CrossRef](#)]
5. Keating, G.M. Sorafenib: A Review in Hepatocellular Carcinoma. *Target. Oncol.* **2017**, *12*, 243–253. [[CrossRef](#)]
6. FDA Approves Atezolizumab Plus Bevacizumab for Unresectable Hepatocellular Carcinoma. Available online: <https://www.fda.gov/drugs/drug-approvals-and-databases/fda-approves-atezolizumab-plus-bevacizumab-unresectable-hepatocellular-carcinoma> (accessed on 15 June 2020).
7. Fire, A.; Xu, S.; Montgomery, M.K.; Kostas, S.A.; Driver, S.E.; Mello, C.C. Potent and specific genetic interference by double-stranded RNA in *Caenorhabditis elegans*. *Nature* **1998**, *391*, 806–811. [[CrossRef](#)]
8. Mansoori, B.; Shotorbani, S.S.; Baradaran, B. RNA interference and its role in cancer therapy. *Adv. Pharm. Bull.* **2014**, *4*, 313–321. [[CrossRef](#)]

9. Setten, R.L.; Rossi, J.J.; Han, S.-P. The current state and future directions of RNAi-based therapeutics. *Nat. Rev. Drug Discov.* **2019**, *8*, 421–446. [[CrossRef](#)]
10. Wang, Q.; Carmichael, G.G. Effects of Length and Location on the Cellular Response to Double-Stranded RNA. *Microbiol. Mol. Biol. Rev.* **2004**, *68*, 432–452. [[CrossRef](#)]
11. Chalbatani, G.M.; Dana, H.; Gharagouzloo, E.; Grijalvo, S.; Eritja, R.; Logsdon, C.D.; Memari, F.; Miri, S.R.; Rad, M.R.; Marmari, V. Small interfering RNAs (siRNAs) in cancer therapy: A nano-based approach. *Int. J. Nanomed.* **2019**, *14*, 3111–3128. [[CrossRef](#)]
12. Guo, J.; Jiang, X.; Gui, S. RNA interference-based nanosystems for inflammatory bowel disease therapy. *Int. J. Nanomed.* **2016**, *11*, 5287–5310. [[CrossRef](#)]
13. Olena, A.F.; Patton, J.G. Genomic Organization of microRNAs. *J. Cell. Physiol.* **2010**, *222*, 540–545. [[CrossRef](#)] [[PubMed](#)]
14. O'Brien, J.; Hayder, H.; Zayed, Y.; Peng, C. Overview of MicroRNA Biogenesis, Mechanisms of Actions, and Circulation. *Front. Endocrinol. (Lausanne)* **2018**, *9*. [[CrossRef](#)] [[PubMed](#)]
15. Khatri, N.; Rath, M.; Baradia, D.; Trehan, S.; Misra, A. In vivo delivery aspects of miRNA, shRNA and siRNA. *Crit. Rev. Ther. Drug Carrier. Syst.* **2012**, *29*, 487–527. [[CrossRef](#)]
16. Burke, J.M.; Kincaid, R.P.; Aloisio, F.; Welch, N.; Sullivan, C.S. Expression of short hairpin RNAs using the compact architecture of retroviral microRNA genes. *Nucleic Acids Res.* **2017**, *45*, 154. [[CrossRef](#)]
17. Paddison, P.J.; Caudy, A.A.; Bernstein, E.; Hannon, G.J.; Conklin, D.S. Short hairpin RNAs (shRNAs) induce sequence-specific silencing in mammalian cells. *Genes Dev.* **2002**, *16*, 948–958. [[CrossRef](#)]
18. Aagaard, L.; Rossi, J.J. RNAi therapeutics: Principles, prospects and challenges. *Adv. Drug Deliv. Rev.* **2007**, *59*, 75–86. [[CrossRef](#)] [[PubMed](#)]
19. Carthew, R.W.; Sontheimer, E.J. Origins and Mechanisms of miRNAs and siRNAs. *Cell* **2009**, *136*, 642–655. [[CrossRef](#)]
20. Matzke, M.A.; Birchler, J.A. RNAi-mediated pathways in the nucleus. *Nat. Rev. Genet.* **2005**, *6*, 24–35. [[CrossRef](#)]
21. Sheu-Gruttadauria, J.; MacRae, I.J. Structural Foundations of RNA Silencing by Argonaute. *J. Mol. Biol.* **2017**, *429*, 2619–2639. [[CrossRef](#)]
22. Adams, D.; Gonzalez-Duarte, P.D.A.; O'Riordan, W.D.; Yang, C.C.; Ueda, M.; Kristen, A.V.; Tournev, I.; Schmidt, H.H.; Coelho, T.; Berk, J.L.; et al. Patisiran, an RNAi Therapeutic, for Hereditary Transthyretin Amyloidosis. *N. Engl. J. Med.* **2018**, *379*, 11–21. [[CrossRef](#)] [[PubMed](#)]
23. Second RNAi Drug Approved. *Nature Biotechnology*, 7 April 2020. [[CrossRef](#)]
24. Thi, E.P.; Mire, C.E.; Lee, A.C.H.; Geisbert, J.B.; Zhou, J.Z.; Agans, K.N.; Snead, N.M.; Deer, D.J.; Barnard, T.R.; Fenton, K.A.; et al. Lipid nanoparticle siRNA treatment of Ebola-virus-Makona-infected nonhuman primates. *Nature* **2015**, *521*, 362–365. [[CrossRef](#)] [[PubMed](#)]
25. Hnisz, D.; Weintraub, A.S.; Day, D.S.; Valton, A.L.; Bak, R.O.; Li, C.H.; Goldmann, J.; Lajoie, B.R.; Fan, Z.P.; Sigova, A.A. Activation of proto-oncogenes by disruption of chromosome neighborhoods. *Science* **2016**, *351*, 1454–1458. [[CrossRef](#)] [[PubMed](#)]
26. Katoh, M.; Katoh, M. FGFR2 and WDR11 are neighboring oncogene and tumor suppressor gene on human chromosome 10q26. *Int. J. Oncol.* **2003**, *22*, 1155–1159. [[CrossRef](#)] [[PubMed](#)]
27. Nieth, C.; Priebisch, A.; Stege, A.; Lage, H. Modulation of the classical multidrug resistance (MDR) phenotype by RNA interference (RNAi). *FEBS Lett.* **2003**, *545*, 144–150. [[CrossRef](#)]
28. Liang, X.; Li, D.; Leng, S.; Zhu, X. RNA-based pharmacotherapy for tumors: From bench to clinic and back. *Biomed. Pharm.* **2020**, *125*, 109997. [[CrossRef](#)]
29. Chiu, Y.-L.; Rana, T.M. RNAi in human cells: Basic structural and functional features of small interfering RNA. *Mol. Cell* **2002**, *10*, 549–561. [[CrossRef](#)]
30. Park, J.; Park, J.; Pei, Y.; Xu, J.; Yeo, Y. Pharmacokinetics and biodistribution of recently-developed siRNA nanomedicines. *Adv. Drug Deliv. Rev.* **2016**, *104*, 93–109. [[CrossRef](#)]
31. Xin, Y.; Huang, M.; Guo, W.W.; Huang, Q.; Zhang, L.Z.; Jiang, G. Nano-based delivery of RNAi in cancer therapy. *Mol. Cancer* **2017**, *16*, 134. [[CrossRef](#)]
32. Ragelle, H.; Vandermeulen, G.; Préat, V. Chitosan-based siRNA delivery systems. *J. Control. Release* **2013**, *172*, 207–218. [[CrossRef](#)]
33. Babu, A.; Muralidharan, R.; Amreddy, N.; Mehta, M.; Munshi, A.; Ramesh, R. Nanoparticles for siRNA-Based Gene Silencing in Tumor Therapy. *IEEE Trans. Nanobiosci.* **2016**, *15*, 849–863. [[CrossRef](#)] [[PubMed](#)]

34. Hnisz, D.; Weintraub, A.S.; Day, D.S.; Valton, A.L.; Bak, R.O.; Li, C.H.; Goldmann, J.; Lajoie, B.R.; Fan, Z.P.; Sigova, A.A. Improving siRNA bio-distribution and minimizing side effects. *Curr. Drug Metab.* **2011**, *12*, 11–23. [[CrossRef](#)]
35. Lee, S.J.; Kim, M.J.; Kwon, I.C.; Roberts, T.M. Delivery Strategies and Potential Targets for siRNA in Major Cancer Types. *Adv. Drug Deliv. Rev.* **2016**, *104*, 2–15. [[CrossRef](#)] [[PubMed](#)]
36. Xu, C.; Lee, S.A.; Chen, X. RNA interference as therapeutics for hepatocellular carcinoma. *Recent Pat. Anticancer Drug Discov.* **2011**, *6*, 106–115. [[CrossRef](#)] [[PubMed](#)]
37. Hajiasgharzadeh, K.; Somi, M.H.; Shanebandi, D.; Mokhtarzadeh, A.; Baradaran, B. Small interfering RNA-mediated gene suppression as a therapeutic intervention in hepatocellular carcinoma. *J. Cell. Physiol.* **2019**, *234*, 3263–3276. [[CrossRef](#)] [[PubMed](#)]
38. Zhang, Q.Y.; Ho, P.Y.; Tu, M.-J.; Jilek, J.L.; Chen, Q.X.; Zeng, S.; Yu, A.M. Lipidation of polyethylenimine-based polyplex increases serum stability of bioengineered RNAi agents and offers more consistent tumoral gene knockdown in vivo. *Int. J. Pharm.* **2018**, *547*, 537–544. [[CrossRef](#)] [[PubMed](#)]
39. Wagner, M.J.; Mitra, R.; McArthur, M.J.; Baze, W.; Barnhart, K.; Wu, S.; Rodriguez-Aguayo, C.; Zhang, X.; Coleman, R.L.; Lopez-Berestein, G. Preclinical Mammalian Safety Studies of EPHARNA (DOPC Nanoliposomal EphA2-Targeted siRNA). *Mol. Cancer Ther.* **2017**, *16*, 1114–1123. [[CrossRef](#)]
40. BioSpace. Simaomics' siRNA Therapeutic Candidate, STP705, Granted Orphan Drug Designation by US FDA for Treatment of Hepatocellular Carcinoma. Available online: <https://www.biospace.com/article/simaomics-sima-therapeutic-candidate-stp705-granted-orphan-drug-designation-by-us-fda-for-treatment-of-hepatocellular-carcinoma/> (accessed on 12 May 2020).
41. Fu, Y.; Liu, S.; Zeng, S.; Shen, H. From bench to bed: The tumor immune microenvironment and current immunotherapeutic strategies for hepatocellular carcinoma. *J. Exp. Clin. Cancer Res.* **2019**, *38*, 396. [[CrossRef](#)]
42. Filliol, A.; Schwabe, R.F. Contributions of Fibroblasts, Extracellular Matrix, Stiffness, and Mechanosensing to Hepatocarcinogenesis. *Semin. Liver Dis.* **2019**, *39*, 315–333. [[CrossRef](#)]
43. Uchimura, K.; Morimoto-Tomita, M.; Bistrup, A.; Li, J.; Lyon, M.; Gallagher, J.; Werb, Z.; Rosen, S.D. HSulf-2, an extracellular endoglucosamine-6-sulfatase, selectively mobilizes heparin-bound growth factors and chemokines: Effects on VEGF, FGF-1, and SDF-1. *BMC Biochem.* **2006**, *7*, 2. [[CrossRef](#)]
44. Montalbano, M.; Rastellini, C.; McGuire, J.T.; Prajapati, J.; Shirafkan, A.; Vento, R.; Cicalese, L. Role of Glypican-3 in the growth, migration and invasion of primary hepatocytes isolated from patients with hepatocellular carcinoma. *Cell Oncol. (Dordr)* **2018**, *41*, 169–184. [[CrossRef](#)] [[PubMed](#)]
45. Sun, W.; Wang, Y.; Cai, M.; Lin, L.; Chen, X.; Cao, Z.; Zhu, K.; Shuai, X. Codelivery of sorafenib and GPC3 siRNA with PEI-modified liposomes for hepatoma therapy. *Biomater. Sci.* **2017**, *5*, 2468–2479. [[CrossRef](#)] [[PubMed](#)]
46. Vlodaysky, I.; Friedmann, Y. Molecular properties and involvement of heparanase in cancer metastasis and angiogenesis. *J. Clin. Investig.* **2001**, *108*, 341–347. [[CrossRef](#)] [[PubMed](#)]
47. Levy-Adam, F.; Feld, S.; Suss-Toby, E.; Vlodaysky, I.; Ilan, N. Heparanase facilitates cell adhesion and spreading by clustering of cell surface heparan sulfate proteoglycans. *PLoS ONE* **2008**, *3*, 2319. [[CrossRef](#)] [[PubMed](#)]
48. Jiang, G.; Zhang, L.; Pu, J.; Mei, H.; Zhao, J.; Huang, K.; Zeng, F.; Tong, Q. Small RNAs targeting transcription start site induce heparanase silencing through interference with transcription initiation in human cancer cells. *PLoS ONE* **2012**, *7*. [[CrossRef](#)]
49. Wang, X.; Ding, J.; Feng, Y.; Weng, L.; Zhao, G.; Xiang, J.; Zhang, M.; Xing, D. Targeting of growth factors in the treatment of hepatocellular carcinoma: The potentials of polysaccharides. *Oncol. Lett.* **2017**, *13*, 1509–1517. [[CrossRef](#)]
50. Fuchs, B.C.; Hoshida, Y.; Fujii, T.; Wei, L.; Yamada, S.; Lauwers, G.Y.; McGinn, C.M.; DePeralta, D.K.; Chen, X.; Kuroda, T.; et al. Epidermal growth factor receptor inhibition attenuates liver fibrosis and development of hepatocellular carcinoma. *Hepatology* **2014**, *59*, 1577–1590. [[CrossRef](#)]
51. Gao, J.; Yu, Y.; Zhang, Y.; Song, J.; Chen, H.; Li, W.; Qian, W.; Deng, L.; Kou, G.; Chen, J. EGFR-specific PEGylated immunoliposomes for active siRNA delivery in hepatocellular carcinoma. *Biomaterials* **2012**, *33*, 270–282. [[CrossRef](#)]
52. Huang, Z.; Dong, L.; Chen, J.; Gao, F.; Zhang, Z.; Chen, J.; Zhang, J. Low-molecular weight chitosan/vascular endothelial growth factor short hairpin RNA for the treatment of hepatocellular carcinoma. *Life Sci.* **2012**, *91*, 1207–1215. [[CrossRef](#)]

53. Li, T.; Xue, Y.; Wang, G.; Gu, T.; Li, Y.; Zhu, Y.Y.; Chen, L. Multi-target siRNA: Therapeutic Strategy for Hepatocellular Carcinoma. *J. Cancer* **2016**, *7*, 1317–1327. [[CrossRef](#)]
54. Wu, Y.-Y.; Chen, L.; Wang, G.-L.; Zhang, Y.-X.; Zhou, J.-M.; He, S.; Qin, J.; Zhu, Y.-Y. Inhibition of hepatocellular carcinoma growth and angiogenesis by dual silencing of NET-1 and VEGF. *J. Mol. Histol.* **2013**, *44*, 433–445. [[CrossRef](#)] [[PubMed](#)]
55. Huang, X.; Jian, W.; Wu, Z.; Zhao, J.; Wang, H.; Li, W.; Xia, J. Small interfering RNA (siRNA)-mediated knockdown of macrophage migration inhibitory factor (MIF) suppressed cyclin D1 expression and hepatocellular carcinoma cell proliferation. *Oncotarget* **2014**, *5*, 5570–5580. [[CrossRef](#)] [[PubMed](#)]
56. Mazumder, S.; DuPree, E.L.; Almasan, A. A dual role of cyclin E in cell proliferation and apoptosis may provide a target for cancer therapy. *Curr. Cancer Drug Targets* **2004**, *4*, 65–75. [[CrossRef](#)]
57. Li, K.; Lin, S.-Y.; Brunicardi, F.C.; Seu, P. Use of RNA interference to target cyclin E-overexpressing hepatocellular carcinoma. *Cancer Res.* **2003**, *63*, 3593–3597. [[PubMed](#)]
58. Bai, T.; Chen, C.-C.; Lau, L.F. Matricellular protein CCN1 activates a proinflammatory genetic program in murine macrophages. *J. Immunol.* **2010**, *184*, 3223–3232. [[CrossRef](#)] [[PubMed](#)]
59. Jia, Q.; Dong, Q.; Qin, L. CCN: Core regulatory proteins in the microenvironment that affect the metastasis of hepatocellular carcinoma. *Oncotarget* **2016**, *7*, 1203–1214. [[CrossRef](#)] [[PubMed](#)]
60. Mizuno, H.; Ogura, M.; Saito, Y.; Sekine, W.; Sano, R.; Gotou, T.; Oku, T.; Itoh, S.; Katabami, K.; Tsuji, T. Changes in adhesive and migratory characteristics of hepatocellular carcinoma (HCC) cells induced by expression of alpha3beta1 integrin. *Biochim. Biophys. Acta* **2008**, *1780*, 564–570. [[CrossRef](#)]
61. Bogorad, R.L.; Yin, H.; Zeigerer, A.; Nonaka, H.; Ruda, V.M.; Zerial, M.; Anderson, D.G.; Kotliansky, V. Nanoparticle-formulated siRNA targeting integrins inhibits hepatocellular carcinoma progression in mice. *Nat. Commun.* **2014**, *5*, 3869. [[CrossRef](#)]
62. Zhou, X.; Xie, F.; Wang, L.; Zhang, L.; Zhang, S.; Fang, M.; Zhou, F. The function and clinical application of extracellular vesicles in innate immune regulation. *Cell. Mol. Immunol.* **2020**, *17*, 323–334. [[CrossRef](#)]
63. Roma-Rodrigues, C.; Fernandes, A.R.; Baptista, P.V. Exosome in tumour microenvironment: Overview of the crosstalk between normal and cancer cells. *Biomed. Res. Int.* **2014**, 179486. [[CrossRef](#)] [[PubMed](#)]
64. Becker, A.; Thakur, B.K.; Weiss, J.M.; Kim, H.S.; Peinado, H.; Lyden, D. Extracellular vesicles in cancer: Cell-to-cell mediators of metastasis. *Cancer Cell* **2016**, *30*, 836–848. [[CrossRef](#)] [[PubMed](#)]
65. Maia, J.; Caja, S.; Moraes, M.C.S.; Couto, N.; Costa-Silva, B. Exosome-Based Cell-Cell Communication in the Tumor Microenvironment. *Front. Cell Dev. Biol.* **2018**, *6*. [[CrossRef](#)] [[PubMed](#)]
66. Pan, J.; Zhou, H.; Zhao, X.; Ding, H.; Li, W.; Qin, L.; Pan, Y. Role of exosomes and exosomal microRNAs in hepatocellular carcinoma: Potential in diagnosis and antitumour treatments (Review). *Int. J. Mol. Med.* **2018**, *41*, 1809–1816. [[CrossRef](#)]
67. Xie, F.; Yuan, Y.; Xie, L.; Ran, P.; Xiang, X.; Huang, Q.; Qi, G.; Guo, X.; Xiao, C.; Zheng, S. miRNA-320a inhibits tumor proliferation and invasion by targeting c-Myc in human hepatocellular carcinoma. *Oncotargets Ther.* **2017**, *10*, 885–894. [[CrossRef](#)]
68. Qu, Z.; Wu, J.; Wu, J.; Luo, D.; Jiang, C.; Ding, Y. Exosomes derived from HCC cells induce sorafenib resistance in hepatocellular carcinoma both in vivo and in vitro. *J. Exp. Clin. Cancer Res.* **2016**, *35*, 30. [[CrossRef](#)]
69. Wang, S.; Xu, M.; Li, X.; Su, X.; Xiao, X.; Keating, A.; Zhao, R.C. Exosomes released by hepatocarcinoma cells endow adipocytes with tumor-promoting properties. *J. Hematol. Oncol.* **2018**, *11*, 14. [[CrossRef](#)]
70. Wang, X.; Shen, H.; Zhang, G.; Huang, R.; Zhang, W.; He, Q.; Jin, K.; Zhuo, H.; Zhang, Z.; Wang, J.; et al. 14-3-3 ζ delivered by hepatocellular carcinoma-derived exosomes impaired anti-tumor function of tumor-infiltrating T lymphocytes. *Cell Death Dis.* **2018**, *9*, 159. [[CrossRef](#)]
71. He, M.; Qin, H.; Poon, T.C.W.; Sze, S.-C.; Ding, X.; Co, N.N.; Ngai, S.-M.; Chan, T.-F.; Wong, N. Hepatocellular carcinoma-derived exosomes promote motility of immortalized hepatocyte through transfer of oncogenic proteins and RNAs. *Carcinogenesis* **2015**, *36*, 1008–1018. [[CrossRef](#)]
72. Zhao, Y.; Jian, W.; Gao, W.; Zheng, Y.; Wang, Y.; Zhou, Z.; Zhang, H.; Wang, C. RNAi silencing of c-Myc inhibits cell migration, invasion, and proliferation in HepG2 human hepatocellular carcinoma cell line: C-Myc silencing in hepatocellular carcinoma cell. *Cancer Cell Int.* **2013**, *13*, 23. [[CrossRef](#)]
73. Haga, Y.; Kanda, T.; Nakamura, M.; Nakamoto, S.; Sasaki, R.; Takahashi, K.; Wu, S.; Yokosuka, O. Overexpression of c-Jun contributes to sorafenib resistance in human hepatoma cell lines. *PLoS ONE* **2017**, *12*. [[CrossRef](#)] [[PubMed](#)]

74. Patt, Y.Z.; Chamsangavej, C.; Yoffe, B.; Smith, R.; Lawrence, D.; Chuang, V.; Carrasco, H.; Roh, M.; Chase, J.; Fischer, H.; et al. Hepatic arterial infusion of floxuridine, leucovorin, doxorubicin, and cisplatin for hepatocellular carcinoma: Effects of hepatitis B and C viral infection on drug toxicity and patient survival. *J. Clin. Oncol.* **1994**, *12*, 1204–1211. [[CrossRef](#)] [[PubMed](#)]
75. Lee, J.E.; Bae, S.H.; Choi, J.Y.; Yoon, S.K.; You, Y.K.; Lee, M.A. Epirubicin, Cisplatin, 5-FU combination chemotherapy in sorafenib-refractory metastatic hepatocellular carcinoma. *World J. Gastroenterol.* **2014**, *20*, 235–241. [[CrossRef](#)] [[PubMed](#)]
76. Ishikawa, T.; Kubota, T.; Abe, S.; Watanabe, Y.; Sugano, T.; Inoue, R.; Iwanaga, A.; Seki, K.; Honma, T.; Yoshida, T. Hepatic arterial infusion chemotherapy with cisplatin before radical local treatment of early hepatocellular carcinoma (JIS score 0/1) improves survival. *Ann. Oncol.* **2014**, *25*, 1379–1384. [[CrossRef](#)]
77. Li, M.; Zhao, P.; Fan, T.; Chen, Y.; Zhang, X.; He, C.; Yang, T.; Lee, R.J.; Khan, M.W.; Raza, S.M.; et al. Biocompatible co-loading vehicles for delivering both nanoplatin cores and siRNA to treat hepatocellular carcinoma. *Int. J. Pharm.* **2019**, *572*, 118769. [[CrossRef](#)]
78. Conigliaro, A.; Costa, V.; Lo Dico, A.; Saieva, L.; Buccheri, S.; Dieli, F.; Manno, M.; Raccosta, S.; Mancone, C.; Tripodi, M.; et al. CD90+ liver cancer cells modulate endothelial cell phenotype through the release of exosomes containing H19 lncRNA. *Mol. Cancer* **2015**, *14*, 155. [[CrossRef](#)]
79. Huang, K.-W.; Lai, Y.-T.; Chern, G.-J.; Huang, S.-F.; Tsai, C.-L.; Sung, Y.-C.; Chiang, C.-C.; Hwang, P.-B.; Ho, T.-L.; Huang, R.-L.; et al. Galactose Derivative-Modified Nanoparticles for Efficient siRNA Delivery to Hepatocellular Carcinoma. *Biomacromolecules* **2018**, *19*, 2330–2339. [[CrossRef](#)]
80. Yao, Y.; Wang, T.; Liu, Y.; Zhang, N. Co-delivery of sorafenib and VEGF-siRNA via pH-sensitive liposomes for the synergistic treatment of hepatocellular carcinoma. *Artif. Cells Nanomed. Biotechnol.* **2019**, *47*, 1374–1383. [[CrossRef](#)]
81. De Clercq, E. AMD3100/CXCR4 Inhibitor. *Front. Immunol.* **2015**, *6*. [[CrossRef](#)]
82. Liu, J.-Y.; Chiang, T.; Liu, C.-H.; Chern, G.-G.; Lin, T.-T.; Gao, D.-Y.; Chen, Y. Delivery of siRNA Using CXCR4-targeted Nanoparticles Modulates Tumor Microenvironment and Achieves a Potent Antitumor Response in Liver Cancer. *Mol. Ther.* **2015**, *23*, 1772–1782. [[CrossRef](#)]
83. Zeisberg, E.M.; Potenta, S.; Xie, L.; Zeisberg, M.; Kalluri, R. Discovery of endothelial to mesenchymal transition as a source for carcinoma-associated fibroblasts. *Cancer Res.* **2007**, *67*, 10123–10128. [[CrossRef](#)] [[PubMed](#)]
84. Anderberg, C.; Pietras, K. On the origin of cancer-associated fibroblasts. *Cell Cycle.* **2009**, *8*, 1461–1462. [[CrossRef](#)]
85. Ishii, G.; Sangai, T.; Oda, T.; Aoyagi, Y.; Hasebe, T.; Kanomata, N.; Endoh, Y.; Okumura, C.; Okuhara, Y.; Magae, J.; et al. Bone-marrow-derived myofibroblasts contribute to the cancer-induced stromal reaction. *Biochem. Biophys. Res. Commun.* **2003**, *309*, 232–240. [[CrossRef](#)]
86. Kalluri, R.; Zeisberg, M. Fibroblasts in cancer. *Nat. Rev. Cancer* **2006**, *6*, 392–401. [[CrossRef](#)] [[PubMed](#)]
87. Elenbaas, B.; Weinberg, R.A. Heterotypic signaling between epithelial tumor cells and fibroblasts in carcinoma formation. *Exp. Cell. Res.* **2001**, *264*, 169–184. [[CrossRef](#)]
88. Birgani, M.T.; Carloni, V. Tumor Microenvironment, a Paradigm in Hepatocellular Carcinoma Progression and Therapy. *Int. J. Mol. Sci.* **2017**, *18*, 405. [[CrossRef](#)]
89. Yang, J.D.; Nakamura, I.; Roberts, L.R. The tumor microenvironment in hepatocellular carcinoma: Current status and therapeutic targets. *Semin. Cancer Biol.* **2011**, *21*, 35–43. [[CrossRef](#)] [[PubMed](#)]
90. Kumar, D.P.; Santhekadur, P.K.; Seneshaw, M.; Mirshahi, F.; Uram-Tuculescu, C.; Sanyal, A.J. A Regulatory Role of Apoptosis Antagonizing Transcription Factor in the Pathogenesis of Nonalcoholic Fatty Liver Disease and Hepatocellular Carcinoma. *Hepatology* **2019**, *69*, 1520–1534. [[CrossRef](#)] [[PubMed](#)]
91. Novikova, M.V.; Khromova, N.V.; Kopnin, P.B. Components of the Hepatocellular Carcinoma Microenvironment and Their Role in Tumor Progression. *Biochem. Mosc.* **2017**, *82*, 861–873. [[CrossRef](#)]
92. Quail, D.F.; Joyce, J.A. Microenvironmental regulation of tumor progression and metastasis. *Nat. Med.* **2013**, *19*, 1423–1437. [[CrossRef](#)]
93. Liu, J.; Chen, S.; Wang, W.; Ning, B.; Chen, F.; Shen, W.; Ding, J.; Chen, W.; Xie, W.; Zhang, X. Cancer-associated fibroblasts promote hepatocellular carcinoma metastasis through chemokine-activated hedgehog and TGF- β pathways. *Cancer Lett.* **2016**, *379*, 49–59. [[CrossRef](#)] [[PubMed](#)]
94. Baluk, P.; Morikawa, S.; Haskell, A.; Mancuso, M.; McDonald, D.M. Abnormalities of basement membrane on blood vessels and endothelial sprouts in tumors. *Am. J. Pathol.* **2003**, *163*, 1801–1815. [[CrossRef](#)]
95. Sun, F.; Wang, J.; Sun, Q.; Li, F.; Gao, H.; Xu, L.; Zhang, J.; Sun, X.; Tian, Y.; Zhao, Q.; et al. Interleukin-8 promotes integrin β 3 upregulation and cell invasion through PI3K/Akt pathway in hepatocellular carcinoma. *J. Exp. Clin. Cancer Res.* **2019**, *38*, 449. [[CrossRef](#)] [[PubMed](#)]

96. Huang, W.; Chen, Z.; Zhang, L.; Tian, D.; Wang, D.; Fan, D.; Wu, K.; Xia, L. Interleukin-8 Induces Expression of FOXC1 to Promote Transactivation of CXCR1 and CCL2 in Hepatocellular Carcinoma Cell Lines and Formation of Metastases in Mice. *Gastroenterology* **2015**, *149*, 1053–1067. [[CrossRef](#)] [[PubMed](#)]
97. Santamato, A.; Fransvea, E.; Dituri, F.; Caligiuri, A.; Quaranta, M.; Niimi, T.; Pinzani, M.; Antonaci, S.; Giannelli, G. Hepatic stellate cells stimulate HCC cell migration via laminin-5 production. *Clin. Sci. (Lond.)* **2011**, *121*, 159–168. [[CrossRef](#)] [[PubMed](#)]
98. Cho, Y.; Park, M.J.; Kim, K.; Park, J.; Kim, J.; Kim, W.; Yoon, J.-H. Tumor-Stroma Crosstalk Enhances REG3A Expressions that Drive the Progression of Hepatocellular Carcinoma. *Int. J. Mol. Sci.* **2020**, *21*, 472. [[CrossRef](#)] [[PubMed](#)]
99. Faouzi, S.; Lepreux, S.; Bedin, C.; Dubuisson, L.; Balabaud, C.; Bioulac-Sage, P.; Desmoulière, A.; Rosenbaum, J. Activation of cultured rat hepatic stellate cells by tumoral hepatocytes. *Lab. Investig.* **1999**, *79*, 485–493.
100. Zhao, W.; Zhang, L.; Yin, Z.; Su, W.; Ren, G.; Zhou, C.; You, J.; Fan, J.; Wang, X. Activated hepatic stellate cells promote tumorigenicity of hepatocellular carcinoma. *Cancer Sci.* **2009**, *100*, 646–653. [[CrossRef](#)]
101. Carloni, V.; Luong, T.V.; Rombouts, K. Hepatic stellate cells and extracellular matrix in hepatocellular carcinoma: More complicated than ever. *Liver Int.* **2014**, *34*, 834–843. [[CrossRef](#)]
102. Mehdizadeh, A.; Somi, M.H.; Darabi, M.; Farajnia, S.; Akbarzadeh, A.; Montazersaheb, S.; Yousefi, M.; Bonyadi, M. Liposome-mediated RNA interference delivery against Erk1 and Erk2 does not equally promote chemosensitivity in human hepatocellular carcinoma cell line HepG2. *Artif. Cells Nanomed. Biotechnol.* **2017**, *45*, 1612–1619. [[CrossRef](#)]
103. Nathan, C.; Ding, A. Nonresolving inflammation. *Cell* **2010**, *140*, 871–882. [[CrossRef](#)] [[PubMed](#)]
104. Murray, P.J. Macrophage Polarization. *Annu. Rev. Physiol.* **2017**, *79*, 541–566. [[CrossRef](#)]
105. Patel, P.; Schutzer, S.E.; Pysopoulos, N. Immunobiology of hepatocarcinogenesis: Ways to go or almost there. *World J. Gastrointest Pathophysiol.* **2016**, *7*, 242–255. [[CrossRef](#)] [[PubMed](#)]
106. Yeung, O.W.H.; Lo, C.-M.; Ling, C.-C.; Qi, X.; Geng, W.; Li, C.X.; Ng, K.T.P.; Forbes, S.J.; Guan, X.-Y.; Poon, R.T.P.; et al. Alternatively activated (M2) macrophages promote tumour growth and invasiveness in hepatocellular carcinoma. *J. Hepatol.* **2015**, *62*, 607–616. [[CrossRef](#)] [[PubMed](#)]
107. Dong, N.; Shi, X.; Wang, S.; Gao, Y.; Kuang, Z.; Xie, Q.; Li, Y.; Deng, H.; Wu, Y.; Li, M.; et al. M2 macrophages mediate sorafenib resistance by secreting HGF in a feed-forward manner in hepatocellular carcinoma. *Br. J. Cancer* **2019**, *121*, 22–33. [[CrossRef](#)]
108. Liu, A.-W.; Cai, J.; Zhao, X.-L.; Jiang, T.-H.; He, T.-F.; Fu, H.-Q.; Zhu, M.-H.; Zhang, S.-H. ShRNA-targeted MAP4K4 inhibits hepatocellular carcinoma growth. *Clin. Cancer Res.* **2011**, *17*, 710–720. [[CrossRef](#)]
109. Zhang, W.; Sun, H.; Shi, X.; Wang, H.; Cui, C.; Xiao, F.; Wu, C.; Guo, X.; Wang, L. SENP1 regulates hepatocyte growth factor-induced migration and epithelial-mesenchymal transition of hepatocellular carcinoma. *Tumor Biol.* **2016**, *37*, 7741–7748. [[CrossRef](#)]
110. Cho, S.-B.; Park, Y.-L.; Song, Y.-A.; Kim, K.-Y.; Lee, G.-H.; Cho, D.-H.; Myung, D.-S.; Park, K.-J.; Lee, W.-S.; Chung, I.-J.; et al. Small interfering RNA-directed targeting of RON alters invasive and oncogenic phenotypes of human hepatocellular carcinoma cells. *Oncol. Rep.* **2011**, *26*, 1581–1586. [[CrossRef](#)] [[PubMed](#)]
111. Zhang, C.; Yu, Y.; Huang, Q.; Tang, K. SIRT6 regulates the proliferation and apoptosis of hepatocellular carcinoma via the ERK1/2 signaling pathway. *Mol. Med. Rep.* **2019**, *20*, 1575–1582. [[CrossRef](#)]
112. Chen, J.; Xia, H.; Zhang, X.; Karthik, S.; Pratap, S.V.; Ooi, L.L.; Hong, W.; Hui, K.M. ECT2 regulates the Rho/ERK signalling axis to promote early recurrence in human hepatocellular carcinoma. *J. Hepatol.* **2015**, *62*, 1287–1295. [[CrossRef](#)]
113. Wang, W.; Wu, F.; Fang, F.; Tao, Y.; Yang, L. Inhibition of invasion and metastasis of hepatocellular carcinoma cells via targeting RhoC in vitro and in vivo. *Clin. Cancer Res.* **2008**, *14*, 6804–6812. [[CrossRef](#)] [[PubMed](#)]
114. Xu, Z.W.; Yan, S.X.; Wu, H.X.; Chen, J.Y.; Zhang, Y.; Li, Y.; Wei, W. The influence of TNF- α and Ang II on the proliferation, migration and invasion of HepG2 cells by regulating the expression of GRK2. *Cancer Chemother. Pharmacol.* **2017**, *79*, 747–758. [[CrossRef](#)] [[PubMed](#)]
115. Shirabe, K.; Mano, Y.; Muto, J.; Matono, R.; Motomura, T.; Toshima, T.; Takeishi, K.; Uchiyama, H.; Yoshizumi, T.; Taketomi, A.; et al. Role of tumor-associated macrophages in the progression of hepatocellular carcinoma. *Surg. Today* **2012**, *42*, 1–7. [[CrossRef](#)] [[PubMed](#)]

116. Zhou, J.; Ding, T.; Pan, W.; Zhu, L.-Y.; Li, L.; Zheng, L. Increased intratumoral regulatory T cells are related to intratumoral macrophages and poor prognosis in hepatocellular carcinoma patients. *Int. J. Cancer* **2009**, *125*, 1640–1648. [[CrossRef](#)] [[PubMed](#)]
117. Kuang, D.-M.; Peng, C.; Zhao, Q.; Wu, Y.; Chen, M.-S.; Zheng, L. Activated monocytes in peritumoral stroma of hepatocellular carcinoma promote expansion of memory T helper 17 cells. *Hepatology* **2010**, *51*, 154–164. [[CrossRef](#)] [[PubMed](#)]
118. Wan, S.S.; Zhao, E.; Kryczek, I.; Vatan, L.; Sadovskaya, A.; Ludema, G.; Simeone, D.M.; Zou, W.; Welling, T.H. Tumor-associated macrophages produce interleukin 6 and signal via STAT3 to promote expansion of human hepatocellular carcinoma stem cells. *Gastroenterology* **2014**, *147*, 1393–1404. [[CrossRef](#)]
119. Xie, Y.; Li, J.; Zhang, C. STAT3 promotes the proliferation and migration of hepatocellular carcinoma cells by regulating AKT2. *Oncol. Lett.* **2018**, *15*, 3333–3338. [[CrossRef](#)]
120. Nicolás-Ávila, J.Á.; Adrover, J.M.; Hidalgo, A. Neutrophils in Homeostasis, Immunity, and Cancer. *Immunity* **2017**, *46*, 15–28. [[CrossRef](#)]
121. Michaeli, J.; Shaul, M.E.; Mishalian, I.; Hovav, A.-H.; Levy, L.; Zolotriov, L.; Granot, Z.; Fridlender, Z.G. Tumor-associated neutrophils induce apoptosis of non-activated CD8 T-cells in a TNF α and NO-dependent mechanism, promoting a tumor-supportive environment. *Oncoimmunology* **2017**, *6*, 1356965. [[CrossRef](#)]
122. Ameratunga, M.; Chénard-Poirier, M.; Candilejo, I.M.; Pedregal, M.; Lui, A.; Dolling, D.; Aversa, C.; Garces, A.I.; Ang, J.E.; Banerji, U.; et al. Neutrophil-lymphocyte ratio kinetics in patients with advanced solid tumours on phase I trials of PD-1/PD-L1 inhibitors. *Eur. J. Cancer* **2018**, *89*, 56–63. [[CrossRef](#)]
123. Jeyakumar, G.; Kim, S.; Bumma, N.; Landry, C.; Silski, C.; Suisham, S.; Dickow, B.; Heath, E.; Fontana, J.; Vaishampayan, U. Neutrophil lymphocyte ratio and duration of prior anti-angiogenic therapy as biomarkers in metastatic RCC receiving immune checkpoint inhibitor therapy. *J. Immunother. Cancer* **2017**, *5*, 82. [[CrossRef](#)] [[PubMed](#)]
124. Margetts, J.; Ogle, L.F.; Chan, S.L.; Chan, A.W.H.; Chan, K.C.A.; Jamieson, D.; Willoughby, C.E.; Mann, D.A.; Wilson, C.L.; Manas, D.M.; et al. Neutrophils: Driving progression and poor prognosis in hepatocellular carcinoma. *Br. J. Cancer* **2018**, *118*, 248–257. [[CrossRef](#)] [[PubMed](#)]
125. Arai, K.; Fukumoto, T.; Kido, M.; Tanaka, M.; Kuramitsu, K.; Kinoshita, H.; Komatsu, S.; Tsugawa, D.; Terai, S.; Matsumoto, T.; et al. Preoperative neutrophil-to-lymphocyte ratio as a predictor of survival after reductive surgery plus percutaneous isolated hepatic perfusion for hepatocellular carcinoma: A retrospective analysis. *Surg. Today* **2017**, *47*, 385–392. [[CrossRef](#)] [[PubMed](#)]
126. Koh, M.Y.; Gagea, M.; Sargis, T.; Lemos, R., Jr.; Grandjean, G.; Charbono, A.; Bekiaris, V.; Sedy, J.; Kiriakova, G.; Liu, X.; et al. A new HIF-1 α /RANTES-driven pathway to hepatocellular carcinoma mediated by germline haploinsufficiency of SART1/HAF in mice. *Hepatology* **2016**, *63*, 1576–1591. [[CrossRef](#)]
127. Zhou, S.L.; Zhou, Z.J.; Hu, Z.Q.; Huang, X.W.; Wang, Z.; Chen, E.B.; Fan, J.; Cao, Y.; Dai, Z.; Zhou, J. Tumor-Associated Neutrophils Recruit Macrophages and T-Regulatory Cells to Promote Progression of Hepatocellular Carcinoma and Resistance to Sorafenib. *Gastroenterology* **2016**, *150*, 1646–1658. [[CrossRef](#)]
128. Zhou, S.-L.; Dai, Z.; Zhou, Z.J.; Wang, X.Y.; Yang, G.H.; Wang, Z.; Huang, X.W.; Fan, J.; Zhou, J. Overexpression of CXCL5 mediates neutrophil infiltration and indicates poor prognosis for hepatocellular carcinoma. *Hepatology* **2012**, *56*, 2242–2254. [[CrossRef](#)] [[PubMed](#)]
129. Ormandy, L.-A.; Farber, A.; Cantz, T.; Petrykowska, S.; Wedemeyer, H.; Horning, M.; Lehner, F.; Manns, M.-P.; Korangy, F.; Greten, T.-F. Direct ex vivo analysis of dendritic cells in patients with hepatocellular carcinoma. *World J. Gastroenterol.* **2006**, *12*, 3275–3282. [[CrossRef](#)]
130. Streba, L.A.M.; Streba, C.T.; Săndulescu, L.; Vere, C.C.; Mitruț, P.; Cotoi, B.V.; Popescu, L.N.; Ion, D.A. Dendritic cells and hepatocellular carcinoma. *Rom. J. Morphol. Embryol.* **2014**, *55*, 1287–1293.
131. Li, P.; Du, Q.; Cao, Z.; Guo, Z.; Evankovich, J.; Yan, W.; Chang, Y.; Shao, L.; Stolz, D.B.; Tsung, A.; et al. Interferon- γ induces autophagy with growth inhibition and cell death in human hepatocellular carcinoma (HCC) cells through interferon-regulatory factor-1 (IRF-1). *Cancer Lett.* **2012**, *314*, 213–222. [[CrossRef](#)]
132. Li, C.; Wang, J.; Zhang, H.; Zhu, M.; Chen, F.; Hu, Y.; Liu, H.; Zhu, H. Interferon-stimulated gene 15 (ISG15) is a trigger for tumorigenesis and metastasis of hepatocellular carcinoma. *Oncotarget* **2014**, *5*, 8429–8441. [[CrossRef](#)]

133. Han, C.; Jiang, Y.; Wang, Z.; Wang, H. Natural killer cells involved in tumour immune escape of hepatocellular carcinoma. *Int. Immunopharmacol.* **2019**, *73*, 10–16. [[CrossRef](#)] [[PubMed](#)]
134. Hasmim, M.; Messai, Y.; Ziani, L.; Thiery, J.; Bouhris, J.-H.; Noman, M.Z.; Chouaib, S. Critical Role of Tumor Microenvironment in Shaping NK Cell Functions: Implication of Hypoxic Stress. *Front. Immunol.* **2015**, *6*, 482. [[CrossRef](#)] [[PubMed](#)]
135. Yang, W.; Sun, T.; Cao, J.; Fan, S. Hypoxia-inducible factor-1 α downregulation by small interfering RNA inhibits proliferation, induces apoptosis, and enhances radiosensitivity in chemical hypoxic human hepatoma SMMC-7721 cells. *Cancer Biother. Radiopharm.* **2011**, *26*, 565–571. [[CrossRef](#)] [[PubMed](#)]
136. Takahashi, Y.; Nishikawa, M.; Takakura, Y. Inhibition of tumor cell growth in the liver by RNA interference-mediated suppression of HIF-1 α expression in tumor cells and hepatocytes. *Gene Ther.* **2008**, *15*, 572–582. [[CrossRef](#)] [[PubMed](#)]
137. Vujanovic, L.; Stahl, E.C.; Pardee, A.D.; Geller, D.A.; Tsung, A.; Watkins, S.C.; Gibson, G.A.; Storkus, W.J.; Butterfield, L.H. Tumor-Derived α -Fetoprotein Directly Drives Human Natural Killer-Cell Activation and Subsequent Cell Death. *Cancer Immunol. Res.* **2017**, *5*, 493–502. [[CrossRef](#)]
138. Yamamoto, M.; Tatsumi, T.; Miyagi, T.; Tsunematsu, H.; Aketa, H.; Hosui, A.; Kanto, T.; Hiramatsu, N.; Hayashi, N.; Takehara, T. α -Fetoprotein impairs activation of natural killer cells by inhibiting the function of dendritic cells. *Clin. Exp. Immunol.* **2011**, *165*, 211–219. [[CrossRef](#)]
139. Langhans, B.; Alwan, A.W.; Krämer, B.; Glässner, A.; Lutz, P.; Strassburg, C.P.; Nattermann, J.; Spengler, U. Regulatory CD4⁺ T cells modulate the interaction between NK cells and hepatic stellate cells by acting on either cell type. *J. Hepatol.* **2015**, *62*, 398–404. [[CrossRef](#)]
140. Li, T.; Yang, Y.; Hua, X.; Wang, G.; Liu, W.; Jia, C.; Tai, Y.; Zhang, Q.; Chen, G. Hepatocellular carcinoma-associated fibroblasts trigger NK cell dysfunction via PGE2 and IDO. *Cancer Lett.* **2012**, *318*, 154–161. [[CrossRef](#)]
141. Venook, A.P.; Papandreou, C.; Furuse, J.; de Guevara, L.L. The incidence and epidemiology of hepatocellular carcinoma: A global and regional perspective. *Oncologist* **2010**, *15*, 5–13. [[CrossRef](#)]
142. Sarker, D.; Plummer, R.; Meyer, T.; Sodergren, M.; Basu, B.; Chee, C.E.; Huang, K.-W.; Palmer, D.H.; Ma, Y.T.; Evans, T.R.J.; et al. MTL-CEBPA, a small activating RNA therapeutic up-regulating C/EBP- α , in patients with advanced liver cancer: A first-in-human, multi-centre, open-label, phase I trial. *Clin. Cancer Res.* **2020**. [[CrossRef](#)]
143. Lin, A.; Giuliano, C.J.; Palladino, A.; John, K.M.; Abramowicz, C.; Yuan, M.L.; Sausville, E.L.; Lukow, D.A.; Liu, L.; Chait, A.R.; et al. Off-target toxicity is a common mechanism of action of cancer drugs undergoing clinical trials. *Sci. Transl. Med.* **2019**, *11*, 11. [[CrossRef](#)]
144. Farra, R.; Musiani, F.; Perrone, F.; Čemažar, M.; Kamensek, U.; Tonon, F.; Abrami, M.; Ručigaj, A.; Grassi, M.; Pozzato, G.; et al. Polymer-Mediated Delivery of siRNAs to Hepatocellular Carcinoma: Variables Affecting Specificity and Effectiveness. *Molecules* **2018**, *23*, 777. [[CrossRef](#)] [[PubMed](#)]
145. Willoughby, J.L.S.; Chan, A.; Sehgal, A.; Butler, J.S.; Nair, J.K.; Racie, T.; Shulga-Morskaya, S.; Nguyen, T.; Qian, K.; Yucius, K.; et al. Evaluation of GalNAc-siRNA Conjugate Activity in Pre-clinical Animal Models with Reduced Asialoglycoprotein Receptor Expression. *Mol. Ther.* **2018**, *26*, 105–114. [[CrossRef](#)] [[PubMed](#)]
146. Thijssen, M.F.; Brüggewirth, I.M.A.; Gillooly, A.; Khvorova, A.; Kowalik, T.F.; Martins, P.N. Gene Silencing With siRNA (RNA Interference): A New Therapeutic Option During Ex Vivo Machine Liver Perfusion Preservation. *Liver Transpl.* **2019**, *25*, 140–151. [[CrossRef](#)] [[PubMed](#)]
147. Bracho-Sanchez, E.; Xia, C.Q.; Clare-Salzler, M.J.; Keselowsky, B.G. Micro and Nano Material Carriers for Immunomodulation. *Am. J. Transplant.* **2016**, *16*, 3362–3370. [[CrossRef](#)] [[PubMed](#)]
148. Théry, C.; Zitvogel, L.; Amigorena, S. Exosomes: Composition, biogenesis and function. *Nat. Rev. Immunol.* **2002**, *2*, 569–579. [[CrossRef](#)]
149. Darband, S.G.; Mirza-Aghazadeh-Attari, M.; Kaviani, M.; Mihanfar, A.; Sadighparvar, S.; Yousefi, B.; Majidinia, M. Exosomes: Natural nanoparticles as bio shuttles for RNAi delivery. *J. Control. Release* **2018**, *289*, 158–170. [[CrossRef](#)]
150. Lu, M.; Xing, H.; Xun, Z.; Yang, T.; Ding, P.; Cai, C.; Wang, D.; Zhao, X. Exosome-based small RNA delivery: Progress and prospects. *Asian J. Pharm. Sci.* **2018**, *13*, 1–11. [[CrossRef](#)]

151. Shahabipour, F.; Barati, N.; Johnston, T.P.; Derosa, G.; Maffioli, P.; Sahebkar, A. Exosomes: Nanoparticulate tools for RNA interference and drug delivery. *J. Cell. Physiol.* **2017**, *232*, 1660–1668. [[CrossRef](#)]
152. Morishita, M.; Takahashi, Y.; Nishikawa, M.; Takakura, Y. Pharmacokinetics of Exosomes—An Important Factor for Elucidating the Biological Roles of Exosomes and for the Development of Exosome-Based Therapeutics. *J. Pharm. Sci.* **2017**, *106*, 2265–2269. [[CrossRef](#)]
153. Lunavat, T.R.; Jang, S.C.; Nilsson, L.; Park, H.T.; Repiska, G.; Lässer, C.; Nilsson, J.A.; Ghossein, Y.S.; Lötvall, J. RNAi delivery by exosome-mimetic nanovesicles—Implications for targeting c-Myc in cancer. *Biomaterials* **2016**, *102*, 231–238. [[CrossRef](#)] [[PubMed](#)]
154. Zhou, Y.; Yuan, Y.; Liu, M.; Hu, X.; Quan, Y.; Chen, X. Tumor-specific delivery of KRAS siRNA with iRGD-exosomes efficiently inhibits tumor growth. *ExRNA* **2019**, *1*, 28. [[CrossRef](#)]



© 2020 by the authors. Licensee MDPI, Basel, Switzerland. This article is an open access article distributed under the terms and conditions of the Creative Commons Attribution (CC BY) license (<http://creativecommons.org/licenses/by/4.0/>).

Review 2

Since my thesis work focused on targeting Akt and its possible use as a treatment in HCC. The next step was to establish a bibliographic background about Akt, its implication in the function of the different cells and its inhibition via chemical inhibitors. This bibliographic background was put in use to write the second review article which was published on the 11th of February 2021.

The article is attached below.



Review

Targeting Akt in Hepatocellular Carcinoma and Its Tumor Microenvironment

Mariam Mroweh ^{1,2,3}, Gaël Roth ^{1,2,4}, Thomas Decaens ^{1,2,4}, Patrice N. Marche ^{1,2}, Hervé Lerat ^{1,2}
and Zuzana Macek Jílková ^{1,2,4,*}

¹ Institute for Advanced Biosciences, Research Center Inserm U 1209/CNRS 5309, 38700 La Tronche, France; mariam.mroweh@univ-grenoble-alpes.fr (M.M.); groth@chu-grenoble.fr (G.R.); tdecaens@chu-grenoble.fr (T.D.); patrice.marche@univ-grenoble-alpes.fr (P.N.M.); herve.lerat@univ-grenoble-alpes.fr (H.L.)

² Université Grenoble-Alpes, 38000 Grenoble, France

³ Laboratory of Cancer Biology and Molecular Immunology, Faculty of Sciences I, Lebanese University, Hadath Beirut 6573-14, Lebanon

⁴ Service d'hépatogastroentérologie, Pôle Digidune, CHU Grenoble Alpes, 38700 La Tronche, France

* Correspondence: ZMacekjilkova@chu-grenoble.fr

Abstract: Hepatocellular carcinoma (HCC) is one of the most common causes of cancer-related deaths worldwide, and its incidence is rising. HCC develops almost exclusively on the background of chronic liver inflammation, which can be caused by chronic alcohol consumption, viral hepatitis, or an unhealthy diet. The key role of chronic inflammation in the process of hepatocarcinogenesis, including in the deregulation of innate and adaptive immune responses, has been demonstrated. The inhibition of Akt (also known as Protein Kinase B) directly affects cancer cells, but this therapeutic strategy also exhibits indirect anti-tumor activity mediated by the modulation of the tumor microenvironment, as demonstrated by using Akt inhibitors AZD5363, MK-2206, or ARQ 092. Moreover, the isoforms of Akt converge and diverge in their designated roles, but the currently available Akt inhibitors fail to display an isoform specificity. Thus, selective Akt inhibition needs to be better explored in the context of HCC and its possible combination with immunotherapy. This review presents a compact overview of the current knowledge concerning the role of Akt in HCC and the effect of Akt inhibition on the HCC and liver tumor microenvironment.

Keywords: AKT; HCC; tumor microenvironment; immune cells

Citation: Mroweh, M.; Roth, G.; Decaens, T.; Marche, P.N.; Lerat, H.; Macek Jilkova, Z. Targeting Akt in Hepatocellular Carcinoma and Its Tumor Microenvironment. *Int. J. Mol. Sci.* **2021**, *22*, 1794. <https://doi.org/10.3390/ijms22041794>

Received: 23 January 2021

Accepted: 9 February 2021

Published: 11 February 2021

Publisher's Note: MDPI stays neutral with regard to jurisdictional claims in published maps and institutional affiliations.



Copyright: © 2021 by the authors. Licensee MDPI, Basel, Switzerland. This article is an open access article distributed under the terms and conditions of the Creative Commons Attribution (CC BY) license (<http://creativecommons.org/licenses/by/4.0/>).

1. Introduction

Hepatocellular carcinoma (HCC) is the most common type of liver malignancy (75–85%), and it ranks fourth among the causes of cancer-related deaths worldwide [1]. HCC generally emerges from a chronic inflammatory environment caused by various reasons. They could be of viral origins, like hepatitis C and B viruses (HCV, HBV), or caused by metabolic disorders leading to non-alcoholic fatty liver diseases (NAFLD) and non-alcoholic steatohepatitis (NASH). Moreover, chronic consumption of alcohol or consumption of toxins (such as aflatoxins) and hereditary diseases such as hemochromatosis lead to chronic liver inflammation, which could further develop into HCC [2].

Chronic liver inflammation often leads to fibrosis followed by cirrhosis and finally HCC. The changes in the state of the liver throughout the development of HCC are accompanied by a change in the tumor microenvironment (TME) profile, which sustains a niche favoring malignancy. The modulations in the status of TME affect an array of cells that include immune cells (resident and migratory), endothelial cells, hepatic stellate cells, and others. This leads to the differentiation of cells into those that support tumor

development and progression: tumor-associated macrophages (TAMs), tumor-associated neutrophils (TANs), and cancer-associated fibroblasts (CAFs) [3]. The changes in the phenotypic and secretory profile of cells of TME result from the change in the transcriptome and/or an altered protein function in the cells accompanied by dysregulation of the complex signaling pathways in the cells. The alteration of the signaling pathways is common in HCC and is crucial for the progression of the tumor. RAS/RAF/MEK/ERK, HGF/MET, VEGF, PDGF, EGF, IGF, JAK/STAT, p53, MAPK, Wnt/ β -catenin, TGF- β , and PI3K/Akt/mTOR [4] are among the altered signaling pathways.

HCC is challenging to diagnose and has limited therapeutic options. HCC patients often remain asymptomatic until they reach an advanced stage, hindering diagnosis. Alpha fetoprotein, the most widely used biomarker for HCC surveillance and diagnosis, is ineffective in accurately detecting early HCC [5,6]. Several advances have been made recently in the field of liver imaging and the development of novel biomarkers to attempt early detection of HCC, but most detected HCC cases are still diagnosed in advanced stages.

At an early stage of the disease, HCC can be treated by surgical resection, percutaneous ablation, or liver transplantation. At a later stage, the therapeutic options have been limited during the last decade to Sorafenib (a multikinase inhibitor) [7,8]. Recently, other first-line treatments such as lenvatinib and second-line treatments such as regorafenib and cabozantinib have been proposed for treatment. However, these drugs demonstrate no superior efficacy compared to Sorafenib [9]. In 2020, immunotherapy re-shuffled the cards with the combination Atezolizumab (an anti-programmed death-ligand 1 (PDL-1) antibody) plus Bevacizumab (an anti-vascular endothelial growth factor (VEGF) antibody), considerably increasing tumor response and survival outcomes and becoming the new first line therapy of advanced HCC. [10]. Nevertheless, only a minority of HCC patients benefit from this therapy, and alternative strategies are needed to augment host immune response [11].

As the search for therapies for HCC continues, several researchers are trying to pinpoint specific effector proteins that could be targeted. In this review, we demonstrate the role played by Akt (also known as Protein Kinase B) in the progression of HCC at the level of the tumor and TME and the growing interest in targeting Akt as a therapeutic option for HCC, Figure 1.

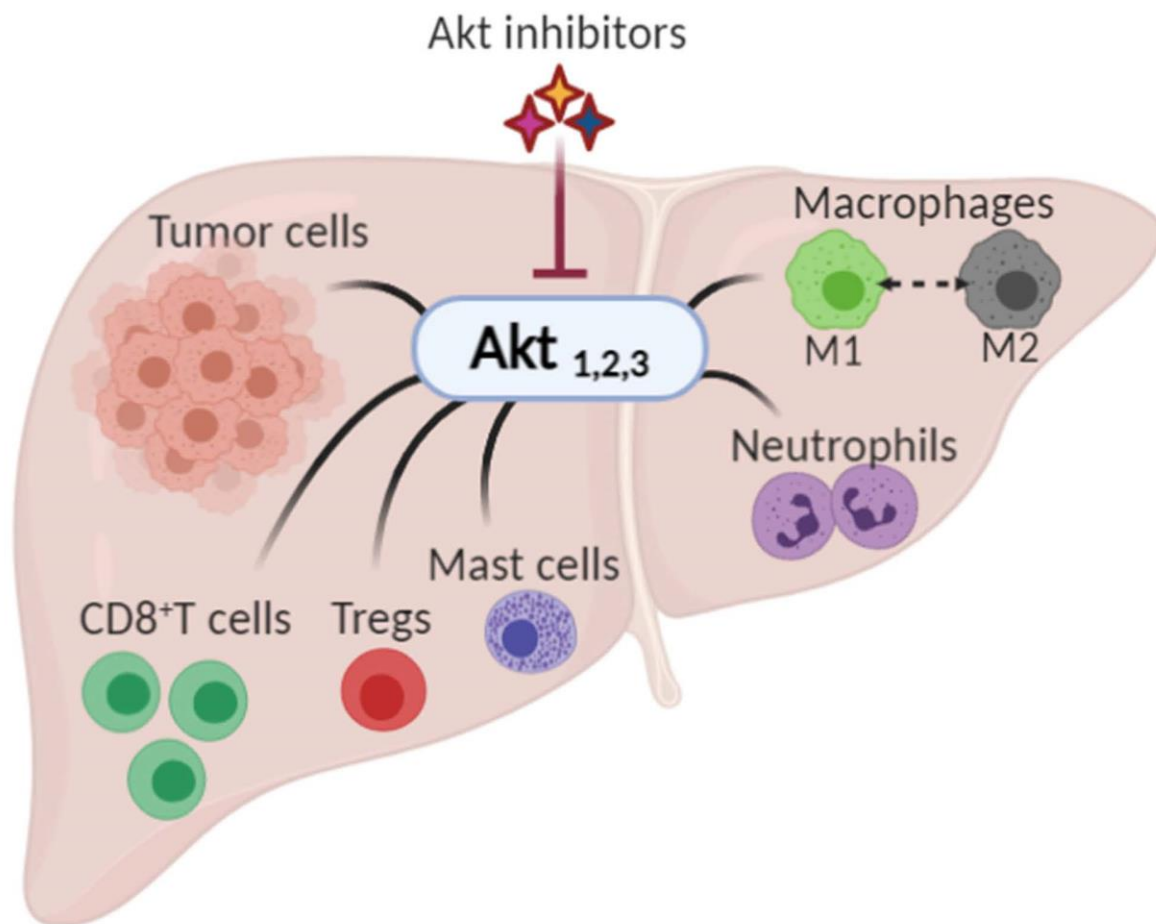


Figure 1. The possible impact of Akt inhibition on hepatocellular carcinoma and its tumor microenvironment. Akt, expressed as three isoforms, Akt1, Akt2, and Akt3, has been shown to play a role in the progression of cancer by controlling the growth, proliferation, and survival in tumor cells, and by modulating tumor microenvironment (namely CD8+ T cells, regulatory T cells (Tregs), mast cells, neutrophils, and macrophages).

2. Akt Isoforms: Differences and Uniqueness

Akt is a serine/threonine protein kinase family member discovered in 1991 [12]. The ~56 kDa protein exists in mammals in three isoforms translated from three distinct genes: Akt1 (PKB alpha), Akt2 (PKB beta), and Akt 3 (PKB gamma). While the first two isoforms are constitutively expressed throughout the body—with a preference for insulin-sensitive tissues for Akt2—Akt3 is said to be expressed in the brain and the testes. On the structural level, Akt consists of the following three domains: (1) the amino-terminal pleckstrin homology (PH) domain, (2) a central domain sharing homology with other cAMP-dependent protein kinases (AGC kinases), and (3) a carboxyl-terminal domain serving as a regulatory domain. These three isoforms share homologies in their catalytic domains, but they diverge in the PH and regulatory domains [13]. Akt is said to be a master regulator serving as the center point in the phosphatidylinositol 3 kinase (PI3K)/Akt pathway, which regulates several cellular processes encompassing cell survival, cell size/growth, survival, proliferation, glucose metabolism, transcription, protein synthesis, genome stability, and neovascularization, and thus any disturbance in this pathway has drastic effects on the cellular homeostasis [13]. The recruitment of various Akt isoforms to the plasma membrane is crucial for their activation. The PH domain binds to the phosphatidylinositol-3,4,5-triphosphate (PIP3) generated by the action of PI3K at the plasma membrane. While there, Akt is prone to two phosphorylation events at the following threonine (Thr) and serine (Ser) residues: Thr 308 and Ser 473 for Akt1,

Thr 309 and Ser 474 for Akt2, and Thr 305 and Ser 472 for Akt3. The Thr phosphorylation events are executed by phosphoinositide-dependent kinase-1 (PDK-1), whereas Ser phosphorylation events are executed by other kinases like the mammalian target of rapamycin complex 2 (mTORC2) and integrin-linked kinases (ILK). These two phosphorylation events are essential for Akt to attain its full function. However, it remains functional only with the Thr phosphorylation. In some instances, the activation of Akt surpasses the PIP3 checkpoint and can be activated by actin, heat shock protein (Hsp) 90, Hsp27, and Posh [13,14]. Various substrates are prone to phosphorylation by Akt, and they are said to be the downstream effectors of this pathway to regulate the various cellular processes. Some of these that can be highlighted are the following: proline-rich Akt substrate of 40 kDa (PRAS40), cyclin-dependent kinase (CDK) inhibitors P21 and P27, paladin and vimentin, inhibitors of KappaB Kinase alpha (IKK α), and tumor progression locus 2 (Tpl2). Moreover, Akt-mediated phosphorylation of tuberous sclerosis (TSC)1/2 complex and mTORC1 regulate cell growth. Survival has also been found among the cellular processes controlled by Akt through the direct inhibition of pro-apoptotic proteins like Bad or the inhibition of pro-apoptotic signals fired by the transcription factors such as Forkhead box protein O1 (FoxO1) [14]. Metabolism-related proteins like glycogen synthase kinase (GSK) 3 β are also among the substrates for Akt. Although the different isoforms show an overlap in their activity, the substrate-specificities of Akt1/2/3 exist. These are dependent on the distribution of the Akt isoforms in the tissues, the differential activation of Akt by external stimuli (amplitude and timing of activation), the preferential intrinsic catalytic activity of the different isoforms, and the specific cell-context factors (subcellular localization and substrate proximity) [15]. Finally, a negative feedback loop exists for turning off this pathway, and this feedback is mediated by protein phosphatase 2A (PP2A), PH domain leucine-rich-repeat-containing protein phosphatase 1/2 (PHLPP2), and phosphatase and tensin homolog (PTEN) [13].

3. Akt in the Development and Progression of Hepatocellular Carcinoma

The PI3K/Akt signaling pathway has been receiving a lot of attention in cancer research as it has been shown to be hyper-activated in different types of cancer. The PI3K/Akt hyper-activation appears often due to the activating mutations in the effector molecules upstream and downstream of Akt rather than in Akt itself—except for the E17K mutation in the PH domain of Akt. The common activating mutations include the following: (i) a mutation hitting the catalytic subunit of PI3K rendering it constitutively active, (ii) loss of PTEN (whose role is to deactivate Akt), (iii) activation mutations of RAS and growth factor receptors, and (iv) gene amplification mutations of Akt and/or its effectors [16].

Activation of the Akt signaling pathway is closely related to the occurrence and development of liver inflammation and fibrosis [17–19] and is associated with a poor prognosis for HCC patients [20]. Importantly, a bioinformatic study analyzed 331 candidates for HCC prognostic factors among which all the three Akt isoforms were selected for further clinical validation, and the results showed a correlation between tumor aggressiveness and poor prognosis [21].

The contribution of the various Akt isoforms in the progression of HCC has been explored by research carried out over the years. As far as Akt1 is concerned, a study in 2019 showed that the Akt1-mediated phosphorylation of mTORC2 is crucial for triggering hepatocarcinogenesis in humans and mice, as it contributes to cellular growth through c-Myc activation [22]. Further, the altered metabolic state of the liver in HCC commonly exhibits a marked up-regulation of aldose reductase. Interestingly, aldose reductase has been shown to interact with the catalytic domain of Akt1, leading to an activation of the Akt/mTOR pathway [23]. Moreover, the TME components can lead to an activation of Akt. For instance, an *in vitro* study mimicking the augmented TME polyamine levels in HCC showed a subsequent increase in the levels of Akt1 along with those of ornithine decarboxylase, spermidine/spermine N1 acetyl transferase, hypoxia

inducing factor 1 α , matrix metalloproteinase 9, VEGF, and downregulated p27. The previous fluctuations resulted in an increase in the proliferation and the migration of HepG2 cells (HCC cell line) [24]. To further support the role of Akt1 in HCC progression, a study demonstrated that the overexpression of myristoylated Akt1—and thus constitutively active Akt1—led to a liver tumor development in mice, and its combination with S-phase kinase-associated protein overexpression exacerbated the phenotype [25]. Interestingly, a real-time imaging study of Akt1 in HCC cells demonstrated that the nuclear translocation of Akt1 is independent of the phosphorylation events at the Thr308 and Ser473 [26]. In contrast, a study showed that a decrease in β -catenin levels in the HepG2 cell line showed no change in the Akt1 expression level, while it decreased the phosphorylated and consequently decreased cell growth. This stresses the cross-communication between the different signaling pathways activated by the signals from TME, which converge onto the Akt1 activity and its effect on HCC progression [27].

Akt2 has also been shown to be a contributor to HCC progression, and some researchers argue that its role in HCC prognosis surpasses that of Akt1. A study by Xu et al. detected overexpression of Akt2 in 38% of the HCC tissues of the studied cohort with a moderate or less expression of Akt1 in all the cases. The high expression of Akt2 correlated with the histopathological differentiation, portal invasion, and the number of tumor nodules, while Akt1 did not correlate with any of these clinicopathological features [28]. An *in vitro* study conducted to investigate the role of Akt2 in the proliferation and migration of HCC cells showed that Akt2 was regulated by STAT3. The ablation of STAT3 by small-interfering RNA (siRNA) led to a decrease in the phosphorylated form of Akt2 and a subsequent decrease in the proliferation and migration of HCC cells. Moreover, the *in vivo* transfection with siRNA against STAT3 decreased the pace of the tumor growth, a process that was reversed by the expression of Akt2. This points to the significant role of Akt2 in the growth of the tumor [29]. Another *in vivo* study highlighted the importance of Akt2 in the process of hepatic steatosis and carcinogenesis. In this study, the hydrodynamic transfection of a mutated form of PI3K subunit alpha alone into mouse livers led to hepatic steatosis, whereas the transfection with a combination of a mutated form of PI3K subunit alpha combined with either NRASV12 or c-Met in the mouse liver led to the development of tumor nodules, which exhibited an increase in the activation of Akt/mTOR and RAS/MAPK signaling pathways. The ablation of Akt2 in mouse livers inhibited both the hepatic steatosis in the former case and tumorigenesis in the latter one [30]. Interestingly, a study of Zebra fish showed that the induced expression of oncogenic Kras led to the development of HCC having great resemblance to the human tumors with an elevated Akt2 activation [31]. On the other hand, the concomitant and systemic deletion of Akt1 and Akt2 in adult mice caused hypoglycemia, liver inflammation, and death [32], pointing to potential toxicities of strong and long-lasting Akt inhibition.

Despite the previous knowledge about the focused expression of Akt3 in the testes and brain, some studies have shown the implication of Akt3 in HCC. A series of studies on micro-RNA (miRNA) profiles in HCC revealed the downregulation of miRNA-144, and miRNA-582-5p. The downregulation of the previously mentioned miRNAs resulted in a sustained expression of their downstream targets. Both the aforementioned miRNAs showed Akt3 among their targets, and their subsequent downregulation supported tumor progression and growth. This supports the contribution of Akt3 in HCC progression [33,34].

4. Akt Modulates the Immune Cells

In addition to direct anti-tumor activity, there is growing evidence that targeting the Akt pathway has an indirect anti-tumor activity that is mediated by the response of immune cells [35]. In fact, TME, which is generally immunosuppressive and metaboli-

cally stressed, can be modulated by Akt, as this pathway is essential to the differentiation, maturation, and functioning of many immune cells. At present, the immunomodulation by Akt is best characterized at the level of T cells and macrophages.

4.1. Akt Regulates the Functions and Fate of T Cells

The regulation of the nutrient metabolism in the T cells is important for the control of their differentiation, as it shapes their function and survival. Quiescent T cells require oxidative catabolic metabolism and use low amounts of nutrients. T cell activation through T cell receptors (TCR) induces a metabolic switch to aerobic glycolysis and anabolic metabolism to sustain cell division and differentiation. Then, different subsets of activated T cells adopt fine-tuning of metabolism homeostasis according to their functions and fate. For example, the glycolytic rates are higher in Th1, Th2, and Th17 than in the T regulatory cells (Tregs). Tregs use fatty acid oxidation for their energy demand, while memory T cells use mitochondrial oxidative phosphorylation and fatty acid oxidation for their long-term persistence [36].

The PI3K-Akt pathway orchestrates the nutrient uptake and utilization within the cell. Thus, it is a key pathway to regulate the functions and fate of T cells. The TCR and CD28 co-stimulation by their respective ligands is known to engage the PI3K/Akt/mTOR signaling cascade [37]. The differentiation into effector T cells and memory T cells is achieved, in part, by asymmetric division, where daughter cells contain different amounts of active mTORC1. Thus, the high levels of active mTORC1 in effector T cells increase glycolytic activity, and the low levels in memory T cells increase lipid metabolism. This event is achieved by RagC mediated translocation of mTOR to the lysosomes through a CD98 and leucine-dependent mechanism [38]. The mTOR inhibition in T cells induces tolerance through the T cell energy [39] and blocks the differentiation to effector T cells leading to the generation of FoxP3⁺, Tregs, and CD8⁺ memory T cells. This is associated with the lower activation of the transactivation factors STAT4, 6, and 3 in response to IL-12, 4, and 6 stimulations. Interestingly, and in contrast with hepatocytes, the Akt-dependent induction of mTORC1 activity in the T cells does not require mTORC2 for their differentiation into Th1 and Th17. In contrast, the T cell differentiation into Th2 requires functional mTORC2 [40]. TCR can induce the mTOR activation through upstream PI3K/Akt activation, which is the signaling that is enhanced by costimulatory receptors (e.g., CD28) [37].

In contrast, cytotoxic T-lymphocyte-associated protein 4 (CTLA-4) and PD-1 can antagonize the mTOR activity via Akt and PI3K inhibition. Indeed, the CTLA-4 mediated inhibition of Akt is dependent on PP2A. The PD-1-induced Akt inhibition involves a blockade of the CD28 cytoplasmic tail function (probably through SHP1/2), thus preventing the synthesis of PI3P by PI3K. In addition, the PD-1-induced PI3K/Akt pathway inhibition is more potent to block T cell differentiation than the CTLA-4-induced PI3K/Akt inhibition [41]. Notably, the PI3K/Akt/mTOR pathway also regulates lymphocyte trafficking through the modulation of CD62L and CCR-7 expression [42].

Regarding the Akt isoform dichotomization in T cell activation, recent publications suggest a divergence in Akt1, 2, or 3 functions. The Akt-1 isoform downregulates proliferation of the thymus-derived Tregs, thus facilitating antigen-specific Th1/Th17 responses. On the other hand, Akt2 increases the proliferation of Tregs and suppresses the antigen-specific Th1/Th17 responses. Furthermore, the treatment with a specific Akt1 inhibitor suppresses disease progression in a mouse model of autoimmune encephalomyelitis [43]. The Akt3 signaling in T cells, and not neurons, is necessary for maintaining the central nervous system integrity during an inflammatory demyelinating disease (in vivo model of myelin-oligodendrocyte glycoprotein-induced experimental autoimmune encephalomyelitis) [44]. Further studies are needed to clarify the role of each Akt isoform in the T cell activation process and antitumor activity.

In conclusion, the Akt pathway is at the epicenter of the T cell activation/differentiation process. This needs to be taken into consideration while choosing the therapeutic targeting of this pathway.

4.2. Macrophage Polarization

Macrophages are a heterogeneous population of cells arising from the myeloid lineage and are involved in innate immunity. The roles of these cells during pathogen encounters are broad, and they encompass antigen processing, presentation, orchestration of inflammatory response, clearance, and repair. A dichotomy between “classically activated macrophages” and “alternatively activated macrophages” depending on different stimuli has been described and led to the emergence of an “M1” versus “M2” terminology. As simple as this classification sounds, in reality, such clear division was challenged by the discovery of TAMs that do not fit in this classification system. Different subsets of M2 macrophages (M2a, M2b, M2c, and M2d) were brought into the spotlight in accordance with their transcription profiles and responses to the different stimuli. Importantly, the presence of TAMs is generally associated with a poor prognosis in solid tumors [45].

The different polarization states of the macrophages result in different modes of action according to the tissue environment based on the signals that they receive from the surrounding cells. M1 macrophages exhibit a pro-inflammatory function along with a microbicide activity and resistance to pathogens. M2 macrophages predominantly mount an anti-inflammatory response, parasite control, tissue remodeling, and immune modulation. The macrophage polarization fate is dictated by the regulation of cytokine production, phagocytosis, autophagy, apoptosis, and metabolism. All of these pathways seemed to have Akt as the converging node. In fact, signaling cascades controlled by PI3K-Akt largely contributed to macrophage polarization [46].

The PI3K/Akt pathway plays a key role in the increase of anti-inflammatory markers such as arginase-1 and IL-10 and inhibition of the production of pro-inflammatory cytokines [47,48]. It has been described that activation of the PI3K-Akt pathway results in increased polarization of M2 macrophages [46], and BMP7 and SMAD 1/5/8 might play a major role in these events [49]. Expectedly, published data also suggest that the inhibition of either PI3K or mTOR results in M1 macrophage polarization [50,51]. For example, rapamycin treatment has been found to promote M1 polarization [52]. Nevertheless, the Akt pathway can also be triggered in macrophages by TLR4 activation [53], activating downstream NF κ B [54] and mTORC1 [55], which are responsible for M1 genes transcription.

While differences in the PI3K/Akt pathway involvement upon macrophage activation might arise from distinct tissue environments or macrophage origins between studies, the differences in the Akt isoforms (Akt 1, 2, or 3) play an important role in this matter [46]. Studies using double and triple gene knockout have showed increasing evidence that each Akt isoform possesses non-overlapping functions. Indeed, in a study using dextran sodium sulfate-induced colitis, the genetic ablation of Akt1 isoform exacerbated the disease; however, the ablation of Akt2 in these mice protected them. This difference was due to the M1 profile and M2 profile in these two cases, respectively [56]. Moreover, studies have shown that knocking down of the Akt1 expression promotes the upregulation of iNOS and IL-12 β (M1 activation) and suppresses TLR4-induced M1 macrophage activation. In contrast, as reviewed previously, the knockout of Akt2 resulted in an M2 phenotype along with elevated M2 markers (Arg1, Ym1, and Fizz1), endotoxin tolerance, and elevated levels of IL-10 [46].

Still, the role of the Akt isoform subcellular localization in macrophages has been poorly documented, and a further level of complexity exists based on the acute versus chronic activation of Akt that remains to be tested in terms of macrophage fate. In conclusion, activation of macrophages is highly dependent on the Akt pathway, but the full

picture of Akt involvement in macrophage polarization remains to be completed, especially concerning the role of each Akt isoform in TME of HCC.

4.3. Other Cells in TME

TANs are major players in the TME of HCC. They recruit both macrophages and Tregs to promote the progression of HCC [57]. Akt signaling cascade is involved in migration, degranulation, and O₂ production, and the Akt2 isoform has a predominant role in regulating neutrophil functions [58].

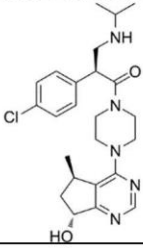
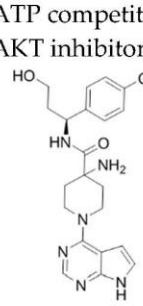
Additionally, mast cells modulate the immune response and mediate angiogenesis. It has been demonstrated that the recruitment of mast cells increases angiogenesis by PI3K-Akt-GSK3 β -AM signaling, which can be reversed by Akt inhibition [59].

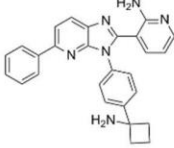
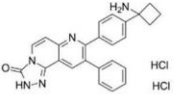
5. Targeting Akt in the Management of HCC

Numerous compounds have been reported to inhibit the PI3K/Akt/mTOR pathway, as reviewed previously [60,61]. Akt inhibitors have been tested as an anti-tumor treatment in several preclinical studies and early clinical phase trials, mostly in gynecologic and prostate cancers. Furthermore, data from preclinical and clinical studies are also available for HCC (as summarized in Table 1).

Classical ATP-competitive Akt inhibitors such as ipatasertib (GDC-0068) and capivasertib (AZD5363) are currently in phase-I and phase-II clinical trials for mono- or combination-therapies. However, because the ATP-binding pocket of Akt is highly conserved among kinases, the selectivity of these inhibitors is limited, and their use is associated with side effects during treatment and lack of efficacy. The efforts to identify more specific and selective small molecules have resulted in the development of allosteric inhibitors such as MK-2206, ARQ092, and ARQ751 [62,63].

Table 1. Akt inhibitors in the management of HCC.

Inhibitor	Mechanism of Action, Structure	Experiment Setup	Antitumor Effect	Effect on TME	Clinical Trial
GDC-0068 [64–66]	ATP competitive AKT inhibitor 	Combination of GDC-0068 with Sorafenib in HepG2 and Huh7 sorafenib-resistant cell-lines	- synergistic antitumor effect - promotion of apoptosis - induction of autophagic cell death	Not investigated	Phase-I/II including multiple solid tumors treated by GDC-0068 in monotherapy or in association with abiraterone + prednisolone: safe and tolerable in monotherapy or in combination
AZD5363 [67,68]	ATP competitive AKT inhibitor 	Single agent in HepG2 and Huh-7 HCC cells Combination with FH535 (β -catenin inhibitor) in THH, Hep3B and HepG2	- inhibition of tumor proliferation - induction of cell-cycle arrest - promotion of apoptosis - promotion of autophagy through p53 activation	Not investigated	Phase-I, AZD5363 in monotherapy, in multiple advanced solid tumors including liver cancer (NCT01895946): safe and tolerable, no data on anti-tumor response Phase-I including multiple solid tumors harboring AKT mutations (NCT02465060)

ARQ 092 [69,70]	allosteric pan-AKT inhibitor 	Single agent and in combination with Sorafenib in a DEN-induced cirrhotic rat model of HCC and in Hep3B, HepG2, Huh-7, PLC/PRF, and HR4 HCC cell lines	- inhibition of tumor proliferation - promotion of apoptosis - synergistic antitumor effect when combined with sorafenib	- anti-angiogenic effect, - improved liver fibrosis - decrease of intrahepatic neutrophils and macrophages	No clinical trial
ARQ 751 [71]	allosteric pan-AKT inhibitor Chemical structure of ARQ 751 is currently unavailable.	Single agent and in combination with sorafenib in DEN-induced cirrhotic rat model of HCC	- inhibition of tumor proliferation - synergistic antitumor effect when combined with sorafenib	Improved liver fibrosis	Phase-Ib (NCT02761694) in solid tumors with PIK3CA/AKT/PTEN mutations including HCC: ongoing
MK-2206 [72,73]	allosteric pan-AKT inhibitor 	Single agent in Human Huh7, Hep3B, and HepG2 HCC cell lines	- Promotion of apoptosis - Inhibition of cell proliferation - Induction of cell cycle arrest	Not investigated	Phase-II trial, MK-2206 in monotherapy in advanced HCC previously treated (NCT01239355): discontinued due to discouraging results

First, an ATP-competitive Akt inhibitor GDC-0068 showed promising antitumor activity, ranging from tumor growth delay to regression in multiple tumor xenograft models as a single agent to the potentialized antitumor activity of classic chemotherapeutic agents [64]. A high basal level of phospho-Akt, PTEN loss, and PIK3CA kinase domain mutations were predictive of a better response to GDC-0068 [64]. More specifically, in an in vitro model of sorafenib-resistant HCC cells, the exposure to GDC-0068 combined with sorafenib restored sensitivity to Sorafenib by switching autophagy, one of the known resistance mechanisms, from a cytoprotective role to a death-promoting mechanism. This association induced a synergistic antitumor effect suggesting, at the time, that GDC-0068 represents a good candidate for further clinical trials in combination with Sorafenib [65]. In clinics, to this day, GDC-0068 was tested in a phase-I basket trial with multiple solid tumors including only one HCC patient without any further study carried out in this pathology [66]. This compound is currently mostly studied in prostate and breast cancers in combination with other anticancer agents.

AZD5363, also known as Capivasertib, is another Akt inhibitor that binds to and inhibits all Akt isoforms. In a large number of cancer cell lines, it has been shown to decrease FOXO3a phosphorylation through Akt inhibition, leading to FOXO3a translocation to the nucleus where it can “switch on” the expression of genes, such as p27, FasL, and BIM by inducing cell-cycle arrest and promoting apoptosis [74]. Moreover, AZD5363 suppresses the proliferation of human HCC cell lines, HepG2 and Huh-7, by inhibiting the phosphorylation of downstream molecules in the Akt signal pathway in a dose- and time-dependent manner [67]. AZD5363 was studied in combination with the β -catenin inhibitor (FH535) in vitro. This combination induced a stronger effect on cell death and displayed antiproliferative effects on transformed human hepatocytes through inhibition of cell-cycle progression, enhanced autophagy marker protein expression, and autophagy-associated death. These promising results suggest that inhibiting

both Akt and β -catenin pathways may represent a new therapeutic way of treating HCC that would, however, require further preclinical and clinical investigations [75]. AZD5363 was tested in a phase-I trial in multiple advanced solid tumors including HCC, and it showed acceptable safety and tolerability profiles [68]. Moreover, it is still under investigation in a large phase-I study, the MATCH screening trial, that includes multiple solid tumors harboring druggable mutations including Akt mutations (NCT02465060).

ARQ 092 is a small allosteric pan-Akt inhibitor that showed interesting results in a diethylnitrosamine- (DEN) induced rat model of HCC developing on cirrhosis, which was assessed by MRI. The ARQ 092 treatment induced downregulation of the mTOR pathway with a decrease in the active phosphorylated form of Akt and its downstream actors. ARQ 092 improved the tumor response, normalized the vascularization, and significantly decreased the fibrosis of the surrounding liver [69]. A combination of ARQ 092 with Sorafenib synergistically decreased the tumor progression with the promotion of apoptosis and reduction of tumor proliferation and angiogenesis [70], and similar effects were observed when ARQ 751, a next-generation allosteric pan-Akt inhibitor, was used [71]. ARQ 751 is now tested in clinics, in a phase-Ib basket trial, as a single agent or in combination with other anticancer drugs in the case of solid tumors with PIK3CA/Akt/PTEN mutations including HCC (NCT02761694).

MK-2206, another allosteric Akt inhibitor that has been studied *in vitro* and *in vivo* in many cancers, has shown interesting *in vitro* activity resulting in cell-cycle arrest, inhibition of cancer cell proliferation, and promotion of apoptosis in human HCC cell lines [72]. It was, later, studied in a phase-II trial including patients with advanced HCC that was previously treated but was prematurely arrested due to discouraging results (NCT01239355). Another phase-II trial in the case of advanced biliary cancer was also stopped after eight inclusions due to the absence of clinical efficacy as a single agent but with an acceptable safety profile (NCT01425879) [73]. Further trials are needed on this front in combination with other targeted therapies.

The data concerning Akt inhibitors in HCC are still preliminary and future clinical development may have to involve combinations with other targeted therapies such as β -catenin inhibitors or immune checkpoint inhibitors to improve the care of HCC patients.

6. Conclusions and Future Perspectives

Although the Akt inhibitors have been intensively studied during the past decade in the context of cancer, their effect on TME has received less attention until very recently. Interestingly, recent studies suggest that apart from their direct anti-tumor activity, the Akt inhibitors have the capacity to modulate TME and to switch it from pro-tumoral to anti-tumoral. The inhibition by AZD8835 in pre-clinical mouse tumor models directly increased CD8⁺ T-cell activation, while Tregs, macrophages, and myeloid-derived suppressor cells were strongly suppressed [76]. Similarly, in several different tumor-bearing mice, the Akt pathway inhibitor, MK-2206, caused the selective depletion of suppressive Tregs, which was associated with enhanced cytotoxic CD8 responses [77]. The Akt inhibitor, AZD5363, was administered as an adjuvant after radiotherapy in tumor-bearing mice which was associated with marked reductions in tumor vascular density, a decrease in the influx of CD11b⁺ myeloid cells, and a failure of tumor regrowth [78]. Similarly, in the rat model of HCC, which accurately recapitulated the scenario and TME of human HCC [79], the Akt inhibition by ARQ 092 was associated with the modulations of TME mainly in the form of a decrease in the accumulation of intrahepatic neutrophils and macrophages [70]. Recent studies have also demonstrated the effect of the Akt inhibitors on TME in cancer patients. For instance, in HER2 negative breast cancer patients, two oral doses of the Akt inhibitor, MK-2206, were associated with a favorable immune profile in TME, including increased CD3⁺CD8⁺ density and greater expression of interferon genes [80]. However, there is no study yet assessing the impact of Akt inhibition on TME in HCC patients.

In conclusion, the Akt pathway plays an important role in the regulation of several processes in the development and progression of HCC. It does this by controlling the growth, proliferation, and survival in tumor cells, on one hand, and by modulating TME, on the other. TME was the underestimated player until recently, but its involvement in HCC progression is now well-recognized. In this article, we have emphasized the importance of considering the effects on TME while developing strategies inhibiting Akt in HCC. Targeting Akt can lead to a favorable change in the immune microenvironment and thus provides a rationale for combining these agents with immunotherapeutics. Additional studies are warranted to pave the way for combining Akt inhibition with immunotherapy in HCC. Furthermore, the isoforms of Akt converge and diverge in their designated roles, but the currently available Akt inhibitors fail to display an isoform specificity. Thus, additional investigations are needed to define the isoform specificity of Akt-related therapeutic targets to trigger a beneficial immune response in HCC patients.

Author Contributions: Conceptualization: M.M., H.L. and Z.M.J.; writing—original draft preparation: M.M., G.R., H.L. and Z.M.J.; writing—review and editing: M.M., G.R., T.D., P.N.M., H.L. and Z.M.J.; project administration: P.N.M., T.D. and Z.M.J.; funding acquisition: T.D. and Z.M.J. All authors have read and agreed to the published version of the manuscript.

Funding: This research was funded by “Dotation Agir pour les Maladies Chroniques” and by “Ligue contre le cancer AURA”, France, by the grant “Exploring the role of AKT in the HCV induced hepatocarcinogenesis” from FINOVI-FUL (2019–2021) and by Agence Nationale de la Recherche sur le SIDA et les Hépatites. M.M. was supported by a fellowship from the Lebanese University, Lebanon.

Acknowledgments: M.M. acknowledges the Lebanese University in Lebanon (namely, Bassam Badran and Nader Hussein) and “Fondation Université Grenoble-Alpes” for their support.

Conflicts of Interest: The authors declare no conflict of interest.

References

1. Fitzmaurice, C.; Abate, D.; Abbasi, N.; Abbastabar, H.; Abd-Allah, F.; Abdel-Rahman, O.; Abdelalim, A.; Abdoli, A.; Abdollahpour, I.; Abdulle, A.S.M. Global, Regional, and National Cancer Incidence, Mortality, Years of Life Lost, Years Lived With Disability, and Disability-Adjusted Life-Years for 29 Cancer Groups, 1990 to 2017: A Systematic Analysis for the Global Burden of Disease Study. *JAMA Oncol.* **2019**, *5*, 1749–1768.
2. Ogunwobi, O.O.; Harricharran, T.; Huaman, J.; Galuza, A.; Odumuwagun, O.; Tan, Y.; Ma, G.X.; Nguyen, M.T. Mechanisms of hepatocellular carcinoma progression. *World J. Gastroenterol.* **2019**, *25*, 2279–2293.
3. Mroweh, M.; Decaens, T.; Marche, P.N.; Macek Jilkova, Z.; Clément, F. Modulating the Crosstalk between the Tumor and Its Microenvironment Using RNA Interference: A Treatment Strategy for Hepatocellular Carcinoma. *Int. J. Mol. Sci.* **2020**, *21*, 5250.
4. Nault, J.C.; Zucman-Rossi, J. Genetics of hepatocellular carcinoma: The next generation. *J. Hepatol.* **2014**, *60*, 224–226.
5. Kim, E.; Viatour, P. Hepatocellular carcinoma: Old friends and new tricks. *Exp. Mol. Med.* **2020**, *52*, 1898–1907.
6. Macek-Jilkova, Z.; Malov, S.I.; Kurma, K.; Charrat, C.; Decaens, T.; Peretolchina, N.P.; Marche, P.N.; Malov, I.V.; Yushchuk, N.D. Clinical and Experimental Evaluation of Diagnostic Significance of Alpha-Fetoprotein and Osteopontin at the Early Stage of Hepatocellular Cancer. *Bull. Exp. Biol. Med.* **2021**, *170*, 340–344.
7. Llovet, J.M.; Ricci, S.; Mazzaferro, V.; Hilgard, P.; Gane, E.; Blanc, J.F.; de Oliveira, A.C.; Santoro, A.; Raoul, J.L.; Forner, A.; et al. Sorafenib in advanced hepatocellular carcinoma. *N. Engl. J. Med.* **2008**, *359*, 378–390.
8. Fan, G.; Wei, X.; Xu, X. Is the era of sorafenib over? A review of the literature. *Ther. Adv. Med. Oncol.* **2020**, *12*, 1758835920927602.
9. Faivre, S.; Rimassa, L.; Finn, R.S. Molecular therapies for HCC: Looking outside the box. *J. Hepatol.* **2020**, *72*, 342–352.
10. Finn, R.S.; Qin, S.; Ikeda, M.; Galle, P.R.; Ducreux, M.; Kim, T.Y.; Kudo, M.; Breder, V.; Merle, P.; Kaseb, A.O.; et al. Atezolizumab plus Bevacizumab in Unresectable Hepatocellular Carcinoma. *N. Engl. J. Med.* **2020**, *382*, 1894–1905.
11. Macek Jilkova, Z.; Aspord, C.; Decaens, T. Predictive Factors for Response to PD-1/PD-L1 Checkpoint Inhibition in the Field of Hepatocellular Carcinoma: Current Status and Challenges. *Cancers* **2019**, *11*, 1554.
12. Bellacosa, A.; Testa, J.R.; Staal, S.P.; Tsichlis, P.N. A retroviral oncogene, akt, encoding a serine-threonine kinase containing an SH2-like region. *Science* **1991**, *254*, 274–277.
13. Martelli, A.M.; Tabellini, G.; Bressanin, D.; Ognibene, A.; Goto, K.; Cocco, L.; Evangelisti, C. The emerging multiple roles of nuclear Akt. *Biochim. Biophys. Acta* **2012**, *1823*, 2168–2178.

14. Nitulescu, G.M.; Margina, D.; Juzenas, P.; Peng, Q.; Olaru, O.T.; Saloustros, E.; Fenga, C.; Spandidos, D.; Libra, M.; Tsatsakis, A.M. Akt inhibitors in cancer treatment: The long journey from drug discovery to clinical use (Review). *Int. J. Oncol.* **2016**, *48*, 869–885.
15. Gonzalez, E.; McGraw, T.E. The Akt kinases: Isoform specificity in metabolism and cancer. *Cell Cycle* **2009**, *8*, 2502–2508.
16. Wang, Q.; Chen, X.; Hay, N. Akt as a target for cancer therapy: More is not always better (lessons from studies in mice). *Br. J. Cancer* **2017**, *117*, 159–163.
17. Ferrín, G.; Guerrero, M.; Amado, V.; Rodríguez-Perálvarez, M.; De la Mata, M. Activation of mTOR Signaling Pathway in Hepatocellular Carcinoma. *Int. J. Mol. Sci.* **2020**, *21*, 1266.
18. Son, M.K.; Ryu, Y.-L.; Jung, K.H.; Lee, H.; Lee, H.S.; Yan, H.H.; Park, H.J.; Ryu, J.-K.; Suh, J.K.; Hong, S.; et al. HS-173, a Novel PI3K Inhibitor, Attenuates the Activation of Hepatic Stellate Cells in Liver Fibrosis. *Sci. Rep.* **2013**, *3*, 3470.
19. Cai, C.X.; Buddha, H.; Castelino-Prabhu, S.; Zhang, Z.; Britton, R.S.; Bacon, B.R.; Neuschwander-Tetri, B.A. Activation of Insulin-PI3K/Akt-p70S6K Pathway in Hepatic Stellate Cells Contributes to Fibrosis in Nonalcoholic Steatohepatitis. *Dig. Dis. Sci.* **2017**, *62*, 968–978.
20. Schmitz, K.J.; Wohlschlaeger, J.; Lang, H.; Sotiropoulos, G.C.; Malago, M.; Steveling, K.; Reis, H.; Cicinnati, V.R.; Schmid, K.W.; Baba, H.A. Activation of the ERK and AKT signalling pathway predicts poor prognosis in hepatocellular carcinoma and ERK activation in cancer tissue is associated with hepatitis C virus infection. *J. Hepatol.* **2008**, *48*, 83–90.
21. Zhang, Y.; Guo, X.; Yang, M.; Yu, L.; Li, Z.; Lin, N. Identification of AKT kinases as unfavorable prognostic factors for hepatocellular carcinoma by a combination of expression profile, interaction network analysis and clinical validation. *Mol. Biosyst.* **2014**, *10*, 215–222.
22. Xu, Z.; Xu, M.; Liu, P.; Zhang, S.; Shang, R.; Qiao, Y.; Che, L.; Ribback, S.; Cigliano, A.; Evert, K.; et al. The mTORC2-Akt1 Cascade Is Crucial for c-Myc to Promote Hepatocarcinogenesis in Mice and Humans. *Hepatology* **2019**, *70*, 1600–1613.
23. Zhao, J.X.; Yuan, Y.W.; Cai, C.F.; Shen, D.Y.; Chen, M.L.; Ye, F.; Mi, Y.J.; Luo, Q.C.; Cai, W.Y.; Zhang, W.; et al. Aldose reductase interacts with AKT1 to augment hepatic AKT/mTOR signaling and promote hepatocarcinogenesis. *Oncotarget* **2017**, *8*, 66987–67000.
24. Dai, F.; Yu, W.; Song, J.; Li, Q.; Wang, C.; Xie, S. Extracellular polyamines-induced proliferation and migration of cancer cells by ODC, SSAT, and Akt1-mediated pathway. *Anti-Cancer Drugs* **2017**, *28*, 457–464.
25. Delogu, S.; Wang, C.; Cigliano, A.; Utpatel, K.; Sini, M.; Longerich, T.; Waldburger, N.; Breuhahn, K.; Jiang, L.; Ribback, S.; et al. SKP2 cooperates with N-Ras or AKT to induce liver tumor development in mice. *Oncotarget* **2015**, *6*, 2222–2234.
26. Zhu, L.; Hu, C.; Li, J.; Xue, P.; He, X.; Ge, C.; Qin, W.; Yao, G.; Gu, J. Real-time imaging nuclear translocation of Akt1 in HCC cells. *Biochem. Biophys. Res. Commun.* **2007**, *356*, 1038–1043.
27. Wang, X.H.; Meng, X.W.; Sun, X.; Liu, B.R.; Han, M.Z.; Du, Y.J.; Song, Y.Y.; Xu, W. Wnt/ β -catenin signaling regulates MAPK and Akt1 expression and growth of hepatocellular carcinoma cells. *Neoplasia* **2011**, *58*, 239–244.
28. Xu, X.; Sakon, M.; Nagano, H.; Hiraoka, N.; Yamamoto, H.; Hayashi, N.; Dono, K.; Nakamori, S.; Umeshita, K.; Ito, Y.; et al. Akt2 expression correlates with prognosis of human hepatocellular carcinoma. *Oncol. Rep.* **2004**, *11*, 25–32.
29. Xie, Y.; Li, J.; Zhang, C. STAT3 promotes the proliferation and migration of hepatocellular carcinoma cells by regulating AKT2. *Oncol. Lett.* **2018**, *15*, 3333–3338.
30. Wang, C.; Che, L.; Hu, J.; Zhang, S.; Jiang, L.; Latte, G.; Demartis, M.I.; Tao, J.; Gui, B.; Pilo, M.G.; et al. Activated mutant forms of PIK3CA cooperate with RasV12 or c-Met to induce liver tumour formation in mice via AKT2/mTORC1 cascade. *Liver Int. Off. J. Int. Assoc. Study Liver* **2016**, *36*, 1176–1186.
31. Chew, T.W.; Liu, X.J.; Liu, L.; Spitsbergen, J.M.; Gong, Z.; Low, B.C. Crosstalk of Ras and Rho: Activation of RhoA abates Kras-induced liver tumorigenesis in transgenic zebrafish models. *Oncogene* **2014**, *33*, 2717–2727.
32. Wang, Q.; Yu, W.N.; Chen, X.; Peng, X.D.; Jeon, S.M.; Birnbaum, M.J.; Guzman, G.; Hay, N. Spontaneous Hepatocellular Carcinoma after the Combined Deletion of Akt Isoforms. *Cancer Cell* **2016**, *29*, 523–535.
33. Zhang, Y.; Huang, W.; Ran, Y.; Xiong, Y.; Zhong, Z.; Fan, X.; Wang, Z.; Ye, Q. miR-582-5p inhibits proliferation of hepatocellular carcinoma by targeting CDK1 and AKT3. *Tumour Biol. J. Int. Soc. Oncodevelopmental Biol. Med.* **2015**, *36*, 8309–8316.
34. Ma, Y.; She, X.G.; Ming, Y.Z.; Wan, Q.Q.; Ye, Q.F. MicroRNA-144 suppresses tumorigenesis of hepatocellular carcinoma by targeting AKT3. *Mol. Med. Rep.* **2015**, *11*, 1378–1383.
35. Okkenhaug, K.; Graupera, M.; Vanhaesebroeck, B. Targeting PI3K in Cancer: Impact on Tumor Cells, Their Protective Stroma, Angiogenesis, and Immunotherapy. *Cancer Discov.* **2016**, *6*, 1090–1105.
36. Kouidhi, S.; Elgaaid, A.B.; Chouaib, S. Impact of Metabolism on T-Cell Differentiation and Function and Cross Talk with Tumor Microenvironment. *Front. Immunol.* **2017**, *8*, 270.
37. Waickman, A.T.; Powell, J.D. mTOR, metabolism, and the regulation of T-cell differentiation and function. *Immunol. Rev.* **2012**, *249*, 43–58.
38. Pollizzi, K.N.; Sun, I.H.; Patel, C.H.; Lo, Y.C.; Oh, M.H.; Waickman, A.T.; Tam, A.J.; Blosser, R.L.; Wen, J.; Delgoffe, G.M.; et al. Asymmetric inheritance of mTORC1 kinase activity during division dictates CD8(+) T cell differentiation. *Nat. Immunol.* **2016**, *17*, 704–711.
39. Powell, J.D.; Lerner, C.G.; Schwartz, R.H. Inhibition of cell cycle progression by rapamycin induces T cell clonal anergy even in the presence of costimulation. *J. Immunol.* **1999**, *162*, 2775–2784.

40. Delgoffe, G.M.; Pollizzi, K.N.; Waickman, A.T.; Heikamp, E.; Meyers, D.J.; Horton, M.R.; Xiao, B.; Worley, P.F.; Powell, J.D. The kinase mTOR regulates the differentiation of helper T cells through the selective activation of signaling by mTORC1 and mTORC2. *Nat. Immunol.* **2011**, *12*, 295–303.
41. Parry, R.V.; Chemnitz, J.M.; Frauwirth, K.A.; Lanfranco, A.R.; Braunstein, I.; Kobayashi, S.V.; Linsley, P.S.; Thompson, C.B.; Riley, J.L. CTLA-4 and PD-1 receptors inhibit T-cell activation by distinct mechanisms. *Mol. Cell Biol.* **2005**, *25*, 9543–9553.
42. Sinclair, L.V.; Finlay, D.; Feijoo, C.; Cornish, G.H.; Gray, A.; Ager, A.; Okkenhaug, K.; Hagenbeek, T.J.; Spits, H.; Cantrell, D.A. Phosphatidylinositol-3-OH kinase and nutrient-sensing mTOR pathways control T lymphocyte trafficking. *Nat. Immunol.* **2008**, *9*, 513–521.
43. Ouyang, S.; Zeng, Q.; Tang, N.; Guo, H.; Tang, R.; Yin, W.; Wang, A.; Tang, H.; Zhou, J.; Xie, H.; et al. Akt-1 and Akt-2 Differentially Regulate the Development of Experimental Autoimmune Encephalomyelitis by Controlling Proliferation of Thymus-Derived Regulatory T Cells. *J. Immunol.* **2019**, *202*, 1441–1452.
44. DuBois, J.C.; Ray, A.K.; Gruber, R.C.; Zhang, Y.; Aflakpui, R.; Macian-Juan, F.; Shafit-Zagardo, B. Akt3-Mediated Protection Against Inflammatory Demyelinating Disease. *Front. Immunol.* **2019**, *10*, 1738.
45. DeNardo, D.G.; Ruffell, B. Macrophages as regulators of tumour immunity and immunotherapy. *Nat. Rev. Immunol.* **2019**, *19*, 369–382.
46. Vergadi, E.; Ieronymaki, E.; Lyroni, K.; Vaporidi, K.; Tsatsanis, C. Akt Signaling Pathway in Macrophage Activation and M1/M2 Polarization. *J. Immunol.* **2017**, *198*, 1006–1014.
47. Weichhart, T.; Saemann, M.D. The PI3K/Akt/mTOR pathway in innate immune cells: Emerging therapeutic applications. *Ann. Rheum. Dis.* **2008**, *67* (Suppl. 3), iii70–4.
48. Martin, M.; Schifferle, R.E.; Cuesta, N.; Vogel, S.N.; Katz, J.; Michalek, S.M. Role of the phosphatidylinositol 3 kinase-Akt pathway in the regulation of IL-10 and IL-12 by Porphyromonas gingivalis lipopolysaccharide. *J. Immunol.* **2003**, *171*, 717–725.
49. Rocher, C.; Singla, D.K. SMAD-PI3K-Akt-mTOR pathway mediates BMP-7 polarization of monocytes into M2 macrophages. *PLoS ONE* **2013**, *8*, e84009.
50. Rauh, M.J.; Ho, V.; Pereira, C.; Sham, A.; Sly, L.M.; Lam, V.; Huxham, L.; Minchinton, A.I.; Mui, A.; Krystal, G. SHIP represses the generation of alternatively activated macrophages. *Immunity* **2005**, *23*, 361–374.
51. Araki, K.; Ellebedy, A.H.; Ahmed, R. TOR in the immune system. *Curr. Opin Cell Biol.* **2011**, *23*, 707–715.
52. Mercalli, A.; Calavita, I.; Dugnani, E.; Citro, A.; Cantarelli, E.; Nano, R.; Melzi, R.; Maffi, P.; Secchi, A.; Sordi, V.; et al. Rapamycin unbalances the polarization of human macrophages to M1. *Immunology* **2013**, *140*, 179–190.
53. Jiang, Z.; Georgel, P.; Du, X.; Shamel, L.; Sovath, S.; Mudd, S.; Huber, M.; Kalis, C.; Keck, S.; Galanos, C.; et al. CD14 is required for MyD88-independent LPS signaling. *Nat. Immunol.* **2005**, *6*, 565–570.
54. Strassheim, D.; Asehnoune, K.; Park, J.S.; Kim, J.Y.; He, Q.; Richter, D.; Kuhn, K.; Mitra, S.; Abraham, E. Phosphoinositide 3-kinase and Akt occupy central roles in inflammatory responses of Toll-like receptor 2-stimulated neutrophils. *J. Immunol.* **2004**, *172*, 5727–5733.
55. Schaeffer, V.; Arbabi, S.; Garcia, I.A.; Knoll, M.L.; Cuschieri, J.; Bulger, E.M.; Maier, R.V. Role of the mTOR pathway in LPS-activated monocytes: Influence of hypertonic saline. *J. Surg Res.* **2011**, *171*, 769–776.
56. Arranz, A.; Doxaki, C.; Vergadi, E.; de la Torre, Y.M.; Vaporidi, K.; Lagoudaki, E.D.; Ieronymaki, E.; Androulidaki, A.; Venihaki, M.; Margioris, A.N.; et al. Akt1 and Akt2 protein kinases differentially contribute to macrophage polarization. *Proc. Natl. Acad. Sci. USA* **2012**, *109*, 9517–9522.
57. Zhou, S.-L.; Zhou, Z.-J.; Hu, Z.-Q.; Huang, X.-W.; Wang, Z.; Chen, E.-B.; Fan, J.; Cao, Y.; Dai, Z.; Zhou, J. Tumor-Associated Neutrophils Recruit Macrophages and T-Regulatory Cells to Promote Progression of Hepatocellular Carcinoma and Resistance to Sorafenib. *Gastroenterology* **2016**, *150*, 1646–1658.e17.
58. Chen, J.; Tang, H.; Hay, N.; Xu, J.; Ye, R.D. Akt isoforms differentially regulate neutrophil functions. *Blood* **2010**, *115*, 4237–4246.
59. Chen, Y.; Li, C.; Xie, H.; Fan, Y.; Yang, Z.; Ma, J.; He, D.; Li, L. Infiltrating mast cells promote renal cell carcinoma angiogenesis by modulating PI3K→AKT→GSK3β→AM signaling. *Oncogene* **2017**, *36*, 2879–2888.
60. Yap, T.A.; Garrett, M.D.; Walton, M.I.; Raynaud, F.; de Bono, J.S.; Workman, P. Targeting the PI3K-AKT-mTOR pathway: Progress, pitfalls, and promises. *Curr. Opin. Pharmacol.* **2008**, *8*, 393–412.
61. Lindsley, C.W.; Barnett, S.F.; Yaroshchak, M.; Bilodeau, M.T.; Layton, M.E. Recent progress in the development of ATP-competitive and allosteric Akt kinase inhibitors. *Curr. Top. Med. Chem.* **2007**, *7*, 1349–1363.
62. Brown, J.S.; Banerji, U. Maximising the potential of AKT inhibitors as anti-cancer treatments. *Pharmacol. Ther.* **2017**, *172*, 101–115.
63. Landel, I.; Quambusch, L.; Depta, L.; Rauh, D. Spotlight on AKT: Current Therapeutic Challenges. *ACS Med. Chem. Lett.* **2020**, *11*, 225–227.
64. Lin, J.; Sampath, D.; Nannini, M.A.; Lee, B.B.; Degtyarev, M.; Oeh, J.; Savage, H.; Guan, Z.; Hong, R.; Kassees, R.; et al. Targeting Activated Akt with GDC-0068, a Novel Selective Akt Inhibitor That Is Efficacious in Multiple Tumor Models. *Clin. Cancer Res.* **2013**, *19*, 1760–1772.
65. Zhai, B.; Hu, F.; Jiang, X.; Xu, J.; Zhao, D.; Liu, B.; Pan, S.; Dong, X.; Tan, G.; Wei, Z.; et al. Inhibition of Akt reverses the acquired resistance to sorafenib by switching protective autophagy to autophagic cell death in hepatocellular carcinoma. *Mol. Cancer Ther.* **2014**, *13*, 1589–1598.
66. Doi, T.; Fujiwara, Y.; Matsubara, N.; Tomomatsu, J.; Iwasa, S.; Tanaka, A.; Endo-Tsukude, C.; Nakagawa, S.; Takahashi, S. Phase I study of ipatasertib as a single agent and in combination with abiraterone plus prednisolone in Japanese patients with advanced solid tumors. *Cancer Chemother. Pharmacol.* **2019**, *84*, 393–404.

67. Zhang, Y.; Zheng, Y.; Faheem, A.; Sun, T.; Li, C.; Li, Z.; Zhao, D.; Wu, C.; Liu, J. A novel AKT inhibitor, AZD5363, inhibits phosphorylation of AKT downstream molecules, and activates phosphorylation of mTOR and SMG-1 dependent on the liver cancer cell type. *Oncol. Lett.* **2016**, *11*, 1685–1692.
68. Dean, E.; Banerji, U.; Schellens, J.H.M.; Krebs, M.G.; Jimenez, B.; van Brummelen, E.; Bailey, C.; Casson, E.; Cripps, D.; Cullberg, M.; et al. A Phase I, open-label, multicentre study to compare the capsule and tablet formulations of AZD5363 and explore the effect of food on the pharmacokinetic exposure, safety and tolerability of AZD5363 in patients with advanced solid malignancies: OAK. *Cancer Chemother. Pharmacol.* **2018**, *81*, 873–883.
69. Roth, G.S.; Jilkova, Z.M.; Kuyucu, A.Z.; Kurma, K.; Pour, S.T.A.; Abbadessa, G.; Yu, Y.; Busser, B.; Marche, P.N.; Leroy, V.; et al. Efficacy of AKT Inhibitor ARQ 092 Compared with Sorafenib in a Cirrhotic Rat Model with Hepatocellular Carcinoma. *Mol. Cancer Ther.* **2017**, *16*, 2157–2165.
70. Jilkova, Z.M.; Kuyucu, A.Z.; Kurma, K.; Pour, S.T.A.; Roth, G.S.; Abbadessa, G.; Yu, Y.; Schwartz, B.; Sturm, N.; Marche, P.N.; et al. Combination of AKT inhibitor ARQ 092 and sorafenib potentiates inhibition of tumor progression in cirrhotic rat model of hepatocellular carcinoma. *Oncotarget* **2018**, *9*, 11145–11158.
71. Kurma, K.; Jilkova, Z.M.; Roth, G.S.; Abbadessa, G.; Yu, Y.; Marche, P.; Decaens, T. Effect of novel AKT inhibitor ARQ 751 as single agent and its combination with sorafenib on hepatocellular carcinoma in a cirrhotic rat model. *J. Hepatol.* **2017**, *66*, S459–S460.
72. Wilson, J.M.; Kunnimalaiyaan, S.; Gamblin, T.C.; Kunnimalaiyaan, M. MK2206 inhibits hepatocellular carcinoma cellular proliferation via induction of apoptosis and cell cycle arrest. *J. Surg. Res.* **2014**, *191*, 280–285.
73. Ahn, D.H.; Li, J.; Wei, L.; Doyle, A.; Marshall, J.L.; Schaaf, L.J.; Phelps, M.A.; Villalona-Calero, M.A.; Bekaii-Saab, T. Results of an abbreviated phase-II study with the Akt Inhibitor MK-2206 in Patients with Advanced Biliary Cancer. *Sci. Rep.* **2015**, *5*, 12122, doi:10.1038/srep12122.
74. Davies, B.R.; Greenwood, H.; Dudley, P.; Crafter, C.; Yu, D.-H.; Zhang, J.; Li, J.; Gao, B.; Ji, Q.; Maynard, J.; et al. Preclinical Pharmacology of AZD5363, an Inhibitor of AKT: Pharmacodynamics, Antitumor Activity, and Correlation of Monotherapy Activity with Genetic Background. *Mol. Cancer Ther.* **2012**, *11*, 873–887.
75. Patra, T.; Meyer, K.; Ray, R.B.; Ray, R. A combination of AZD5363 and FH5363 induces lethal autophagy in transformed hepatocytes. *Cell Death Dis.* **2020**, *11*, 540, doi:10.1038/s41419-020-02741-1.
76. Carnevalli, L.S.; Sinclair, C.; Taylor, M.A.; Gutierrez, P.M.; Langdon, S.; Coenen-Stass, A.M.L.; Mooney, L.; Hughes, A.; Jarvis, L.; Staniszewska, A.; et al. PI3K α/δ inhibition promotes anti-tumor immunity through direct enhancement of effector CD8⁺ T-cell activity. *J. Immunother. Cancer* **2018**, *6*, 158.
77. Abu-Eid, R.; Samara, R.N.; Ozbun, L.; Abdalla, M.Y.; Berzofsky, J.A.; Friedman, K.M.; Mkrtichyan, M.; Khleif, S.N. Selective Inhibition of Regulatory T Cells by Targeting the PI3K–Akt Pathway. *Cancer Immunol. Res.* **2014**, *2*, 1080–1089.
78. Searle, E.J.; Telfer, B.A.; Mukherjee, D.; Forster, D.M.; Davies, B.R.; Williams, K.J.; Stratford, I.J.; Illidge, T.M. Akt inhibition improves long-term tumour control following radiotherapy by altering the microenvironment. *Embo Mol. Med.* **2017**, *9*, 1646–1659.
79. Macek Jilkova, Z.; Kurma, K.; Decaens, T. Animal Models of Hepatocellular Carcinoma: The Role of Immune System and Tumor Microenvironment. *Cancers* **2019**, *11*, 1487.
80. Marks, D.K.; Gattrell, R.D.; El Asmar, M.; Boboila, S.; Hart, T.; Lu, Y.; Pan, Q.; Yu, J.; Hibshoosh, H.; Guo, H.; et al. Akt Inhibition Is Associated With Favorable Immune Profile Changes Within the Tumor Microenvironment of Hormone Receptor Positive, HER2 Negative Breast Cancer. *Front. Oncol.* **2020**, *10*, 968.